**University of Southampton**

Faculty of Physical Sciences and Engineering

Physics and Astronomy

# Holographic correlators and scattering amplitudes: $\mathcal{N} = 4$ **SYM and beyond**

by

Ross Glew

A thesis submitted for the degree of

Doctor of Philosophy

January 2023

# <u>ABSTRACT</u>

**HOLOGRAPHIC CORRELATORS AND SCATTERING AMPLITUDES: $\mathcal{N} = 4$ SYM AND BEYOND**

by Ross Glew

In the first part of this thesis we study string corrections to one-loop amplitudes of single-particle half-BPS operators $\mathcal{O}_p$ in $AdS_5 \times S^5$ . The tree-level correlators (dual to AdS scattering amplitudes via the AdS/CFT correspondence) in supergravity enjoy an accidental 10d conformal symmetry. Consequently, one observes a partial degeneracy in the spectrum of anomalous dimensions of double-trace operators and at the same time equality of many different correlators for different external charges $p_{i=1,2,3,4}$. The one-loop contribution is expected to lift such bonus properties, and its precise form can be predicted from tree-level data and consistency with the operator product expansion.

Here we present a closed-form Mellin space formula for $\langle \mathcal{O}_{p_1} \mathcal{O}_{p_2} \mathcal{O}_{p_3} \mathcal{O}_{p_4} \rangle$ at order $\lambda^{-3/2}$ in the expansion around large $\lambda$ valid for arbitrary external charges $p_i$. Our formula makes explicit the lifting of the bonus degeneracy among different correlators through a feature we refer to as 'sphere splitting'. While tree-level Mellin amplitudes come with a single crossing symmetric kernel, which defines the pole structure of the $AdS_5 \times S^5$ amplitude, our one-loop amplitude naturally splits the $S^5$ part into two separate contributions. The amplitude also exhibits a remarkable consistency with the corresponding flat space IIB amplitude through the large $p$ limit.

In the second part of this thesis we study the relation between the branch cut structure of scattering amplitudes in planar $\mathcal{N} = 4$ SYM and Grassmannian cluster algebras using the novel language of Gröbner theory. We detail how to extract the familiar $\mathcal{A}$-coordinates and their respective adjacency conditions from the Gröbner fan of the Plücker ideal. Having established this connection we apply similar techniques to the case of non dual conformal invariant five-point kinematics where we extract the full non-planar symbol alphabet relevant for the construction of five-point integrals/amplitudes.

Finally, we continue to study the connection between cluster algebras and scattering amplitudes by considering the family of partial flag cluster algebras $F(2, 4, n)$ in order to extract information on the symbol alphabet for amplitudes with five-point and six-point non dual conformal invariant kinematics.

# Table of Contents

# Declaration of Authorship

I, Ross Glew, declare that this thesis entitled *Holographic correlators and scattering amplitudes: $\mathcal{N} = 4$ SYM and beyond* and the work presented in it are my own and have been generated by me as the result of my own original research.

I confirm that:

1. This work was done wholly or mainly while in candidature for a research degree at this University;

2. Where any part of this thesis has previously been submitted for a degree or any other qualification at this University or any other institution, this has been clearly stated;

3. Where I have consulted the published work of others, this is always clearly attributed;

4. Where I have quoted from the work of others, the source is always given. With the exception of such quotations, this thesis is entirely my own work;

5. I have acknowledged all main sources of help;

6. Where the thesis is based on work done by myself jointly with others, I have made clear exactly what was done by others and what I have contributed myself;

7. Either none of this work has been published before submission, or parts of this work have been published as: [1–3]

Signed:

Date:

x

# Acknowledgements

First I would like to thank my supervisor James Drummond for introducing me to the beautiful subject of scattering amplitudes and for the continual help, support and long discussions over the last four years. I would like to thank my collaborators Hynek, Michele, Francesco and Ömer from whom I have learnt a lot and without which this thesis would not exist. Also, a thank-you in advance to my examiners for having to read my thesis.

Next, I would like to thank my parents Gary and Jodie whose love made this thesis (not to mention the last 25 years) possible, as well as my family: Shannon, Carlie, Nanny Bam-Bam, Anthony, Charlie, Jordan, Brian, Elaine, Mick, John and Pat. Some special thanks to:

- Carlie and Charlie for housing me and making life fun in the first lockdown.

- Shannon and Jordan for all the snacks and vape juice.

- Jodie for making me a cup of tea on the 18th of June.

I would also like to thank Tesh, Matt, Michele, *Justine*[1] and Billy whose friendships I have valued over the course of my PhD.

Finally, I would like to thank Maëlle Leggiadro who will forever be my greatest discovery.

---

[1] À prononcer avec un accent français.

*To Gary and Jodie*

# Chapter 1

# Introduction

Scatttering experiments such as those performed at the Large Hadron Collider (LHC) have been an invaluable tool for testing our most fundamental theories of nature. The object measured in scattering experiments is the *scattering cross-section* which broadly speaking measures the probability for a particular interaction to take place amongst a collection of particles. To obtain the cross-section requires knowledge of the more fundamental object, the *scattering amplitude*[1], which can be calculated within the framework of Quantum Field Theory (QFT). Scattering amplitudes then constitute some of the most fundamental measurements we can make on the theories which govern our universe. But the limit of their interest goes beyond just the experimental results they provide. They can also reveal deep insights into the structure of QFTs which are often obscured by the familiar Lagrangian description.

As an example consider processes relevant for physics at the LHC. The protons collided at the LHC are made up of quarks and gluons whose interactions are governed by Quantum Chromodynamics (QCD). One possible process which can take place is that a collection of gluons come together to interact. Therefore we might ask what is the associated amplitude for the scattering of $n$ gluons. The usual starting point for any QFT calculation is the Lagrangian from which the Feynman rules defining the interaction vertices can be read off.

---

[1]We may think of the scattering amplitude in QFT being analogous to the wavefunction in Quantum Mechanics.

**Figure 1.1:** The three-point and four-point gluon vertices of QCD.

If the theory is weakly coupled we can organise the calculation into a perturbative expansion in Feynman diagrams ordered by the number of loops. The Feynman rules can then be used to convert each Feynman diagram into a mathematical expression. Thus, to calculate the scattering amplitude of $n$ gluons at leading order (the tree-level contribution) we sum over all possible Feynman diagrams with $n$ external legs, and no internal loops, which can be built from the three-point and four-point point gluon vertices of Figure 1.1. However, these calculations become intractable very quickly due to the combinatorial explosion which takes place for the number of diagrams.

$$
\begin{aligned}
2g \to 2g \quad & \text{4 diagrams} \\
2g \to 3g \quad & \text{25 diagrams} \\
2g \to 4g \quad & \text{220 diagrams} \\
2g \to 5g \quad & \text{2485 diagrams}
\end{aligned}
$$

By the time we consider $2g \to 8g$ there are over ten million diagrams, eventually there reaches a point where even these most powerful computers cannot handle the computations. But, as shown by Parke-Taylor [4] this complexity is artificial, a remnant from the fact we are trying to build an on-shell gauge independent object from gauge dependent diagrams containing virtual off-shell particles. In fact, when written in the *correct* variables, these ten million diagrams collapse to a single term. The same remains true for an arbitrary number of gluons, where the result is summarised as[1]

$$
A_n^{\mathrm{MHV}} = \frac{\langle ij \rangle^4}{\langle 12 \rangle \dots \langle n1 \rangle}. \tag{1.1}
$$

Such a drastic simplification is a calling card to move away from the Feynman description in search for a new understanding which makes this simplicity manifest!

The search for this simplicity has sparked an array of new efficient techniques for the calculation of scattering amplitudes including: the on-shell tree level BCFW recursion

---

[1]Where the brackets are spinor-helicty variables and the $i^{\mathrm{th}}$ and $j^{\mathrm{th}}$ gluon are taken to have negative helicity.

relations [5, 6], which effectively reduce the problem of computing any $n$-point gluon amplitude to consistently stitching together three-point amplitudes, in some cases, such as the scattering of $n$ gluons [7], this allows a closed form solution to the recursion relations; whereas beyond tree level methods such as generalised unitarity [8] have been developed to tackle the more complex analytic structure.

The perfect toy model for exploring these ideas further is provided by $\mathcal{N} = 4$ Super Yang-Mills (SYM) theory in 4d, which has many symmetries to make the theory tractable, whilst still retaining rich mathematical structure, so as not to be trivial. The intensive study of $\mathcal{N} = 4$ has led to the discovery of beautiful mathematical structures hidden within scattering amplitudes. At weak coupling, and in the planar limit, an all-loop integrand [9] has been written down, extending the BCFW recursion relation to all loop orders. This construction is closely related to the Grassmannian[1] $G(k, n)$ [10–12], which makes manifest both the superconformal invariance, and its long illusive counterpart dual superconformal conformal invariance [13].

However, of most relevance to this thesis, are the results for the amplitudes themselves. In particular we will be interested in the branch cut structure of perturbative amplitudes in planar $\mathcal{N} = 4$ and their relation to certain structures in algebraic geometry. Considering the branch cut structure of amplitudes has allowed the analytic bootstrap program to obtain impressive results up to high loop orders [14–24]. The foundation of the bootstrap relies on the link between the Grassmannian $G(4, n)$ cluster algebras[2] and the location of potential branch cut singularities of the amplitude. This relation, first discovered in [28] and further developed in [29], linked the $\mathcal{A}$-coordinates of the cluster algebra to the *symbol alphabet* (the positions of potential logarithmic singularities) of the amplitude. Furthermore, the link was endowed with a geometric significance by the discovery of *cluster adjacency* [30] encoding which consecutive branch cuts have non-zero residues. The bootstrap program has mainly focused on six and seven points as their associated cluster algebras $G(4, 6)$ and $G(4, 7)$ are of finite type.

Exploring the connection between the symbol alphabets of amplitudes in planar $\mathcal{N} = 4$ SYM and the Grassmannian will be the focus of the second part of this thesis. Inspired by the recent success of the application of Tropical geometry to scattering amplitudes [31–34], and results from the mathematics literature [35, 36], we first set out to reformulate existing results in the new language of the Gröbner fan. Having established this connection we ask the exciting question of whether similar techniques may be applied to cases beyond $\mathcal{N} = 4$ SYM where dual conformal symmetry is no longer present. Note, these question have begun to be asked at the level of individual Feynman diagrams for instance in [37–39] where cluster algebraic structures have also been seen to emerge. Our main example will be the non dual

---

[1] The Grassmannian $G(k, n)$ is the set of $k$-planes in n dimensions.
[2] First discovered in [25–27].

conformal invariant five-point kinematics whose planar and non-planar symbol alphabet have been proposed in [37, 40]. In the final chapter of this section we will also return to the question of how much a generalisation of the Grassmannian cluster algebras, the partial flag cluster algebras, have to say about the symbol alphabet of non dual conformal invariant five and six -point amplitudes.

But, the reasons to study $\mathcal{N} = 4$ are not at an end yet. At strong coupling this theory also provides a vital tool in the study of quantum gravity through the AdS/CFT correspondence!

The AdS/CFT correspondence [41] relates theories of quantum gravity in AdS to non-gravitational Conformal Field Theories (CFT's) living at the boundary in one less dimension, the prime example being the duality between $\mathcal{N} = 4$ SYM and type IIB string theory on AdS$_5 \times$S$^5$. We will be particularly interested in the limit where we take the number of colours $N$ large and further take the 't Hooft coupling $\lambda = g_{YM}^2 N$ to infinity. In this limit the bulk theory reduces to weakly coupled IIB supergravity in AdS whose single particle states are the supergravity fields.
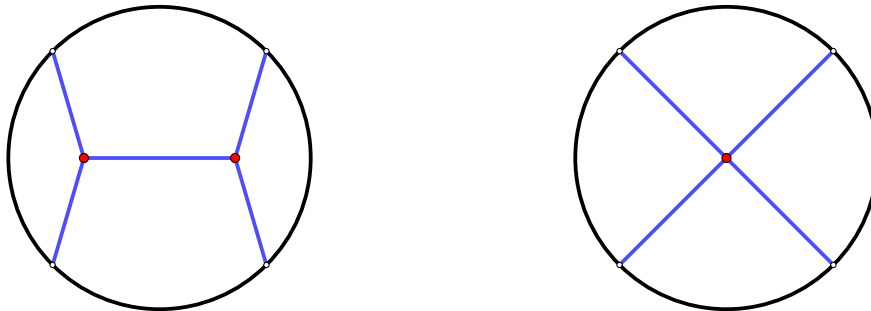


**Figure 1.2:** Examples of exchange (left) and contact (right) Witten diagrams entering the scattering amplitude at tree-level.

Let's consider scattering amplitudes in this weakly coupled supergravity theory. Through the AdS/CFT correspondence scattering amplitudes on the supergravity side are mapped to correlation functions of gauge invariant operators on the CFT side. Our main point of interest will be four-point correlation functions of half-BPS operators

$$\langle \mathcal{O}_{p_1}(x_1)\mathcal{O}_{p_2}(x_2)\mathcal{O}_{p_3}(x_3)\mathcal{O}_{p_4}(x_4)\rangle, \tag{1.2}$$

where the dual description of $\mathcal{O}_2$ corresponds to a state belonging to the graviton super-multiplet and $\mathcal{O}_{p>2}$ its Kaluza-Klein (KK) partners. The standard algorithm for computing such holographic correlators follows closely the example above for flat space amplitudes. As before we can compute the supergravity amplitudes in a diagrammatic expansion in powers of the small Newton constant, where the Feynman diagrams of flat space are replaced with their AdS equivalent the Witten Diagrams. Consider the tree-level contribution, which we obtain by summing over all tree-level exchange and contact Witten diagrams. This approach

requires detailed knowledge of the cubic and quartic vertices appearing in the AdS effective action, obtained by Kaluza-Klein reduction of IIB supergravity on $S^5$. The effective action is extremely complicated [42–44], with the scalar quartic vertices [43] alone filling 15 pages. Furthermore, the number of exchange Witten diagrams grows rapidly with the KK level. All in all making it practically impossible to go beyond the simplest cases of the lowest KK modes [45–50], even where a solution does exist, it is given in the unenlightening form as a sum of $\bar{D}$ functions with complicated analytic structure.

These problems were solved in [51, 52] by rephrasing the question in Mellin space [53, 54] where the analytic structure of the amplitude simplifies dramatically. In Mellin space the holographic correlator becomes a rational expression in mandelstam-like invariants $s, t, u$, whose poles and residues are dictated by Operator Product Expansion (OPE) factorization analogous to their flat-space counterparts. This allowed [51, 52] to write down a beautifully simple formula for the tree-level correlator for arbitrary KK modes! The result can be summarised in a single term given by[1]

$$\mathcal{M}^{(1,0)} = \frac{1}{(\mathbf{s}+1)(\mathbf{t}+1)(\mathbf{u}+1)}. \tag{1.3}$$

Since this landmark result there have been many exciting developments. The tree-level result above allowed for a detailed study of the double-trace spectrum [56] at leading large $N$, culminating in a general expression for the tree-level anomalous dimensions [56] which itself hinted towards a hidden 10d conformal symmetry at tree-level [57]. Another direction which has received attention is the study of stringy corrections arising from higher derivative corrections to the AdS effective action [58–61]. If it were possible to resum the string corrections at tree-level the resulting expression would be the analog to the Virasoro-Shapiro amplitude in AdS!

Beyond tree-level a handful of correlators have been computed at one-loop both for supergravity [55, 62–66] and its stringy corrections [1, 62, 67]. Beyond this no general correlator has been computed. Note, also at two loops results are further constrained to only the simplest correlator of four supergraviton multiplets [68, 69]. The focus of the first part of this thesis will be to remedy this for the first one-loop string correction where we shall write down a general formula for arbitrary KK modes!

The above examples at strong and weak coupling exemplify not only the richness of $\mathcal{N} = 4$, but, also the power of the *bootstrap philosophy*, which can be summarised as follows: Instead of performing lengthy QFT calculations why don't we simply write down the only answer with the correct analytic structure consistent with symmetries?

The remainder of this thesis is split into two topics which can be read independently. The

---

[1]Note, the result was first written in this form by [55].

first discussing holographic correctors in $\mathcal{N} = 4$ SYM around the supergravity limit, the second discussing the mathematical structure of scattering amplitudes in planar $\mathcal{N} = 4$ SYM and beyond, a content outline for each can be found below.

## 1.1   Outline: Part I

In the first part of this thesis we study the correlation function of 1/2-BPS operators in $\mathcal{N} = 4$ SYM theory i.e.

$$\langle \mathcal{O}_{p_1}(x_1)\mathcal{O}_{p_2}(x_2)\mathcal{O}_{p_3}(x_3)\mathcal{O}_{p_4}(x_4)\rangle. \tag{1.4}$$

We will study these objects at tree level and one loop in Newton's constant (or equivalently, $1/N^2$ and $1/N^4$ corrections in the CFT) and at the leading orders in string corrections to Einstein gravity, i.e. leading orders in the $\alpha' \sim \lambda^{-\frac{1}{2}}$ expansion, where $\lambda$ is the 't Hooft coupling.

At tree level much is known about the structure of these correlators and general explicit results exist both at the level of supergravity [51, 52], as well as its stringy corrections [60, 61] up-to high orders in $\lambda^{-1/2}$. However, at one-loop no such general formulae exist. The one-loop supergravity correlator was studied for the simplest correlator $\langle \mathcal{O}_2\mathcal{O}_2\mathcal{O}_2\mathcal{O}_2\rangle$ in [64, 70] and more generally in [66] where a position space algorithm was presented for boostrapping arbitrary one-loop correlators from tree level data. The one-loop supergravity result was also studied in Mellin space in [63] where an explicit formula was presented for the simplified family of correlators $\langle \mathcal{O}_2\mathcal{O}_2\mathcal{O}_p\mathcal{O}_p\rangle$. Furthermore, knowledge of one-loop stringy correlators is known [1, 58, 59, 62, 67, 71] but only restricted to low charges and simplified cases.

Our main focus will be to remedy this sorry state of affairs by presenting a formula for the first one-loop string correction at order $(\lambda)^{-3/2}$ for arbitrary external charges. Along the way we will discuss the general picture for higher $\lambda$ in order to (somewhat) systematise the one-loop bootstrap, or at least provide a more educated ansatz than has otherwise existed. The results presented in the first part of this thesis originate from [1, 2] where the one-loop string correction was calculated for the simpler setting of $\langle \mathcal{O}_2\mathcal{O}_2\mathcal{O}_p\mathcal{O}_p\rangle$ in [1] and later generalised to arbitrary KK modes in [2].

The remainder of Part I is organised as follows: In sections 2-5 we introduce the relevant material to appreciate the construction of the one-loop amplitude including: a discussion of correlation functions in Conformal Field Theories (CFT's), the conformal block expansion in $\mathcal{N} = 4$ SYM, the AdS/CFT correspondence and the Mellin space formalism.

Next, at the beginning of Chapter 6, we describe in detail how the OPE (Operator Product Expansion) can be used to build the one-loop amplitude from tree level data. It is also in this chapter that we present our main result: a completely general formula for the one-loop

correlator at $(\lambda)^{-3/2}$. Finally, in section 6.3 we show consistency of the one-loop amplitude with the large $p$ limit and the flat space limit in type IIB string theory.

## 1.2  Outline: Part II

In the second part of this thesis we begin with a study of perturbative scattering amplitudes in planar $\mathcal{N} = $ SYM and the underlying mathematical structures which govern them. As we will see the branch cut structure of these dual conformal invariant $n$-point amplitudes are intimately connected with the Grassmannian cluster algebras $G(4, n)$.

To motivate why an unfamiliar space such as the Grassmannian should appear in this discussion it is enough to consider the question: *what is the best way to describe the kinematic space of massless amplitudes*? Naively, amplitudes are functions of the external momenta $p_i^\mu$. However, the momenta are constrained by the massless on-shell condition and momentum conservation via

$$p_i^2 = 0; \qquad \sum_{i=1}^{n} p_i^\mu = 0, \tag{1.5}$$

and hence it is natural to search for a set of variables which automatically satisfy these constraints. The majority of the next two chapters will be focused on introducing this new set of variables. This will lead us from spinor-helicity variables to momentum-twistors and eventually, for the dual conformal invariant case of $\mathcal{N} = 4$ SYM, to the Grassmannian $G(4, n)$ itself. In the more general setting where dual conformal symmetry is not present the kinematic space is instead naturally associated to the partial flag $F(2, 4, n)$.

With the *correct* variables to hand we continue to review the well established language of the amplitude bootstrap programme and the important role the Grassmannian cluster algebras have to play. Most importantly we introduce the notion of the symbol, an object encoding the consecutive discontinuities of the amplitude, which is built upon the $\mathcal{A}$-coordinates of the cluster algebras $G(4, n)$. We will review how the geometric structure of the $G(4, n)$ cluster algebra constrains the form of the symbol through *cluster adjacency.*

Having reviewed this necessary material we move on in Chapter 11 to the first result of this section, to extract the $\mathcal{A}$-coordinates and cluster adjacency rules, relevant for constructing amplitudes in $\mathcal{N} = 4$ SYM, from the $G(4, n)$ cluster algebras via the novel language of the Gröbner fan. A benefit of this approach is that it makes no reference to the cluster algebra directly and hence has the potential to be more widely applicable for instance to the case of amplitudes where dual conformal symmetry is no longer present. With this larger goal in mind we conclude Chapter 11 with an application of the Gröbner fan technology to the non dual conformal invariant five-point kinematics to see what we can learn about its symbol alphabet. These results were originally presented in [3].

Finally, in Chapter 12 we return to the study of a generalisation of the Grassmannian cluster

algebras, the partial flag cluster algebras $F(2, 4, n)$, to see what role they have to play in determining the symbol alphabet for non dual conformal invariant massless 5 and 6 point amplitudes.

# PART I

## HOLOGRAPHIC CORRELATORS

# Chapter 2

# Conformal Field Theory

This section provides a basic introduction to Conformal Field Theory emphasising on: primary operators, their correlations functions, the Operator Product Expansion, and conformal blocks. The main references followed are [72, 73].

The conformal transformations are given by the subset of diffeomorphisms $x \mapsto x'(x)$ which keep the metric[1] fixed up to a local rescaling. In $d > 2$ they are generated by the usual isometries of flat space: translations $P_\mu$ and Lorentz transformations $M_{\mu\nu}$; along with dilatations $D$ and special conformal transformations $K_\mu$, which close to form the conformal group $SO(d, 2)$. A subset of the conformal algebra is given by

$$[D, P_\mu] = P_\mu, \quad [D, K_\mu] = -K_\mu. \tag{2.1}$$

As such we may think of $P_\mu$ and $K_\mu$ as raising and lowering operators for the dilatations. Using the raising and lowering operators leads us to the classification of local operators, $\mathcal{O}_i$, with scaling dimensions $\Delta_i$ defined by

$$[D, \mathcal{O}_j(0)] = i\Delta_j \mathcal{O}_j(0), \tag{2.2}$$

into two types: *primaries* and *descendants*. The primary operators are defined as being annihilated by special conformal transformations at the origin

$$[K, \mathcal{O}(0)] = 0. \tag{2.3}$$

Whereas the descendants can be obtained by acting on the primary operators with a linear combination of derivatives, or in other words by repeatedly applying the generator of translations $P_\mu$. A primary operator together with its tower of descendants together form a conformal multiplet.

---

[1]For our purposes we take this to be the metric of $d$-dimensional Minkowski space.

The generators $P_\mu$ and $K_\mu$ act as raising and lowering operators of the scaling dimension which move us around a conformal multiplet, with condition (2.3) defining the *lowest weight* operator. Since we will be interested in CFT correlations functions, and descendants are obtained trivially from their primaries by acting with derivatives, it follows that the correlation functions of descendent operators can be obtained directly from that of their primaries. Hence, from now we will discuss only primary operators.

## 2.1   Correlation functions of primary operators

We now demonstrate the power of conformal symmetry in fixing the form of conformal correlation functions of primary operators. At two points, after having fixed a normalisation, the correlation function of two scalar primary operators $\phi_i(x_i)$ is completely fixed to be

$$\langle \phi_1(x_1)\phi_2(x_2) \rangle = \frac{\delta_{\Delta_1 \Delta_2}}{x_{12}^{\Delta_1 + \Delta_2}}, \tag{2.4}$$

where we have defined $x_{ij} = x_i - x_j$.

Again, at three points the correlation function is fixed, this time up to an overall constant given by

$$\langle \phi_1(x_1)\phi_2(x_2)\phi_3(x_3) \rangle = \frac{\lambda_{123}}{|x|_{12}^{\Delta_1 + \Delta_2 - \Delta_3}|x|_{23}^{\Delta_2 + \Delta_3 - \Delta_1}|x|_{31}^{\Delta_3 + \Delta_1 - \Delta_2}}. \tag{2.5}$$

The overall constant $\lambda_{123}$ is known as the three-point coupling or OPE coefficient[1] (for reasons which will become clear).

However, at four points it is possible to form the conformal invariant cross ratios

$$u = \frac{x_{12}x_{34}}{x_{13}x_{24}} \quad \text{and} \quad v = \frac{x_{14}x_{23}}{x_{13}x_{24}}, \tag{2.6}$$

on which the four point function can depend non trivially. As an example consider the four-point function of identical operators $\phi$ with dimension $\Delta$, this takes the most general form

$$\langle \phi(x_1)\phi(x_2)\phi(x_3)\phi(x_4) \rangle = \frac{f(u,v)}{x_{12}^{2\Delta}x_{34}^{2\Delta}}, \tag{2.7}$$

where $f(u,v)$ is some function of the conformal cross ratios.

Note, the left hand side of this equation is invariant under permutations of the positions of the operators, therefore the function $f(u,v)$ must also satisfy these *crossing* constraints. The permutations are generated by the crossing $1 \leftrightarrow 2$ implying

$$f(u,v) = f(u/v, 1/v), \tag{2.8}$$

---

[1]These two terms will be used interchangeably.

and $1 \leftrightarrow 3$ implying

$$f(u,v) = \left(\frac{u}{v}\right)^{\Delta} f(v,u). \tag{2.9}$$

In the next section we will see how the OPE completely fixes[1] the function $f(u,v)$ in terms of the spectrum of primary operators $\Delta$, and the coefficients $\lambda_{ijk}$ appearing in the three-point functions.

## 2.2 The OPE and conformal block expansion

A concept from CFT that will be used extensively in the next section is the OPE (Operator Product Expansion). As the name suggests the OPE allows us to expand a product of operators at two nearby space-time points over a linear combination of primaries and descendants, this is summarised as

$$\overbrace{\phi_i(x)\phi_j}(0) = \sum_{\mathcal{O}} \lambda_{ij\mathcal{O}}\mathcal{L}_{\mathcal{O}}(x,\partial_y)\mathcal{O}(y)|_{y=0}, \tag{2.10}$$

where the sum runs over all primary operators of the theory, $\lambda_{ijk}$ are the coefficients appearing in the three-point functions, and $\mathcal{L}_{\mathcal{O}}(x,\partial_y)$ is a differential operator which reproduces the contribution coming from all descendants whose form is completely fixed by conformal symmetry.

Under insertion of the OPE an $n$-point correlation function can be reduced to a sum over $(n-1)$-point functions. Therefore, under repeated insertion, we can reduce the task of calculating any $n$-point correlation functions to consistently stitching together three-point functions with the correct OPE coefficients. In this way all correlation functions are fixed by the knowledge of the spectrum of primary operators and the couplings of the three-point functions $\{\Delta_i, \lambda_{ijk}\}$ which collectively is known as the *CFT Data*.

Let us see this explicitly for the case of the four-point function. We can insert the OPE twice into the correlation function as

$$\langle \overbrace{\phi(x_1)\phi(x_2)}\overbrace{\phi(x_3)\phi(x_4)}\rangle = \sum_{\mathcal{O}} \lambda_{12\mathcal{O}}\lambda_{34\mathcal{O}} \left[ \mathcal{L}_{\mathcal{O}}(x_{12},\partial_y)\mathcal{L}_{\mathcal{O}}(x_{34},\partial_z)\langle \mathcal{O}(y)\mathcal{O}(z)\rangle|_{z=x_{(34)}}^{y=x_{(12)}} \right], \tag{2.11}$$

where we have defined $x_{(ij)} = (x_i + x_j)/2$. Note, the function in the square bracket, known as the Conformal Partial Wave (CPW), is completely fixed by conformal symmetry! The above can be written as
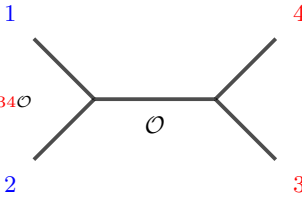
$$\langle \overbrace{\phi(x_1)\phi(x_2)}\overbrace{\phi(x_3)\phi(x_4)}\rangle = \frac{1}{x_{12}^{2\Delta_\phi}x_{34}^{2\Delta_\phi}} \sum_{\mathcal{O}} \lambda_{12\mathcal{O}}\lambda_{34\mathcal{O}}g_{\Delta,\ell}(u,v), \tag{2.12}$$

---

[1]In fact to fix the correlation function from the OPE we need to also consider the two-point and three-point functions with one spinning operator.
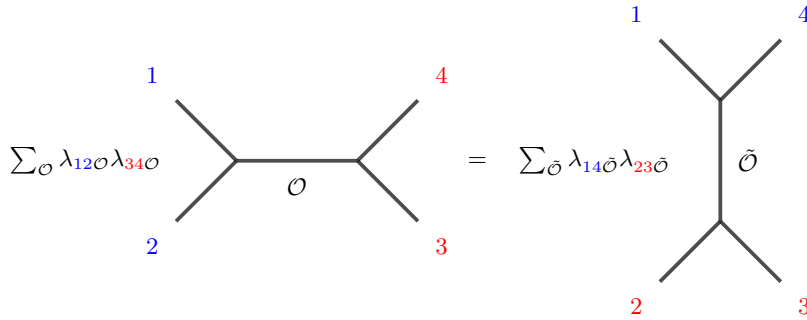
Where $g_{\Delta,\ell}(u,v)$ are known as *conformal blocks*[1] and $(\Delta,\ell)$ label the dimension and spin of the operator $\mathcal{O}$. These functions represent the contribution to the four point function from the conformal multiplet with primary operator $\mathcal{O}$.

Since the CFT data defines all correlation functions, and hence the entire theory, we may ask whether any random set $\{\Delta_i, \lambda_{ijk}\}$ corresponds to a consistent CFT? The answer is no! This can be seen by again considering CPW expansion of the four-point function. Above we chose to perform the OPE as $\langle\phi(x_1)\phi(x_2)\phi(x_3)\phi(x_4)\rangle$ which we represent diagrammatically in Figure 2.1.



$$\langle\phi_1(x_1)\phi_2(x_2)\phi_3(x_3)\phi_4(x_4)\rangle = \sum_{\mathcal{O}} \lambda_{12\mathcal{O}}\lambda_{34\mathcal{O}}$$

**Figure 2.1:** The CPW expansion of the four-point function in the s-channel.

Alternatively we could have chose to perform the OPE as $\langle\phi(x_1)\phi(x_2)\phi(x_3)\phi(x_4)\rangle$, and since the choice was arbitrary, both expansions must agree. This condition imposes constraints on the CFT data which must be satisfied in order to define a consistent CFT. These consistency conditions are referred to as *crossing symmetry* and are demonstrated pictorially in Figure 2.2. The crossing equations provide powerful constraints on the CFT data and form the foundation of the conformal bootstrap [75, 76].



$$\sum_{\mathcal{O}} \lambda_{12\mathcal{O}}\lambda_{34\mathcal{O}} \qquad = \qquad \sum_{\tilde{\mathcal{O}}} \lambda_{14\tilde{\mathcal{O}}}\lambda_{23\tilde{\mathcal{O}}}$$

**Figure 2.2:** The CPW expansion of the four-point function in the $s$ and $t$ channels.

In the next section we will review these ideas in the explicit example of $\mathcal{N}=4$ SYM where we will identify the (super) primary operators we will focus on in the first part of this thesis and provide explicit formulae for the conformal blocks.

---

[1]The form of the conformal blocks was originally developed in [74].

# Chapter 3

# $\mathcal{N} = 4$ **SYM**

The field content of $\mathcal{N} = 4$ SYM[1] includes: one gauge field $A_\mu$; four chiral fermions $\lambda_\alpha^A$ with $A = 1, .., 4$; six real scalars $\phi^I$ with $I = 1, ..., 6$ transforming in the fundamental representation of the R-symmetry group $SO(6) \cong SU(4)$; with all fields transforming in the adjoint representation of the gauge group $SU(N)$. The $\mathcal{N} = 4$ SYM Lagrangian in four dimensions is given uniquely by [78]

$$\mathcal{L}_4 = \text{Tr}\Big\{ -\frac{1}{2}F_{\mu\nu}F^{\mu\nu} - (D_\mu\phi^{AB})(D^\mu\bar{\phi}_{AB}) + 2i\bar{\lambda}_A\bar{\sigma}^\mu D_\mu\lambda^A + \frac{1}{2}g_{\text{YM}}^2[\phi^{AB},\phi^{CD}][\bar{\phi}_{AB},\bar{\phi}_{CD}]$$

$$- 2g_{\text{YM}}(\lambda^A[\bar{\phi}_{AB},\lambda^B] - \bar{\lambda}_A[\phi^{AB},\bar{\lambda}_B])\Big\},$$

where the trace is taken over the gauge group $SU(N)$; the six complex scalars $\phi^{AB}$, transforming in the antisymmetric rank-two representation of $SU(4)$, are subject to the reality condition, and are related to the six real scalars mentioned above by linear transformations.

At the classical level the theory is invariant under the conformal group $SO(2,4) \sim SU(2,2)$ and by construction $\mathcal{N} = 4$ supersymmetry. Together these combine into the larger group of superconformal symmetries $PSU(2,2|4)$ under which the theory is invariant. Remarkably, calculations of correlation functions have revealed no ultra-violet divergences under perturbative quantization, and as a consequence, the renormalization group $\beta$-function vanishes identically. As a result the superconformal group $PSU(2,2|4)$ remains an exact symmetry of $\mathcal{N} = 4$ SYM at the quantum level.

As mentioned the superconformal group $PSU(2,2|4)$ contains the conformal group $SU(2,2)$, reviewed in the last section, whose generators are given by: translations $P_\mu$, Lorentz transformations $M_{\mu\nu}$, dilatations $D$ and special conformal transformations $K_\mu$. The $\mathcal{N} = 4$ supersymmetry is then generated by adding four fermionic Poincaré supercharges $Q_\alpha^a$ and

---

[1]The material covered in this section follows closely the review [77].

$\bar{Q}_{\dot{\alpha}a}$ with $a = 1, \ldots, 4$ along with the $SO(6) \sim SU(4)$ R-symmetry generators $T^A$ with $A = 1, \ldots, 15$. As the Poincaré supercharges and special conformal transformations do not commute it is necessary to add the conformal supercharges $S_\alpha^a$ and $\bar{S}_{\dot{\alpha}a}$ which together close to form the $\mathcal{N} = 4$ superconformal algebra. We will now see how the operators of the theory organise into representations of the superconformal group.

## 3.1   Superconformal symmetry and local operators

As discussed in the last section, primary operators satisfy the condition of being annihilated by the generators of the special conformal transformations and define the *highest weight state* of a conformal multiplet from which we can generate all descendants by acting with derivatives (the generators of translations) which act as raising operators of the scaling dimensions.

We follow an analogous story here to organise operators into representations of the superconformal group. In addition to the generators of translations and special conformal transformations we have another set of raising and lowering operators given by the supercharges $Q$ and $S$ which raise and lower the scaling dimensions by units of $1/2$. This allows us to define a *superconformal primary* operator as satisfying the condition[1]

$$[S, \mathcal{O}(0)] = 0. \tag{3.1}$$

Note, this in fact implies the weaker notion of a conformal primary. Having identified the highest weight states as the superconformal primaries we continue as before, acting with the raising operators $Q$ and $P$ to build the entire superconformal multiplet. Note, the supercharges themselves anticommute to give the generator of translations

$$\{Q_\alpha^a, \bar{Q}_{\dot{\beta}b}\} = 2\sigma_{\alpha\dot{\beta}}^\mu P_\mu \delta_b^a, \tag{3.2}$$

and in fact the entire multiplet can already be generated just by the supercharges. In particular, there are only finitely many ways to combine the supercharges before arriving at a derivative, and therefore a superconformal multiplet contains finitely many conformal primaries.

Let us see how to construct such superconformal primaries explicitly. As we have just argued any operator arising from the action of the supercharges $Q$ on the fundamental fields cannot be a primary operator. It is useful then to understand how the supercharges act on the fundamental fields, this is given schematically by

$$[Q, \phi] \sim \lambda, \ [Q, F] \sim D\lambda, \ \{Q, \lambda\} \sim F + [\phi, \phi], \ \{Q, \bar{\lambda}\} \sim D\phi, \tag{3.3}$$

---

[1]Note, for a superconformal primary we must also have $[\bar{S}, O(0)] = 0$.

where $D$ is the covariant derivative, $F$ is the field strength tensor, and we have dropped the dependence on indices. With these expressions we conclude that a superconformal primary cannot contain any expression appearing on the r.h.s of (3.3). Therefore, the only way to construct a superconformal primary is through a combination of scalars $\phi^I$ in a symmetrised way. The simplest such example is given by the single trace operators

$$\text{str}(\phi^{I_1} \ldots \phi^{I_p})(x) \tag{3.4}$$

where the $I_n$ are $SO(6)$ fundamental indices; str denotes the symmeterised trace over the gauge group $SU(N)$ and as a consequence of $\text{tr}\{\phi^I\} = 0$ we have $p \geq 2$. Generally, these operators transform under reducible representations, i.e. the symmeterised product of $n$ fundamental represractions, and irreducible representations can be obtained by removing the traces, the simplest such example being the irreducible operators

$$\sum_I \text{tr}(\phi^I \phi^I) \;\leftrightarrow\; \text{Konishi multiplet},$$

$$\text{tr}(\phi^{\{I_1} \phi^{I_2\}}) \;\leftrightarrow\; \text{Supergravity multiplet}, \tag{3.5}$$

where the curly braces indicate the traceless symmetrisation of the $SO(6)$ indices. Through the AdS/CFT correspondence the Konishi operator corresponds to an excited string state and vanishes from the spectrum upon taking the supergravity limit (more on the supergravity limit in the next chapter). Therefore, we will be most interested in the second class of operator, which are more generally given by

$$\mathcal{O}_p^{I_1,\ldots,I_p}(x) = \text{tr}(\phi^{\{I_1} \ldots \phi^{I_p\}})(x). \tag{3.6}$$

The R-symmetry indices can be conveniently dealt with by introducing auxiliary $SO(6)$ vectors $y^I$ satisfying the null condition $y \cdot y = 0$, resulting in

$$\mathcal{O}_p(x, y) = y_{I_1} \ldots y_{I_p} \text{tr}(\phi^{I_1} \ldots \phi^{I_p})(x). \tag{3.7}$$

These operators transform in the symmetric traceless representation $[0, p, 0]$ of the $SO(6)$ R-symmetry. They make up the $1/2$-*BPS* operators, meaning they are annihilated by half of the supercharges and, as a consequence, have protected scaling dimensions $\Delta = p$. As we will see in the next section, in the limit of large $N$, the AdS/CFT correspondence maps these operators to the supergravity multiplet and its KK partners. Therefore, by studying the correlation functions of these $1/2$-BPS operators, which we will next introduce, we are dually probing scattering amplitudes of type IIB supergravity in AdS.

A variety of multi-trace operators may be constructed from products of the single-trace operators introduced above. The simplest such example being the double-trace operators

which take the schematic form

$$\mathcal{O}_p \Box^n \partial^{\{\mu_1,\ldots,\mu_l\}} \mathcal{O}_q|_{[a,b,a]}.$$

As we shall see in the next chapter these will be the operators appearing in the long sector of the OPE of two $1/2$-BPS operators.

## 3.2   Four point functions of $1/2$-BPS operators

We will be interested in correlation functions of these $1/2$-BPS operators. As mentioned in Chapter 2 the two and three-point functions are fixed, up to an overall constant, by conformal symmetry. Moreover, the operators $\mathcal{O}_p$ we consider here are protected by supersymmetry, meaning their two and three-point functions are controlled completely by their free field expressions. Therefore, the first non-trivial case is the four point correlator. Its most general form is constrained by superconformal symmetry [79, 80], which splits the function into a free theory contribution ($g = \lambda = 0$) plus an interacting term,

$$\langle \mathcal{O}_{p_1} \mathcal{O}_{p_2} \mathcal{O}_{p_3} \mathcal{O}_{p_4} \rangle = \langle \mathcal{O}_{p_1} \mathcal{O}_{p_2} \mathcal{O}_{p_3} \mathcal{O}_{p_4} \rangle_{\text{free}} + \langle \mathcal{O}_{p_1} \mathcal{O}_{p_2} \mathcal{O}_{p_3} \mathcal{O}_{p_4} \rangle_{\text{int}} . \tag{3.8}$$

The free theory contribution can be computed via Wick contractions of the elementary fields and contains disconnected and connected contributions,

$$\langle \mathcal{O}_{p_1} \mathcal{O}_{p_2} \mathcal{O}_{p_3} \mathcal{O}_{p_4} \rangle_{\text{free}} = \langle \mathcal{O}_{p_1} \mathcal{O}_{p_2} \mathcal{O}_{p_3} \mathcal{O}_{p_4} \rangle_{\text{free,disc}} + \langle \mathcal{O}_{p_1} \mathcal{O}_{p_2} \mathcal{O}_{p_3} \mathcal{O}_{p_4} \rangle_{\text{free,conn}} . \tag{3.9}$$

The interacting term is further constrained [79] to take the form

$$\langle \mathcal{O}_{p_1} \mathcal{O}_{p_2} \mathcal{O}_{p_3} \mathcal{O}_{p_4} \rangle_{\text{int}} = p_1 p_2 p_3 p_4 N^{\Sigma - 2} \tilde{\mathcal{I}} \mathcal{P}_{\vec{p}} \mathcal{H}_{\vec{p}}(U, V, \tilde{U}, \tilde{V}), \tag{3.10}$$

where we have introduced the short hand notation $\vec{p} = (p_1, p_2, p_3, p_4)$ to indicate the dependence on charges and $\Sigma = \frac{p_1 + p_2 + p_3 + p_4}{2}$, as well as the conformal and R-symmetry cross ratios:

$$U = x\bar{x} = \frac{x_{12}^2 x_{34}^2}{x_{13}^2 x_{24}^2}, \qquad\qquad V = (1-x)(1-\bar{x}) = \frac{x_{14}^2 x_{23}^2}{x_{13}^2 x_{24}^2},$$

$$\tilde{U} = y\bar{y} = \frac{y_{12}^2 y_{34}^2}{y_{13}^2 y_{24}^2}, \qquad\qquad \tilde{V} = (1-y)(1-\bar{y}) = \frac{y_{14}^2 y_{23}^2}{y_{13}^2 y_{24}^2}, \tag{3.11}$$

using the notation $x_{ij} = (x_i - x_j)$, and similarly $y_{12}^2 = y_1 \cdot y_2$. The prefactor

$$\mathcal{P}_{\vec{p}} = \frac{\prod_{i<j} g_{ij}^{p(ij)}}{(g_{13} g_{24})^{\Sigma}}; \qquad g_{ij} = \frac{y_{ij}^2}{x_{ij}^2},$$

carries the correct conformal and R-symmetry weights, with $g_{ij}$ denoting the propagator; and the superconformal Ward identities fix $\tilde{\mathcal{I}}$ to take the form

$$\tilde{\mathcal{I}} = (x - y)(x - \bar{y})(\bar{x} - y)(\bar{x} - \bar{y}). \tag{3.12}$$

The only piece of the correlator depending on the gauge coupling $g_{YM}$ (or $\lambda$) is the function $\mathcal{H}_{\vec{p}}$, which we will naturally refer to as the interacting part. It contains all non-trivial dynamical information of the theory, and therefore only receives contributions from unprotected operators. It is a polynomial in the R-symmetry cross-ratios $(\tilde{U}, \tilde{V})$, with a more complicated analytic structure in the conformal cross-ratios $(U, V)$.

## 3.3 The superconformal block decomposition

We now wish to use the OPE to relate the expressions for the correlators to the CFT data. The $\mathcal{N} = 4$ SYM OPE for two 1/2-BPS operators can be summarised as

$$\overbrace{\mathcal{O}_{p_1}(x_1)\mathcal{O}_{p_2}(x_2)} \sim \sum_{\mathcal{O}_{\vec{\tau}}} C_{p_1 p_2 \mathcal{O}} \mathcal{L}_{\mathcal{O}}(x_{12}, \partial_{x_2}) \mathcal{O}_{\vec{\tau}}(x_2), \tag{3.13}$$

where we have introduced the *twist* of the operator $\tau = \Delta - \ell$, and the short hand notation for the quantum numbers $\vec{\tau} = (\tau, \ell, a, b)$. The sum above runs over all primary operators $\mathcal{O}_{\vec{\tau}}$ of twist $\tau$, spin $\ell$ and $su(4)$ representation $[a, b, a]$ appearing in the tensor product $[0, p_1, 0] \otimes [0, p_2, 0]$, and as before the operator $\mathcal{L}_{\mathcal{O}}$ generates the contribution from all descendants. Upon inserting the double OPE expansion into the four-point correlator as $\langle \overbrace{\mathcal{O}_{p_1}(x_1)\mathcal{O}_{p_2}(x_2)} \overbrace{\mathcal{O}_{p_3}(x_3)\mathcal{O}_{p_4}(x_4)} \rangle$ we obtain the SCPW expansion.

The operators entering the SCPW expansion are either: short multiplets whose dimensions and OPE coefficients are protected and are independent of the coupling $g_{YM}$; or long multiplets whose dimensions and OPE coefficients depend on the coupling and acquire quantum corrections. The protected multiplets come entirely from the free theory contributions, while unprotected (or long) multiplets come from both free theory and interacting contributions

$$\langle \mathcal{O}_{p_1}\mathcal{O}_{p_2}\mathcal{O}_{p_3}\mathcal{O}_{p_4} \rangle = \langle \mathcal{O}_{p_1}\mathcal{O}_{p_2}\mathcal{O}_{p_3}\mathcal{O}_{p_4} \rangle_{\text{free}}^{\text{prot.}} + \langle \mathcal{O}_{p_1}\mathcal{O}_{p_2}\mathcal{O}_{p_3}\mathcal{O}_{p_4} \rangle_{\text{free}}^{\text{long}} + \langle \mathcal{O}_{p_1}\mathcal{O}_{p_2}\mathcal{O}_{p_3}\mathcal{O}_{p_4} \rangle_{\text{int}}. \tag{3.14}$$

Our focus will be on the superconformal block decomposition of the long sector

$$\langle \mathcal{O}_{p_1}\mathcal{O}_{p_2}\mathcal{O}_{p_3}\mathcal{O}_{p_4} \rangle^{\text{long}} = \langle \mathcal{O}_{p_1}\mathcal{O}_{p_2}\mathcal{O}_{p_3}\mathcal{O}_{p_4} \rangle_{\text{free}}^{\text{long}} + \langle \mathcal{O}_{p_1}\mathcal{O}_{p_2}\mathcal{O}_{p_3}\mathcal{O}_{p_4} \rangle_{\text{int}}. \tag{3.15}$$

We denote the quantum numbers of the exchanged multiplet by $\vec{\tau} = (\tau, l, a, b)$ for a superconformal primary of twist $\tau = \Delta - l$, spin $l$ and $su(4)$ representation with Dynkin labels

$[aba]$. The expansion of the long part of the correlator into super blocks is then given by

$$\langle \mathcal{O}_{p_1} \mathcal{O}_{p_2} \mathcal{O}_{p_3} \mathcal{O}_{p_4} \rangle^{\text{long}} = \sum_{\vec{\tau}} c_{\vec{\tau}}^{\vec{p}} \, \mathbb{L}_{\vec{\tau}}^{\vec{p}} \,, \tag{3.16}$$

where $\mathbb{L}$ is the superblock for long multiplets (see e.g. [81]),

$$\mathbb{L}_{\vec{\tau}}^{\vec{p}} = \tilde{\mathcal{I}} \mathcal{P}_{\vec{p}} \left( \frac{V}{\bar{V}} \right)^{p_{(23)}} \mathcal{B}_{\tau,l}^{\vec{p}}(x, \bar{x}) \Upsilon_{[aba]}^{\vec{p}}(y, \bar{y}) \,. \tag{3.17}$$

The conformal and $su(4)$ factors of $\mathbb{L}$ are given by

$$\mathcal{B}_{\tau,l}^{\vec{p}}(x, \bar{x}) = \frac{F_{l+\tau/2+2}^{(\alpha,\beta)}(x) F_{\tau/2+1}^{(\alpha,\beta)}(\bar{x}) - F_{l+\tau/2+2}^{(\alpha,\beta)}(\bar{x}) F_{\tau/2+1}^{(\alpha,\beta)}(x)}{x - \bar{x}} \,,$$

$$\Upsilon_{[aba]}^{\vec{p}}(y, \bar{y}) = \frac{F_{-b/2}^{(-\alpha,-\beta)}(y) F_{-b/2-a-1}^{(-\alpha,-\beta)}(\bar{y}) - F_{-b/2}^{(-\alpha,-\beta)}(\bar{y}) F_{-b/2-a-1}^{(-\alpha,-\beta)}(y)}{y - \bar{y}} \,, \tag{3.18}$$

where

$$F_{\rho}^{(\alpha,\beta)}(x) = x^{\rho-1} {}_2F_1(\rho + \alpha, \rho + \beta, 2\rho; x) \,. \tag{3.19}$$

For compactness of notation we have introduced $\alpha = \frac{p_2 - p_1}{2}$ and $\beta = \frac{p_3 - p_4}{2}$. A more general treatment, including the short multiplets, is considerably more subtle and has been detailed in [81–84]. The block coefficients $c_{\vec{\tau}}^{\vec{p}}$ are given in terms of product of OPE coefficients

$$c_{\vec{\tau}}^{\vec{p}} = \sum_{\mathcal{O}} C_{p_1 p_2 \mathcal{O}} C_{p_3 p_4 \mathcal{O}}.$$

where again the sum runs over all superconformal primary operators $\mathcal{O}$ of twist $\tau$, spin $\ell$ and $su(4)$ representations $[a, b, a] \in ([0, p_1, 0] \times [0, p_2, 0]) \cap ([0, p_3, 0] \times [0, p_4, 0])$.

Generally, there exist many operators with the same quantum numbers $\vec{\tau}$ leading to a mixing problem for the block coefficients $c_{\vec{\tau}}^{\vec{p}}$, which are not in one-to-one correspondence with the OPE coefficients. To understand the OPE predictions we must first get a handle on the spectrum of exchanged operators in the OPE, for this we now turn to understanding the dual gravity description provided by the AdS/CFT correspondence. Having identified the spectrum of operators we can then return to address the mixing problem.

# Chapter 4

# Holographic correlators and AdS/CFT

Having introduced the four-point function of 1/2-BPS operators in $\mathcal{N} = 4$ SYM we now wish to show how through the AdS/CFT this is mapped to calculating string scattering amplitudes in $\mathrm{AdS}_5 \times \mathrm{S}^5$. In this section we first review the original motivation for the AdS/CFT correspondence. We will see how the coupling constants of both sides of the correspondence are related, as well as how CFT operators and their correlators map to supergravity states and their scattering amplitudes. The four-point correlator will be studied in the supergravity limit and the traditional calculation using Witten diagrams will be reviewed. The material covered in this section follows [77, 85, 86].

## 4.1   AdS/CFT from D3-branes

We are interested in the prototype example of the AdS/CFT correspondence, the equivalence between $\mathcal{N} = 4$ SYM theory in 4d with $\mathrm{SU}(N)$ gauge group, and IIB string theory on $\mathrm{AdS}_5 \times \mathrm{S}^5$. To motivate this equivalence we follow the original argument of Maldacena and consider a stack of $N$ coincident $D3$-branes in the low energy, $\alpha' \to 0$, limit [41].

The stack of D3-branes can be studied from two perspectives. The first is to consider them within IIB string theory in flat-space. In this setup we have two types of excitations: the open strings with end points on the D-branes, and the closed strings describing excitations of empty space. Upon taking the low energy limit only massless string states survive. The massless closed string excitations describe $\mathcal{N} = 4$ SYM theory with SU(N) gauge group living on the 4d world-volume of the branes. The massless closed string excitations then describe free IIB supergravity in the bulk. Therefore, in the low energy limit, we have two decoupled systems, the 4d CFT living on the branes, and free gravity propagating in the

bulk, schematially

$$\mathcal{N} = 4 \text{ SYM} \ \oplus \ \text{IIB supergravity on } \mathbb{R}^{10}. \tag{4.1}$$

The dual (gravity) description is to consider the D-branes, which themselves carry charge/mass and therefore deform the metric, as a solution to type IIB supergravity itself. The D3-brane solution takes the form

$$ds^2 = H^{-1/2}(-dt^2 + dx_1^2 + dx_2^2 + dx_3^2) + H^{1/2}(dr^2 + r^2 d\Omega_5^2), \tag{4.2}$$

$$H = 1 + \frac{R^4}{r^4}, \quad R^4 = 4\pi g_s \alpha'^2 N.$$

We would like to see the same phenomenon as before, that upon taking the low-energy limit, we are left with two decoupled theories. First, note that the energy $E$ as measured by an observer at infinity and the energy $E_r$ measured by an observer at position $r$ are related by a redshift factor given by

$$E = H^{-1/4} E_r. \tag{4.3}$$

This implies that the same process brought closer and closer to $r = 0$ would appear, to an observer at infinity, to have lower and lower energy. Therefore, upon taking the low energy limit we will have two types of excitations: the massless excitations propogating in the bulk region, and any kind of excitation that is sufficiently close to $r = 0$. Let us inspect the metric (4.2) in these two regions. When $r \gg R$ the metric reduces to 10d Minkowski space. However, in the near-horizon limit $r \ll R$ the metric reduces to

$$ds^2 = \frac{r^2}{R^2}(-dt^2 + dx_1^2 + dx_2^2 + dx_3^2) + \frac{R^2}{r^2} dr^2 + R^2 d\Omega_5^2, \tag{4.4}$$

i.e. the geometry of $\text{AdS}_5 \times \text{S}^5$ with common radius $R$. We see again that, in the low energy limit, we have two decoupled systems: supergravity in flat space, and the full IIB string theory living on $\text{AdS}_5 \times \text{S}^5$ i.e.

$$\text{IIB superstring on } \text{AdS}_5 \times \text{S}^5 \oplus \text{IIB supergravity on } \mathbb{R}^{10}. \tag{4.5}$$

Note, in both viewpoints one of the decoupled systems is given by supergravity in flat space. This led Maldacena [41] to the conjecture that $\mathcal{N} = 4$ SYM in 4d with gauge group SU(N) is dual to IIB superstring theory on $\text{AdS}_5 \times \text{S}^5$! The relation between the parameters of both theories, where $g_s$ and $g_{YM}$ are the string and gauge theory couplings respectively, are given by

$$g_s = \frac{g_{YM}^2}{4\pi}, \qquad R^4 = 4\pi g_s \alpha'^2 N. \tag{4.6}$$

## 4.2 The supergravity limit

The conjecture as formulated above is valid for all values of $N$ and string coupling $g_s \sim g_{YM}$. However, since string theory quantization on curved manifolds is currently out of reach, it is interesting to study the correspondence in a more tractable limit in which the bulk theory corresponds to IIB supergravity.

To arrive at the supergravity approximation we first take the 't Hooft limit. In this limit we fix the 't Hooft coupling defined by $\lambda = g_{YM}^2 N$ and subsequently take $N \to \infty$. On the field theory side this corresponds to a topological expansion of Feynman diagrams with the leading order given by planar diagrams. On the gravity side we notice that $g_s \propto \lambda/N$, and since $\lambda$ is being held fixed, taking $N \to \infty$ will correspond to weak coupling string perturbation theory. Having taken this limit the only remaining parameter is the 't Hooft coupling $\lambda = R^4/\alpha'^2$ itself. To arrive at the supergravity limit strings must be well approximated by point particles, this approximation is good when we take $\lambda \to \infty$. As we see an expansion around strong coupling on the CFT side corresponds to an expansion around weakly coupled supergravity on the gravity side. It is this strong/weak duality which makes the AdS/CFT correspondence so powerful.

Throughout the remainder of this section we will work in an expansion around the supergravity limit at large N and large $\lambda$. In this way corrections to supergravity are organised in a double expansion: with $1/N$ corrections corresponding to a loop expansion in the bulk, and the $1/\lambda$ expansion corresponding to adding a tower of string corrections.

## 4.3 State operator map

We now wish to map the four-point function of 1/2-BPS operators on the CFT side to its gravity dual, this problem was originally addressed in [87, 88]. First, we must identify which are the CFT operators dual to single particle states on the gravity side. In the strict large N limit the single-trace 1/2-BPS operators are in fact dual to the supergravity spectrum: with $\mathcal{O}_2$ dual to the graviton supermultiplet; and all higher operators $\mathcal{O}_{p \geq 3}$ dual to Kaluza-Klein modes arising from the compactifcation of $S^5$. However, as we include $1/N$ corrections this is no longer true, and the *single particle operators*, dual to single particle supergravity states, acquire contributions from multi-trace operators[1] which come supressed in $1/N$:

$$\mathcal{O}_p(x, y) = y^{I_1} \dots y^{I_p} \text{tr}\{\phi_{I_1} \dots \phi_{I_p}\}(x) + (\text{multi-trace}). \tag{4.7}$$

As first proposed in [56] the multi-trace terms in the definition of the single-particle supergravity operators are fixed by the condition that *single particle operators are orthogonal to all multi-trace operators* i.e. $\langle \mathcal{O}_p [\mathcal{O}_{q_1} \dots \mathcal{O}_{q_n}] \rangle = 0$. With this definition the multi-trace

---

[1]This was already noted in [89, 90] and more recently discussed in [52, 56, 63, 66, 91, 92].

terms can be computed entirely by considering only the free theory. Building on the previous work of [93], the multi-trace contributions for a general single-particle state was given in [92]. As an example consider $\mathcal{O}_4$, the first case for which the multi-trace terms are non-vanishing [56], which is given by

$$\mathcal{O}_4 = \text{Tr}(\phi^4) - \frac{2N^2 - 3}{N(N^2 + 1)} \mathcal{O}_2 \mathcal{O}_2. \tag{4.8}$$

It is more correctly these operators that we consider and it is their correlation functions which correspond to supergravity scattering amplitudes on $\text{AdS}_5 \times \text{S}^5$.

## 4.4  Holographic correlators in the supergravity expansion

We will be interested in the expansion of the correlator around the supergravity limit at large $N$ and large $\lambda$. In particular we will be interested in the block decomposition of the part of the correlator containing long multiplets which receives contributions from both the free and interacting terms

$$\langle \mathcal{O}_{p_1} \mathcal{O}_{p_2} \mathcal{O}_{p_3} \mathcal{O}_{p_4} \rangle_{\text{long}} = \langle \mathcal{O}_{p_1} \mathcal{O}_{p_2} \mathcal{O}_{p_3} \mathcal{O}_{p_4} \rangle_{\text{free long}} + \langle \mathcal{O}_{p_1} \mathcal{O}_{p_2} \mathcal{O}_{p_3} \mathcal{O}_{p_4} \rangle_{\text{int}}. \tag{4.9}$$

In the supergravity limit the free theory contribution is given by the expansion

$$\langle \mathcal{O}_{p_1} \mathcal{O}_{p_2} \mathcal{O}_{p_3} \mathcal{O}_{p_4} \rangle_{\text{free long}} = N^\Sigma \left[ \langle \mathcal{O}_{p_1} \mathcal{O}_{p_2} \mathcal{O}_{p_3} \mathcal{O}_{p_4} \rangle_{\text{free long}}^{(0)} + \frac{1}{N^2} \langle \mathcal{O}_{p_1} \mathcal{O}_{p_2} \mathcal{O}_{p_3} \mathcal{O}_{p_4} \rangle_{\text{free long}}^{(1)} + \dots \right] \tag{4.10}$$

Note, the free theory only contributes to leading order in $1/\lambda$ as it does not depend on the gauge coupling. The leading large $N$ contribution is of order[1] $N^\Sigma$ with $\Sigma = \frac{p_1 + p_2 + p_3 + p_4}{2}$ and comes from the disconnected free theory term, it is given by the products of two-point functions,

$$\langle \mathcal{O}_{p_1} \mathcal{O}_{p_2} \mathcal{O}_{p_3} \mathcal{O}_{p_4} \rangle_{\text{disc}} = \langle \mathcal{O}_{p_1} \mathcal{O}_{p_2} \rangle \langle \mathcal{O}_{p_3} \mathcal{O}_{p_4} \rangle + \langle \mathcal{O}_{p_1} \mathcal{O}_{p_3} \rangle \langle \mathcal{O}_{p_2} \mathcal{O}_{p_4} \rangle + \langle \mathcal{O}_{p_1} \mathcal{O}_{p_4} \rangle \langle \mathcal{O}_{p_2} \mathcal{O}_{p_3} \rangle. \tag{4.11}$$

Where the operators $\mathcal{O}_p$ are orthogonal and normalised as follows[2],

$$\langle \mathcal{O}_{p_1} \mathcal{O}_{p_2} \rangle = \delta_{p_1 p_2} (g_{12})^{p_1} R_{p_1}, \qquad R_{p_1} = p_1 N^{p_1} + O(N^{p_1 - 2}), \qquad g_{ij} = \frac{y_{ij}^2}{x_{ij}^2}. \tag{4.12}$$

The interacting term contributes solely to the long sector taking the form

$$\langle \mathcal{O}_{p_1} \mathcal{O}_{p_2} \mathcal{O}_{p_3} \mathcal{O}_{p_4} \rangle_{\text{int}} = p_1 p_2 p_3 p_4 N^{\Sigma - 2} \tilde{\mathcal{I}} \mathcal{P}_{\vec{p}} \mathcal{H}_{\vec{p}}(U, V, \tilde{U}, \tilde{V}; \lambda). \tag{4.13}$$

---

[1]Note that $\sum_i p_i$ is always even and so $\Sigma$ is integer.

[2]The full normalisation is $R_p = p^2(p-1) \left[ \frac{1}{(N-p+1)_{p-1}} - \frac{1}{(N+1)_{p-1}} \right]^{-1} = p_1 N^{p_1} + O(N^{p_1 - 2})$ [92].

As the only piece of the correlator dependent on the gauge coupling $\mathcal{H}_{\vec{p}}$ admits a double expansion. First, we expand around large $N$ as

$$\mathcal{H}_{\vec{p}} = \mathcal{H}_{\vec{p}}^{(1)} + \frac{1}{N^2}\mathcal{H}_{\vec{p}}^{(2)} + \dots, \tag{4.14}$$

corresponding to a loop expansion in the bulk. While the tree level and one-loop coefficients above are themselves expanded for large $\lambda$ as follows

$$\mathcal{H}_{\vec{p}}^{(1)} = \mathcal{H}_{\vec{p}}^{(1,0)} + \lambda^{-\frac{3}{2}}\mathcal{H}_{\vec{p}}^{(1,3)} + \lambda^{-\frac{5}{2}}\mathcal{H}_{\vec{p}}^{(1,5)} + \lambda^{-3}\mathcal{H}_{\vec{p}}^{(1,6)} + \dots,$$
$$\mathcal{H}_{\vec{p}}^{(2)} = \lambda^{\frac{1}{2}}\mathcal{H}_{\vec{p}}^{(2,-1)} + \mathcal{H}_{\vec{p}}^{(2,0)} + \lambda^{-\frac{1}{2}}\mathcal{H}_{\vec{p}}^{(2,1)} + \lambda^{-1}\mathcal{H}_{\vec{p}}^{(2,2)} + \lambda^{-\frac{3}{2}}\mathcal{H}_{\vec{p}}^{(2,3)} + \dots, \tag{4.15}$$

corresponding to adding stringy corrections to the leading order supergravity contribution. These string corrections arise directly from higher derivative terms in the IIB supergravity effective action.

At order $N^{\Sigma-2}$, we have the contribution from connected free theory and the contribution from the interacting part. The connected free theory along with the term $\mathcal{H}_{\vec{p}}^{(1,0)}$ correspond together to the tree level supergravity contribution. The tree level supergravity term was shown by [51, 52] to have a particularly compact expression in Mellin space (to be introduced in the next chapter). The tree level supergravity contribution is then followed by an infinite tower of stringy corrections $\mathcal{H}_{\vec{p}}^{(1,n)}$, which arise from contact terms in the IIB string theory effective action. Their structure is related to the Virasoro-Shapiro amplitude in 10d flat-space via the flat space limit. The resummation of these terms has received much attention [58–61, 71, 94] and are currently known (up to a handful of ambiguities not fixed by the conformal bootstrap) to order $\lambda^{-9/2}$. Again, their expressions are most conveniently expressed in Mellin space.

The terms of order $N^{\Sigma-4}$ in the double expansion (4.15) correspond to one-loop contributions in AdS$_5$. The leading term $\mathcal{H}_p^{(2,-1)}$ corresponds to the presence of a quadratic divergence at one loop in ten-dimensional supergravity, and is regulated by a $\mathcal{R}^4$ counterterm at one loop in string theory. The term $\mathcal{H}_p^{(2,0)}$ is the one-loop supergravity term, addressed in [63–66, 95]. The term $\mathcal{H}_p^{(2,1)}$ corresponds to the genus-one contribution to the modular completion of the $\mathcal{H}_p^{(1,5)}$ term. The corresponding modular function is an Eisenstein series which receives perturbative contributions only at genus zero and genus two [96] and we therefore expect $\mathcal{H}_p^{(2,1)}$ to vanish, consistent with the localisation analysis of [97, 98]. The term $\mathcal{H}_p^{(2,2)}$ gives rise, in the flat space limit, to the analytic part of the one-loop string amplitude studied in [99]. It is non-vanishing and corresponds to the genus-one contribution to the modular completion of the $\mathcal{H}_p^{(1,6)}$ term. Finally, the term $\mathcal{H}_p^{(2,3)}$ is the genuine one-loop string correction induced by the presence of the $\mathcal{H}_p^{(1,3)}$ term at tree level. This is the term which we will construct in the first part of this thesis. The position space structure of one-loop IIB supergravity amplitudes has been addressed in [64, 65, 70], culminating in a general

algorithm for constructing correlators with arbitrary external charges [66]. Considering further string corrections at one-loop has revealed a new type of singularity in their analytic structure compared to the supergravity case [67].

More recently the two-loop supergravity contribution $\mathcal{H}_{\vec{p}}^{(3,0)}$, not shown in the expansion above, has be considered for four graviton multiplets in [68, 69].

## 4.5   Witten diagram computation: tree level supergravity

As mentioned we will be working in an expansion around large $N$ and large $\lambda$. In this limit the bulk theory becomes weakly coupled type IIB supergravity with a small five-dimensional Newton constant. Therefore, the task of computing correlation functions in the CFT is mapped to computing scattering amplitudes in weakly coupled IIB supergravtiy on AdS$_5$. The standard method for computing the AdS amplitudes is through a perturbative Witten diagram expansion in the small Newton constant. Therefore, to compute the supergravity contribution to the four-point function of 1/2-BPS operators we sum over tree level exchange and contact Witten depicted below. The rules for evaluating Witten diagram are analogous
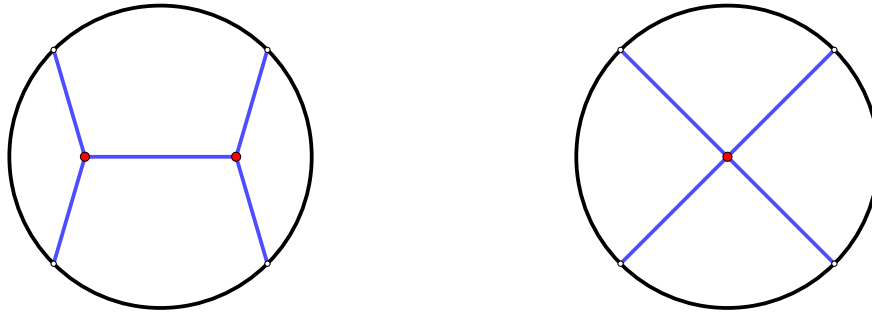


**Figure 4.1:** Examples of exchange (left) and contact (right) Witten diagrams entering the scattering amplitude at tree level.

to their flat-space Feynman counterparts: to each line connecting to bulk points $z$ and $w$ we assign a bulk-to-bulk propogator $G_{BB}(z, w)$, and similarly to each line connecting the bulk point $x$ to the boundary point $\vec{x}$ we assign a bulk-to-boundary propogator $G_{B\partial}(z, \vec{x})$, and we integrate over all bulk interaction vertices. The propogators $G_{BB}(z, w)$ and $G_{B\partial}(z, \vec{x})$ are AdS Green's functions with the appropriate boundary conditions.

The simplest such example of a contact Witten diagram is the four-point contact diagram of external scalars with no derivatives in the quartic vertex given by the so called D-functions

$$D_{\Delta_1\Delta_2\Delta_3\Delta_4}(x_1, x_2, x_3, x_4) = \int_0^\infty \frac{dz_0}{z_0^{d+1}} \int d^d x \prod_{i=1}^4 G_{B\partial}(z, \vec{x}_i), \tag{4.16}$$

where the scalar bulk-to-boundary propogotar is given by

$$G_{B\partial}(z, \vec{x}_i) = \left( \frac{z_0}{z_0^2 + (\vec{z} - \vec{x}_i)^2} \right)^{\Delta_i}, \tag{4.17}$$

and $\Delta_i$ is the scaling dimension of the $i^{\text{th}}$ boundary CFT operator. The more complicated exchange diagrams take the form

$$\mathcal{A}_{\text{ex}}^{(4)} = \int_{\text{AdS}} dz dw G_{B\partial}(z, \vec{x}_1) G_{B\partial}(z, \vec{x}_2) G_{BB}(z, w) G_{B\partial}(w, \vec{x}_3) G_{B\partial}(w, \vec{x}_4). \tag{4.18}$$

Following this approach requires detailed knowledge of the cubic and quartic vertices appearing in the AdS effective action, obtained by Kaluza-Klein reduction of IIB supergravity on $S^5$. The effective action is extremely complicated [42–44], with the scalar quartic vertices [43] filling 15 pages. Furthermore, the number of exchange Witten diagrams grows rapidly with the KK level, making it practically impossible to go beyond the simplest cases of the lowest KK modes [45–50]. The extension to arbitrary charges, made in [51, 52], was achieved by translating the problem into Mellin space which we shall now introduce.

# Chapter 5

# Mellin space formalism

As first shown by Mack [53], and improved later by Pendones [54] in the context of holographic theories in *AdS*, the CFT correlators are most conveniently represented in Mellin space. In Mellin space the amplitude shares many similarities with a scattering amplitude, and in fact can be understood as a curved completion of a flat space scattering amplitude, with the latter recovered in the limit of large Mellin variables. The Mellin amplitude also has the benefit of a simpler analytic structure than its position space counterpart whose poles and residues are controlled by the OPE.

For holographic correlators in $AdS_5 \times S^5$, it is possible to improve further the Mellin space representation, by considering a double Mellin transform which treats equally the conformal AdS and internal S space[1]. This double Mellin transform reads,

$$\langle \mathcal{O}_{p_1} \mathcal{O}_{p_2} \mathcal{O}_{p_3} \mathcal{O}_{p_4} \rangle_{\mathrm{int}} = p_1 p_2 p_3 p_4 N^{\Sigma-2} \hat{\mathcal{I}} \int d\hat{s}_{ij} \sum_{\check{s}_{ij}} \prod_{i<j} \left[ \frac{x_{ij}^{2\hat{s}_{ij}} y_{ij}^{2\check{s}_{ij}} \Gamma[-\hat{s}_{ij}]}{\Gamma[\check{s}_{ij}+1]} \right] \mathcal{M}_{\vec{p}}(\hat{s}_{ij}, \check{s}_{ij}), \quad (5.1)$$

where $\hat{s}_{ij}$ are AdS Mellin variables and $\check{s}_{ij}$ are sphere Mellin variables subject to the constraints,

$$\sum_i \hat{s}_{ij} = -p_j - 2, \qquad \sum_i \check{s}_{ij} = p_j - 2. \quad (5.2)$$

The factor $\hat{\mathcal{I}}$, which removes two units of weight w.r.t. to the charges $p_i$, is a consequence of superconformal symmetry [79], and takes the form

$$\hat{\mathcal{I}} = (x_{13}^2 x_{24}^2 y_{13}^2 y_{24}^2)^2 \tilde{\mathcal{I}}, \qquad \tilde{\mathcal{I}} = (x-y)(x-\bar{y})(\bar{x}-y)(\bar{x}-\bar{y}), \quad (5.3)$$

where $x, \bar{x}, y, \bar{y}$ parametrise the invariant cross-ratios as given in (3.11), this factor is invariant under permutations of the external operators.

---

[1]This idea was first advocated in [55] and further refined in [60] and [61].

The constraints on the Mellin variables can be solved as follows,

$$\hat{s}_{12} + \tfrac{p_1+p_2}{2} = \hat{s}_{34} + \tfrac{p_3+p_4}{2} = \hat{s}, \qquad\qquad \check{s}_{12} - \tfrac{p_1+p_2}{2} = \check{s}_{34} - \tfrac{p_3+p_4}{2} = \check{s},$$

$$\hat{s}_{14} + \tfrac{p_1+p_4}{2} = \hat{s}_{23} + \tfrac{p_2+p_3}{2} = \hat{t}, \qquad\qquad \check{s}_{14} - \tfrac{p_1+p_4}{2} = \check{s}_{23} - \tfrac{p_2+p_3}{2} = \check{t},$$

$$\hat{s}_{13} + \tfrac{p_1+p_3}{2} = \hat{s}_{24} + \tfrac{p_2+p_4}{2} = \hat{u}, \qquad\qquad \check{s}_{13} - \tfrac{p_1+p_3}{2} = \check{s}_{24} - \tfrac{p_2+p_4}{2} = \check{u}, \qquad (5.4)$$

with

$$\hat{s} + \hat{t} + \hat{u} = \Sigma - 2\,, \qquad \check{s} + \check{t} + \check{u} = -\Sigma - 2 \qquad ; \qquad \Sigma = \tfrac{p_1+p_2+p_3+p_4}{2}. \qquad (5.5)$$

We shall say that the variables $\hat{s}, \check{s}$ define the **s**-channel and similarly for the other channels. The variables $\hat{s}, \check{s}$ and $\hat{t}, \check{t}$ will be taken to be independent. The integral and the sum in (5.1) only run over the independent variables $\hat{s}, \check{s}$ and $\hat{t}, \check{t}$, and the sum will actually be finite, as we will see. We can further accompany each channel in position and internal space with the following combinations of charges,

$$c_s = \tfrac{p_1+p_2-p_3-p_4}{2} \qquad ; \qquad c_t = \tfrac{p_1+p_4-p_2-p_3}{2} \qquad ; \qquad c_u = \tfrac{p_2+p_4-p_1-p_3}{2} \qquad (5.6)$$

The parametrisation of $\vec{p}$ in terms of $\{\Sigma, c_s, c_t, c_u\}$ is invertible, with $\Sigma$ being an invariant under permutation, and the various triplets $\{\hat{s}, \check{s}, c_s\}$, $\{\hat{t}, \check{t}, c_t\}$, $\{\hat{u}, \check{u}, c_u\}$ transforming into one another under crossing.

It is convenient to rewrite the correlator (5.1) by making manifest the dependence on the cross-ratios, namely

$$\langle \mathcal{O}_{p_1}\mathcal{O}_{p_2}\mathcal{O}_{p_3}\mathcal{O}_{p_4}\rangle_{\mathrm{int}} = p_1 p_2 p_3 p_4 N^{\Sigma-2} \tilde{\mathcal{I}} \frac{\prod_{i<j} g_{ij}^{\frac{p_i+p_j}{2}}}{(g_{13}g_{24})^{\Sigma}} \mathcal{H}_{\vec{p}}(U, V, \tilde{U}, \tilde{V}), \qquad (5.7)$$

where

$$\mathcal{H}_{\vec{p}}(U, V, \tilde{U}, \tilde{V}) = \int d\hat{s}d\hat{t} \sum_{\check{s},\check{t}} U^{\hat{s}} V^{\hat{t}} \tilde{U}^{\check{s}} \tilde{V}^{\check{t}} \, \mathbf{\Gamma}\, \mathcal{M}_{\vec{p}}. \qquad (5.8)$$

By definition, $\mathbf{\Gamma} = \Gamma_{\mathbf{s}}\Gamma_{\mathbf{t}}\Gamma_{\mathbf{u}}$ with

$$\Gamma_{\mathbf{s}} = \frac{\Gamma_{\hat{s}}}{\Gamma_{\check{s}}} \qquad ; \qquad \begin{aligned} \Gamma_{\hat{s}} &= \Gamma[\tfrac{p_1+p_2}{2} - \hat{s}]\Gamma[\tfrac{p_3+p_4}{2} - \hat{s}] = \Gamma[\tfrac{\Sigma}{2} \pm \tfrac{c_s}{2} - \hat{s}] \\ \Gamma_{\check{s}} &= \Gamma[1 + \tfrac{p_1+p_2}{2} + \check{s}]\Gamma[1 + \tfrac{p_3+p_4}{2} + \check{s}] = \Gamma[1 + \tfrac{\Sigma}{2} \pm \tfrac{c_s}{2} + \check{s}]. \end{aligned} \qquad (5.9)$$

Similarly for $\Gamma_{\mathbf{t}}$ and $\Gamma_{\mathbf{u}}$. The $\pm$ abbreviation stands for taking the product of both $\Gamma$ with $+$ and $-$ signs. Note, the sum over $\check{s}$ and $\check{t}$ is automatically truncated by the $\Gamma$ functions in the denominator of $\mathbf{\Gamma}$, thus it is finite. See also section 5.1.1.

Under crossing transformation, the factor $\mathbf{\Gamma}$ is invariant while for the Mellin amplitude we

find the following table.

$$
\begin{aligned}
\mathcal{M}_{p_1 p_2 p_3 p_4}(\hat{s}, \hat{t}, \check{s}, \check{t}) &= \mathcal{M}_{p_2, p_1, p_3, p_4}(\hat{s}, \hat{u}, \check{s}, \check{u}) &= \mathcal{M}_{c_s, +c_u, +c_t}(\hat{s}, \hat{u}, \check{s}, \check{u}) \\
&= \mathcal{M}_{p_1, p_2, p_4, p_3}(\hat{s}, \hat{u}, \check{s}, \check{u}) &= \mathcal{M}_{c_s, -c_u, -c_t}(\hat{s}, \hat{u}, \check{s}, \check{u})
\end{aligned}
$$

$$
\begin{aligned}
\mathcal{M}_{p_1 p_2 p_3 p_4}(\hat{s}, \hat{t}, \check{s}, \check{t}) &= \mathcal{M}_{p_4, p_2, p_3, p_1}(\hat{u}, \hat{t}, \check{u}, \check{t}) &= \mathcal{M}_{c_u, +c_t, +c_s}(\check{u}, \check{t}, \check{u}, \check{t}) \\
&= \mathcal{M}_{p_1, p_3, p_2, p_4}(\hat{u}, \hat{t}, \check{u}, \check{t}) &= \mathcal{M}_{-c_u, c_t, -c_s}(\hat{u}, \hat{t}, \check{u}, \check{t})
\end{aligned}
\tag{5.10}
$$

$$
\begin{aligned}
\mathcal{M}_{p_1 p_2 p_3 p_4}(\hat{s}, \hat{t}, \check{s}, \check{t}) &= \mathcal{M}_{p_1, p_4, p_3, p_2}(\hat{t}, \hat{s}, \check{t}, \check{s}) &= \mathcal{M}_{c_t, +c_s, +c_u}(\hat{t}, \hat{s}, \check{t}, \check{s}) \\
&= \mathcal{M}_{p_3, p_2, p_1, p_4}(\hat{t}, \hat{s}, \check{t}, \check{s}) &= \mathcal{M}_{-c_t, -c_s, c_u}(\hat{t}, \hat{s}, \check{t}, \check{s})
\end{aligned}
$$

The dependence on $\Sigma$ is left implicit since $\Sigma$ does not transform under crossing. It is clear that crossing has simple properties w.r.t. the triplets $\{\hat{s}, \check{s}, c_s\}$, $\{\hat{t}, \check{t}, c_t\}$, $\{\hat{u}, \check{u}, c_u\}$.

We will focus on the quantum regime of $\mathcal{N} = 4$ SYM where the theory is dual to classical supergravity (i.e. the regime where we first take $N$ large and then take large 't Hooft coupling $\lambda$), and we will study the tree level and the one-loop contribution to the Mellin amplitude,

$$
\mathcal{M} = \mathcal{M}^{(1)} + \frac{1}{N^2} \mathcal{M}^{(2)} + \dots,
\tag{5.11}
$$

with both contributions themselves expanded for large $\lambda$ as follows,

$$
\begin{aligned}
\mathcal{M}^{(1)} &= \mathcal{M}^{(1,0)} + \lambda^{-\frac{3}{2}} \mathcal{M}^{(1,3)} + \lambda^{-\frac{5}{2}} \mathcal{M}^{(1,5)} + \dots \\
\mathcal{M}^{(2)} &= \lambda^{\frac{1}{2}} \mathcal{M}^{(2,-1)} + \mathcal{M}^{(2,0)} + \lambda^{-1} \mathcal{M}^{(2,2)} + \lambda^{-\frac{3}{2}} \mathcal{M}^{(2,3)} + \dots
\end{aligned}
\tag{5.12}
$$

Where the large $\lambda$ expansion corresponds to curvature/derivative corrections[1].

## 5.1 tree level supergravity

The combination of analytic bootstrap techniques and the knowledge about the spectrum of supergravity, which consists of protected half-BPS single-particle states and multi-particle states (but no excited string states), allows one to solve the problem of computing the tree level contribution to the four-point correlators. The expression for $\mathcal{M}^{(1,0)}$ was given in

---

[1]The term $\lambda^{\frac{1}{2}} \mathcal{M}^{(2,-1)}$ corresponds to the $R^4$ counterterm. A term $\lambda^{-\frac{1}{2}} \mathcal{M}^{(2,1)}$ would correspond to the genus one contribution to the modular completion of $\lambda^{-\frac{5}{2}} \mathcal{M}^{(1,5)}$ and it vanishes. The term $\lambda^{-1} \mathcal{M}^{(2,2)}$ corresponds to the genus one contribution to the modular completion of $\mathcal{M}^{(1,6)}$.

[51, 52], building on previous work [100]. In our notation

$$\mathcal{M}^{(1,0)} = \frac{1}{(\mathbf{s}+1)(\mathbf{t}+1)(\mathbf{u}+1)}\,, \tag{5.13}$$

where the bold variables are given by

$$\mathbf{s} = \hat{s} + \check{s} \quad ; \quad \mathbf{t} = \hat{t} + \check{t} \quad ; \quad \mathbf{s}+\mathbf{t}+\mathbf{u} = -4\,. \tag{5.14}$$

Let us study this expression in detail, in particular emphasising the link between poles in Mellin space and exchanged operators in the OPE. This will help us to fully understand the superconformal block decomposition and the operators which appear.

### 5.1.1   Tree Level OPE: poles vs quantum numbers

The interacting part of the correlator (5.7) is written as an expansion in monomials $\tilde{U}^{\check{s}}\tilde{V}^{\check{t}}$ over a triangle in the $(\check{s}, \check{t})$ plane given by

$$\check{s} \geq -\min(\tfrac{p_1+p_2}{2}, \tfrac{p_3+p_4}{2}) \quad ; \quad \check{t} \geq -\min(\tfrac{p_1+p_4}{2}, \tfrac{p_2+p_3}{2}) \quad ; \quad \check{u} \geq -\min(\tfrac{p_1+p_3}{2}, \tfrac{p_2+p_4}{2}) \tag{5.15}$$

where $\check{u} = -\Sigma - 2 - \check{s} - \check{t}$. Finiteness of this sum is due to the sphere $\Gamma$ functions in the denominator of $\mathbf{\Gamma}$ factor, i.e. outside of (5.15) the factor $1/\Gamma_{\check{s}}\Gamma_{\check{t}}\Gamma_{\check{u}}$ vanishes. The amplitude is thus polynomial in $\tilde{U}$ and $\tilde{V}$. The triangle (5.15) is also in correspondence with the $su(4)$ representations $[aba]$ flowing between the OPEs $\mathcal{O}_{p_1}(x_1) \times \mathcal{O}_{p_2}(x_2)$ and $\mathcal{O}_{p_3}(x_3) \times \mathcal{O}_{p_4}(x_4)$. In particular, we will think of $\check{s}$ as the conjugate variable to 'twist' for the sphere, i.e. $b$, and $\check{t}$ as the conjugate variable for 'spin' on sphere, i.e. $a$.

The number of long $su(4)$ channels a correlator contributes to depends only on the charges, and can be accounted by introducing the degree of extremality $\kappa$. A nice and fully symmetric expression for $\kappa$ can be given as follows,

$$\kappa = \min(\tfrac{p_1+p_2}{2}, \tfrac{p_3+p_4}{2}) + \min(\tfrac{p_1+p_4}{2}, \tfrac{p_2+p_3}{2}) + \min(\tfrac{p_1+p_3}{2}, \tfrac{p_2+p_4}{2}) - \Sigma - 2 \tag{5.16}$$

The number of long $su(4)$ channels is then $\frac{(\kappa+1)(\kappa+2)}{2}$. The reps $[aba]$ flowing in the OPE instead depend on the orientation of the charges and they are

$$a = 0, 1, \ldots, \kappa \quad ; \quad \begin{aligned} & b = b_{min}, b_{min}+2, \ldots, b_{min}+2\kappa \\ & b_{min} = \max(|p_1-p_2|, |p_4-p_3|) \end{aligned} \tag{5.17}$$

Let us now translate the triangle in $su(4)$ labels into the one in $\check{s}$ and $\check{t}$. We shall focus on $\check{s}$ first, since this is relevant for the $(\alpha')^3$ amplitude.

It is almost immediate to see that

$$
\begin{aligned}
\check{s} &= \check{s}_{min}, \check{s}_{min} + 1, \dots, \check{s}_{max} \\
b &= b_{max}, b_{max} - 2, \dots, b_{min}
\end{aligned}
\quad ; \quad
\begin{cases}
\check{s}_{min} = -\min(\frac{p_1+p_2}{2}, \frac{p_3+p_4}{2}) \\
\check{s}_{max} = -\max(\frac{|p_1-p_2|}{2}, \frac{|p_4-p_3|}{2}) - 2
\end{cases}
\tag{5.18}
$$

where $\check{s}$ is max when $\check{t}$ and $\check{u}$ are minimum and $\check{s}_{max} - \check{s}_{min} = \kappa$. In sum

$$
\frac{b}{2} = -\check{s} - 2.
\tag{5.19}
$$

The change from $su(4)$ harmonics $Y_{[0b0]}$ and monomials $\tilde{U}^{\check{s}}$ is a triangular matrix of the form

$$
\begin{bmatrix}
Y_{[0,b_{min},0]} \\
\vdots \\
Y_{[0,b_{max},0]}
\end{bmatrix}
=
\boxed{\phantom{XXXXXX} 0 \phantom{XXXXX}}
\begin{bmatrix}
\tilde{U}^{\check{s}_{max}} \\
\vdots \\
\tilde{U}^{\check{s}_{min}}
\end{bmatrix}
\tag{5.20}
$$

In particular, the monomial $\tilde{U}^{\check{s}_{min}}$ is the one and only one contributing to $[0b_{max}0]$, but as we lower $b \leq b_{max}$ sequentially a new monomial each time starts contributing. The inclusion of $\check{t}$ and $a$ for each $\check{s}$ and $b$ is straightforward at this point. The total range of $\check{t}$ simply covers $\check{t} = \check{t}_{min}, \check{t}_{min} + 1, \dots, \check{t}_{max} = \check{t}_{min} + \kappa$ with $\check{t}_{min} = -\min(\frac{p_1+p_4}{2}, \frac{p_2+p_3}{2})$. In the same way the total range of $a$ covers $a = 0, 1, \dots, \kappa$.

Now that we have understood how the 4pt Mellin amplitude contributes to the various $su(4)$ channels, we would like to explain how the poles of

$$
\mathcal{M}^{(1,0)} = \frac{1}{(\mathbf{s}+1)(\mathbf{t}+1)(\mathbf{u}+1)},
\tag{5.21}
$$

are in correspondence with contributions in twist for each $su(4)$ channel. This will then lead us to our classification of the three regions Below Window, Window, and Above Window.

The simple pole at $\mathbf{s} + 1 = 0$ is equivalently described by $\hat{s} = -1 - \check{s}$. It follows from (5.20) that if we look at $[0b0]$ channels we find

|  | lowest pole from $\mathbf{s} + 1 = 0$ |  |
|---|---|---|
| $[0b_{max}0]$ | $\hat{s} = -1 - \check{s}_{min} = -1 + \min(\frac{p_1+p_2}{2}, \frac{p_3+p_4}{2})$ | $= \frac{b_{max}}{2} + 1$ |
| $\vdots$ | $\vdots$ | $\vdots$ |
| $[0b_{min}0]$ | $\hat{s} = -1 - \check{s}_{max} = +1 + \max(\frac{|p_1-p_2|}{2}, \frac{|p_4-p_3|}{2})$ | $= \frac{b_{min}}{2} + 1$ |
|  |  | $=$ unitarity bound |

(5.22)

Since there is a triangular transformation between monomials and $su(4)$ harmonics the value

of $\hat{s}$ written in the above table is actually the minimum value. Thus for labels $[aba]$ simple poles are given by

$$\hat{s} = [a + \tfrac{b}{2} + 1, \ldots, \min(\tfrac{p_1+p_2}{2}, \tfrac{p_3+p_4}{2}) - 1] \tag{5.23}$$

Each simple pole contributes with a $U^{\hat{s}}$. Now, because a long block of twist $\tau$ has a leading power in $U$ given by $U^{\tau/2}$, we find that poles in (5.22) imply the presence of a contribution in twist starting at the unitarity bound $\tau = 2a + b + 2$. Then, other simple poles coming from $(\mathbf{s} + 1) = 0$ add a *new* contribution in twist up to $\tau = \min(p_1 + p_2, p_3 + p_4) - 2$. We refer to this region as 'Below Window'.

Another sequence of simple poles contributing to the correlator comes from the $\mathbf{\Gamma}$ factor. We define the Window Region by the sequence of simple poles at

$$\hat{s} = p_{min}, \ldots, p_{\max} - 1 \qquad ; \qquad \text{Window Region,} \tag{5.24}$$

where $p_{\min} = \min(\tfrac{p_1+p_2}{2}, \tfrac{p_3+p_4}{2})$ and $p_{\max} = \max(\tfrac{p_1+p_2}{2}, \tfrac{p_3+p_4}{2})$.

Finally, also from $\mathbf{\Gamma}$, we have an infinite sequence of double poles:

$$\hat{s} \geq p_{\max} \qquad ; \qquad \text{Above Window.} \tag{5.25}$$

These double poles give rise to $\log U$ terms at tree level, upon performing the Mellin integral over $\hat{s}$. We should notice that for $p_1 + p_2 = p_3 + p_4$ the Window is empty. In this case, Above Window simply means above the threshold for exchange of long double traces, as defined in (5.25).

The operators exchanged in the regions described in (5.23)-(5.24)-(5.25), whose OPE data we are interested in, are two-particle operators which we will now introduce.

### 5.1.2   Two-particle spectrum

In the supergravity limit ($N \to \infty$ and $\lambda \gg 1$) the only operators surviving are: the single-particle operators $\mathcal{O}_p$, where the energy-momentum tensor, $\mathcal{O}_2$, corresponds to the graviton multiplet; and $\mathcal{O}_{p \geq 3}$ corresponding to higher Kaluza-Klein modes coming from the compactification of $\mathrm{S}^5$; and multi particle-states built from products of these. All other operators correspond to massive string excitations which acquire infinite mass and decouple from the spectrum.

The simplest of the multi-particle operators are the double-trace operators, $\mathcal{O}_{pq;\vec{\tau}}$, with classical dimension $\Delta^{(0)} = \tau + \ell$ and spin $\ell$. They have the property that their leading order three-point functions with external operators are non-vanishing. This is not true for higher multi-particle operators built from a higher number of single-particle operators, which have three-point couplings further suppressed by powers of $1/N$. Therefore, at leading large $N$ in the supergravity limit the contributions to the OPE are controlled by the double-trace

operators $\mathcal{O}_{pq;\vec{\tau}}$ [1].

For a given twist $\tau$, spin and $su(4)$ channel $[a, b, a]$ a basis of long superconformal primary operators is given schematically by [56]

$$\mathcal{O}_{pq;\vec{\tau}} = \mathcal{O}_p \partial^l \Box^{\frac{1}{2}(\tau - p - q)} \mathcal{O}_q, \qquad (p \le q). \tag{5.26}$$

Where $(pq)$ run over the $d = \mu(t - 1)$ pairs, with $t = \frac{\tau - b}{2} - a$,

$$\mathcal{D}_{\vec{\tau}} = \{(pq)|p = i + a + 1 + r; q = i + a + 1 - r + b\}, \tag{5.27}$$

parameterised by

$$i = 1, \ldots, (t - 1), \qquad r = 0, \ldots, (\mu - 1), \qquad \mu = \begin{cases} \lfloor \frac{b+2}{2} \rfloor & a + l \text{ even}, \\ \lfloor \frac{b+1}{2} \rfloor & a + l \text{ odd}. \end{cases} \tag{5.28}$$

This may be visualised as sweeping out a rectangle in the $(p, q)$ plane pictured below. Note, long operators have a minimum twist $\tau \ge 2a + b + 4$ one step above the unitarity bound.



$A = (a + 2, a + b + 2);$
$B = (a + 1 + \mu, a + b + 3 - \mu);$
$C = (a + \mu + t, a + b + 2 + t - \mu);$
$D = (a + 1 + t, a + b + 1 + t);$
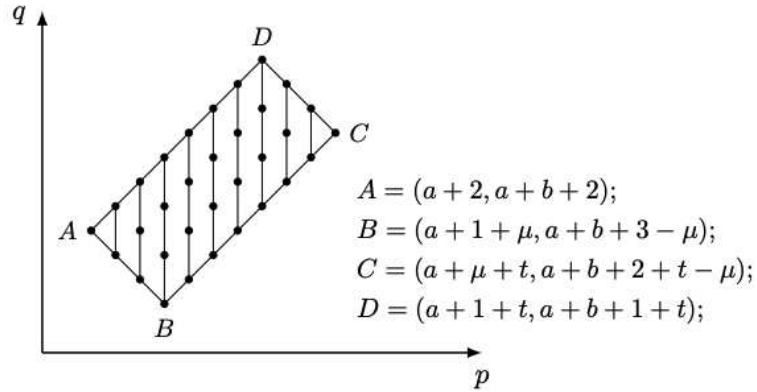
**Figure 5.1:** The set $\mathcal{D}_{\vec{\tau}}$ pictured in the $(p, q)$ plane. With vertical lines indicating operators with the same anomalous dimension see [56] for full details.

Generally, for a given set of classical quantum numbers there exist many degenerate operators causing operator mixing. We must then define the true scaling eigenstates, $\mathcal{K}_{rs}$, with well defined scaling dimensions. This implies that the block coefficients of

$$\langle \mathcal{O}_{p_1} \mathcal{O}_{p_2} \mathcal{O}_{p_3} \mathcal{O}_{p_4} \rangle^{\text{long}} = \sum_{\vec{\tau}} c_{\vec{\tau}}^{\vec{p}} \mathbb{L}_{\vec{\tau}}^{\vec{p}}, \tag{5.29}$$

are not in one-to-one correspondence with the three-point functions $C_{pq;\mathcal{K}_{rs}} \sim \langle \mathcal{O}_p \mathcal{O}_q \mathcal{K}_{rs} \rangle$,

---

[1] For fixed $p, q, \tau$ and $su(4)$ labels there exists a unique double trace operator of spin $\ell$. This is not true for higher multi-particle states which have a growing number of operators with increasing spin.

and instead we must sum over all degenerate operators in the set $\mathcal{D}_{\vec{\tau}}$

$$c_{\vec{\tau}}^{\vec{p}} = \sum_{(rs) \in \mathcal{D}_{\vec{\tau}}} C_{p_1 p_2; \mathcal{K}_{rs}} C_{p_1 p_2; \mathcal{K}_{rs}}. \tag{5.30}$$

The parameters $N$ and $\lambda^{-\frac{1}{2}}$ enter through the quantities $C_{pq;\mathcal{K}_{rs}}$ and the dimensions $\Delta$, where $C_{pq;\mathcal{K}_{rs}}$ admit the double expansion

$$C_{pq;\mathcal{K}_{rs}} = N^{\frac{p+q}{2}} \left[ \left( C_{pq;\mathcal{K}_{rs}}^{(0,0)} + \lambda^{-3/2} C_{pq;\mathcal{K}_{rs}}^{(0,3)} + \lambda^{-5/2} C_{pq;\mathcal{K}_{rs}}^{(0,5)} + \dots \right) \right.$$
$$\left. + \frac{1}{N^2} \left( C_{pq;\mathcal{K}_{rs}}^{(1,0)} + \lambda^{-3/2} C_{pq;\mathcal{K}_{rs}}^{(1,3)} + \lambda^{-5/2} C_{pq;\mathcal{K}_{rs}}^{(1,5)} + \dots \right) + O(N^{-4}) \right]. \tag{5.31}$$

Similarly, the scaling dimensions admit the expansion,

$$\Delta_{\mathcal{K}_{rs}} = \tau + \ell + \frac{2}{N^2} \left( \eta_{\mathcal{K}_{rs}}^{(1,0)} + \lambda^{-3/2} \eta_{\mathcal{K}_{rs}}^{(1,3)} + \lambda^{-\frac{5}{2}} \eta_{\mathcal{K}_{rs}}^{(1,5)} + \dots \right)$$
$$+ \frac{2}{N^4} \left( \lambda^{\frac{1}{2}} \eta_{\mathcal{K}_{rs}}^{(2,-1)} + \eta_{\mathcal{K}_{rs}}^{(2,0)} + \lambda^{-\frac{1}{2}} \eta_{\mathcal{K}_{rs}}^{(2,1)} + \lambda^{-1} \eta_{\mathcal{K}_{rs}}^{(2,2)} + \lambda^{-3/2} \eta_{\mathcal{K}_{rs}}^{(2,3)} + \dots \right) + O(N^{-6}). \tag{5.32}$$

The Equation (5.30), after expanding around large $N$ and $\lambda$, defines the *mixing equations.* Using these equations, along with results of Rastelli-Zhou for the general tree level supergravity correlator [51, 52], the mixing problem at various levels of generality was solved in [64, 65, 101], culminating in explicit formulae for the leading order three-point functions, and a fully factorised formula for the supergravity anomalous dimensions

$$\eta_{\mathcal{K}_{pq}}^{(1,0)} = -\frac{2 M_t^{(4)} M_{t+l+1}^{(4)}}{(\ell_{10} + 1)_6}, \tag{5.33}$$

where

$$M_t^{(4)} \equiv (t-1)(t+a)(t+a+b+1)(t+2a+b+2), \tag{5.34}$$

$$\ell_{10} = l + 2(p-2) - a + \frac{1 - (-)^{a+l}}{2}. \tag{5.35}$$

It is important to notice that $\ell_{10}$ only depends on $p$, which indicates the presence of a residual degeneracy for operators on the vertical lines of, Figure (5.1). We will show later that this makes certain OPE data needed for the one-loop computation impossible to un-mix directly.

The tree level mixing problem has also been studied for the first string correction [56], where

$$\eta_{\mathcal{K}_{22+b}}^{(1,3)} = -\frac{\zeta_3}{840} \delta_{l,0} \delta_{a,0} M_t^{(4)} M_{t+1}^{(4)} (t-1)_3 (t+b+1)_3, \tag{5.36}$$

exhibits a simple pattern, namely only the lightest state acquires a non-vanishing anomalous dimension, corresponding to the left most operator in the rectangle and to $\ell_{10} = 0$. Furthermore, the first string correction to the three-point functions was shown to vanish $C^{(0,3)}_{pq;\mathcal{K}_{rs}} = 0$. The structure of the anomalous dimensions at higher string corrections has since elucidated in [59, 60]. We will revisit the unmixing equations in full detail in Chapter 6.

## 5.2   tree level string-corrections

Much progress has been made in understanding $\lambda^{-\frac{1}{2}}$ corrections to the supergravity result. Such stringy corrections arise from higher-derivative interaction terms to the $\text{AdS}_5 \times \text{S}^5$ effective action, taking the general form $\partial^{2n}\mathcal{R}$, where $\mathcal{R}$ is the ten-dimensional Riemann curvature.

$$\mathcal{M}^{(1)} = \mathcal{M}^{(1,0)} + \lambda^{-\frac{3}{2}}\mathcal{M}^{(1,3)} + \lambda^{-\frac{5}{2}}\mathcal{M}^{(1,5)} + \dots. \tag{5.37}$$

The first two terms given by $\mathcal{M}^{(1,3)}$ and $\mathcal{M}^{(1,5)}$ descend from the $\mathcal{R}^4$ and $\partial^2\mathcal{R}^4$ supervertices respectively, which upon dimensional reduction generate quartic vertices in $\text{AdS}_5$ for all KK modes. The analytic structure of the general correction term $\partial^{2n}\mathcal{R}^4$ in Mellin space is simply polynomial in the Mellin variables whose degree is dictated by $n$. Note, the polynomiality of the tree level string corrections in Mellin space corresponds to the fact that they arise from corrections to unprotected double-trace operators, whose poles are already included by the $\mathbf{\Gamma}$ factor in the definition of the Mellin amplitude. Such polynomial solutions correspond to spin truncated solutions to the crossing equations [71, 94, 102, 103].

Through the flat space limit [54, 104] the Mellin space expressions are related to the type IIB closed string four-point scattering amplitude of four super-gravitons i.e. the Virasoro-Shapiro amplitude. Comparison to the low energy $(\lambda^{-\frac{1}{2}})$ expansion of the Virasoro-Shapiro amplitude completely fixes the leading terms in the polynomial Mellin amplitudes order by order in $\lambda^{-\frac{1}{2}}$. This relation was used first in [103] to fix the correlator of four super-gravitons and later extended in [71, 94] to the $\langle\mathcal{O}_2\mathcal{O}_2\mathcal{O}_p\mathcal{O}_p\rangle$ family of correlators to the first few order in the $\lambda^{-\frac{1}{2}}$ expansion.

Our focus will be on the first tree level $(\alpha')^3$ string correction given simply by [58]

$$\mathcal{M}^{(1,3)} = 2\zeta_3(\Sigma - 1)_3. \tag{5.38}$$

Note, this correction being constant is quite special, and corresponds to the truncation of the spectrum to spin zero. Higher order $\alpha'$ corrections come with non trivial polynomials in the Mellin variables and have been studied systematically via the bootstrap programme [58, 71, 103]. To various orders, fully explicit results have been computed in [59–61].

Both $\mathcal{M}^{(1,0)}$ and $\mathcal{M}^{(1,3)}$ come with interesting properties which are simple to see in our

formalism: We would expected $\mathcal{M}^{(1,0)}$ to be function of all variables $\{\hat{s}, \hat{t}, \check{s}, \check{t}, p_1, p_2, p_3, p_4\}$ but it happens to depend only on the specific combinations $\mathbf{s} = \hat{s} + \check{s}$ and $\mathbf{t} = \hat{t} + \check{t}$, $\mathbf{u} = -\mathbf{s} - \mathbf{t} - 4$. Moreover, it does not depend explicitly on the charges $p_i$ at all. In a similar way, $\mathcal{M}^{(1,3)}$ is just a constant, but for the factor of $(\Sigma - 1)_3$ (which is singlet under crossing). The crucial observation is that both $\mathcal{M}^{(1,0)}$ and $\mathcal{M}^{(1,3)}$ can be understood as 10d objects. In the case of supergravity, it was shown in [57] that $\mathcal{M}^{(1,0)}$ enjoys a 10d conformal symmetry. In the case of tree level $\alpha'$ corrections, the authors of [61] showed that $\mathcal{M}^{(1,3)}$ (and in fact $\mathcal{M}^{(1,i\geq 3)}$) is the dimensional reduction of a 10d contact diagram in $AdS_5 \times S^5$. Since the operators $\mathcal{O}_p(x, y)$ are Kaluza-Klein modes, the 10d structure of the tree level correlators implicitly constrains the way the Mellin amplitude depends on the charges.

At tree level the ultimate goal would be to resum all the $\alpha'$ corrections to $\mathcal{M}^{(1,0)}$. The resummed $\mathcal{M}^{(1)}$, as function of $\alpha'$, would then give the Virasoro-Shapiro amplitude in $AdS_5 \times S^5$, i.e. the generalisation of the well known type IIB flat space amplitude. It is a non-trivial problem because the bootstrap program leaves unfixed a number of ambiguities at each order in $\alpha'$. Additional input, from supersymmetric localisation [94, 97, 98], is already crucial to fix the ambiguities that appear at $(\alpha')^5$ [59].

## 5.3    Loop corrections

Higher order corrections in $1/N^2$ have been considered both at the level of supergravity and its stringy corrections. At one-loop, $\mathcal{O}(1/N^4)$, the supergravity term $\mathcal{M}^{(2,0)}$ was considered in Mellin space by [55, 62, 63, 71] with the most general formula given for the $\langle \mathcal{O}_2 \mathcal{O}_2 \mathcal{O}_p \mathcal{O}_p \rangle$ family of correlators. A complimentary position space approach was developed in [64, 65, 95] resulting in a general algorithm for constructing the one-loop correlator [66]. The one-loop string corrections have also been considered both in Mellin and position space [1, 62, 67] with the most general correlator considered being $\langle \mathcal{O}_2 \mathcal{O}_2 \mathcal{O}_p \mathcal{O}_p \rangle$ at $\lambda^{-3/2}$. Recently the two-loop, $\mathcal{O}(1/N^6)$, supergravity contribution $\mathcal{M}^{(3,0)}_{\vec{p}}$ was constructed in position space for the $\langle \mathcal{O}_2 \mathcal{O}_2 \mathcal{O}_2 \mathcal{O}_2 \rangle$ correlator [68, 69].

However, up to now *no general expressions for the correlator beyond tree level are known*! At one-loop the supergravity expression has been studied in [66] but proven too complicated to write down a general closed form expression. The perfect candidate to uncover the structure of one-loop amplitudes is given by the first string correction $\mathcal{M}^{(2,3)}$ at one-loop in $AdS_5 \times S^5$, due to the simplifcation of the double trace spectrum which truncates to 10d spin zero. In the next chapter we will construct explicit formulae for $\mathcal{M}^{(2,3)}$, for arbitrary external charges, generalising previous work done in [1, 58, 59, 62, 67, 71], and we will outline what is the general picture to go higher order in $\lambda$. This will involve implementing a one-loop bootstrap programme similar to that in [66] to extract pieces of the one-loop correlator from tree level results which we will also review.

# Chapter 6

# One-loop string corrections in AdS$_5 \times$ S$^5$

This chapter is dedicated to the study of one-loop string contributions beyond the one-loop supergravity correlators $\mathcal{M}^{(2,0)}$ studied in [66], the work here was originally presented in [1, 2]. We will focus on $\mathcal{M}^{(2,3)}$ at $(\alpha')^3$, generalising previous work done in [1, 58, 59, 62, 67, 71]. Along the way we will discuss the general picture for higher orders in $\alpha'$. We will explain how the bootstrap program works in the next section. Here we would like to summarise our main results and novelties, compared to the existing literature.

The OPE determines the gravity amplitude from CFT data of exchanged two-particle operators at tree level.[1] In the case of $\mathcal{M}^{(2,3)}$, the CFT data comes from $\mathcal{M}^{(1,0)}$ and $\mathcal{M}^{(1,3)}$, which we reviewed above in (5.13) and (5.38). Within certain ranges of twist which we refer to as Above Window, Window, and Below Window, the tree level OPE carries information about the maximal $\log^2 U$ discontinuity, the $\log U$ discontinuity and the analytic contribution, respectively. The Above Window region contains the $\log^2 U$ discontinuity and is fully determined by the OPE. The Window and the Below Window are finite ranges in the twist and give additional information on the structure of the amplitude. Indeed, as for $\mathcal{M}^{(2,0)}$ in supergravity [66], the $\log^2 U$ discontinuity is not enough to bootstrap the full one-loop amplitude, and the information coming from Window and Below Window is crucial to obtain the final result.

In order to appreciate the various novelties of one-loop physics, let us begin by noting that the $\mathbf{\Gamma}$ factor used to define the Mellin transform in (5.7) has itself a *bonus property*. It is invariant under *variations* of the charges $p_i$ which swap pairs of values $p_i + p_j$ for $i, j$ in the

---

[1]Up to a handful of ambiguities which cannot be fixed by the current bootstrap program.

s, or t, or u channel. For instance, if we highlight the s channel in,

$$\mathbf{\Gamma} = \frac{\Gamma[\frac{p_1+p_2}{2} - \hat{s}]\Gamma[\frac{p_3+p_4}{2} - \hat{s}]}{\Gamma[1 + \frac{p_1+p_2}{2} + \check{s}]\Gamma[1 + \frac{p_3+p_4}{2} + \check{s}]}\Gamma_{\mathtt{t}}\Gamma_{\mathtt{u}} \tag{6.1}$$

this is invariant under variations of the charges such that the values of $p_1 + p_2$ and $p_3 + p_4$ swap, but the other combinations $p_i + p_j$ remain unchanged. Let us emphasise that this property is not crossing symmetry, hence the use of the term *variations*. In terms of the $c_s, c_t, c_u$ parametrisation of the charges, see e.g. (5.9), the variations we are discussing just amount to exchange the values $\pm c_s$. In (6.1) we looked at the s channel, but of course the same reasoning applies to the other channels.

To have a concrete and simple example of the bonus property in mind, consider the case of correlators $\vec{p} = (4424)$ and $\vec{p} = (3335)$. These correlators have indeed the same $\mathbf{\Gamma}$, but more importantly, since the Mellin amplitudes $\mathcal{M}^{(1,0)}$ and $\mathcal{M}^{(1,3)}$ are themselves invariant under the aforementioned variations, the interacting correlators are equal at the corresponding orders in the expansion,

$$\mathcal{H}_{4424}(U, V, \tilde{U}, \tilde{V}) = \mathcal{H}_{3335}(U, V, \tilde{U}, \tilde{V}). \tag{6.2}$$

Recall that $\mathcal{H}_{\vec{p}}$ is introduced in (5.7) and, up to numerical factors normalisations dictated by (5.7) and free propagators removed, is just the interacting part of $\langle \mathcal{O}_{p_1} \mathcal{O}_{p_2} \mathcal{O}_{p_3} \mathcal{O}_{p_4} \rangle$.

More generally, we shall say that two correlators are degenerate when they have the same values of $\Sigma$ and $|c_s|, |c_t|, |c_u|$. We will show that whenever two correlators are degenerate in the tree level $\alpha'$ expansion, this degeneracy is lifted at one-loop at the corresponding order in $\alpha'$. This lift was first discussed in supergravity [66] but its expression at the level of the Mellin amplitude was not yet investigated. In this paper we provide very concrete formulae which exhibit the degeneracty lifting in the case of $\mathcal{M}^{(2,3)}$, and we believe that analogous formulae will hold at higher orders in $\alpha'$.

The Mellin amplitude will be written in the following way,

$$\mathcal{M}^{(2,3)}_{\vec{p}} = \left[\mathcal{W}^{(AW)}_{\vec{p}}(\hat{s}, \check{s}) + \mathcal{R}^{(W)}_{\vec{p}}(\hat{s}, \check{s}) + \mathcal{B}^{(BW)}_{\vec{p}}(\hat{s}, \check{s})\right] + \mathtt{crossing}, \tag{6.3}$$

where the superscripts indicate which region of OPE data was used to fix the function, i.e. Above Window (AW), Window (W) and Below Window (BW).

<u>The first term</u> in (6.3) is given by

$$\mathcal{W}^{(AW)}_{\vec{p}} = w_{\vec{p}}(\hat{s}, \check{s})\, \tilde{\psi}^{(0)}(-\mathbf{s}), \tag{6.4}$$

where $w_{\vec{p}}(\hat{s}, \check{s})$ is a polynomial and $\tilde{\psi}^{(0)}(-\mathbf{s}) \equiv \psi^{(0)}(-\mathbf{s}) + \gamma_E$ is the digamma function shifted by the Euler constant. This term is entirely determined by the OPE prediction for the

$\log^2 U$ discontinuity, corresponding to exchange of two-particle operators Above Window (AW).

The second term in (6.3) represents the novelty of the one-loop function. It takes the form,

$$\mathcal{R}_{\vec{p}}^{(W)}(\hat{s}, \check{s}) = \sum_{z=0}^{6} \frac{1}{\mathbf{s} - z}\left[ (\check{s} + \tfrac{p_1+p_2}{2} - z)_{z+1}\, r_{\vec{p};z}^{+}(\hat{s}, \check{s}) + (\check{s} + \tfrac{p_3+p_4}{2} - z)_{z+1}\, r_{\vec{p};z}^{-}(\hat{s}, \check{s}) \right], \quad (6.5)$$

where crossing implies that $r^{\pm}$ are related to each other, and given in terms of a single function with certain residual symmetry in the charges $\vec{p}$:

$$\begin{cases} r_{\vec{p}}^{+} = r_{\{-c_s, -c_t, c_u\}} \\ r_{\vec{p}}^{-} = r_{\{+c_s, +c_t, c_u\}} \end{cases} \quad ; \quad r_{\{c_s, c_t, c_u\}} = r_{\{c_s, -c_t, -c_u\}} \quad ; \quad r_{\{c_s, c_t, c_u\}} = r_{\{c_s, c_u, c_t\}}. \quad (6.6)$$

The function $r_{\vec{p};z}(\hat{s}, \check{s})$ is a polynomial, for each $z$, determined by OPE predictions for the $\log^1 U$ discontinuity in the Window. The poles in $z$ come with the bold font variables, and the structure of poles in $\hat{s}, \check{s}$, follows. We will explain this in the next sections.

Let us comment on the reason why $\mathcal{R}^{(W)}$ represents a novelty: When we look at $\mathcal{R}^{(W)}$ together with the $\boldsymbol{\Gamma}$ functions, say we focus on $\Gamma_{\mathbf{s}}$ in the $\mathbf{s}$-channel, the total amplitude undergoes the following split,

$$\frac{\mathcal{R}_{\vec{p}}^{(W)}}{\Gamma[1 + \tfrac{p_1+p_2}{2} + \check{s}]\Gamma[1 + \tfrac{p_3+p_4}{2} + \check{s}]}$$

$$(6.7)$$

$$= \frac{1}{\mathbf{s} - z}\left[ \frac{r_{\vec{p};z}^{+}}{\Gamma[-z + \tfrac{p_1+p_2}{2} + \check{s}]\Gamma[1 + \tfrac{p_3+p_4}{2} + \check{s}]} + \frac{r_{\vec{p};z}^{-}}{\Gamma[1 + \tfrac{p_1+p_2}{2} + \check{s}]\Gamma[-z + \tfrac{p_3+p_4}{2} + \check{s}]} \right]$$

In particular the sphere $\Gamma$ functions (in $\boldsymbol{\Gamma}$) split into two $z$-dependent gamma functions, with residues $r^{\pm}$ respectively. Since we will find that $r^{\pm}$ have generic charge dependence, i.e. they depend on $c_t$ and $c_u$ non trivially, it follows that $r^{\pm}$ do not map to each other under variations of charges that leave $\boldsymbol{\Gamma}$ invariant, and therefore the bonus property, exemplified for instance in (6.2), is lifted. All together we refer to this phenomenon as *sphere splitting*.

The third term in (6.3) is found to take the form

$$\mathcal{B}_{\vec{p}}^{(BW)}(\hat{s}, \check{s}) = \sum_{z=0}^{2} \frac{(\check{s} + \tfrac{p_1+p_2}{2} - z)_{z+1}(\check{s} + \tfrac{p_3+p_4}{2} - z)_{z+1}}{\mathbf{s} - z}\, b_{\vec{p};z}(\hat{s}, \check{s}), \quad (6.8)$$

where again $b_{\vec{p}}(\hat{s}, \check{s}; z)$ are polynomials. This contribution is determined by OPE predictions from the $\log^0 U$ term in the Below Window region.

Remarkably, we find that $\sum_z$ in (6.5) and (6.8) are finite and moreover the number of poles

indexed by $z$ is independent of the charges! This feature was already observed in [1] by studying $\langle \mathcal{O}_2 \mathcal{O}_2 \mathcal{O}_p \mathcal{O}_p \rangle$ in the Window. It is not manifest from the form of the OPE, which instead depends on charges by construction. In fact, in order for this truncation to happen, there is a delicate interplay between $\mathcal{W}^{(AW)}$ and $\mathcal{R}^{(W)}$, and $\mathcal{B}^{(BW)}$.

The function $\mathcal{W}^{(AW)}$ contributes to $\log^2 U$ discontinuity by construction, but also contributes to the $\log^1 U$ discontinuity in the Window and the analytic term $\log^0 U$ in the Below Window regions. Similarly, $\mathcal{R}^{(W)}$ contributes to $\log^1 U$ in the Window region by construction but also to the analytic term $\log^0 U$ in the Below Window region. This cascading behaviour results from our choice to use the bold font variables, $\mathbf{s}, \mathbf{t}, \mathbf{u}$, in the parametrisation of the poles of $\mathcal{M}$, say $\tilde{\psi}^{(0)}(-\mathbf{s})$ and $\mathbf{s} - z$ in the $\mathbf{s}$ channel. This choice of parametrisation then reveals an additional simplicity: the truncation of the number of poles in $z$. In particular, we find that $\mathcal{R}^{(W)}$ only contains seven poles $z = 0, \ldots 6$ at order $(\alpha')^3$.

We can argue that the use of the bold font variables, $\mathbf{s}, \mathbf{t}, \mathbf{u}$ in the parametrisation of the poles of $\mathcal{M}$ is natural from the perspective of large $p$ limit [55], i.e. from the expected behaviour of the amplitude when the charges $\vec{p}$ are taken to be large. The large $p$ limit is well established in various $AdS \times S$ backgrounds. In the case we are interested in, the crucial observation is that, in the large $\vec{p}$ limit, the $AdS_5 \times S^5$ Mellin amplitude asymptotes the flat space amplitude of IIB supergravity, where $\mathbf{s}$ is identified with the corresponding ten-dimensional Mandelstam invariant of the flat space amplitude. Now, the flat space amplitude of the one-loop IIB amplitude has various log contributions, e.g. $\log(-\mathbf{s})$. It is natural that such logs should arise from the digamma in the limit of large $\mathbf{s}$ as $\tilde{\psi}^{(0)}(-\mathbf{s}) \to \log(-\mathbf{s})$. It follows that $\mathbf{s}$ is the natural variable entering $\tilde{\psi}^{(0)}(-\mathbf{s})$ in the $AdS_5 \times S^5$ Mellin amplitude. More evidence supporting the use of $\mathbf{s}, \mathbf{t}, \mathbf{u}$, in parametrising the poles of $\mathcal{M}$ also comes from our preliminary investigations on the $(\alpha')^{n+3}$ terms for $n > 0$, which show that the number of poles grows with $n$, but remains finite, and is independent of tree level ambiguities.

Following similar logic, the poles of the function $\mathcal{B}^{(BW)}$, are parametrised by $\mathbf{s}, \mathbf{t}, \mathbf{u}$. This function was previously studied for the single correlator $\langle \mathcal{O}_3 \mathcal{O}_3 \mathcal{O}_3 \mathcal{O}_3 \rangle$ in [1]. We find that only three poles at $z = 0, 1, 2$ are needed to match the OPE data. Again, this truncation depends on the delicate interplay with both $\mathcal{W}^{(AW)}$ and $\mathcal{R}^{(W)}$. Finally, combining all contributions we are able to explicitly verify consistency with the ten-dimensional flat space limit. Since this property was not used in the detailed construction of the individual contributions, this provides a strong consistency check on the form of our final results.

## 6.1    The AdS$_5 \times$ S$^5$ OPE

Having reviewed the necessary material we now revisit the OPE to see which information is accessible to us at one-loop, focusing particularly on string-corrected one-loop amplitudes, given explicitly at $\lambda^{-3/2}$ in the next section. It draws mainly from [66] where it was explained

how the CFT data collected from tree-level correlators must be organised at one-loop, in order to initiate the bootstrap program for arbitrary external operators $\vec{p}$.

### 6.1.1 Large $N$ expansion

With the spectrum of operators exchanged in the OPE at hand we can now begin to make predictions for the block coefficients. Recall, the conformal block decomposition for the long part of the correlator is given by

$$\langle \mathcal{O}_{p_1} \mathcal{O}_{p_2} \mathcal{O}_{p_3} \mathcal{O}_{p_4} \rangle^{\mathrm{long}} = \sum_{\vec{\tau}} c_{\vec{\tau}}^{\vec{p}} \, \mathbb{L}_{\vec{\tau}}^{\vec{p}} \, . \tag{6.9}$$

As mentioned in Section 5.1.2 the double-trace operators entering the OPE are degenerate in free theory: for fixed free quantum numbers, $\vec{\tau}$, there are as many operators $\mathcal{O}_{pq}$ as integer pairs $(pq)$ in the rectangle $\mathcal{D}_{\vec{\tau}}$ described in [56]. Therefore, the block coefficients $c_{\vec{\tau}}^{\vec{p}}$ are not in one-to-one correspondence with the CFT data and instead we must sum over all degenerate operators

$$c_{\vec{\tau}}^{\vec{p}} = \sum_{(rs) \in \mathcal{D}_{\vec{\tau}}} C_{p_1 p_2 \mathcal{K}_{rs}} C_{p_3 p_4 \mathcal{K}_{rs}}, \tag{6.10}$$

where $\mathcal{K}_{rs}$ are the true scaling eignestates. Upon expanding the scaling dimensions and the three-point couplings[1] $C_{p_i p_j \mathcal{K}_{rs}}$ of the double-trace operators with the external single-particle operators $\mathcal{O}_{p_i}$ and $\mathcal{O}_{p_j}$,

$$\Delta_{\mathcal{K}_{rs}} = \tau + l + \frac{2}{N^2} \eta_{\mathcal{K}_{rs}}^{(1)} + \dots, \quad C_{p_i p_j \mathcal{K}_{rs}} = N^{\frac{p_i + p_j}{2}} \Big[ C_{p_i p_j \mathcal{K}_{rs}}^{(0)} + \frac{1}{N^2} C_{p_i p_j \mathcal{K}_{rs}}^{(1)} + \dots \Big], \tag{6.11}$$

we can go ahead and write down the OPE predictions for the block coefficients in the large $N$ expansion. The long multiplet contribution to the *full* correlator (free+interacting) up to one-loop is given by[2]

$$\langle \mathcal{O}_{p_1} \mathcal{O}_{p_2} \mathcal{O}_{p_3} \mathcal{O}_{p_4} \rangle_{\mathrm{long}} = \sum_{\vec{\tau} \in AW} L_{\vec{p};\vec{\tau}}^{(0)} \mathbb{L}_{\vec{\tau}}^{\vec{p}} \tag{6.12}$$

$$+ \frac{1}{N^2} \Bigg[ \sum_{\vec{\tau} \in W} N_{\vec{p};\vec{\tau}}^{(1)} + \sum_{\vec{\tau} \in AW} V_{\vec{p};\vec{\tau}}^{(1)} \log(u) \Bigg] \mathbb{L}_{\vec{\tau}}^{\vec{p}} + \dots$$

$$+ \frac{1}{N^4} \Bigg[ \sum_{\vec{\tau} \in BW} K_{\vec{p};\vec{\tau}}^{(2)} + \sum_{\vec{\tau} \in W} H_{\vec{p};\vec{\tau}}^{(2)} \log(u) + \sum_{\vec{\tau} \in AW} M_{\vec{p};\vec{\tau}}^{(2)} \log^2(u) \Bigg] \mathbb{L}_{\vec{\tau}}^{\vec{p}} + \dots$$

To understand the above formula we note that $C_{p_i p_j \mathcal{K}_{\vec{\tau}}}^{(0)} = 0$ for $\tau < p_i + p_j$. This follows from the form of the long contribution to disconnected free theory, which is only non-zero in

---

[1] Note, the dependance of the anomalous dimensions and three-point coupling on the quantum numbers $\vec{\tau}$ has been suppressed.

[2] We have omitted terms with derivatives acting on the blocks as they do not affect the leading logs for each region.

the above-window region. Therefore, when taking the product of two three-point functions $C_{p_1p_2}(\mathcal{O}_{\vec{\tau}})C_{p_3p_4}(\mathcal{O}_{\vec{\tau}})$ as in (6.10) we define three regions in the large $N$ counting. Using the notation $\tau_{max} = \max(p_1 + p_2, p_3 + p_4)$ and $\tau_{min} = \min(p_1 + p_2, p_3 + p_4)$, the three regions are shown in Figure 6.1 and their OPE predictions are given by:

**Above Window** $(\tau \geq \tau_{max})$: Both three point functions $C^{(0)}_{p_1p_2,\mathcal{K}_{rs}}$ and $C^{(0)}_{p_3p_4,\mathcal{K}_{rs}}$ have leading order contributions in the $1/N$ expansion. The terms $L^{(0)}$, $M^{(1)}$ and $N^{(2)}$ only receive contributions within the above window region where we have

$$L_{\vec{p}}^{(0)} = \sum_{(rs)\in\mathcal{D}_{\vec{\tau}}} C^{(0)}_{p_1p_2;\mathcal{K}_{rs}} C^{(0)}_{p_3p_4;\mathcal{K}_{rs}}, \tag{6.13}$$

$$V_{\vec{p}}^{(1)} = \sum_{(rs)\in\mathcal{D}_{\vec{\tau}}} C^{(0)}_{p_1p_2;\mathcal{K}_{rs}} \eta^{(1)}_{\mathcal{K}_{rs}} C^{(0)}_{p_3p_4;\mathcal{K}_{rs}}, \tag{6.14}$$

$$M_{\vec{p}}^{(2)} = \sum_{(rs)\in\mathcal{D}_{\vec{\tau}}} \frac{1}{2} C^{(0)}_{p_1p_2;\mathcal{K}_{rs}} \eta^{(1)}_{\mathcal{K}_{rs}} \eta^{(1)}_{\mathcal{K}_{rs}} C^{(0)}_{p_3p_4;\mathcal{K}_{rs}}. \tag{6.15}$$

**Window** $(\tau_{min} \leq \tau < \tau_{max})$: One three point function is leading order, the other is $1/N$ suppressed. Within this region we may calculate the terms $N^{(1)}$ and $H^{(2)}$ given by

$$N_{\vec{p}}^{(1)} = \sum_{(rs)\in\mathcal{D}_{\vec{\tau}}} C^{(0)}_{p_1p_2;\mathcal{K}_{rs}} C^{(1)}_{p_3p_4;\mathcal{K}_{rs}} + C^{(1)}_{p_1p_2;\mathcal{K}_{rs}} C^{(0)}_{p_3p_4;\mathcal{K}_{rs}}, \tag{6.16}$$

$$H_{\vec{p}}^{(2)} = \sum_{(rs)\in\mathcal{D}_{\vec{\tau}}} \left( C^{(1)}_{p_1p_2;\mathcal{K}_{rs}} C^{(0)}_{p_3p_4;\mathcal{K}_{rs}} + C^{(0)}_{p_1p_2;\mathcal{K}_{rs}} C^{(1)}_{p_3p_4;\mathcal{K}_{rs}} \right) \eta^{(1)}_{\mathcal{K}_{rs}}. \tag{6.17}$$

**Below window** $(2a + b + 2 \leq \tau < \tau_{min})$: Both three-point functions are $1/N$ suppressed leading to a genuine $1/N^4$ effect. Within this region we may calculate the term $K^{(2)}$ given by

$$K_{\vec{p};\vec{\tau}}^{(2)} = \sum_{(rs)\in\mathcal{D}_{\vec{\tau}}} C^{(1)}_{p_1p_2;\mathcal{K}_{rs}} C^{(1)}_{p_3p_4;\mathcal{K}_{rs}}. \tag{6.18}$$

Note, all of these expressions contain at most tree-level data, meaning we are able to predict parts of the one-loop correlator with known tree-level results, this includes: the entire double log discontinuity $M_{\vec{p}}^{(2)}$; the log discontinuity $H_{\vec{p}}^{(2)}$ in the Window; and the analytic piece $K_{\vec{p}}^{(2)}$ below window!
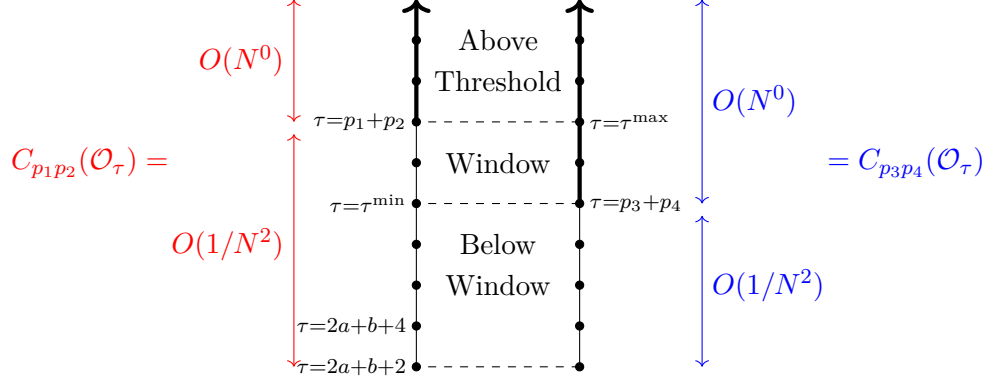
**Figure 6.1:** The large $N$ structure of $C_{p_1p_2,\vec{\tau}} C_{p_3p_4,\vec{\tau}}$ for two particle operators $\mathcal{O}_\tau$ in an $su(4)$ representation $[aba]$, and varying twist.

### 6.1.2 Tree-level OPE

Due to the operator mixing the OPE data is better organised into matrices. Let us package the anomalous dimensions $\eta^{(1)}_{\mathcal{K}_{rs}}$ into a diagonal $|\mathcal{D}_{\vec{\tau}}| \times |\mathcal{D}_{\vec{\tau}}|$ matrix $\boldsymbol{\eta}^{(1)}_{\vec{\tau}}$. We then arrange the leading order three-point functions into an $|\mathcal{D}_{\vec{\tau}}| \times |\mathcal{D}_{\vec{\tau}}|$ matrix $\mathbf{C}^{(0)}_{\vec{\tau}}$

$$\left(\mathbf{C}^{(0)}_{\vec{\tau}}\right)_{(rs),(pq)} = C^{(0)}_{pq;\mathcal{K}_{rs}}; \quad (pq),(rs) \in \mathcal{D}_{\vec{\tau}}. \tag{6.19}$$

Similarly, we construct the full rank $|\mathcal{D}_{\vec{\tau}}| \times |\mathcal{D}_{\vec{\tau}}|$ matrices $\mathbf{L}^{(0)}_{\vec{\tau}}$ and $\mathbf{V}^{(1)}_{\vec{\tau}}$ for fixed $\vec{\tau}$

$$\left(\mathbf{L}^{(0)}_{\vec{\tau}}\right)_{(p_1p_2),(p_3p_4)} = L^{(0)}_{\vec{p};\vec{\tau}}; \quad (p_1p_2),(p_3p_4) \in \mathcal{D}_{\vec{\tau}}, \tag{6.20}$$

$$\left(\mathbf{V}^{(1)}_{\vec{\tau}}\right)_{(p_1p_2),(p_3p_4)} = V^{(1)}_{\vec{p};\vec{\tau}}; \quad (p_1p_2),(p_3p_4) \in \mathcal{D}_{\vec{\tau}}. \tag{6.21}$$

The matrix $\mathbf{L}^{(0)}_{\vec{\tau}}$ gives the (diagonal) CPW coefficients from disconnected free theory, while $\mathbf{V}^{(1)}_{\vec{\tau}}$ comes from the $\log U$ terms arising from the double poles in the tree-level interacting part. With these definitions we may re-write (6.13) and (6.14) as

$$\mathbf{L}^{(0)}_{\vec{\tau}} = \mathbf{C}^{(0)}_{\vec{\tau}} \cdot \mathbf{C}^{(0)T}_{\vec{\tau}}; \qquad \mathbf{V}^{(1)}_{\vec{\tau}} = \mathbf{C}^{(0)}_{\vec{\tau}} \cdot \boldsymbol{\eta}^{(1)}_{\vec{\tau}} \cdot \mathbf{C}^{(0)T}_{\vec{\tau}} \tag{6.22}$$

A similar organisation principle holds for the subleading three-point couplings $C^{(1)}$ which arise from the window region. This time it is more naturally arranged into a vector $\mathbf{C}^{(1)}_{(q_1q_2);\vec{\tau}}$, labelled by $\vec{\tau}$ and a fixed pair $q_1q_2$, such that $q_1 + q_2 > \tau \geq 2a + b + 4$, with the vector index running over the operators

$$\left(\mathbf{C}^{(1)}_{(q_1q_2);\vec{\tau}}\right)_{(rs)} = C^{(1)}_{q_1q_2\mathcal{K}_{rs};\vec{\tau}}; \quad (rs) \in \mathcal{D}_{\vec{\tau}}. \tag{6.23}$$
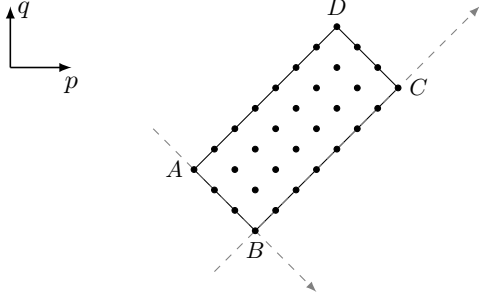
$A = (a+2, a+b+2);$
$B = (a+1+\mu, a+b+3-\mu);$
$C = (a+\mu+t-1, a+b+1+t-\mu);$
$D = (a+t, a+b+t);$

**Figure 6.2:** The set $\mathcal{R}_{\vec{\tau}}$ pictured in the $(p, q)$ plane. With vertical lines indicating operators with the same anomalous dimension see [56] for full details.

The non-log tree-level data for the correlator $\langle \mathcal{O}_{q_1} \mathcal{O}_{q_2} \mathcal{O}_{p_3} \mathcal{O}_{p_4} \rangle$ in the window region is also best encoded by the vector,

$$\left( \mathbf{N}^{(1)}_{(q_1 q_2);\vec{\tau}} \right)_{(p_3 p_4)} = \sum_{(rs) \in \mathcal{D}_{\vec{\tau}}} C^{(1)}_{q_1 q_2 \mathcal{K}_{rs}} C^{(0)}_{p_3 p_4 \mathcal{K}_{rs}}; \quad (p_3 p_4) \in \mathcal{D}_{\vec{\tau}} \tag{6.24}$$

In this case it is crucial to consider both the tree-level contribution to $\langle \mathcal{O}_{q_1} \mathcal{O}_{q_2} \mathcal{O}_{p_3} \mathcal{O}_{p_4} \rangle_{\text{int}}$ and connected free theory in the long sector. With these definitions we can thus re-write (6.16) as

$$\mathbf{N}^{(1)}_{(q_1 q_2);\vec{\tau}} = \mathbf{C}^{(1)}_{(q_1 q_2);\vec{\tau}} \cdot \mathbf{C}^{(0)\,T}_{\vec{\tau}}, \tag{6.25}$$

where the first term has vanished since $C^{(0)}_{q_1 q_2 \mathcal{K}_{rs}} = 0$.

The above discussion holds for any value of the 't Hooft coupling $\lambda$, but let us recall that we are interested in the regime of large $\lambda$ and expand the anomalous dimensions and three-point functions accordingly,

$$\begin{aligned}
\eta^{(1)}_{\mathcal{K}_{rs}} &= \eta^{(1,0)}_{\mathcal{K}_{rs}} &&+ \lambda^{-\frac{3}{2}} \eta^{(1,3)}_{\mathcal{K}_{rs}} &&+ \lambda^{-\frac{5}{2}} \eta^{(1,5)}_{\mathcal{K}_{rs}} + \dots, \\
C^{(0)}_{p_i p_j \mathcal{K}_{rs}} &= C^{(0,0)}_{p_i p_j \mathcal{K}_{rs}} &&+ \lambda^{-\frac{3}{2}} C^{(0,3)}_{p_i p_j \mathcal{K}_{rs}} &&+ \lambda^{-\frac{5}{2}} C^{(0,5)}_{p_i p_j \mathcal{K}_{rs}} + \dots \\
C^{(1)}_{p_i p_j \mathcal{K}_{rs}} &= C^{(1,0)}_{p_i p_j \mathcal{K}_{rs}} &&+ \lambda^{-\frac{3}{2}} C^{(1,3)}_{p_i p_j \mathcal{K}_{rs}} &&+ \lambda^{-\frac{5}{2}} C^{(1,5)}_{p_i p_j \mathcal{K}_{rs}} + \dots.
\end{aligned}$$

The matrix $\mathbf{L}^{(0)}_{\vec{\tau}}$ is independent of $\lambda$, being derived from the disconnected part of the free theory correlator, hence we can also write $\mathbf{L}^{(0)}_{\vec{\tau}} = \mathbf{L}^{(0,0)}_{\vec{\tau}}$. The matrix $\mathbf{V}^{(1)}_{\vec{\tau}}$ has an expansion for large $\lambda$,

$$\mathbf{V}^{(1)}_{\vec{\tau}} = \mathbf{V}^{(1,0)}_{\vec{\tau}} + \lambda^{-\frac{3}{2}} \mathbf{V}^{(1,3)}_{\vec{\tau}} + \lambda^{-\frac{5}{2}} \mathbf{V}^{(1,5)}_{\vec{\tau}} + \dots. \tag{6.26}$$

When we expand the mixing equations (6.22) order by order in $\lambda^{-\frac{1}{2}}$ we find the following equations at leading order,

$$\mathbf{L}^{(0,0)}_{\vec{\tau}} = \mathbf{C}^{(0,0)}_{\vec{\tau}} \mathbf{C}^{(0,0)\,T}_{\vec{\tau}},$$

$$\mathbf{V}_{\vec{\tau}}^{(1,0)} = \mathbf{C}_{\vec{\tau}}^{(0,0)} \boldsymbol{\eta}_{\vec{\tau}}^{(1,0)} \mathbf{C}_{\vec{\tau}}^{(0,0)\,T} \,. \tag{6.27}$$

These equations give the eigenvalue problem solved in [56, 101], yielding the double-trace spectrum of anomalous dimensions in supergravity which exhibit the partial residual degeneracy associated with the hidden conformal symmetry [57]. The supergravity contributions to the anomalous dimensions of the operators are given by a very simple formula [56],

$$\eta_{\mathcal{K}_{pq}}^{(1,0)} = -\frac{2M_t^{(4)} M_{t+l+1}^{(4)}}{(\ell_{10}+1)_6} \tag{6.28}$$

where

$$M_t^{(4)} \equiv (t-1)(t+a)(t+a+b+1)(t+2a+b+2)\,, \tag{6.29}$$

$$\ell_{10} = l + 2(p-2) - a + \frac{1-(-)^{a+l}}{2}\,. \tag{6.30}$$

The notation for $\ell_{10}$ reflects the fact that this quantity can be interpreted as a ten-dimensional spin [57]. For $\mu > 1$ and $t > 2$ there is a residual degeneracy because $\ell_{10}$ depends only on $p$ and not on $q$. This degeneracy is illustrated in Figure 6.2 which gives a sketch of the rectangle $\mathcal{D}_{\vec{\tau}}$ with operators of common anomalous dimension connected by vertical lines. The residual degeneracy is a reflection of the ten-dimensional conformal symmetry described in [57].

At the next orders in the expansion we find at order $\lambda^{-\frac{3}{2}}$,

$$\mathbf{C}_{\vec{\tau}}^{(0,3)} \mathbf{C}_{\vec{\tau}}^{(0,0)\,T} + \mathbf{C}_{\vec{\tau}}^{(0,0)} \mathbf{C}_{\vec{\tau}}^{(0,3)\,T} = 0\,,$$
$$\mathbf{C}_{\vec{\tau}}^{(0,0)} \boldsymbol{\eta}_{\vec{\tau}}^{(1,3)} \mathbf{C}_{\vec{\tau}}^{(0,0)\,T} + \mathbf{C}_{\vec{\tau}}^{(0,3)} \boldsymbol{\eta}_{\vec{\tau}}^{(1,0)} \mathbf{C}_{\vec{\tau}}^{(0,0)\,T} + \mathbf{C}_{\vec{\tau}}^{(0,0)} \boldsymbol{\eta}_{\vec{\tau}}^{(1,0)} \mathbf{C}_{\vec{\tau}}^{(0,3)\,T} = \mathbf{V}_{\vec{\tau}}^{(1,3)}\,. \tag{6.31}$$

At this order the anomalous dimensions are even simpler [58]. Only operators with $\ell_{10} = 0$, i.e. with $a = l = 0$, $i = 1$, $r = 0$ (and hence $(p,q) = (2, 2+b)$) receive an anomalous dimension. In relation to the diagram Fig. 6.2, these operators sit at the left-most corner of the rectangle $\mathcal{D}_{\vec{\tau}}$. Their anomalous dimensions read,

$$\eta_{\mathcal{K}_{22+b}}^{(1,3)} = -\frac{\zeta_3}{840} \delta_{l,0} \delta_{a,0} M_t^{(4)} M_{t+1}^{(4)} (t-1)_3 (t+b+1)_3\,. \tag{6.32}$$

At order $\lambda^{-\frac{5}{2}}$ the mixing equations read,

$$\mathbf{C}_{\vec{\tau}}^{(0,5)} \mathbf{C}_{\vec{\tau}}^{(0,0)\,T} + \mathbf{C}_{\vec{\tau}}^{(0,0)} \mathbf{C}_{\vec{\tau}}^{(0,5)\,T} = 0\,,$$
$$\mathbf{C}_{\vec{\tau}}^{(0,0)} \boldsymbol{\eta}_{\vec{\tau}}^{(1,5)} \mathbf{C}_{\vec{\tau}}^{(0,0)\,T} + \mathbf{C}_{\vec{\tau}}^{(0,5)} \boldsymbol{\eta}_{\vec{\tau}}^{(1,0)} \mathbf{C}_{\vec{\tau}}^{(0,0)\,T} + \mathbf{C}_{\vec{\tau}}^{(0,0)} \boldsymbol{\eta}_{\vec{\tau}}^{(1,0)} \mathbf{C}_{\vec{\tau}}^{(0,5)\,T} = \mathbf{V}_{\vec{\tau}}^{(1,5)}\,. \tag{6.33}$$

Their solution was first given in [59]. Since then the general strucutre of the tree-level

anomalous has been elucidated [60].

Here we are mostly concerned with the order $\lambda^{-\frac{3}{2}}$ equations, which in fact yield $\mathbf{C}^{(0,3)} = 0$ as part of their solution [58]. Note that this simplification does not hold at the next order, i.e. $\mathbf{C}^{(0,5)} \neq 0$ [59]. By expanding the subleading couplings $C^{(1)}$ in $\lambda^{-\frac{1}{2}}$ we have,

$$\mathbf{C}^{(1,0)}_{(q_1 q_2);\vec{\tau}} \cdot \mathbf{C}^{(0,0)T}_{\vec{\tau}} = \mathbf{N}^{(1,0)}_{(q_1 q_2);\vec{\tau}},$$

$$\mathbf{C}^{(1,3)}_{(q_1 q_2);\vec{\tau}} \cdot \mathbf{C}^{(0,0)T}_{\vec{\tau}} + \mathbf{C}^{(1,0)}_{(q_1 q_2);\vec{\tau}} \cdot \mathbf{C}^{(0,3)T}_{\vec{\tau}} = \mathbf{N}^{(1,3)}_{(q_1 q_2);\vec{\tau}},$$

$$\mathbf{C}^{(1,5)}_{(q_1 q_2);\vec{\tau}} \cdot \mathbf{C}^{(0,0)T}_{\vec{\tau}} + \mathbf{C}^{(1,0)}_{(q_1 q_2);\vec{\tau}} \cdot \mathbf{C}^{(0,5)T}_{\vec{\tau}} = \mathbf{N}^{(1,5)}_{(q_1 q_2);\vec{\tau}}. \tag{6.34}$$

Again the order $\lambda^{-\frac{3}{2}}$ equation simplifies since $\mathbf{C}^{(0,3)}_{\vec{\tau}} = 0$.

### 6.1.3   One loop OPE

Having reviewed tree level data, we are ready to use it to study one-loop string theory in $AdS_5 \times S^5$. This amounts to bootstrap the one-loop correlators by knowing

$$\langle \mathcal{O}_{p_1} \mathcal{O}_{p_2} \mathcal{O}_{p_3} \mathcal{O}_{p_4} \rangle_{\text{long}} = \ldots + \frac{1}{N^4} \left[ \sum_{\vec{\tau} \in BW} K^{(2)}_{\vec{p};\vec{\tau}} + \sum_{\vec{\tau} \in W} H^{(2)}_{\vec{p};\vec{\tau}} \log(u) + \sum_{\vec{\tau} \in AW} M^{(2)}_{\vec{p};\vec{\tau}} \log^2(u) \right] \mathbb{L}^{\vec{p}}_{\vec{\tau}} + \ldots$$

i.e. by knowing the values of $M^{(2)}_{\vec{p};\vec{\tau}}$, $H^{(2)}_{\vec{p};\vec{\tau}}$, and $K^{(2)}_{\vec{p};\vec{\tau}}$.

$\underline{\log^2(U)}$: The OPE data gathered from the disconnected and tree-level contributions allows us to predict the $\log^2 U$ terms at one loop. Such terms arise purely in the above window region and, for fixed quantum numbers $\vec{\tau}$, can be arranged into a matrix $\mathbf{M}^{(2)}_{\vec{\tau}}$ given by

$$\mathbf{M}^{(2)}_{\vec{\tau}} = \tfrac{1}{2} \, \mathbf{C}^{(0)}_{\vec{\tau}} \cdot (\boldsymbol{\eta}^{(1)}_{\vec{\tau}})^2 \cdot \mathbf{C}^{(0)T}_{\vec{\tau}} = \tfrac{1}{2} \, \mathbf{V}^{(1)}_{\vec{\tau}} \cdot (\mathbf{L}^{(0)}_{\vec{\tau}})^{-1} \cdot \mathbf{V}^{(1)}_{\vec{\tau}}. \tag{6.35}$$

Thus the $\log^2 U$ terms are entirely predicted from the disconnected and tree-level CPW coefficients $\mathbf{L}$ and $\mathbf{V}$. The above relation can be expanded in $\lambda^{-\frac{1}{2}}$ resulting in

$$\mathbf{M}^{(2,0)}_{\vec{\tau}} = \tfrac{1}{2}\mathbf{C}^{(0,0)}_{\vec{\tau}} \cdot (\boldsymbol{\eta}^{(1,0)}_{\vec{\tau}})^2 \cdot \mathbf{C}^{(0,0)T}_{\vec{\tau}} = \tfrac{1}{2}\mathbf{V}^{(1,0)}_{\vec{\tau}} \cdot (\mathbf{L}^{(0)}_{\vec{\tau}})^{-1} \cdot \mathbf{V}^{(1,0)}_{\vec{\tau}}, \tag{6.36}$$

$$\mathbf{M}^{(2,3)}_{\vec{\tau}} = \mathbf{C}^{(0,0)}_{\vec{\tau}} \cdot \boldsymbol{\eta}^{(1,0)}_{\vec{\tau}} \cdot \boldsymbol{\eta}^{(1,3)}_{\vec{\tau}} \cdot \mathbf{C}^{(0,0)T}_{\vec{\tau}} + \tfrac{1}{2} \left[ \mathbf{C}^{(0,3)}_{\vec{\tau}} \cdot \boldsymbol{\eta}^{(1,0)}_{\vec{\tau}} \cdot \boldsymbol{\eta}^{(1,0)}_{\vec{\tau}} \cdot \mathbf{C}^{(0,0)T}_{\vec{\tau}} + \text{tr.} \right]$$

$$= \tfrac{1}{2} \left( \mathbf{V}^{(1,3)}_{\vec{\tau}} \cdot (\mathbf{L}^{(0)}_{\vec{\tau}})^{-1} \cdot \mathbf{V}^{(1,0)}_{\vec{\tau}} + \mathbf{V}^{(1,0)}_{\vec{\tau}} \cdot (\mathbf{L}^{(0)}_{\vec{\tau}})^{-1} \cdot \mathbf{V}^{(1,3)}_{\vec{\tau}} \right). \tag{6.37}$$

In the second line above we have used $\mathbf{C}^{(0,3)}_{\vec{\tau}} \mathbf{C}^{(0,0)T}_{\vec{\tau}} + \mathbf{C}^{(0,0)}_{\vec{\tau}} \mathbf{C}^{(0,3)T}_{\vec{\tau}} = 0$, and that $\boldsymbol{\eta}^{(1,0)}_{\vec{\tau}}$ and $\boldsymbol{\eta}^{(1,3)}_{\vec{\tau}}$ are diagonal and hence commute. The first condition at $(\alpha')^3$ is obvious, since $C^{(0,3)}_{\vec{\tau}} = 0$. A formula like (6.37) holds at $(\alpha')^5$ upon replacing $\mathbf{V}^{(1,5)}_{\vec{\tau}}$.

$\underline{\log^1(U)}$: In fact, for general charges, more information can be predicted about the structure

of the one-loop amplitude. In the window region it is possible to predict the form of the single $\log U$ behaviour. We arrange the one-loop partial wave coefficients into a vector $\mathbf{H}^{(2)}_{(q_1 q_2);\vec{\tau}}$ labelled by a fixed pair of charges $(q_1 q_2)$ as above,

$$\mathbf{H}^{(2)}_{(q_1 q_2);\vec{\tau}} = \mathbf{C}^{(1)}_{(q_1 q_2);\vec{\tau}} \cdot \boldsymbol{\eta}^{(1)}_{\vec{\tau}} \cdot \mathbf{C}^{(0)T}_{\vec{\tau}} = \mathbf{N}^{(1)}_{(q_1 q_2);\vec{\tau}} \cdot \left( \mathbf{L}^{(0)}_{\vec{\tau}} \right)^{-1} \cdot \mathbf{V}^{(1)}_{\vec{\tau}} . \tag{6.38}$$

Recall that $\mathbf{C}^{(1)}_{(q_1 q_2);\vec{\tau}}$ exists only for operators $\mathcal{K}_{\vec{\tau}}$ such that $\tau < q_1 + q_2$. Recall also that for a correlator $\langle \mathcal{O}_p \mathcal{O}_q \mathcal{O}_p \mathcal{O}_q \rangle$ there is no Window.

In the cases with no residual degeneracy of the tree-level supergravity anomalous dimension [56] the leading order three-point functions may themselves be un-mixed as in [64, 65, 101]. They can then be used to calculate the $\mathbf{C}^{(1)}_{q_1 q_2;\vec{\tau}}$ using (6.25), and finally the one-loop $\log(u)$ contribution from the first equality above. This was the procedure used in [1] to construct the $\langle \mathcal{O}_2 \mathcal{O}_2 \mathcal{O}_p \mathcal{O}_p \rangle$ family of correlators and led to much new OPE data as described in Appendix A. However, for the general case where the residual degeneracy makes this impossible we must instead use the matrix equations given by the second equality.

If we now expand in $\lambda^{-\frac{1}{2}}$ we find

$$\mathbf{H}^{(2,0)}_{(q_1 q_2);\vec{\tau}} = \mathbf{N}^{(1,0)}_{(q_1 q_2);\vec{\tau}} \cdot \left( \mathbf{L}^{(0,0)}_{\vec{\tau}} \right)^{-1} \cdot \mathbf{V}^{(1,0)}_{\vec{\tau}} , \tag{6.39}$$

$$\mathbf{H}^{(2,3)}_{(q_1 q_2);\vec{\tau}} = \mathbf{N}^{(1,3)}_{(q_1 q_2);\vec{\tau}} \cdot \left( \mathbf{L}^{(0,0)}_{\vec{\tau}} \right)^{-1} \cdot \mathbf{V}^{(1,0)}_{\vec{\tau}} + \mathbf{N}^{(1,0)}_{(q_1 q_2);\vec{\tau}} \cdot \left( \mathbf{L}^{(0,0)}_{\vec{\tau}} \right)^{-1} \cdot \mathbf{V}^{(1,3)}_{\vec{\tau}} . \tag{6.40}$$

$\underline{\log^0(U)}$: Finally, we can also obtain information about the $(\log U)^0$ terms in the below-window region,

$$\mathbf{K}^{(2)}_{q_1 q_2 q_3 q_4} = \mathbf{C}^{(1)}_{(q_1 q_2);\vec{\tau}} \cdot \mathbf{C}^{(1)}_{(q_3 q_4);\vec{\tau}}{}^{T} = \mathbf{N}^{(1)}_{(q_1 q_2);\vec{\tau}} \cdot \left( \mathbf{L}^{(0)}_{\vec{\tau}} \right)^{-1} \cdot \mathbf{N}^{(1)}_{(q_3 q_4);\vec{\tau}}{}^{T} . \tag{6.41}$$

Once again we can expand in $\lambda^{-\frac{1}{2}}$ to obtain,

$$\mathbf{K}^{(2,0)}_{q_1 q_2 q_3 q_4} = \mathbf{N}^{(1,0)}_{(q_1 q_2);\vec{\tau}} \cdot \left( \mathbf{L}^{(0,0)}_{\vec{\tau}} \right)^{-1} \cdot \mathbf{N}^{(1,0)}_{(q_3 q_4);\vec{\tau}}{}^{T} , \tag{6.42}$$

$$\mathbf{K}^{(2,3)}_{q_1 q_2 q_3 q_4} = \mathbf{N}^{(1,3)}_{(q_1 q_2);\vec{\tau}} \cdot \left( \mathbf{L}^{(0,0)}_{\vec{\tau}} \right)^{-1} \cdot \mathbf{N}^{(1,0)}_{(q_3 q_4);\vec{\tau}}{}^{T} + \mathbf{N}^{(1,0)}_{(q_1 q_2);\vec{\tau}} \cdot \left( \mathbf{L}^{(0,0)}_{\vec{\tau}} \right)^{-1} \cdot \mathbf{N}^{(1,3)}_{(q_3 q_4);\vec{\tau}}{}^{T} . \tag{6.43}$$

which give the OPE predictions in terms of tree level data. Note, the Below Window predictions are non trivial for the first time only at one-loop!

The double logarithmic behaviour at one-loop in supergravity has been studied extensively [1, 63, 64, 66, 70]. It has been used to make predictions for the form of the one-loop correlator both in position [1, 64, 66] and Mellin space [55, 63]. The relations (6.39) and (6.42) only become relevant for correlators with multiple $su(4)$ channels. These have been studied in [66] with several explicit examples constructed in position space. The complication in supergravity comes from the fact that both Window and Below Window predictions are non-trivial at all spins, and it remains difficult to find the one-loop Mellin amplitude

explicitly for generic external charges.

Our focus will be on the $(\alpha')^3$ one-loop correlator and thus equations (6.37), (6.40) and (6.43). The advantage of studying the $\mathcal{M}^{(2,3)}$ amplitude, compared to supergravity, stems from the truncation in spin of the spectrum of two-particle operators exchanged. This simplifies the structure of the OPE predictions in the Window and Below Window regions, and will indeed allow us to find an expression for the Mellin amplitude $\mathcal{M}^{(2,3)}_{\vec{p}}$ for general $\vec{p}$. Given our understanding here, we believe that the same pattern applies at all orders in $\alpha'$, even though computationally it will become a bit more involved.

### 6.1.4   Window splitting

We already mentioned the existence of degenerate correlators, i.e. correlators that have the same values of $\Sigma$ and $|c_s|, |c_t|, |c_u|$, and therefore such that $\mathbf{\Gamma}$ is unchanged. For example, two correlators whose values of $p_1 + p_2$ and $p_3 + p_4$ swap, and the other $p_i + p_j$ are unchanged. At order $\mathcal{M}^{(1,0)}$ and $\mathcal{M}^{(1,3)}$ these correlators are necessarily proportional to each other since both these Mellin amplitudes do not distinguish them. The situation at one loop is quite different. The crucial point is that the OPE predictions now involve a sum over operators which mixes degenerate and non-degenerate data at tree level.

The example of $\langle \mathcal{O}_3 \mathcal{O}_3 \mathcal{O}_3 \mathcal{O}_5 \rangle$ and $\langle \mathcal{O}_4 \mathcal{O}_4 \mathcal{O}_2 \mathcal{O}_4 \rangle$ discussed in (6.2) is quite useful to see what is going on. The one-loop predictions in the Window will involve

$$
\begin{aligned}
\left[ \mathbf{N}^{(1,0)}_{35} \right]_{(rs)=(24),(33)} &\quad ; \quad \left[ \mathbf{N}^{(1,0)}_{44} \right]_{(rs)=(24),(33)}, \\
\left[ \mathbf{N}^{(1,3)}_{35} \right]_{(rs)=(24),(33)} &\quad ; \quad \left[ \mathbf{N}^{(1,3)}_{44} \right]_{(rs)=(24),(33)},
\end{aligned}
\tag{6.44}
$$

with indices $(rs)$ running over the rectangle at $\tau = 6$ in [020], i.e. $\{(24), (33)\}$. So even though the purple colored coefficients come from correlators degenerate at tree level, and which are therefore proportional to each other, the remaining data is genuinely distinct. Thus, after matrix multiplication (see (6.38) and (6.41)), the one-loop result will distinguish these correlators. The general statement will be that one-loop OPE predictions in the window lift the tree-level degeneracy of correlators. This was first noticed in supergravity in [66], and the same mechanism is at work here.

## 6.2   The one loop Mellin amplitude $\mathcal{M}^{(2,3)}$

In this section we translate the structure of the one-loop OPE data into the Mellin space amplitude. We claim that

$$
\mathcal{M}^{(2,3)}_{\vec{p}} = \left[ \mathcal{W}^{(AW)}_{\vec{p}}(\hat{s}, \check{s}) + \mathcal{R}^{(W)}_{\vec{p}}(\hat{s}, \check{s}) + \mathcal{B}^{(BW)}_{\vec{p}}(\hat{s}, \check{s}) \right] + \texttt{crossing}\,.
\tag{6.45}
$$

i.e. $\mathcal{M}_{\vec{p}}^{(2,3)}$ naturally splits into three pieces, described below.

Our starting point will be to use the data from the OPE, at tree level Above Window, to completely fix $\mathcal{W}^{(AW)}$. We will find that

$$\mathcal{W}_{\vec{p}}^{(AW)}(\hat{s}, \check{s}) = \tilde{\psi}^{(0)}(-\mathbf{s}) \; w(\hat{s}, \check{s}, c_s; \Sigma) \tag{6.46}$$

where $w$ is a determined polynomial, and $\tilde{\psi}^{(0)} = \psi^{(0)} + \gamma_E$ is a digamma function. The latter accounts for the fact that $\mathcal{W}^{AW}$ has to contribute to triple poles in order to generate a $\log^2 U$ discontinuity, and the $\mathbf{\Gamma}$ factor only gives at most double poles Above Window.[1] The restricted dependence of $w$ on the Mellin variables comes from the fact that the OPE has support only on $a = l = 0$, and therefore $w$ is function of $\mathbf{s}$-type variables only, thus $w(\hat{s}, \check{s}, c_s; \Sigma)$.

Note: The argument of $\tilde{\psi}^{(0)}$ being $-\mathbf{s}$ implies that contributions from $\mathcal{W}^{(AW)}$ are not restricted to Above Window, but actually start at $\mathbf{s} = 0$. As we explained in the previous section, this is one unit above the unitarity bound $\mathbf{s} + 1 = 0$, therefore $\mathcal{W}^{(AW)}$ contributes also to the $\log^1 U$ and $\log^0 U$ discontinuities, respectively, in the Window and Below Window. This fact will play an important role as observed in [1], and explained below.

Next, we will use window OPE data, and also contributions coming from $\mathcal{W}^{(AW)}$, to fix the remainder function in the Window

$$\mathcal{R}_{\vec{p}}^{(W)}(\hat{s}, \check{s}) = \sum_{z=0}^{6} \frac{(\check{s} + \frac{p_1+p_2}{2} - z)_{z+1} \; r_{\vec{p};z}^{+}(\hat{s}, \check{s}) + (\check{s} + \frac{p_3+p_4}{2} - z)_{z+1} \; r_{\vec{p};z}^{-}(\hat{s}, \check{s})}{\mathbf{s} - z} \,, \tag{6.47}$$

with $r^{\pm}$ are polynomials. We shall call $\mathcal{R}$ a remainder function since it gives the part of the OPE Window predictions not captured by $\mathcal{W}^{(AW)}$. Remarkably, the interplay with $\mathcal{W}^{(AW)}$ will truncate the sum over $z$ to a maximum of seven poles! It will be clear that this function should also be extended to contribute to the Below Window region.

The determination of the function $\mathcal{R}^{(W)}$ is a central result of our investigation, since it characterises the way the *window splitting* is implemented in Mellin space. We called this phenomenon "sphere splitting", and it will be discussed in more detail in section 6.2.2.

Finally, using Below Window data, as well as contributions now coming from both $\mathcal{W}^{(AW)}(\hat{s}, \check{s})$ and $\mathcal{R}^{(W)}(\hat{s}, \check{s})$, we fix the last piece of our ansatz[2]

$$\mathcal{B}_{\vec{p}}^{(BW)}(\hat{s}, \check{s}) = \sum_{z=0}^{2} \frac{(\check{s} + \frac{p_1+p_2}{2} - z)_{z+1} (\check{s} + \frac{p_3+p_4}{2} - z)_{z+1}}{\mathbf{s} - z} b_{\vec{p};z}(\hat{s}, \check{s}) \,. \tag{6.48}$$

---

[1] Note the formula $\Gamma[-\hat{s} + \frac{p_1+p_2}{2}]\Gamma[-\hat{s} + \frac{p_3+p_4}{2}]\psi(-\mathbf{s})\mathcal{W}^{(AW)}U^{\hat{s}} \to \frac{1}{2}\left[\partial_{\hat{s}}^2 \frac{1}{(\hat{s}-\mathfrak{n})}\right]\mathcal{W}^{(AW)}U^{\hat{s}}$.

[2] The division between $\mathcal{R}^{(W)}$ and $\mathcal{B}^{(BW)}$ is our choice. We do so because the explicit solution for $\mathcal{R}^{(W)}$ will have nice analytic properties Below Window, see section 6.2.2.

This is also a remainder function, capturing the predictions of the OPE in the Below Window region after contributions from both $\mathcal{W}^{(AW)}(\hat{s}, \check{s})$ and $\mathcal{R}^{(W)}(\hat{s}, \check{s})$ are taken into account. We find that $\mathcal{B}^{(BW)}(\hat{s}, \check{s})$ also truncates, this time to just three poles in $z$. Again $b_{\vec{p};z}(\hat{s}, \check{s})$ is polynomial.

In practice to arrive at the above expressions we first make an ansatz in Mellin space and perform the contour integration to arrive at an expression in position space which we can then expand in conformal blocks and match against the known OPE data.

### 6.2.1   Above window

The $\log^2 U$ terms at order $\lambda^{-\frac{3}{2}}$ have a very simple form [1]. The reason behind this is that only operators with $\ell_{10} = 0$ receive an order $\lambda^{-\frac{3}{2}}$ contribution to their anomalous dimensions. Therefore, in the following expression for $\mathbf{M}_{\vec{\tau}}^{(2,3)}$,

$$[\mathbf{M}_{\vec{\tau}}^{(2,3)}]_{(p_1 p_2),(p_3 p_4)} = \sum_{\mathcal{K} \in R_{\vec{\tau}}} C_{p_1 p_2 \mathcal{K}}^{(0,0)} \eta_{\mathcal{K}}^{(1,0)} \eta_{\mathcal{K}}^{(1,3)} C_{p_3 p_4 \mathcal{K}}^{(0,0)} . \tag{6.49}$$

only a single operator $\mathcal{K}$ contributes to the sum for a given $\tau$ and $b$! In Figure 6.2 this is the operator labelled by the leftmost corner of the rectangle. If we now insert this expression into the sum over long superconformal blocks to obtain the expansion of the $\log^2 U$ discontinuity, we find an expression that is almost identical to the expansion of the $\log U$ discontinuity at tree level,[1] but for the insertion of a factor of $\eta^{(1,0)}$ restricted to $\ell_{10} = 0$. By construction this factor is a number (which includes the value of the denominator of $\eta^{(1,0)}$) multiplying the eigenvalue of a certain eight-order Casimir operator $\Delta^{(8)}$ introduced in [57] in position space, see in particular [1].

In Mellin space, the $\log^2 U$ contribution comes from $\mathbf{\Gamma} \times \tilde{\psi}^{(0)}(-\mathbf{s})$, which is the source of all triple poles. The knowledge of the $\log^2 U$ coefficient will therefore fully fix

$$\mathcal{W}_{\vec{p}}^{(AW)}(\hat{s}, \check{s}) = \tilde{\psi}^{(0)}(-\mathbf{s}) \; w(\hat{s}, \check{s}, c_s; \Sigma). \tag{6.50}$$

From the discussion about the special form of (6.49) we infer that, apart for an overall prefactor, the polynomial $w$ is given by applying $\Delta^{(8)}$ (rewritten in Mellin space) to 1, where the latter is (up to a numerical factor) the tree level amplitude in the Virasoro Shapiro amplitude at order $(\alpha')^3$.

We have written the full expression of $w(\hat{s}, \check{s}, c_s; \Sigma)$ in the Appendix. Expanded in all variables it has the form

$$w(\hat{s}, \check{s}, c_s; \Sigma) = +\frac{(\Sigma - 1)_3}{180}\Big( -36c_s^2 + 9c_s^4 + 36c_s^2 \check{s} + \ldots + 8\check{s}\hat{s}^3 \Sigma^4 + 2\hat{s}^4 \Sigma^4 \Big). \tag{6.51}$$

---

[1]i.e. $\sum_{\mathcal{K} \in R_{\vec{\tau}}} C_{(p_1 p_2)\mathcal{K}}^{(0,0)} \eta_{\mathcal{K}}^{(1,3)} C_{p_3 p_4 \mathcal{K}}^{(0,0)}$.

A more compact representation can be given by the following double integral,

$$w(\hat{s}, \check{s}) = \frac{i}{2\pi} \int_0^\infty \frac{d\alpha}{\alpha} \int_\mathcal{C} d\beta \; e^{-\alpha-\beta} \alpha^{\Sigma+2} (-\beta)^{-\Sigma+1} \; \widetilde{w}(\alpha, \beta) \tag{6.52}$$

where $\mathcal{C}$ is the Hankel contour. The $\alpha$ integral is the $\Gamma$ function integral, and the $\beta$ integral the reciprocal $\Gamma$ function integral. Note that the integral in $\alpha$ is nothing but the integral used by Penedones to study flat space limit [54], and the $\beta$-integral generalises that to the compact space.

Then, $\widetilde{w}_{\vec{p}}(\alpha, \beta)$ is defined in terms of the following variables,

$$S = \alpha\hat{s} - \beta\check{s}, \qquad \tilde{S} = \alpha\hat{s} + \beta\check{s}, \tag{6.53}$$

by the expression

$$\widetilde{w}(\alpha, \beta, c_s; \Sigma) = \tag{6.54}$$
$$\frac{1}{90} (S - 3\Sigma)(S - 2\Sigma)(S - \Sigma) S + \tfrac{\Sigma^2 - c_s^2}{20} (2S^2 - 6S\Sigma + 5\Sigma^2 - c_s^2) +$$
$$- \frac{1}{30} \tilde{S}(2S^2 - 9S\Sigma + 11\Sigma^2 - 3c_s^2) + \frac{1}{180} (S^2 - 36S\Sigma + 36(\Sigma^2 - c_s^2) + 7\tilde{S}^2).$$

It is immediate to see that only $c_s^{2\mathbb{N}}$ appear. In fact, since $w$ is a function of $\mathbf{s}$ variables only, the crossing relations,

$$
\begin{array}{ccc}
\mathcal{M}_{p_1 p_2 p_3 p_4}(\hat{s}, \hat{t}, \check{s}, \check{t}) & = & \mathcal{M}_{p_4, p_3, p_2, p_1}(\hat{s}, \hat{t}, \check{s}, \check{t}) \\
\| & & \| \\
\mathcal{M}_{c_s, c_t, c_u}(\hat{s}, \hat{t}, \check{s}, \check{t}) & & \mathcal{M}_{-c_s, c_t, -c_u}(\hat{s}, \hat{t}, \check{s}, \check{t})
\end{array}
\tag{6.55}
$$

implies that $w$ is function of $c_s^2$, i.e. since there is no $c_u$ dependence the invariance under $c_s \leftrightarrow -c_s$ follows. In particular, as for $\boldsymbol{\Gamma}$ factor, the polynomial $w(\hat{s}, \check{s}, c_s; \Sigma)$ has the same bonus property.

Let us emphasise that the OPE does not immediately predict $\tilde{\psi}^{(0)}(-\mathbf{s})$. The Above Window region only requires $\Gamma[\frac{p_1+p_2}{2} - \hat{s}]\Gamma[\frac{p_3+p_4}{2} - \hat{s}]\tilde{\psi}^{(0)}(-\hat{s} + p_{\max})$, since $\hat{s} \geq p_{\max}$ is where the triple poles are. However, the presence of $\tilde{\psi}^{(0)}(-\mathbf{s})$ is strongly motivated by the limit in which the charges $p_i$ are large, and therefore $\mathbf{s}$ is large [55]. As explained already in the Introduction, the key observation is that in this limit $\mathbf{s}$ becomes a 10d Mandelstam invariant and the Mellin amplitude asymptotes the 10d flat space scattering amplitude. In the present case we must recover the $\log(-\mathbf{s})$ of the type IIB flat space amplitude, and the latter comes from $\tilde{\psi}^{(0)}(-\mathbf{s})$ in the limit of large $\mathbf{s}$. We will later show in section 6.3 that in the large $p$ limit we recover exactly the type-IIB flat space amplitude!

It follows from the presence of $\tilde{\psi}^{(0)}(-\mathbf{s})$ that the range of twists where $\mathcal{W}^{(AW)}$ contributes

is not restricted to the Above Window region, $\hat{s} \geq p_{\text{max}}$, where $\mathcal{W}^{(AW)}$ naturally lives, but embraces the bigger region bounded from below by the locus $\mathbf{s} = 0$. We now understand that $\mathcal{W}^{(AW)}$ contributes to the one-loop correlator starting from the first two-particle operator in the Below Window region at $\tau = 2a + b + 4$. Consequently $\mathcal{W}^{(AW)}$ gives contributions that will add to those of $\mathcal{R}^{(W)}$ function and $\mathcal{B}^{(BW)}$ in- and below- Window, respectively. The choice to write the Above Window contribution as described above has the consequence of revealing the truncation of sum over $z$ in the Window contribution to $z = 0, \ldots, 6$, rather than a range growing with the charges.

**Flat space relation of the $AdS_5 \times S^5$ amplitude**

The fact that the polynomial $w(\hat{s}, \check{s}, c_s; \Sigma)$ can be written in terms of a pre-polynomial (6.54), as in the case of the Virasoro-Shapiro amplitude studied in [60], suggests the following little game: In flat space the part of the $(\alpha')^3$ amplitude at one loop which accompanies $\log(-s)$ is $s^4$, and the tree-level $(\alpha')^7$ amplitude is proportional to $s^4 + t^4 + u^4$. Therefore, if we assemble

$$\mathcal{M}_7 \equiv w(\hat{s}, \check{s}, c_s; \Sigma) + w(\hat{t}, \check{t}, c_t; \Sigma) + w(\hat{u}, \check{u}, c_u; \Sigma) \tag{6.56}$$

we expect by construction that this quantity has the correct 10d flat space limit. Is there something more? Upon inspection, it turns out that $\mathcal{M}_7$ so constructed is actually the tree-level $(\alpha')^7$ amplitude constructed in [60, 61], up to an overall coefficient and a certain choice of ambiguities! This observation stands at the moment as a curiosity, though quite intriguing. It would be interesting to understand its origin further, and whether or not it generalises beyond this case. We will leave this for a future investigation.

### 6.2.2   The Window

The $\log^1 U$ projection of the $(\alpha')^3$ correlator in the Window has the following one-loop OPE expansion, for fixed quantum numbers $\vec{\tau}$,

$$\sum_{\mathcal{K} \in \mathcal{R}_{\vec{\tau}}} C^{(0,0)}_{p_1 p_2, \mathcal{K}} \left( \eta^{(1,3)}_{\mathcal{K}} C^{(1,0)}_{p_3 p_4, \mathcal{K}} + \eta^{(1,0)}_{\mathcal{K}} C^{(1,3)}_{p_3 p_4, \mathcal{K}} \right) + \sum_{\mathcal{K} \in \mathcal{R}_{\vec{\tau}}} C^{(0,0)}_{p_3 p_4, \mathcal{K}} \left( \eta^{(1,3)}_{\mathcal{K}} C^{(1,0)}_{p_1 p_2, \mathcal{K}} + \eta^{(1,0)}_{\mathcal{K}} C^{(1,3)}_{p_1 p_2, \mathcal{K}} \right) \tag{6.57}$$

Formula (6.57) contains two terms symmetric under $(p_1, p_2) \leftrightarrow (p_3, p_4)$. However, the two terms never contribute together. This is because the (free theory value of the) twist of the two-particle operator $\mathcal{K}$ is greater equal than $\max(p_1 + p_2, p_3 + p_4)$, and therefore in the Window either $C^{(0,0)}_{p_1 p_2, \mathcal{K}} = 0$ or $C^{(0,0)}_{p_3 p_4, \mathcal{K}} = 0$. It follows that when we compute the OPE predictions we only have access to one of the two terms at once. Nevertheless, we do expect a final formula for the coefficients which is at the same time symmetric under $(p_1, p_2) \leftrightarrow (p_3, p_4)$ and also analytic in the charges. We can imagine several scenarios of

which the simplest one is perhaps the one where a single contribution, say for concreteness the one for $p_1 + p_2 < p_3 + p_4$, is such that upon a natural analytic continuation in the charges, it automatically vanishes when $p_1 + p_2 > p_3 + p_4$, and vice-versa. The final symmetric result will then be the sum of the two contributions. This simple scenario is indeed the one realised by the amplitude.

In the analysis that follows it will prove useful to move between a Mellin space formula of the type,

$$\mathcal{H}_{\vec{p}}(U, V, \tilde{U}, \tilde{V}) = \int d\hat{s} d\hat{t} \sum_{\check{s}, \check{t}} U^{\hat{s}} V^{\hat{t}} \tilde{U}^{\check{s}} \tilde{V}^{\check{t}} \; \mathbf{\Gamma} \; \mathcal{M}_{\vec{p}}(\check{s}, \check{t}), \tag{6.58}$$

and a formula where we perform the sum over $\check{s}$ and $\check{t}$ and decompose into the basis of spherical harmonics $Y_{[aba]}$. We can start in the monomial basis, with an expression of the form

$$\int d\hat{s} d\hat{t} \; U^{\hat{s}} V^{\hat{t}} \; \Gamma_{\hat{s}} \Gamma_{\hat{t}} \Gamma_{\hat{u}} \sum_{\check{s}, \check{t}} \frac{\tilde{U}^{\check{s}} \tilde{V}^{\check{t}}}{\Gamma_{\check{s}} \Gamma_{\check{t}} \Gamma_{\check{u}}} \; \mathcal{F}_{\vec{p}}(\hat{s}, \check{s}), \tag{6.59}$$

valid for $\mathcal{F} = \{\mathcal{W}^{(AW)}, \mathcal{R}^{(W)}, \mathcal{B}^{(BW)}\}$, i.e. each one of the three functions that builds up our amplitude. The sum over $\check{s}$ and $\check{t}$ is finite, as we explained already. Then, upon decomposing into spherical harmonics we can alternatively write,

$$\int d\hat{s} d\hat{t} \; U^{\hat{s}} V^{\hat{t}} \; \Gamma_{\hat{s}} \Gamma_{\hat{t}} \Gamma_{\hat{u}} \sum_{[0b0]} Y_{[0b0]} \; \mathcal{F}_{\vec{p}}(\hat{s}, b). \tag{6.60}$$

The notation $\mathcal{F}(\hat{s}, \check{s})$ and $\mathcal{F}(\hat{s}, b)$ will then refer to $\mathcal{F}$ as being written in the monomial basis and spherical harmonic basis, respectively.

As an example, we reproduce an interesting formula for the Above Window function

$$\begin{aligned} w_{\vec{p}}(\hat{s}, b) = & \frac{(\Sigma - 1)_3}{\Gamma_{[0b0]}} \times \frac{1}{15 \times 3!} \sum_{i=0}^{4} (-1)^i \binom{4}{i} (\hat{s}(\hat{s} + 2 - i) - \tfrac{b}{2}(\tfrac{b}{2} + 2)) \\ & \times \left( \hat{s} - \frac{b+2}{2} \right)_{3-i} \left( \hat{s} + \frac{b+2}{2} \right)_{3-i} \left( \frac{p_1 + p_2}{2} - \hat{s} \right)_i \left( \frac{p_3 + p_4}{2} - \hat{s} \right)_i \end{aligned} \tag{6.61}$$

where the analogous factor of $\Gamma_{[aba]}$ function was found in [59].[1]

With either representation, i.e. $\mathcal{F}(\hat{s}, \check{s})$ and $\mathcal{F}(\hat{s}, b)$, we can perform the $\hat{s}$ and $\hat{t}$ integration, to arrive at an expression in position space which we can then decompose into conformal blocks and match against OPE predictions.

---

[1]

$$\Gamma_{[aba]}^{-1} = \frac{(\Sigma - 2)! b! (b+1)! (2 + a + b)}{\Gamma[\pm \frac{p_1 - p_2}{2} + \frac{b+2}{2}] \Gamma[\frac{p_1 + p_2}{2} + \frac{b+2}{2}] \Gamma[\frac{p_1 + p_2}{2} - \frac{b + 2a + 2}{2}] \Gamma[\pm \frac{p_3 - p_4}{2} + \frac{b+2}{2}] \Gamma[\frac{p_3 + p_4}{2} + \frac{b+2}{2}] \Gamma[\frac{p_3 + p_4}{2} - \frac{b + 2a + 2}{2}]}.$$

**Spherical harmonic basis**

We wish to compute first $\mathcal{R}_{\vec{p}}^W(\hat{s}, b)$ in the spherical harmonic basis. This is derived from matching the $\log^1 U$ projection of the amplitude, i.e.

$$\int d\hat{s}d\hat{t} \; U^{\hat{s}} V^{\hat{t}} \; \Gamma_{\hat{s}}\Gamma_{\hat{t}}\Gamma_{\hat{u}} \left( \sum_b Y_{[0b0]} \left[ \mathcal{W}_{\vec{p}}^{(AW)}(\hat{s}, b) + \mathcal{R}_{\vec{p}}^{(W)}(\hat{s}, b) \right] + \texttt{crossing} \right) \Bigg|_{\log^1 U} \qquad (6.62)$$

with the prediction from the OPE in the Window. Schematically, we expect

$$\mathcal{R}_{\vec{p}}^{(W)}(\hat{s}, b) = \sum_n \frac{\#}{\hat{s} - n} \qquad ; \qquad n \geq \min\left(\frac{p_1 + p_2}{2}, \frac{p_3 + p_4}{2}\right). \qquad (6.63)$$

The task will be to find the residues $\#$ for the various values of the twist in the Window Region, here labelled by values of $\tau = 2n$. In (6.62) we have already restricted the summation to $a = 0$, as a consequence of the truncation to spin zero valid at order $(\alpha')^3$.

In practice, say we focus on the **s** channel, we will pick double poles in $\hat{s}$ in the Window (this will select the $\log^1 U$ contribution), perform the $\hat{t}$ integral, and obtain a function in position space. This function contains up to $\log^1 V$ and $\log^0 V$ contributions (since there is no $\tilde{\psi}(-\mathbf{t})$ in the **s** channel). Note that for given power of $U$, both $\log^1 V$ and $\log^0 V$ come with a non trivial rational function of $V$. These contributions are analytic in the small $x, \bar{x}$ expansion, which is the expansion of the blocks we want to match.[1]

As in the case of $\langle \mathcal{O}_2 \mathcal{O}_2 \mathcal{O}_p \mathcal{O}_p \rangle$ considered in [1], we find that *only five poles* are necessary to fit the OPE predictions[2]. In the sector $p_1 + p_2 \leq p_3 + p_4$, we find

$$\mathcal{R}_{\vec{p}}^-(\hat{s}, b) = \sum_{n \geq \frac{p_1 + p_2}{2}} \frac{\gamma_{\vec{p}}(n, b)}{\Gamma[5 - n + \frac{p_1 + p_2}{2}]\Gamma[\frac{p_3 + p_4}{2} - n]} \frac{\mathtt{R}_{\vec{p}}^-(n, b)}{(\hat{s} - n)}, \qquad (6.64)$$

where the minus superscript stands for $p_1 + p_2 \leq p_3 + p_4$, then $n = \frac{p_1 + p_2}{2}, \frac{p_1 + p_2}{2} + 1, \ldots$ runs over half-twists, and

$$\gamma_{\vec{p}}(n, b) = \frac{b!(b+1)!(b+2)}{\Gamma\left[\pm\frac{p_{12}}{2} + \frac{b+2}{2}\right]\Gamma\left[\pm\frac{p_{43}}{2} + \frac{b+2}{2}\right]} \frac{\left(\frac{p_1 + p_2}{2} - \frac{b+2}{2}\right)_3 \left(\frac{p_1 + p_2}{2} + \frac{b+2}{2}\right)_3}{\Gamma\left[n - \frac{b+2}{2}\right]\Gamma\left[n + \frac{b+2}{2}\right]} \qquad (6.65)$$

---

[1] It is actually convenient to resum the OPE predictions to exhibit the $\log V$ contribution explicitly, then match. This type of resummation was called a one-variable resummation in [66] see section 4.3.

[2] In $\langle ppqq \rangle$, fix the $su(4)$ channel to start with, and look at the residue of the first pole as function of $p$ and $q$. The range of $p, q$ is infinite and this gives a $p, q$ dependent polynomial in the numerator and three $\Gamma$ functions in the denominator. We then vary the $su(4)$ channel, introducing $b$. By studying in the same way the second pole, the third pole, etc..., we recognise $\Gamma[\frac{p_3 + p_4}{2} - n]\Gamma[n - \frac{b+2a+2}{2}]\Gamma[n + \frac{b+2}{2}]$. Thus, even though we can access five values of the twist, i.e. five poles, we can single out $\Gamma[5 + \frac{p_1 + p_2}{2} - n]$ from looking at $B^3$ where $B := \frac{b(b+4)}{4}$.

and

$$\mathtt{R}_{\vec{p}}^{-}(n,b) = \frac{B^3}{15} + \frac{(\Sigma^2 + 14\Sigma - (c_s)^2 - 10c_s + 28 - 2(c_{tu})^2)B^2}{60} + \dots$$
$$- 2n\left[\frac{(\Sigma+3)B^2}{15} + \frac{(\Sigma^2 + 7\Sigma - (c_s)^2 - c_s + 12 - (c_{tu})^2(\Sigma+3))B}{30} + \dots\right] \qquad ; \qquad B := \frac{b(b+4)}{4}.$$

(6.66)

The full expression for $\mathtt{R}^-$ can be found in the appendix, it is made of simple polynomials. Note that above we have used the notation $c_{tu} = c_t + c_u$.

The fact that only five poles in $\mathcal{R}^-$ are needed to fit the OPE data is reflected by the factor $1/\Gamma[5 + \frac{p_1+p_2}{2} - n]$, which automatically truncates when $n \geq \frac{p_1+p_2}{2} + 5$. It implies that beyond the fifth pole, the OPE predictions are fully captured already by the function $\mathcal{W}^{AW}$! This is quite remarkable given that we are evaluating $\mathcal{W}^{AW}$ in the Window. Let us also emphasise that $\mathtt{Res}_{\vec{p}}$ turns out to be only a linear polynomial in $n$. Considering that we are fitting five poles, this is a non-trivial consistency check of our formula. A closely related formula holds for $\mathcal{R}^+$ in the sector $p_1 + p_2 \geq p_3 + p_4$. Let us see why:

Above we considered the case $p_1 + p_2 < p_3 + p_4$ and found $\mathcal{R}^-$, but note that it automatically vanishes when $p_1 + p_2 > p_3 + p_4$. This is because of $1/\Gamma[\frac{p_3+p_4}{2} - n]$ and the fact that $n \geq \frac{p_1+p_2}{2}$ in the sum. Therefore, we are free to add both contributions in one formula and write the following symmetric and analytic expression

$$\mathcal{R}_{\vec{p}}^{(W)}(\hat{s},b) = \mathcal{R}_{\vec{p}}^{-}(\hat{s},b) + \mathcal{R}_{\vec{p}}^{+}(\hat{s},b) \qquad ; \qquad \mathcal{R}_{p_1p_2p_3p_4}^{+}(\hat{s},b) = \mathcal{R}_{p_4p_3p_2p_1}^{-}(\hat{s},b) \qquad (6.67)$$

where $\mathcal{R}^+$ is related to $\mathcal{R}^-$ by swapping charges in the appropriate way. Using the $c_s, c_t, c_u$ parametrisation, $\mathcal{R}_{\{c_s,c_t,c_u\}}^{+}(\hat{s},b) = \mathcal{R}_{\{-c_s,c_t,-c_u\}}^{-}(\hat{s},b)$.

Let us now come back to the Window splitting mentioned in section 6.1.4. There, we explained that degenerate correlators at tree level are those correlators with the same values of $\Sigma$ and $|c_s|, |c_t|, |c_u|$ which therefore are proportional to each other at order $\mathcal{M}^{(1,0)}$ and $\mathcal{M}^{(1,3)}$, because the bonus property is preserved. We can see from the explicit expressions for $\mathtt{Res}_{\vec{p}}(n,b)$ that at one-loop this is not the case anymore. Coming back to our guiding example of $\vec{p} = (3335)$ and $\vec{p} = (4424)$, we can see that

$$\mathtt{R}_{\vec{p}=3335}^{-}(n=3, b=2) = -\frac{336}{5} \qquad ; \qquad \mathtt{R}_{\vec{p}=4424}^{+}(n=3, b=2) = -\frac{348}{5} \qquad (6.68)$$

where the LHS is simply the evaluation of (6.66), while the RHS is obtained from the (6.66) upon $c_s \to -c_s$ and $c_u \to -c_u$. As promised, the one-loop OPE distinguishes these two correlators in the Window. Note instead that if we project the correlators onto the $\log^2 U$ discontinuity Above Window, the corresponding contributions are still degenerate.

Figure 6.3 illustrates the general structure of poles of the remainder function, as we have obtained it from OPE data. Notice now that $\mathcal{R}^{(W)}(\hat{s},b)$ can be analytically continued Below
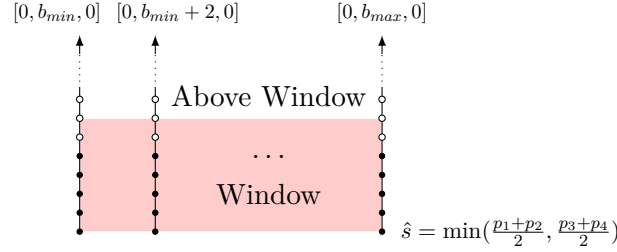
**Figure 6.3:** Pole structure of the remainder function in the basis of spherical harmonics. Black dots indicate a non-zero residue. Un-filled dots only receive contributions from $\mathcal{W}^{(AW)}$.

Window. Quite nicely, the factor $1/\Gamma\left[n - \frac{b+2}{2}\right]$ ensures vanishing at the unitarity bound, thus giving the correct physical behaviour not just in the Window, where the function was fitted, but also Below Window! We infer that the remainder function can be understood more properly to descend onto the range of twists above the unitarity bound, which means we are free to start the sum in (6.64) from $n \geq \frac{b+4}{2}$. At this point it is clear that the pole structure of $\mathcal{R}^{(W)}$ will be naturally labelled by bold font variables, in complete analogy with the way $\mathcal{W}^{(AW)}$ descends in- and below- Window. Figure 6.4 illustrates the poles from the latter viewpoint.
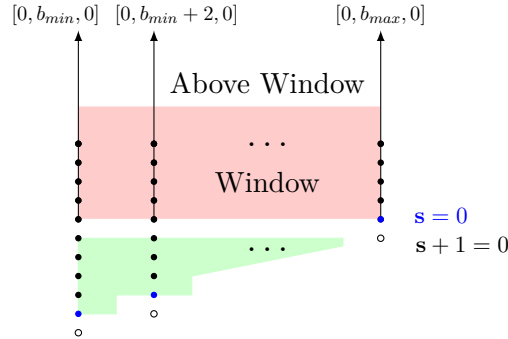


**Figure 6.4:** Pole structure of the remainder function after continuation Below Window.

To see more clearly the structure of poles in $\mathbf{s}$, from the Window down to the Below Window, let us point out that when we look at the $[0b_{max}0]$ channel, the locus $\mathbf{s} = 0$ pinpoints the bottom of the window, below there is only the unitarity bound at $\mathbf{s} + 1 = 0$. Lowering $b < b_{max}$, and looking at the $[0b0]$ channels, the same locus $\mathbf{s} = 0$ enters the below window region depicted in green.

**Monomial basis, Crossing, and Sphere splitting**

In this section we will turn the expression $\mathcal{R}^{(W)}(\hat{s}, b)$, written in the basis of harmonics $Y_{[0b0]}$, into the monomials basis $U^{\check{s}} V^{\check{t}}$, yielding the final Mellin amplitude corresponding to

the Window region. The result right away is

$$\mathcal{R}_{\vec{p}}^{(W)}(\hat{s}, \check{s}) = \sum_{z=0}^{6} \frac{1}{\mathbf{s} - z} \left[ (\check{s} + \tfrac{p_1+p_2}{2} - z)_{z+1} \ r_{\vec{p};z}^{+}(\hat{s}, \check{s}) + (\check{s} + \tfrac{p_3+p_4}{2} - z)_{z+1} \ r_{\vec{p};z}^{-}(\hat{s}, \check{s}) \right], \quad (6.69)$$

where the notation $r^{\pm}$ refers to the fact that $p_1 + p_2 = \Sigma + c_s$ and $p_3 + p_4 = \Sigma - c_s$. The polynomials $r^{\pm}$ are related to each other,

$$r_{\vec{p}}^{+} = r_{\{-c_s, -c_t, c_u\}} \qquad ; \qquad r_{\vec{p}}^{-} = r_{\{+c_s, +c_t, c_u\}}, \quad (6.70)$$

and given in the appendix. There are seven of them, since $z = 0, \ldots, 6$. The first few are are simple to write down, see the list in (6.74).

The result for $\mathcal{R}^{(W)}$ in (6.69) has two important properties, which are tied to the window splitting described in the previous section. These properties go together and are 1) the split of $\mathbf{\Gamma}$, and 2) the dependence of $r$ on the charges $\vec{p}$. Both these properties provide the way to distinguish between $p_1 + p_2 < p_3 + p_4$ and $p_1 + p_2 > p_3 + p_4$ at the level of the Mellin amplitude. All together this is the sphere splitting we already mentioned in the summary.

In more details: Assume $\hat{s}$ belongs to the Window, then $\hat{s} = \min(\tfrac{p_1+p_2}{2}, \tfrac{p_3+p_4}{2}) + n$ for some positive integer, $n \geq 0$. Now, from $\mathbf{s} - z = 0$ we obtain the value of $\check{s}$, through the relation $-z + \min(\tfrac{p_1+p_2}{2}, \tfrac{p_3+p_4}{2}) + \check{s} = -n$. Considering that

$$\frac{\mathcal{R}_{\vec{p}}^{(W)}(\hat{s}, \check{s})}{\Gamma[1 + \tfrac{p_1+p_2}{2} + \check{s}]\Gamma[1 + \tfrac{p_3+p_4}{2} + \check{s}]} \rightarrow$$

$$\sum_{z=0}^{6} \frac{1}{\mathbf{s} - z} \left[ \frac{r_{\vec{p};z}^{+}}{\Gamma[-z + \tfrac{p_1+p_2}{2} + \check{s}]\Gamma[1 + \tfrac{p_3+p_4}{2} + \check{s}]} + \frac{r_{\vec{p};z}^{-}}{\Gamma[1 + \tfrac{p_1+p_2}{2} + \check{s}]\Gamma[-z + \tfrac{p_3+p_4}{2} + \check{s}]} \right]$$

$$(6.71)$$

we see that only one of the two terms contributes, because

| | |
|---|---|
| $p_1 + p_2 > p_3 + p_4$ | $p_1 + p_2 < p_3 + p_4$ |
| $-z + \tfrac{p_3+p_4}{2} + \check{s} = -n$ | $-z + \tfrac{p_1+p_2}{2} + \check{s} = -n$ |
| only $r^{+}$ contributes | only $r^{-}$ contributes |

$$(6.72)$$

This splitting is analytic in the arguments of the $\Gamma$ functions, and therefore the function $r^{\pm}$, will be polynomial, i.e. there are no absolute value discontinuities. When we change basis, the sum over $z$ truncates to seven poles $z = 0, \ldots, 6!$ and we find

$$r_{\vec{p}}^{+} = r_{\{-c_s, -c_t, c_u\}} \qquad ; \qquad r_{\vec{p}}^{-} = r_{\{+c_s, +c_t, c_u\}}, \quad (6.73)$$

where $r$ is given in the appendix. Here we will quote for illustration

$$
\begin{aligned}
r_{\vec{p};6} &= \frac{(\check{s}+\frac{\Sigma+c_s}{2}-1)(\check{s}+\frac{\Sigma+c_s}{2})}{15} \,, \\
r_{\vec{p};5} &= \frac{(\check{s}+\frac{\Sigma+c_s}{2})(-30+11c_s+2c_s^2+9\Sigma+3c_s\Sigma+\Sigma^2+c_{tu}^2+30\check{s}-2\check{s}\Sigma-12\check{s}^2)}{30} \,, \\
r_{\vec{p};4} &= \frac{30\check{s}^4+10\check{s}^3(\Sigma-9)-5\check{s}(-30+11c_s+2c_s^2+11\Sigma+3c_s\Sigma+\Sigma^2+c_{tu}^2)+\ldots}{15} \,, \\
&\;\;\vdots
\end{aligned}
\tag{6.74}
$$

It is now clear how the sphere splitting on the Mellin amplitude achieves the window splitting of section 6.1.4 coming from the OPE. As mentioned already, to break the bonus property of the $\boldsymbol{\Gamma}$ we need $r_{\{c_s,c_t,c_u\}}$ to depend not only on $c_s$, but generically on all $c_s, c_t, c_u$. Considering (6.74) for the s-channel, this indeed has non trivial dependence on $c_t$ and $c_u$ (actually here only on $c_{tu} = c_t + c_u$)[1] and therefore breaks the degeneracy of correlators $\mathcal{M}^{(1,0)}$ and $\mathcal{M}^{(1,3)}$.

As an example let us consider the correlator $\langle \mathcal{O}_2 \mathcal{O}_2 \mathcal{O}_p \mathcal{O}_p \rangle$, for which we have $c_s = 2-p, \Sigma = 2+p, c_{tu} = 0$ and $\check{s} = -2$, after substituting in these values the above formulae reduce to

$$
r_{22pp;n} = 16 \binom{4}{n} \frac{(p+1)_2}{\Gamma[n+2]}.
\tag{6.75}
$$

Note, the vanishing of $r_{22pp;5}$ and $r_{22pp;6}$ ensuring consistency with the five pole picture in the spherical harmonic basis.

Let us comment further on crossing symmetry, verifying that (6.73) is consistent with crossing, and checking additional symmetries of $r$. By starting from the following (subset of crossing) relations,

$$
\mathcal{R}^{(W)}_{p_1,p_2,p_3,p_4}(\hat{s},\hat{t},\check{s},\check{t}) = \mathcal{R}^{(W)}_{p_2,p_1,p_4,p_3}(\hat{s},\hat{t},\check{s},\check{t}) = \mathcal{R}^{(W)}_{c_s,-c_t,-c_u}(\hat{s},\hat{t},\check{s},\check{t})
\tag{6.76}
$$

$$
= \mathcal{R}^{(W)}_{p_4,p_3,p_2,p_1}(\hat{s},\hat{t},\check{s},\check{t}) = \mathcal{R}^{(W)}_{-c_s,c_t,-c_u}(\hat{s},\hat{t},\check{s},\check{t})
\tag{6.77}
$$

$$
= \mathcal{R}^{(W)}_{p_3,p_4,p_1,p_2}(\hat{s},\hat{t},\check{t},\check{s}) = \mathcal{R}^{(W)}_{-c_s,-c_t,c_u}(\hat{s},\hat{t},\check{s},\check{t})
\tag{6.78}
$$

we find that $r^{\pm}$ are related to each other, and in fact are given in terms of a single function,

$$
r_{\vec{p}}^{+} = r_{\{-c_s,-c_t,c_u\}} \qquad ; \qquad r_{\vec{p}}^{-} = r_{\{+c_s,+c_t,c_u\}}.
\tag{6.79}
$$

---

[1] otherwise crossing would imply invariance under $c_s \leftrightarrow -c_s$.

Moreover, crossing shows that $r$ has the following residual symmetry[1]

$$r_{\{c_s,c_t,c_u\}} = r_{\{c_s,-c_t,-c_u\}} \qquad ; \qquad r_{\{c_s,c_t,c_u\}} = r_{\{c_s,c_u,c_t\}}. \qquad (6.80)$$

This is in fact what happens when we look at the explicit expressions of $r^{\pm}_{\vec{p};z}(\hat{s},\check{s})$.

Two final comments.

1) The truncation in the number of poles can be seen to be in one-to-one correspondence with the bound in the degree of the non factorisable polynomial appearing in the numerator of $r_{\vec{p};z}$. Under this logic we cannot have a numerator past $r_{\vec{p};6}$.

2) Notice also that $r_{\vec{p};6}$ and $r_{\vec{p};5}$ vanish in the Window precisely because of the factors $(\check{s} + \frac{p_1+p_2}{2} - 1)$ and $(\check{s} + \frac{p_1+p_2}{2})$, thus guaranteeing consistency with the five poles picture in Figure 6.3. The new picture for the poles in the monomial basis is displayed in Figure 6.5.
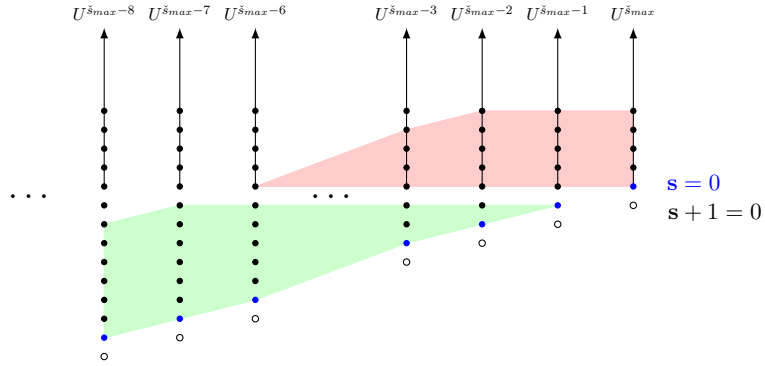


**Figure 6.5:** The pole structure of $\mathcal{R}^{(W)}$ in the monomial basis. Red: contributions lying in the window. Green: contributions lying in the Below window.

### 6.2.3 Below Window completion

So far we have focussed on the Window region. We also understood that $\mathcal{R}^{(W)}$ has an immediate analytic continuation to Below Window. Now we should ask whether we need or not an additional reminder function Below Window? The answer is affirmative and in fact we need a contribution $\mathcal{B}^{(BW)}$ of the following form,

$$\mathcal{B}^{(BW)}_{\vec{p}}(\hat{s},\check{s}) = \sum_{z=0}^{2} \frac{(\check{s} + \frac{p_1+p_2}{2} - z)_{z+1}(\check{s} + \frac{p_3+p_4}{2} - z)_{z+1}}{\mathbf{s} - z} b_{\vec{p};z}(\hat{s},\check{s}). \qquad (6.81)$$

---

[1] The second property on the l.h.s. does not follow from (6.76)-(6.78). It has to do with exchanging $c_t \leftrightarrow c_u$ and it comes from imposing (5.10) etc., on the full Mellin amplitude

$$\mathcal{R}^{(W)}_{c_s,c_t,c_u}(\hat{s},\check{s}) + \mathcal{R}^{(W)}_{c_t,c_u,c_s}(\hat{t},\check{t}) + \mathcal{R}^{(W)}_{c_u,c_s,c_t}(\hat{u},\check{u}).$$

Then, together, the contribution from $\mathcal{B}^{(BW)}$ and the contributions from both $\mathcal{W}^{(AW)}$ and $\mathcal{R}^{(W)}$ Below Window will reproduce the correct OPE prediction.

We find that only poles $z = 0, 1, 2$ receive a Below Window completion. Their explicit form is

$$\begin{aligned}
\textit{b}_{\vec{p};2} &= \tfrac{4(\check{s}+\Sigma-1)}{15} \,, \\
\textit{b}_{\vec{p};1} &= \tfrac{(1-2\check{s}-\Sigma)(4\check{s}^2-4\check{s}(1+2\Sigma)+16-c_s^2+4\Sigma-11\Sigma^2)}{15} \,, \\
\textit{b}_{\vec{p};0} &= \tfrac{16\check{s}^5-64\check{s}^4\Sigma-8\check{s}^3(c_s^2-15\Sigma^2+4)+16\check{s}^2\Sigma(c_s^2+26\Sigma^2-29)+...}{60} \,,
\end{aligned} \tag{6.82}$$

and can be read in the Appendix.

Again the truncation to three poles is in one-to-one correspondence with the bound on the degree of the polynomial. It is interesting to note the below window region does not exhibit the sphere splitting. For example in the **s**-channel these functions depend just on $c_s^2$ and thus are symmetric under $p_1 + p_2 \leftrightarrow p_3 + p_4$.

With the knowledge of $\mathcal{W}^{(AW)}$, $\mathcal{R}^{(W)}$ and $\mathcal{B}^{(BW)}$ the bootstrap program for $\mathcal{M}^{(2,3)}$ is completed, up to the following ambiguities:

**Ambiguities.**   The ambiguities we can add to the one loop function are tree-like contributions of the form of contributions to the Virasoro-Shapiro tree amplitude and do not spoil the one-loop OPE predictions in- and below- Window. For the case of $\mathcal{M}^{(2,3)}$ we can add the same as the functions corresponding to $\mathcal{M}^{(1,n=3,5,6)}$. The case $\mathcal{M}^{(1,n=7)}$ is simple to exclude since it will contribute to the flat space limit, and there is no such a contribution in flat space. Note that by construction the ambiguities listed above will contribute to the $\log^1(U)$ discontinuity, Above Window, rather than in the Window, and for the analytic part they will contribute, in the Window, rather than Below Window. In other words, they lie on top of what we fixed by the OPE data at one-loop, and therefore contribute with a free coefficient, as far as the bootstrap program is concerned.

## 6.3   Large $p$ and the flat space amplitude

In this section we will compute the large $p$ limit of [55], i.e. the limit of $\mathcal{M}^{(2,3)}$ when the external charges $p_i$ (and thus the Mellin variables) are taken to be large. By the arguments in [55], this limit reduces the amplitude to the full flat space amplitude of IIB supergravity where $\mathbf{s}, \mathbf{t}, \mathbf{u}$ become 10d Mandelstam invariants. The flat space amplitude is quite a simple amplitude, but $\mathcal{M}^{(2,3)}$ involves various pieces and therefore it will be quite an interesting computation to show the final result.

Let us focus on the **s**-channel, and introduce for convenience $\tilde{\mathbf{s}} = 2\check{s} + \Sigma$. To take the limit,

we simply need to consider

$$\{\mathbf{s}, \tilde{\mathbf{s}}, c_s\} \;\to p\,\{\mathbf{s}, \tilde{\mathbf{s}}, c_s\} \quad ; \quad \Sigma \to p\Sigma, \qquad ; \qquad p \to \infty \qquad (6.83)$$

on the various entries in the Mellin amplitude, which we know explicitly as function of $\vec{p}$. The limit on $\mathcal{W}_{\vec{p}}^{AW}$ is straightforward and reads

$$\lim_{p\to\infty} \frac{\mathcal{W}_{\vec{p}}^{AW}}{p^8} = \lim_{p\to\infty} \frac{w(\hat{s}, \check{s}, c_s; \Sigma)\psi(-\mathbf{s})}{p^8} = \frac{\zeta_3}{90}\Sigma^4 \mathbf{s}^4 \log(-\mathbf{s}) \qquad (6.84)$$

This is already the corresponding IIB flat space result [105]. We conclude that for the large $p$ limit to hold the contributions from $\mathcal{R}^{(W)}$ and $\mathcal{B}^{(BW)}$ must give vanishing contributions in the limit.

One can see that the contribution from $\mathcal{B}^{(BW)}$ are subleading w.r.t to $p^8$ in the limit. However, for each one of the $z$ poles, the contribution from $\mathcal{R}^{(W)}$ individually is not subleading! In fact, we find the following contributions:

| pole | $\displaystyle\lim_{p\to\infty} \frac{\text{contribution from pole}\,(z)}{p^8}$ |
|------|------|
| $z = 6$ | $\dfrac{(\tilde{\mathbf{s}}-c_s)^2(\tilde{\mathbf{s}}-c_s-2\Sigma)^3((\tilde{\mathbf{s}}-\Sigma-c_{tu})(\tilde{\mathbf{s}}-\Sigma+c_{tu}))^2}{7680\mathbf{s}}$ |
| $\vdots$ | $\vdots$ |
| $z = 0$ | $\dfrac{(\tilde{\mathbf{s}}-c_s)^7(\tilde{\mathbf{s}}+c_s)^2}{7680\mathbf{s}}$ |

$$(6.85)$$

By inspection of (6.85), we find that the leading term of each pole $z$ is as leading as (6.84): It has degree 8 in $p$. However, when *summing* over all contributions in the second column, the result vanishes! This cancellation is quite remarkable, given that non trivial functions of $\tilde{\mathbf{s}}$ and charges are involved. We find then that the large $p$ limit of the one-loop amplitude $\mathcal{M}^{(2,3)}$, and the flat space IIB S-matrix, match perfectly. As a byproduct of our analysis here we have given a non-trivial confirmation of the geometric picture associated with the large $p$ limit, as described in [55], and shown the self-consistency of the one-loop bootstrap program.

# Chapter 7

# Conclusions

In the first part of this thesis we studied one-loop stringy corrections to the Mellin amplitude of four single-particle operators $\langle \mathcal{O}_{p_1} \mathcal{O}_{p_2} \mathcal{O}_{p_3} \mathcal{O}_{p_4} \rangle$. We started from the $AdS_5 \times S^5$ Mellin representation in terms of variables conjugated to cross ratios, $\hat{s}, \check{s}, \hat{t}, \check{t}$, the Mellin amplitude $\mathcal{M}_{\vec{p}}$, and the following kernel of Gamma function,

$$\mathbf{\Gamma} = \frac{\Gamma[\frac{p_1+p_2}{2} - \hat{s}]\Gamma[\frac{p_3+p_4}{2} - \hat{s}]}{\Gamma[1 + \frac{p_1+p_2}{2} + \check{s}]\Gamma[1 + \frac{p_3+p_4}{2} + \check{s}]} \Gamma_\mathbf{t}\Gamma_\mathbf{u}, \tag{7.1}$$

see discussion around (5.9). Then, we gave explicit formulas for the leading order $(\alpha')^3$ amplitude at one-loop, in the form,

$$\mathcal{M}_{\vec{p}}^{(2,3)} = \left[ \mathcal{W}_{\vec{p}}^{(AW)}(\hat{s}, \check{s}) + \mathcal{R}_{\vec{p}}^{(W)}(\hat{s}, \check{s}) + \mathcal{B}_{\vec{p}}^{(BW)}(\hat{s}, \check{s}) \right] + \texttt{crossing}\,. \tag{7.2}$$

The various functions $\mathcal{W}^{(AW)}, \mathcal{R}^{(W)}, \mathcal{B}^{(BW)}$, introduced in (6.3), are described in full details in sections 6.2.1, 6.2.2, and 6.2.3, respectively. Each one is bootstrapped from the OPE, and labelled by a corresponding region of twists for the exchange of long two-particle operators. We called these regions Above Window, Window and Below Window, following [66], where the same classification was used to bootstrap the one-loop supergravity amplitude, mainly in position space. The supergravity amplitude is still a rather complicated function, due to the fact that the OPE has support for all spins. The $\alpha'$ corrections have instead finite spin supports and therefore are simpler to deal with. We believe however that the lessons from the study of $\alpha'$ amplitudes are general, and in fact best expressed in Mellin space.

The advantage of using Mellin space stems from the observation that the whole structure of poles in Mellin space can be put in correspondence with the OPE, a result due to Mack [53], which here we have upgraded to $AdS_5 \times S^5$. The pole structure takes into account both $\mathbf{\Gamma}$ and $\mathcal{M}$. The poles of $\mathcal{M}$ at tree level were shown to be captured by bold-font variables [55], i.e. poles given by equations of the form $\mathbf{s} + 1 = 0$, where $\mathbf{s} = \hat{s} + \check{s}$, similarly for $\mathbf{t}$, or

**u**. Quite nicely, this way of parametrising the poles works at one loop, with two important modifications: Poles of $\mathcal{M}$ are now of the form $\psi(-\mathbf{s})$ or $\mathbf{s} - z = 0$ for $z = 0, \dots, 6$, and the residues, compared to tree level, have generic dependence on the charges $\vec{p}$.

Considering the various contributions to $\mathcal{M}^{(2,3)}$ in (7.2) we have found:

(1) The double logarithmic discontinuity of the one-loop amplitude comes from $\mathcal{W}^{(AW)}$ and is fixed by OPE data Above Window. It takes the form of $\psi(-\mathbf{s})$ times a non-trivial polynomial in the Mellin variables, and for many aspects fits into the discussion of the tree level Virasoro-Shapiro amplitude, as given in [60]. In particular, it can be given as $\Delta^{(8)}$ on a preamplitude. This expectation will be true to all orders in $\alpha'$.

(2) The structure of $\mathcal{R}^{(W)}$ is the main novelty of the one-loop amplitude. This is determined by OPE data in the Window. This OPE data is the one responsible for lifting a bonus property of the supergravity amplitude, i.e. the fact that certain correlators are equal to each other. Such a degeneracy of amplitudes follows from the special (crossing symmetric) form of $\mathbf{\Gamma}$, and the peculiar charge dependence of the Mellin amplitudes, i.e. no dependence at all in supergravity, and $(\frac{p_1+p_2+p_3+p_4}{2} - 1)_3$ at order $(\alpha')^3$.

The first crucial result is that $\mathcal{R}^{(W)}$ takes the form,

$$\mathcal{R}^{(W)}_{\vec{p}}(\hat{s}, \check{s}) = \sum_{z=0}^{6} \frac{1}{\mathbf{s} - z} \left[ (\check{s} + \tfrac{p_1+p_2}{2} - z)_{z+1} \, r^+_{\vec{p};z}(\hat{s}, \check{s}) + (\check{s} + \tfrac{p_3+p_4}{2} - z)_{z+1} \, r^-_{\vec{p};z}(\hat{s}, \check{s}) \right], \quad (7.3)$$

and comes with two separate contributions, singled out by the $z$-dependent Pochhammers. This implies that when we look at $\mathcal{R}^{(W)}$ together with the $\mathbf{\Gamma}$ functions, the total amplitude undergoes the following split,

$$\frac{\mathcal{R}^{(W)}_{\vec{p}}}{\Gamma[1 + \tfrac{p_1+p_2}{2} + \check{s}]\Gamma[1 + \tfrac{p_3+p_4}{2} + \check{s}]}$$

$$\tag{7.4}$$

$$= \frac{1}{\mathbf{s} - z} \left[ \frac{r^+_{\vec{p};z}}{\Gamma[-z + \tfrac{p_1+p_2}{2} + \check{s}]\Gamma[1 + \tfrac{p_3+p_4}{2} + \check{s}]} + \frac{r^-_{\vec{p};z}}{\Gamma[1 + \tfrac{p_1+p_2}{2} + \check{s}]\Gamma[-z + \tfrac{p_3+p_4}{2} + \check{s}]} \right]$$

The polynomials $r^{\pm}$ are related by crossing, $r^+_{\vec{p}} = r_{\{-c_s, -c_t, c_u\}}$, $r^-_{\vec{p}} = r_{\{+c_s, +c_t, c_u\}}$, and crucially have generic charge dependence. This structure, which all together we called "sphere splitting", follows from the OPE.[1] Our result for $\mathcal{R}^{(W)}$ shows neatly how the OPE structure translates into a structure in Mellin space.

The second crucial result is the use of bold font variables to parametrise the poles of $\mathcal{M}$. For $\mathcal{W}^{(AW)}$, this implies that $\mathcal{W}^{(AW)}$ not only contributes to the OPE Above Window, where it

---

[1]From the OPE viewpoint this is also true at one-loop in supergravity [66].

was bootstrapped, but cascades to Window and Below Window regions. Because of this, the OPE predictions in the Window pick the contributions of both $\mathcal{W}^{(AW)}$ and $\mathcal{R}^{(W)}$. In this sense, $\mathcal{R}^{(W)}$ is a remainder function, but precisely for this reason, the sum over $z$ in (7.3) truncates to finitely many poles, $z = 0, \ldots 6$, rather than depending on the external charges. Quite remarkably, the result for $\mathcal{R}^{(W)}$ can itself be continued Below Window. Thus, with the same logic,

(3) The function $\mathcal{B}^{(BW)}$ is

$$\mathcal{B}_{\vec{p}}^{(BW)}(\hat{s}, \check{s}) = \sum_{z \geq 0} \frac{\left(\check{s} + \frac{p_1 + p_2}{2} - z\right)_{z+1}\left(\check{s} + \frac{p_3 + p_4}{2} - z\right)_{z+1}}{\mathbf{s} - z} \, b_{\vec{p};z}(\hat{s}, \check{s}), \tag{7.5}$$

and is itself a remainder function for $\mathcal{W}^{(AW)}$ and $\mathcal{R}^{(W)}$ in the Below Window region. In sum, the analytic properties of all these functions are quite spectacular: they properly continue from the Above Window down to the Below Window region, and correctly switch off outside the physical range of relevance.

Finally, we studied the 10d flat space limit, using the large $p$ limit of [55]. The consistency with the flat space amplitude of IIB supergravity is again quite remarkable. The limit on $\mathcal{W}^{(AW)}$ is already giving the flat amplitude, and naively, each pole in $z$ from $\mathcal{R}^{(W)}$ adds a non vanishing contribution, non trivial in both $\check{s}$ and the charges. However, upon summing over $z$ all these extra contributions correctly cancel out!

Let us conclude with an outlook. Our main focus has been understanding the structure of the amplitude and the way Mellin space realises the various features of the OPE predictions at one-loop. We focused on the $(\alpha')^3$ contribution, but we believe that the logic behind the construction of $\mathcal{M}^{(2,3)}$ is valid to all orders in $(\alpha')^{n+3}$. In particular the sphere splitting is generic, and the number of poles in $z$ increases with $n$ but stays finite! It is only a matter of computational effort to fix the various residues in the Window and Below Window. The one-loop bootstrap program in $AdS_5 \times S^5$ is thus understood at all orders in $\alpha'$, but for the usual ambiguities, which needs additional input to be fixed. It would be interesting to find these extra constraints, either from localisation [94, 97, 98], or from sum rules [106, 107].

It would be also interesting to understand the "sphere splitting" from a diagrammatic point of view. Perhaps a 10d master amplitude can be found which undergoes the "sphere splitting" onto $\mathcal{R}^{(W)}$ in a natural way. This is partially suggested by the remarkable cancellations that take place when we tested the large $p$ flat space limit in section 6.3, and the fact that poles are parametrised by bold font variables. Perhaps this point of view would give insight on the way to arrange the one-loop supergravity result in a simple form.

# Part II

# Scattering amplitudes

# Chapter 8

# Massless kinematics

In this section we begin the study of how best to describe the kinematic space on which the amplitudes live. The momenta, $p_i^\mu$, of an $n$-point massless scattering amplitude are constrained via the massless on-shell condition and momentum conservation. As we shall see in this chapter the massless on-shell condition can be trivialised through the use of *spinor-helicity variables* $(\lambda, \tilde{\lambda})$ which we now introduce.

## 8.1 The little group

To best appreciate the benefit of introducing these new variables we begin with a general discussion, following [108–110], of particles and their transformation properties under the Lorentz group. A particle is defined as being a unitary irreducible representation of the Poincaré group. Usually, in order to diagonalise translations, particles are labelled by their momentum $p^\mu$, however, generally they can carry additional labels which we collectively call $\sigma$. To label the one-particle states of a theory we can start from a reference momentum $k^\mu$, and a basis of states $|k, \sigma\rangle$, from which we can define a basis for general momentum $p^\mu$ given by

$$|p, \sigma\rangle := U(L(p, k))|k, \sigma\rangle, \tag{8.1}$$

where $p^\mu = L^\mu_\nu(p, k)k^\nu$ and $U(L(p, k))$ is a unitary operator acting on the Hilbert space of states.

We wish to understand how the $|p, \sigma\rangle$ transforms under a general Lorentz transformation $\Lambda$, acting on our state we have

$$
\begin{aligned}
U(\Lambda)|p, \sigma\rangle &= U(\Lambda)U(L(p, k))|k, \sigma\rangle \\
&= U(L(\Lambda p, k))U(\underbrace{L^{-1}(\Lambda p, k)\Lambda L(p, k)}_{W})|k, \sigma\rangle,
\end{aligned}
$$

where moving to the second line we inserted the identity operator as $U(L(\Lambda p, k))U(L^{-1}(\Lambda p, k))$, and used the fact that $U(\Lambda_1)U(\Lambda_2) = U(\Lambda_1\Lambda_2)$.

Note, the Lorentz transformation $W$ leaves the reference momentum invariant, $W^\mu_\nu k^\nu = k^\mu$, this subset of transformations is known as the *little group*. Since the $|k, \sigma\rangle$ already provide a basis of states for momentum $k$, we may write

$$U(\Lambda)|p, \sigma\rangle = U(L(\Lambda p, k)) \sum_{\sigma'} D_{\sigma\sigma'}|k, \sigma'\rangle,$$

$$= \sum_{\sigma'} D_{\sigma\sigma'}|\Lambda p, \sigma'\rangle,$$

where $D_{\sigma\sigma'}$ furnishes a representation of the little group.

In four dimensions, for massless particles $p^2 = 0$, the reference momentum can be taken to be $k^\mu = (E, 0, 0, E)$ i.e. a particle travelling along the $z$-axis. The little group is therefore given by $SO(2) \cong U(1)$, corresponding to rotations around the $z$-axis, the representations of which are labelled by the *helicity $h$* of the particle.

The consequence of this discussion for amplitudes is that, under a Lorentz transformation of the momentum, the amplitudes transform under representations of the little group for each particle i.e. we have

$$\mathcal{A}(\{p_i, h_i\}) \mapsto \prod_i (e^{-i2h_i\theta})\mathcal{A}(\{p_i, h_i\}). \tag{8.2}$$

It is this property that we wish to make manifest by introducing the spinor-helicity variables. As we will see the spinor-helicity variables also have the desired property of trivially satisfying the massless on-shell condition $p^2 = 0$.

## 8.2   The spinor-helicity formalism

The starting point is to define the matrix $p_{\alpha\dot\alpha}$ obtained by contracting the momentum $p_\mu$ with the Pauli matrices given by

$$p_{\alpha\dot\alpha} = p_\mu \sigma^\mu_{\alpha\dot\alpha} = \begin{pmatrix} p_0+p_3 & p_1-ip_2 \\ p_1+ip_2 & p_0-p_3 \end{pmatrix}, \quad \sigma^\mu = (\mathbb{1}, \vec\sigma). \tag{8.3}$$

In these variables the on-shell condition becomes the vanishing of the determinant

$$\det(p_{\alpha\dot\alpha}) = p_0^2 - p_1^2 - p_2^2 - p_3^2 = 0. \tag{8.4}$$

This implies that the matrix $p_{\alpha\dot\alpha}$ is not full rank, and that the massless on-shell condition can be trivially satisfied by writing $p_{\alpha\dot\alpha}$ as the outer product of two vectors given by

$$p_{\alpha\dot\alpha} = \lambda_\alpha \tilde\lambda_{\dot\alpha}, = \begin{pmatrix} \lambda_1\tilde\lambda_{\dot1} & \lambda_1\tilde\lambda_{\dot2} \\ \lambda_2\tilde\lambda_{\dot1} & \lambda_2\tilde\lambda_{\dot2} \end{pmatrix}. \tag{8.5}$$

For general complex momenta $(\lambda, \tilde{\lambda})$ are independent, however, for real momenta $\lambda$ and $\tilde{\lambda}$ are taken to be complex conjugates.

On the spinor-helicity variables the little group transformations act as the scaling

$$(\lambda, \tilde{\lambda}) \mapsto (t\lambda, t^{-1}\tilde{\lambda}), \tag{8.6}$$

which leaves the momentum invariant. Generally, $t$ can be taken to be any complex number[1], for the case of real momenta we have $\tilde{\lambda} = \lambda^*$, which implies $t = e^{-i\theta}$.

Since the little group now acts simply as scalings on the $(\lambda, \tilde{\lambda})$, the particle helicity information of the amplitude is directly encoded in its scalings under (8.6) by

$$\mathcal{A}(\{t_i \lambda_i, t_i^{-1} \tilde{\lambda}_i, h_i\}) = \prod_i (t_i^{-2h_i}) \mathcal{A}(\{\lambda_i, \tilde{\lambda}_i, h_i\}). \tag{8.7}$$

In summary, we can view an amplitude as a Lorentz invariant function of the $(\lambda, \tilde{\lambda})$ which scales correctly under a little group transformation (8.7).

The Lorentz invariants are constructed using the anti-symmetric tensor $\epsilon^{\alpha\beta}$ and $\epsilon^{\dot{\alpha}\dot{\beta}}$ which we denote as

$$\langle ij \rangle = \epsilon^{\alpha\beta} \lambda_\alpha \lambda_\beta,$$
$$[ij] = \epsilon^{\dot{\alpha}\dot{\beta}} \tilde{\lambda}_{\dot{\alpha}} \tilde{\lambda}_{\dot{\beta}}.$$

The familiar Mandelstam invariants $s_{ij}$ are then given by

$$s_{ij} = (p_i + p_j)^2 = 2p_i \cdot p_j = \langle ij \rangle [ij]. \tag{8.8}$$

Since, the $(\lambda, \tilde{\lambda})$ are nothing other than two-dimensional vectors, any three or more must be linearly dependent. This fact is summarised by the Schouten identity

$$\langle ij \rangle \langle kl \rangle + \langle ik \rangle \langle lj \rangle + \langle il \rangle \langle jk \rangle = 0, \tag{8.9}$$

and analogously for the square brackets. Furthermore, the angle and square brackets are constrained by momentum conservation which implies

$$\sum_{j=1}^{n} \langle ij \rangle [jk] = 0, \quad \forall \ (i, k). \tag{8.10}$$

Note, this is the first instance of the Grassmannians appearing in the discussion of massless kinematic since the same data can be expressed as the Grassmannian $G(2, n)$, one each for

---

[1]Strictly the general complex scaling is not the little group of the previous discussion, $U(1)$, but rather its (non-compact) complexification $GL(1)$.

the $\lambda$ and $\tilde{\lambda}$, where the Schouten identity tells us the dependancy of minors, and momentum conservation implies that the $\lambda$ and $\tilde{\lambda}$ two-planes are orthogonal.

## 8.3   Three-particle kinematics

The little-group scaling properties provide strong constraints on the form of amplitudes, in fact, at three points, it is enough to fix the amplitude completely. To see this first consider the momentum conservation condition for three-points given by

$$(p_1 + p_2 + p_3)^2 = 0 \quad \Longrightarrow \quad \langle 12 \rangle [12] = \langle 13 \rangle [13] = \langle 23 \rangle [23] = 0. \tag{8.11}$$

This condition has two classes of solution those in which the $\lambda$'s are parallel

$$\langle 12 \rangle = \langle 13 \rangle = \langle 23 \rangle = 0, \tag{8.12}$$

and those in which the $\tilde{\lambda}$'s are parallel

$$[12] = [13] = [23] = 0. \tag{8.13}$$

This implies that the three-particle amplitude is either a function of the $\langle ij \rangle$ or $[ij]$. Note, when taking the momenta to be real, we take the $\lambda$ and $\tilde{\lambda}$ to be complex conjugates and only the trivial case where all brackets vanish remains, hence the three-point amplitudes strictly only exist only for complexified momenta.

Imposing the correct little group scalings for each particle completely fixes the form of the amplitude, for the case of three gluons the two choices correspond to the MHV and $\overline{\text{MHV}}$ colour ordered amplitudes respectively

$$A^{\text{MHV}}(1^-, 2^-, 3^+) = \frac{\langle 12 \rangle^4}{\langle 12 \rangle \langle 23 \rangle \langle 31 \rangle}, \quad A^{\overline{\text{MHV}}}(1^+, 2^+, 3^-) = \frac{[12]^4}{[12][23][31]}. \tag{8.14}$$

These three-point amplitudes constitute the building blocks for building higher point functions through, for instance, the BCFW recursion realtions [5, 6]. Two particularly simple, and famous, classes of solutions are given by the Parke-Taylor [4] formula

$$A_n^{\text{MHV}} = \frac{\langle ij \rangle^4}{\langle 12 \rangle \dots \langle n1 \rangle}, \quad A_n^{\overline{\text{MHV}}} = \frac{[ij]^4}{[12] \dots [n1]}, \tag{8.15}$$

where we have taken the two negative or positive helicities to be on the $i^{\text{th}}$ and $j^{\text{th}}$ legs respectively.

As discussed in the introduction, the textbook (off-shell) approach would have consisted of calculating an enormous number of Feynman diagrams, all for them to collapse to a single

term, emphasising the power of the on-shell approach. In fact many well known results for identifying consistent QFT's, for instance the restriction to spin $s < 2$ particles, in the on-shell approach, can be reformulated algebraically as consistency conditions coming from unitarity on tree-level four-point amplitudes [111].

**Colour ordering**

In a gauge theory such as YM, or its supersymmetric cousin $\mathcal{N} = 4$ SYM, with gauge group $SU(N)$ it is always possible, by repeated application of the Fierz identity,

$$(T^a)_i^j (T^a)_k^l = \delta_i^l \delta_k^j - 1/N \delta_i^j \delta_k^l, \tag{8.16}$$

to decompose the colour structures appearing in expressions for the planar amplitudes as a sum over the individual trace components. Where the $T^a$ are the generators of the fundamental representation of $SU(N)$. As an example consider the four gluon amplitude s-channel diagram which contains the factor $c_s = f^{a_1 a_2 a} f^{a a_3 a_4}$ this can be decomposed as

$$c_s = f^{a_1 a_2 a} f^{a a_1 a_2} \propto \text{Tr}[T^{a_1} T^{a_2} T^{a_3} T^{a_4}] - \text{Tr}[T^{a_1} T^{a_2} T^{a_4} T^{a_3}]$$
$$+ \text{Tr}[T^{a_1} T^{a_4} T^{a_3} T^{a_2}] - \text{Tr}[T^{a_1} T^{a_3} T^{a_4} T^{a_2}]. \tag{8.17}$$

Generally, in the planar limit (taking $N \to \infty$) we can express the amplitude as a sum over the individual trace structures as

$$\mathcal{A}_n^{(p)} = g_{YM}^{n-2} \sum_{\sigma_n \in \mathcal{S}_n / \mathbb{Z}_n} \text{Tr}[T^{a_{\sigma_1}} \dots T^{a_{\sigma_n}}] A_n(\sigma_1, \dots, \sigma_n), \tag{8.18}$$

where the $A_n$ are known as the colour ordered partial amplitudes.

# Chapter 9

# More $\mathcal{N} = 4$ SYM

Before moving forward to consider the condition of momentum conservation let us take a step back and return to discuss the symmetries of $\mathcal{N} = 4$ SYM. As we have seen in Chapter 3 the symmetries[1] include conformal symmetry, and $\mathcal{N} = 4$ supersymmetry, which combine into superconformal symmetry. However, colour ordered amplitudes in the planar limit possess an additional *dual superconformal symmetry* [13], hidden from the Lagrangian description, acting in a dual space-time.

In this section we begin by organising amplitudes according to supersymmetry. This will lead us to collect the component helicity dependant amplitudes into a single supersymmetric object, the *superamplitude*, making manifest the relations imposed by the supersymmetric Ward identities. Next, we introduce *twistor* variables, which linearise the form of the conformal generators. Finally, we introduce the *momentum twistor* variables, which simarly linearise the action of the dual conformal transformations, as well as manifesting momentum conservation. By the end of this section we will understand the connection between the kinematic space of scattering amplitudes in planar $\mathcal{N} = 4$ SYM and the Grassmannian $G(4, n)$.

## 9.1 Supersymmetry

The particle content of $\mathcal{N} = 4$ SYM consists of: a single positive helicity gluon, 4 helicity $+1/2$ fermions, 6 scalars, 4 helicity $-1/2$ fermions, and one negative helicity gluon. The particles are related by the $\mathcal{N} = 4$ SUSY algebra part of which reads

$$\{Q_\alpha^A, \bar{Q}_{\dot{\alpha}B}\} = 2P_{\alpha\dot{\alpha}}\delta_B^A, \tag{9.1}$$

---

[1]The introduction of maximal SUSY may seem far removed from its non supersymmetric counterpart, however, at tree-level, pure gluon scattering amplitudes are insensitive to the number of supersymmetries.

where all other combinations of $Q$ and $\bar{Q}$ anticommute, and $A, B = 1, \ldots, 4$ are $SU(4)$ R-symmetry indices. We can define the vacuum states $|+\rangle$ and $|-\rangle$ associated to the positive and negative helicity gluons respectively which satisfy

$$Q_\alpha^A| + 1\rangle = 0, \qquad \bar{Q}_{\dot{\alpha}A}| - 1\rangle = 0. \tag{9.2}$$

From (9.2) we generate the full tower of states by acting on those defined above with the SUSY generators $Q$ and $\bar{Q}$ which act as raising and lowering operators of the helicity by units of $1/2$.

It is useful to manifest the action of as many SUSY's as possible. Due to the anti-commutator, we can either choose this to be the $Q$ or the $\bar{Q}$. For this purpose we introduce the on-shell chiral[1] superfield [112] which re-packages all 16 states as

$$|\Phi\rangle = |+1\rangle + \eta^A| + 1/2\rangle_A + \frac{1}{2!}\eta^A\eta^B|0\rangle_{AB} + \frac{1}{3!}\eta^A\eta^B\eta^C| - 1/2\rangle_{ABC} + \eta^1\eta^2\eta^3\eta^4| - 1\rangle. \tag{9.3}$$

Here the $\eta^A$ are Grassmann variables which carry fundamental $SU(4)$ indices. On this chiral superfield the SUSY generator $Q$ acts as

$$Q_\alpha^A|\Phi\rangle = q_\alpha^A|\Phi\rangle, \tag{9.4}$$

where $q_\alpha^A = \lambda_\alpha \eta^A$ is the *supermomentum.*

Note, this book-keeping device is particularly powerful in the case of $\mathcal{N} = 4$ SYM as all particles are contained within a single multiplet. In the on-shell formalism the action of the SUSY generators is given by

$$P_{\alpha\dot{\alpha}} = \lambda_\alpha\tilde{\lambda}_{\dot{\alpha}}, \quad Q_\alpha^A = \lambda_\alpha\eta^A, \quad \bar{Q}_{\dot{\alpha}A} = \tilde{\lambda}_{\dot{\alpha}}\frac{\partial}{\partial\eta^A}. \tag{9.5}$$

### 9.1.1   Superamplitudes

The supersymmetric ward identities [113, 114] relate amplitudes whose external states are related by supersymmetry, i.e. with the same total helicity. To make this property manifest we introduce the superamplitude, $\mathcal{A}(\{\lambda, \tilde{\lambda}, \eta\})$, which as well as being a function of $(\lambda, \tilde{\lambda})$, is also polynomial in the $\eta$.

As a consequence of (super) momentum conservation, and the simple multiplicative action of their corresponding operators, the most general form of the superamplitude is given by

$$\mathcal{A}_n(\{\lambda, \tilde{\lambda}, \eta\}) = \frac{\delta^{(0|8)}(\sum_{i=1}^n \lambda_i\eta_i)\delta^4(\sum_{i=1}^n \lambda_i\tilde{\lambda}_i)}{\langle 12\rangle \ldots \langle n1\rangle}\hat{\mathcal{A}}_n(\{\lambda, \tilde{\lambda}, \eta\}), \tag{9.6}$$

---

[1]Note, we could have equally chosen to manifest the action of the $\bar{Q}$.

where $\delta^{(a|b)}$ indicates $a$ bosonic delta functions and $b$ fermionic. Note, the behaviour of the fermionic delta function $\delta^{(0|1)}(\eta) = \eta$ implies

$$\delta^{(0|8)}(\sum_{i=1}^{n} \lambda_i \eta_i) = \prod_{\alpha=1}^{2} \prod_{A=1}^{4} \sum_{i=1}^{n} \lambda_{i\alpha} \eta_i^A. \tag{9.7}$$

Since the SUSY Ward identities relate expressions with the same total helicity it is convenient to decompose the superamplitude as

$$\hat{\mathcal{A}}_n(\{\lambda, \tilde{\lambda}, \eta\}) = \sum_{k=0}^{n-4} \hat{\mathcal{A}}_{n,4k}(\{\lambda, \tilde{\lambda}, \eta\}), \tag{9.8}$$

where $\hat{\mathcal{A}}_{n,4k} \sim \mathcal{O}(\eta^{4k})$ is called the N$^k$MHV sector. The steps of 4 in the order of the $\eta$'s is a consequence of R-symmetry, with the only invariant contraction being with the anti-symmetric tensor $\epsilon_{ABCD}$.

This superamplitude acts as a generating function for all helicity configurations, where to obtain a specific amplitude we need only find the relevant term in the $\eta$ expansion. As an example consider the MHV super-amplitude, for which we have $\hat{\mathcal{A}}_{n,0} = 1$, given by

$$\mathcal{A}_n^{\text{MHV}}(\{\lambda, \tilde{\lambda}, \eta\}) = \frac{\delta^{(0|8)}(\sum_{i=1}^{n} \lambda_i \eta_i) \delta^4(\sum_{i=1}^{n} \lambda_i \tilde{\lambda}_i)}{\langle 12 \rangle \ldots \langle n1 \rangle}. \tag{9.9}$$

This contains the terms[1]

$$\mathcal{A}_n^{\text{MHV}}(\{\lambda, \tilde{\lambda}, \eta\}) = (\eta_i)^4 (\eta_j)^4 \delta^{(4)}(\sum_{i=1}^{n} \lambda_i \tilde{\lambda}_i) \frac{\langle ij \rangle^4}{\langle 12 \rangle \ldots \langle n1 \rangle} + \ldots, \tag{9.10}$$

corresponding to the Parke-Taylor amplitude from Equation (8.15). More generally, the N$^k$MHV sector contains the amplitude with $(k+2)$ negative helicity gluons and $(n-k-2)$ positive helicity gluons, along with all other amplitudes related by SUSY.

Let us remark that from the view of the superamplitude it is trivial to see that the all positive and one-negative helicity amplitudes (and their conjugates) vanish [113, 114] due to the supermomentum conserving factor which is already of order eight in the $\eta$'s. Note, at three points there is an exception due to the special properties of three-point kinematics where a $k = -1$ amplitude does in fact exist.

---

[1]Using the definition $\eta^4 = \frac{1}{4!} \epsilon_{ABCD} \eta^A \eta^B \eta^C \eta^D$.

### 9.1.2   Three-particle kinematics

Having introduced the superamplitudes let us return to the example at three-points. As before we have the two types of amplitude the one in which $\tilde{\lambda}_1 \propto \tilde{\lambda}_2 \propto \tilde{\lambda}_3$ given by

$$\mathcal{A}_3(\{\lambda, \eta\}) = \frac{\delta^{(0|8)}(\lambda_1 \eta_1 + \lambda_2 \eta_2 + \lambda_3 \eta_3)}{\langle 12 \rangle \langle 23 \rangle \langle 31 \rangle}, \tag{9.11}$$

and the other amplitude with $\lambda_1 \propto \lambda_2 \propto \lambda_3$ given by[1]

$$\mathcal{A}_3(\{\tilde{\lambda}, \eta\}) = \frac{\delta^{(0|4)}([12]\eta_3 + [23]\eta_1 + [31]\eta_2)}{[12][23][31]}. \tag{9.12}$$

Again, these three-particle amplitudes serve as the building blocks for the supersymmetric version of the BCFW recursion [115–117]. In fact, in the case of $\mathcal{N} = 4$ SYM, a closed form formula has been given for all tree-level superamplitudes [7].

## 9.2   Twistor space

As we have already seen $\mathcal{N} = 4$ SYM possesses (super) conformal symmetry. However, in our current coordinates $(\lambda, \tilde{\lambda})$ the representation of the conformal generators are non-uniform: for example the Lorentz generators are linear in derivatives whereas the generators of the special conformal transformations come with two-derivatives. It is therefore desirable to search for new coordinates in which the representation of the conformal generators become linear.

These new coordinates are intimately connected to the question of how to best parameterise null rays in space-time, which after all is a conformal invariant notion. We can specify a null ray by choosing two points which lie on the ray $x_1^\mu$ and $x_2^\mu$ say, where we have

$$(x_2^\mu - x_1^\mu)^2 = 0 \quad \Longrightarrow \quad \det(x_2 - x_1)^{\alpha\dot{\alpha}} = 0. \tag{9.13}$$

The second equality implies that every point $x_{\alpha\dot{\alpha}}$ on the null ray specified by the two points must satisfy the *incidence relation* given by

$$\lambda^\alpha x_{\alpha\dot{\alpha}} = \mu_{\dot{\alpha}}, \tag{9.14}$$

for some choice of $\mu_{\dot{\alpha}}$. Therefore, for some choice of $(\lambda^\alpha, \mu_{\dot{\alpha}})$ we can construct a null ray in space-time, we can collect these into a single *twistor*[2], $Z^I$, given by

$$Z^A = \begin{pmatrix} \lambda^\alpha \\ \mu_{\dot{\alpha}} \end{pmatrix}. \tag{9.15}$$

---

[1] Notice, the fermionic delta function is only of degree 4.

[2] Twistor variables were first introduced by Penrose in [118] and their supersymmetric version was later given by [119].

Note, these objects are only defined projectively i.e. $Z^A \sim tZ^A$ since through (9.14) both twistors define the same null ray. In this way we have identified null rays in space time with points in $\mathbb{CP}^3$. In fact, it is exactly these twistor coordinates in which the representation of the conformal generators become linear, acting as $sl_4$ on the $A$ index!

We can construct $sl_4$ conformal invariant objects by contracting with the epsilon symbol given by

$$\langle ijkl \rangle = \epsilon_{ABCD} Z_i^A Z_j^B Z_k^C Z_l^D . \tag{9.16}$$

**Points $\iff$ Lines**

So we have seen a point in twistor space corresponds to a null ray in space-time. Let us make complete the correspondence by considering a line in twistor space labelled by two points $Z_A$ and $Z_B$ and ask what this is mapped to in space-time, it turns out to be the point

$$x_{AB}^{\alpha\dot\alpha} = \frac{\lambda_A^\alpha \mu_B^{\dot\alpha} - \lambda_B^\alpha \mu_A^{\dot\alpha}}{\langle AB \rangle} . \tag{9.17}$$

This makes clear the correspondence of points/lines in space-time with lines/points in twistor space.

**Null-seperation $\iff$ Intersection**

A final exercise, which will prove useful in the next section, is to ask what is the distance between the two points $x_{AB}$ and $x_{CD}$ specified by the lines $(Z_A Z_B)$ and $(Z_C Z_D)$ in twistor space, this distance is given by

$$(x_{AB} - x_{CD})^2 = \frac{\langle ABCD \rangle}{\langle AB \rangle \langle CD \rangle} . \tag{9.18}$$

In particular, this tells us that two points in space-time become null-seperated when the corresponding lines in twistor space intersect i.e. when $\langle ABCD \rangle = 0$ as shown in Figure 9.1.
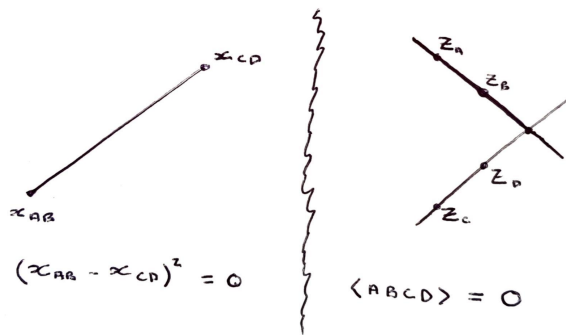
**Figure 9.1:** Two null-separated points in space-time, $x_{AB}$ and $x_{CD}$, correspond to two intersecting lines, $(Z_A Z_B)$ and $(Z_C Z_D)$, in twistor space. With the intersection point in twistor space being dual to the null ray in space-time.

## 9.3   Momentum twistor space

We have just seen that, for a theory with conformal symmetry, a natural set of coordinates, on which the action of conformal symmetry is linear, are the twistor variables, i.e. points in $\mathbb{CP}^3$. In fact, for planar colour-ordered amplitudes in $\mathcal{N} = 4$ SYM, there is a hidden dual conformal symmetry[1] [13], on top of the regular conformal symmetry, which acts in a dual coordinate space. Naturally, we now introduce new variables that make *this* symmetry manifest, this will lead to the notion of *momentum twistor* variables [121].

To motivate the definition of momentum-twistors let us first return to the goal set out at the beginning of Chapter 8, to find some set of variables which trivialise both the on-shell and momentum conservation conditions

$$p_i^2 = 0, \qquad \sum_{i=1}^{n} p_i^{\mu} = 0. \tag{9.19}$$

We have seen how to solve the on-shell condition through the use of spinor-helicity variables, instead lets now consider the momentum-conservation condition.

Given some ordering on the external momenta, naturally handed to us in the case of planar $\mathcal{N} = 4$ SYM by the colour ordered amplitudes, we can interpret momentum-conservation as the closing of a light-like polygon constructed by joining the momentum end to end as depicted in Figure 9.2. This polygon, instead of being labelled by its faces, i.e. the momenta, can equally be described by providing its vertices, which leads us to the definition of the

---

[1]In fact the conformal and dual conformal symmetries combine into an infinite dimensional Yangian symmetry under which the amplitudes are invariant [120].

*dual coordinates* $x_i$ [122] defined by[1]

$$p_i^{\alpha\dot\alpha} = \lambda_i^\alpha \tilde\lambda_i^{\dot\alpha} = x_{i+1}^{\alpha\dot\alpha} - x_i^{\alpha\dot\alpha}, \tag{9.20}$$

upon which the hidden dual conformal symmetry acts. Note, under identifying $x_{n+1} = x_1$, these coordinates trivially satisfy momentum conservation

$$\sum_{i=1}^n p_i^\mu = x_2^\mu - x_1^\mu + x_3^\mu - x_2^\mu + \ldots + x_n^\mu - x_{n-1}^\mu + x_1^\mu - x_n^\mu = 0. \tag{9.21}$$

With the dual coordinates to hand we can perform the same exercise as before and transform to momentum twistor space. Again, the points $x_i^{\alpha\dot\alpha}$ are mapped to a collection of lines in $\mathbb{CP}^3$. Where, as we have seen from the last exercise in 9.2, that null separation of consecutive points $p_i^2 = (x_{i+1} - x_i)^2 = 0$ in the dual space translates to the intersection of consecutive lines in momentum twistors space. This defines another polygon now in momentum twistor space as depicted in Figure 9.2. Again, we can specify this polygon not by its edges but by its vertices $Z_i^A$ i.e. the momentum twistors. It is these variables which trivialise both the massless on-shell condition and momentum-conservation, and transform linearly under dual conformal transformations!

To summarise, given a collection of $n$ *arbitrary* points, $Z_i^A$, in momentum twistor space, $\mathbb{CP}^3$, we can construct $n$ null momenta which satisfy momentum conservation! The map between momentum twistors and the dual space follows directly from the formulae in the last section where we have

$$Z_i^A = \begin{pmatrix} \lambda_i^\alpha \\ \mu_{\dot\alpha}^i \end{pmatrix}, \quad x_i^{\alpha\dot\alpha} = \frac{\lambda_i^\alpha \mu_{i+1}^{\dot\alpha} - \lambda_{i+1}^\alpha \mu_i^{\dot\alpha}}{\langle ii+1 \rangle}. \tag{9.22}$$

Where, as before, dual conformal invariant objects are constructed by contraction with the epsilon symbol

$$\langle ijkl \rangle = \epsilon_{ABCD} Z_i^A Z_j^B Z_k^C Z_l^D. \tag{9.23}$$

---

[1]Let us emphasise that the $x's$ are NOT space-time points. For instance notice they have mass dimension 1.
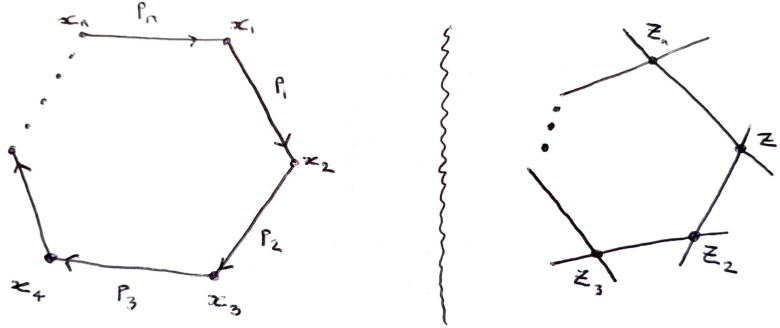
**Figure 9.2:** Momentum conservation pictured as a null polygon both in the dual space-time (left) and momentum twistor space (right).

In this notation the multi-particle Mandelstam invariants become

$$s_{i,\dots j-1} = (p_i + \dots + p_{j-1})^2 = (x_j - x_i)^2 = x_{ji}^2 \tag{9.24}$$

$$= \frac{\langle i-1\,i\,j-1\,j\rangle}{\langle i-1\,i\rangle\langle j-1\,j\rangle}. \tag{9.25}$$

Which, as can be seen from the denominator, are themselves not dual conformal invariant. However, dual conformal invariant objects can be constructed by taking homogenous rational combinations in which the two brackets cancel.

### 9.3.1   $G(4,n)$

We can finally understand why the Grassmannian appears in the discussion of scattering amplitudes in planar $\mathcal{N} = 4$ SYM. The $n$ twistors can be organised into a $4 \times n$ matrix as

$$\left(Z_i \dots Z_n\right), \tag{9.26}$$

which parameterises a point in the Grassmannian $G(4,n)$ modulo the rescaling of the $Z_i$. The dual conformal symmetry implies that the amplitudes must be functions of the $sl_4$ invariant Plücker coordinates

$$\langle ijkl\rangle = \det(Z_i Z_j Z_k Z_l). \tag{9.27}$$

Therefore we conclude the kinematic space of dual-conformal invariant massless kinematics is identified with

$$\mathrm{Conf}_n(\mathbb{P}^3) = Gr(4,n)/(\mathbb{C}^*)^{n-1}. \tag{9.28}$$

As we shall see in Chapter **??** this space can be associated with a *cluster algebra* whose combinatorial structure provides crucial information for the analytic structure of amplitudes.

### 9.3.2 Super momentum-twistors

The above discussion has a supersymmetric extension which follows a similar construction. The supermomentum conservation can be trivialised by introducing the dual coordinates

$$q_i^{\alpha A} = \lambda_i^\alpha \eta_i^A = \theta_{i+1}^{\alpha A} - \theta_i^{\alpha A}, \tag{9.29}$$

from which we introduce the *momentum super-twistors* given by

$$\mathcal{Z}_i = \begin{pmatrix} Z_i \\ \chi_i \end{pmatrix}, \quad \chi_i^A = \langle i\theta_i^A \rangle = \langle i\theta_{i+1}^A \rangle. \tag{9.30}$$

Again, we have the equivalence $\mathcal{Z}_i \sim t_i \mathcal{Z}_i$, and therefore the momentum super-twistors are also defined projectively.

## 9.4 Bootstrapping loop amplitudes

Having reviewed the relevant kinematics, and introduced the variables on which our amplitudes will depend, we now turn to the study of loop amplitudes in planar $\mathcal{N} = 4$ SYM.

### 9.4.1 The BDS-like ansatz

When considering loop-amplitudes it is important to take into account the structure of infrared divergences. This can be achieved by factoring out an infrared divergent piece leaving over a finite remainder function

$$\mathcal{A}_n = \mathcal{A}_n^{\text{IR}} \mathcal{A}_n^{\text{fin}}. \tag{9.31}$$

However, the choice of $\mathcal{A}_n^{\text{IR}}$ is not unique, and with different choices, the finite remainder function can make manifest (or not) certain physical and mathematical properties. Therefore, it is desirable to choose $\mathcal{A}_n^{\text{IR}}$ such that $\mathcal{A}^{\text{fin}}$ is as simple to compute as possible. Originally, the factor was chosen to be the so called BDS ansatz [123, 124], the exact form of which will not be relevant. However, this has the undesirable quality that neither the BDS ansatz, nor the finite remainder function, satisfy the Steinmann relations [125]

$$\text{Disc}_{s_{jj+1j+2}}(\text{Disc}_{s_{ii+1i+2}}\mathcal{A}) = 0, \quad \forall j = i \pm 1, i \pm 2, \tag{9.32}$$

whereas their product, the full amplitude, does! The Steinmann relations above are the statement that the amplitude cannot have consecutive discontinuities in overlapping three-particle (and their generalisation to higher point) Mandelstam invariants.

To restore the Steinmann relations, for $n \neq 0 \mod 4$, we can instead define the so called BDS-like[1] ansatz [127]

$$\mathcal{A}_n = \mathcal{A}_n^{\text{BDS-like}} \mathcal{E}_n, \tag{9.33}$$

Again, the exact form of $\mathcal{A}_n^{\text{BDS-like}}$ is not of relevance here. The important point is that the function $\mathcal{E}_n$ is dual conformal invariant and satisfies the Steinmann relations, it can be written entirely in terms of the momentum super twistors $\mathcal{Z}_i$, and has an expansion into $\text{N}^k\text{MHV}$ sectors similar to Equation (9.8), given by

$$\mathcal{E}_n = \mathcal{E}_{n,\text{MHV}} + \mathcal{E}_{n,\text{NMHV}} + \dots. \tag{9.34}$$

The MHV term is degree zero in the Grassmann $\chi_i$ variables, and is simply a function of the $Z_i$, with dual conformal symmetry implying dependance only on of the $\langle ijkl \rangle$ four-brackets. It has an homogeneity in each of the $Z_i$ of degree zero, and is therefore a function on the configuration space of $n$ points in $\mathbb{P}^3$, which we had already denoted as $\text{Conf}_n(\mathbb{P}^3)$.

The NMHV term is degree four in the Grassmann variables and can be written as

$$\mathcal{E}_{n,\text{NMHV}} = \sum [ijklm] E_{ijklm}(Z_1, \dots, Z_n), \tag{9.35}$$

where the *Yangian invariants* are given by,

$$[ijklm] = \frac{(\chi_i \langle jklm \rangle + \text{cyclic})^4}{\langle ijkl \rangle \langle jklm \rangle \langle klmi \rangle \langle lmij \rangle \langle mijk \rangle}, \tag{9.36}$$

and again the $E_{ijklm}$ are dual conformally invariant functions on $\text{Conf}_n(\mathbb{P}^3)$.

Since we will be most interested in the six and seven point hexagon and heptagon amplitudes these are the only terms in the $\text{N}^k\text{MHV}$ expansion which need be considered, since all others can be obtained upon parity conjugation.

Moving forward all terms discussed above, collectively denoted $F$, will admit the perturbative loop expansion

$$F = \sum_{L=0}^{\infty} g^{2L} F^{(L)}. \tag{9.37}$$

### 9.4.2   Polylogarithms and their symbols

At six and seven points all available data for planar $\mathcal{N} = 4$ SYM suggests that the $L$ loop amplitude can be expressed as *weight* $2L$ polylogarithms (polylogs for short). The polylogs $f^{(k)}$ are a class of iterated integrals over logarithmic singularities, which at weight $k$ can be defined recursively to obey

$$df^{(k)} = \sum_{a \in \mathcal{A}} f_a^{(k-1)} d\log a, \tag{9.38}$$

---

[1]Further refinements on the choice of normalisation have also been considered, for a review see [126].

where $a$ are rational (algebraic) functions of the relevant kinematic variables, referred to as *letters*, they run over the finite set of letters $\mathcal{A}$ known as the *alphabet*. By specifying the alphabet we are provided with a class of polylogs defined recursively in weight. At weight-one the function space is simply given by $\{\log a | a \in \mathcal{A}\}$. As an example for $\mathcal{A} = \{x, 1-x\}$ we generate the harmonic polylogs [128].

Alternatively, we can define polylogarithms directly in terms of iterated integrals. The so called Goncharov polylogs [129] are defined recursively as

$$G(\underbrace{a_1, a_2 \ldots, a_k}_{\text{weight k}}; x) = \int_0^x \frac{dt}{t - a_1} G(a_2, \ldots, a_k; t), \tag{9.39}$$

where we have

$$G(a; x) = \int_0^x \frac{dt}{t - a}, \quad a \neq 0, \quad G(\underbrace{0, 0, \ldots, 0}_{k}; x) = \frac{1}{k!} \log^k x, \tag{9.40}$$

from which the more familiar classical polylogs $\mathrm{Li}_k(x)$ are obtained as a special case by

$$\mathrm{Li}_k(x) = G(\underbrace{0, 0, \ldots, 0}_{k-1}, 1; x). \tag{9.41}$$

The total derivative formulation (9.38) can also be seen as defining the $(k-1, 1)$ piece of the *coproduct* [29] of $f^{(k)}$ through

$$f^{(k-1,1)} = \sum_{a \in \mathcal{A}} f_a^{(k-1)} \otimes d \log a. \tag{9.42}$$

Where, as a consequence of $d^2 f^{(k)} = 0$, the $(k-1, k)$ coproduct satisfies the integrability condition

$$\sum_{a \in \mathcal{A}} df_a^{(k-1)} \wedge d \log a = 0. \tag{9.43}$$

By applying the $(n, 1)$ coproduct to the component functions $f^{(k-1)}$ all the way down to weight zero we arrive at the notion of the *symbol* of the function $f^{(k)}$, alternatively the $(1, \ldots, 1)$ piece of the coproduct, given by an element of the $k$-fold tensor product of the space of one-forms spanned by the $d \log a$

$$\begin{aligned} \mathcal{S}(f^{(k)}) = f^{(1,\ldots,1)} &= \sum_{\vec{a} \in \mathcal{A}^k} c_{a_1 \ldots a_k} \left[ d \log a_1 \otimes \ldots \otimes d \log a_k \right]. \\ &:= \sum_{\vec{a} \in \mathcal{A}^k} c_{a_1 \ldots a_k} \left[ a_1 \otimes \ldots \otimes a_k \right]. \end{aligned}$$

In the second line we have used the notational convention of only recording the letters $a$

in the arguments of the tensor product, for example the symbol of the classical polylogs is given by

$$\mathcal{S}(\mathrm{Li}_k(x)) = -[(1-x) \otimes \underbrace{x \otimes \ldots \otimes x}_{k-1}]. \tag{9.44}$$

Note, the symbol inherits the familiar properties of logarithms namely

$$[a \otimes b_1 b_2 \otimes c] = [a \otimes b_1 \otimes c] + [a \otimes b_2 \otimes c], \tag{9.45}$$

and

$$[a \otimes b^p \otimes c] = p[a \otimes b \otimes c] \quad p \in \mathbb{Q}. \tag{9.46}$$

The symbol is a useful tool when dealing with polylogs as it provides an efficient route to simplifying lengthy expressions, as demonstrated in [130] for the two-loop MHV amplitude at six points [131]. It also encodes the branch cut and differential structure of the function $f^{(k)}$. The derivative action is encoded by the right most element by

$$d\left[a_1 \otimes \ldots \otimes a_k\right] = \left[a_1 \otimes \ldots \otimes a_{k-1}\right] d\log a_k. \tag{9.47}$$

Wheras the logarithmic branch cut structure is encoded in the first element, where to take the singularity around $a_1 = 0$ say we take all terms with initial entry is $a_1$, the discontinuity is then given by

$$\mathrm{disc}_{a_1=0}\left[a_1 \otimes \ldots \otimes a_k\right] = 2\pi i \left[a_2 \otimes \ldots \otimes a_k\right]. \tag{9.48}$$

### 9.4.3   The amplitude boostrap

The bootstrap programme [14–23] has used the symbol technology to great effect in order to compute six and seven point amplitudes. The first step in the bootstrap program, after having been provided with some alphabet[1], is to build the associated function space (up to weight $2L$ for the $L$ loop amplitude) in which the amplitude lives. Note, this is not in fact the entire $k$-fold tensor product space, since a general element (a *word*)

$$\sum_{\vec{a} \in \mathcal{A}^k} c_{a_1 \ldots a_k}[a_1 \otimes \ldots \otimes a_k], \tag{9.49}$$

is not necessarily associated to the symbol of some function. To ensure that it is we must impose the integrability conditions

$$\sum_{\vec{a} \in \mathcal{A}^k} c_{a_1 \ldots a_k} \underbrace{a_1 \otimes \ldots \otimes a_k}_{a_j \otimes a_{j+1}} d\log a_j \wedge \log a_{j+1} = 0, \quad \forall\, j = \{1, \ldots, k-1\}, \tag{9.50}$$

---

[1]In our case the symbol alphabet is handed to us by the $\mathcal{A}$ coordinates of the Grassmannian cluster algebras $G(4,6)$ and $G(4,7)$ for six and seven points respectively.

which follow from the fact that $d^2 f = 0$ for all functions and encode the commutativity of partial derivatives. The elements of $\mathcal{A} \otimes \ldots \otimes \mathcal{A}$ which satisfy these conditions is known as the space of *integrable words*[1]. After determining a basis of integrable words at some low weight we can then iteratively construct bases at higher weight as outlined in [22, 132].

With a basis, $b_i^{(2L)}$, of integrable weight $2L$ words to hand we can make an ansatz for the $L$ loop amplitude

$$F^{(L)} = \sum_i c_i b_i^{(2L)}, \tag{9.51}$$

with some free coefficients $c_i$. These coefficients can then be fixed by imposing consistency conditions which the symbol of the amplitude is expected to obey. These include initial and final entry [133] conditions, as well as constraints coming from the Steinmann relations, collinear limits, multi-regge kinematics, discrete symmetries and as we shall see in the next chapter cluster adjacency [30], for a review of the bootstrap program see [126].

---

[1]Note an integrable word is a linear combination of words which is itself integrable.

# Chapter 10

# Grassmannian cluster algebras

The link between cluster algebras associated to the Grassmannians $G(4,n)$, or more correctly the $3(n-5)$-dimensional spaces $\mathrm{Conf}_n(\mathbb{P}^3)$, and $n$-point scattering amplitudes in $\mathcal{N} = 4$ SYM was originally proposed in [28], where it was observed that the symbol of the two-loop MHV remainder functions of [133] could be constructed explicitly in terms of cluster $\mathcal{A}$-coordinates.

This connection explains the 9 and 42 letter alphabets for 6 and 7 point amplitudes respectively, conjectured to be polylogarithmic with symbol alphabets given by the $\mathcal{A}$-coordinates of $G(4,6)$ and $G(4,7)$ to all loop orders, and has facilitated impressive calculations in the context of the analytic bootstrap upto high loop orders [14–23]. Furthermore, the link between $\mathcal{A}$-coordinates and the singularities of the amplitudes was endowed with a geometric interpretation with the discovery of *cluster adjacecny* [30, 132]. With cluster adjacency stating that consecutive singularities can only appear in the symbol if there exists a cluster in which both letters appear.

In this section we review the details of the $G(4,6)$ and $G(4,7)$ cluster algebras relevant for 6 and 7 point amplitudes. This will set us up to reformulate the same ideas in the new language of the (to be introduced) Gröbner fan in the next chapter. In addition we point out the complications which arise at 8 points and beyond due to the appearance of non-rational square root letters in the symbol alphabet of 8-point scattering amplitudes, and the fact that the set of $\mathcal{A}$-coordinates of $G(4,8)$ is no longer finite. We will return to discuss both complications in detail in Chapter 12 of this thesis in the context of 6-point scattering amplitudes with general kinematics.

## 10.1  The Grassmannian

The Grassmannian $G(k,n)$ is the space of $k$-planes in $n$ dimensions. A point of which can be specified by $k$ many $n$-component vectors organised into a $k \times n$ matrix. These matrices are

defined up to row operations which leave the plane invariant, the resulting space of matrices modulo $GL(k)$ transformations is $k(n-k)$ dimensional.

Alternatively, the Grassmannian can be described through the set of $\binom{n}{k}$ maximal minors $p_{i_1 \ldots i_k}$ or Plücker coordinates. On the set of Plücker coordinates row operations act as an overall scaling and, modulo this overall scaling, the vector of Plücker coordinates may be thought of as a point in the projective space $\mathbb{P}^{\binom{n}{k}-1}$. However, an arbitrary point in $\mathbb{P}^{\binom{n}{k}-1}$ is not necessarily realisable as a matrix, since the set of $k \times k$ minors of any $k \times n$ matrix are not independent, and instead obey homogenous quadratic relations known as the Plücker relations which take the form

$$p_{i_1 \ldots i_r [i_{r+1} \ldots i_k} p_{j_1 \ldots j_{r+1}] j_{r+2} \ldots j_k} = 0. \tag{10.1}$$

We call the ideal generated by the Plucker relations inside the ring of polynomials in the Plucker coordinates the Plücker ideal $I_{k,n}$. The Grassmannian can then be thought as the projective variety inside $\mathbb{P}^{\binom{n}{k}-1}$ whose points vanish on the Plücker ideal. We will discuss this algebraic formulation of the Grassmannian in much detail in the next chapter. As an example consider the case of $G(2,n)$, whose Plücker ideal is generated by the relations
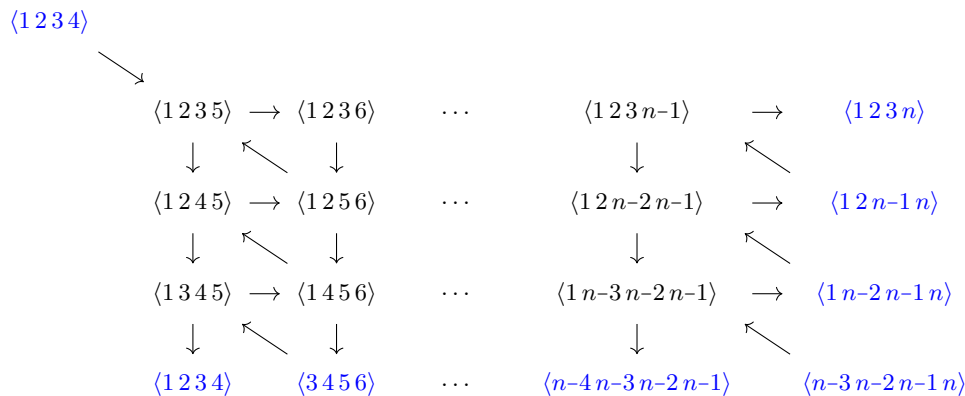
$$I_{2,n} = \langle p_{ij}p_{kl} - p_{ik}p_{jl} + p_{il}p_{jk} : 1 \leq i < j < k < l \leq n \rangle. \tag{10.2}$$

In fact the Plücker relations are homogenous with respect to $n$ independent rescalings $p_{i_1 \ldots i_k} \mapsto t_{i_1} \ldots t_{i_k} p_{i_1 \ldots i_k}$ for $t_i \in \mathbb{C}^*$. By modding out these *local* scalings we obtain the $(k-1)(n-k-1)$ dimensional configuration space of $n$ points in $\mathbb{P}^{k-1}$

$$\mathrm{Conf}_n(\mathbb{P}^{k-1}) = G(k,n)/(\mathbb{C}^{*n-1}). \tag{10.3}$$

## 10.2   Cluster algebras

A cluster algebra, originally developed in [25–27], can be specified by a choice of initial cluster encoded by a quiver diagram. Where a quiver diagram is a collection of *active* and *frozen* nodes, connected by arrows, with each node being assigned its own $\mathcal{A}$-coordinate. As an example consider Figure 10.1 which depicts the cluster algebra for $G(4,n)$: it has $m = 3(n-5)$ active nodes and $n$ frozen nodes indicated by the blue vertices. In addition to the initial cluster there are also a set of mutation rules which detail how the quiver diagram and $\mathcal{A}$-coordinates of one cluster transform into another. In the case of $n = 6$ and $n = 7$ the mutation rules generate finitely many clusters, hence finitely many $\mathcal{A}$-coordinates, and are referred to as being of finite type.

$$\langle 1\,2\,3\,4 \rangle$$

$$
\begin{array}{ccccccc}
\langle 1\,2\,3\,5 \rangle & \rightarrow & \langle 1\,2\,3\,6 \rangle & \cdots & \langle 1\,2\,3\,n\text{-}1 \rangle & \rightarrow & \langle 1\,2\,3\,n \rangle \\
\downarrow & \nwarrow & \downarrow & & \downarrow & \nwarrow & \\
\langle 1\,2\,4\,5 \rangle & \rightarrow & \langle 1\,2\,5\,6 \rangle & \cdots & \langle 1\,2\,n\text{-}2\,n\text{-}1 \rangle & \rightarrow & \langle 1\,2\,n\text{-}1\,n \rangle \\
\downarrow & \nwarrow & \downarrow & & \downarrow & \nwarrow & \\
\langle 1\,3\,4\,5 \rangle & \rightarrow & \langle 1\,4\,5\,6 \rangle & \cdots & \langle 1\,n\text{-}3\,n\text{-}2\,n\text{-}1 \rangle & \rightarrow & \langle 1\,n\text{-}2\,n\text{-}1\,n \rangle \\
\downarrow & \nwarrow & \downarrow & & \downarrow & \nwarrow & \\
\langle 1\,2\,3\,4 \rangle & & \langle 3\,4\,5\,6 \rangle & \cdots & \langle n\text{-}4\,n\text{-}3\,n\text{-}2\,n\text{-}1 \rangle & & \langle n\text{-}3\,n\text{-}2\,n\text{-}1\,n \rangle
\end{array}
$$

**Figure 10.1:** The initial cluster of G$(4, n)$.

The arrows of the quiver diagram are described by the *exchange matrix*, $b$, with the elements

$$b_{ij} = (\text{no. of arrows } i \rightarrow j) - (\text{no. of arrows } j \rightarrow i). \tag{10.4}$$

Here the exchange matrix is skew-symmetric with indices running over all nodes (active and frozen) and in the case of $G(4, n)$ has dimension $(m + n) \times (m + n)$. Note, we need not record arrows between frozen nodes so the bottom right $(n \times n)$ submatrix of $b$ is irrelevant. By performing a mutation on any *active* node $k$ we obtain a new cluster with the exchange matrix

$$b'_{ij} = \begin{cases} -b_{ij} & \text{if } i = k \text{ or } j = k. \\ b_{ij} + [-b_{ik}]_+ b_{kj} + b_{ik}[b_{kj}]_+ & \text{otherwise.} \end{cases} \tag{10.5}$$

with $[x]_+ = \max(x, 0)$. Where the $\mathcal{A}$-coordinate associated to the mutated node becomes

$$a'_k = \frac{1}{a_k} \prod_{i=1}^{m+n} a_i^{[b_{ik}]_+} + \prod_{i=1}^{m+n} a_i^{[-b_{ik}]_+}. \tag{10.6}$$

Given the initial cluster and mutation rules we can obtain the data for every other cluster by repeated mutation on active nodes.

On top of the $\mathcal{A}$-coordinates and $b$ matrix we may assign additional data to the initial cluster. We also have the *coefficient matrix*, given by the $(m \times m)$ identity matrix whose mutation rules are given by

$$c'_{ij} = \begin{cases} -c_{ij} & \text{if } j = k. \\ c_{ij} - [-c_{ik}]_+ b_{kj} + c_{ik}[-b_{kj}]_+ & \text{otherwise.} \end{cases} \tag{10.7}$$

Additionally, to each active node $a_i$ we associate the **g**-vector $\mathbf{e}_i$, the unit vector in the $i$th

direction, which upon mutating on the $k^{th}$ node transform as

$$\mathbf{g}'_k = -\mathbf{g}_k + \sum_{i=1}^{n}[-b_{ik}]_+\mathbf{g}_i + \sum_{j=1}^{n}[c_{jk}]_+\mathbf{b}^0_j, \tag{10.8}$$

where $\mathbf{b}^0_j$, $j \in \{1, \ldots, m\}$ corresponds to the $j$th column of $b^0$, the exchange matrix for the initial cluster. By following these mutation rules each $\mathcal{A}$-coordinate generated will be associated to its own unique $\mathbf{g}$-vector.

A cluster subalgebra of codimension-one consisting of all clusters containing a given $\mathcal{A}$-coordinate can be generated by searching for some cluster with the chosen $\mathcal{A}$-coordinate, *freezing it*, and performing all possible mutations on the remaining active nodes. Similarly, we can generate subalgbras of higher codimension by choosing some subset of coordinates $\mathcal{S}$, so long as they all appear in a single cluster together, freezing them, and performing all mutations on the remaining active nodes to obtain a subalgebra of codimension-$|\mathcal{S}|$. This procedure terminates when we have specified all $3(n-5)$ $\mathcal{A}$-coordinates appearing in a single cluster together i.e. a zero dimensional cluster algebra.

In the case where two $\mathcal{A}$-coordinates appear together in a cluster we call them *adjacent* otherwise we call them *forbidden*. The fact that some coordinates appear together in clusters and others do not has been shown to have physical significance for scattering amplitudes. Where in [30, 132] the notion of *cluster adjacency* was introduced which can be summarised as follows: *two letters (A-coordinates) can appear adjacent in the symbol of the amplitude iff they appear in some cluster together.* This can be used to significantly reduce the space of integrable words needed in the amplitude bootstrap.

Note, the $\mathcal{A}$-coordinates are not homogenous under rescaling the individual twistors and hence do not strictly define coordinates on $\mathrm{Conf}_n(\mathbb{P})^3$. However, we can instead define the homogenous $\mathcal{X}$-coordinates with respect to a cluster given by

$$x_j = \prod_i a_i^{b_{ij}}, \tag{10.9}$$

where $j$ labels an active node and $i$ runs over all nodes of the cluster. They have their own mutation rules given by

$$x'_i = \begin{cases} 1/x_i & k = i, \\ x_i\left(1 + x_k^{\mathrm{sgn}(b_{ik})}\right)^{b_{ik}} & k \neq i. \end{cases} \tag{10.10}$$

for mutations on node $i$.

Since the $\mathcal{X}$-coordinates range over $0 < x < \infty$, in the real case, they can be seen as defining a positive region in $\mathrm{Conf}_n(\mathbb{RP}^3)$. This region can be visualised as a polytope whose facets correspond to the codimension-one subalgebras described above. Where the boundaries of the facets correspond to codimension-two subalgebras, and so on, all the way down to

the vertices of the polytope, corresponding to the individual clusters or dimension zero subalgebras. In this picture the $\mathcal{X}$-coordinates are viewed as *edge coordinates*, in the sense that they correspond to the edges connecting to each vertex/cluster where they run over $0 < x < \infty$. Note, this is compatible with the fact that, under mutation along an edge (10.10), the associated $\mathcal{X}$-coordinate inverts.

### 10.2.1  $G(4, 6)$

Let us see the above definitions at work in the simplest case of the cluster algebra associated to $G(4, 6)$[1]. The quiver diagram of the initial cluster is given in Figure 10.2 with the three active coordinates

$$a_1 = \langle 1235 \rangle, \quad a_2 = \langle 1245 \rangle, \quad a_3 = \langle 1345 \rangle, \tag{10.11}$$

together with the 6 frozen coordinates. The full list of 9 active coordinates are distributed over 14 clusters connected in the topology of the Stasheff or $A_3$ polytope as depicted in Figure 10.3.

As mentioned each facet corresponds to the subalgebra obtained by freezing one of the active coordinates: three square facets, or $A_1 \times A_1$ subalgebra, obtained by freezing e.g. $\langle 1245 \rangle$, and six pentagonal facets, or $A_2$ subalgebra, obtained by freezing e.g. $\langle 1235 \rangle$. The clusters appear as the 14 vertices of the polytope: where the $\mathcal{A}$-coordinates contained in a cluster correspond to the three facets which intersect at the given vertex. As an example the initial cluster can be seen as top left vertex of the Stasheff polytope highlighted in red.

The content of cluster adjacency is encoded by which facets share a codimension-two subalgebra. As an example consider the adjacent pair $\{\langle 1235 \rangle, \langle 2456 \rangle\}$ which share an $A_1$ subalgebra corresponding to the shared edge in the intersection of the two facets. However, the pair of square faces defined by $\{\langle 1245 \rangle, \langle 2356 \rangle\}$ share no such boundary and are a *forbidden pair*.
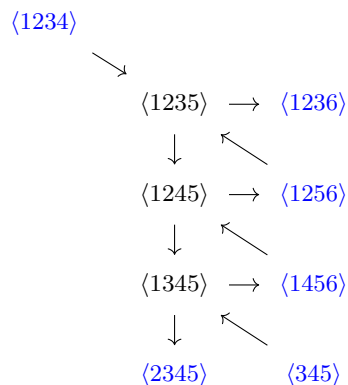
Note, the polytope depicted in 10.3 should not be thought simply in the abstract sense of encoding the connections between clusters. But instead the interior, when restricting to real momentum twistors, can be thought as the region inside the three-dimensional space $\mathrm{Conf}_6(\mathbb{RP}^3)$ where all the $\mathcal{X}$-coordinates are strictly positive. Each vertex of the polytope is then the origin in the set of $\mathcal{X}$-coordinates defined by the cluster. For example the $\mathcal{X}$-coordinates of the initial cluster are given by

$$x_1 = \frac{\langle 1234 \rangle \langle 1256 \rangle}{\langle 1236 \rangle \langle 1245 \rangle}, \quad x_2 = \frac{\langle 1235 \rangle \langle 1456 \rangle}{\langle 1256 \rangle \langle 1345 \rangle}, \quad x_3 = \frac{\langle 1245 \rangle \langle 3456 \rangle}{\langle 2345 \rangle \langle 1456 \rangle}. \tag{10.12}$$

The point $(0, 0, 0)$ in the $(x_1, x_2, x_3)$ coordinate system defines the vertex corresponding to

---

[1]More correctly the cluster algebra is associated to $\mathrm{Conf}_6(\mathbb{P}^3)$ but we will continue to refer to the Grassmannian.

the initial cluster, with the $\mathcal{X}$-coordinates running from 0 to $\infty$ along the three connected edges.

$$\langle 1234 \rangle$$

$$\searrow$$

$$\langle 1235 \rangle \;\longrightarrow\; \langle 1236 \rangle$$

$$\downarrow \qquad \nwarrow$$

$$\langle 1245 \rangle \;\longrightarrow\; \langle 1256 \rangle$$

$$\downarrow \qquad \nwarrow$$

$$\langle 1345 \rangle \;\longrightarrow\; \langle 1456 \rangle$$

$$\downarrow \qquad \nwarrow$$

$$\langle 2345 \rangle \qquad\quad \langle 345 \rangle$$

**Figure 10.2:** The initial cluster of the $G(4,6)$ cluster algebra.

Alternatively we can define the set of homogeneous *dihedral* coordinates given by

$$u_{ij} = \frac{\langle ij+1\rangle\langle i+1j\rangle}{\langle ij\rangle\langle i+1j+1\rangle}, \quad 0 < u_{ij} < 1, \tag{10.13}$$

where the labels $i$ and $j$ are separated by at least two. Here we have introduced the two bracket notation which replaces the four brackets with their complements for example $\langle 1234 \rangle \to \langle 56 \rangle$. In the case of $n = 6$ the dihedral coordinates form a complete set of nine multiplicatively independent homogenous combinations of the $\mathcal{A}$-coordinates. Hence, they can be used as an alphabet for the construction of the hexagon polylogarithmic function space.
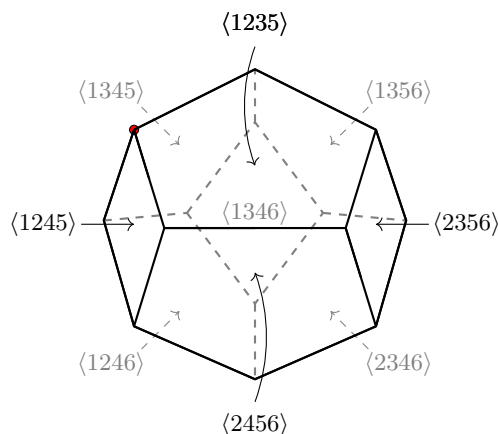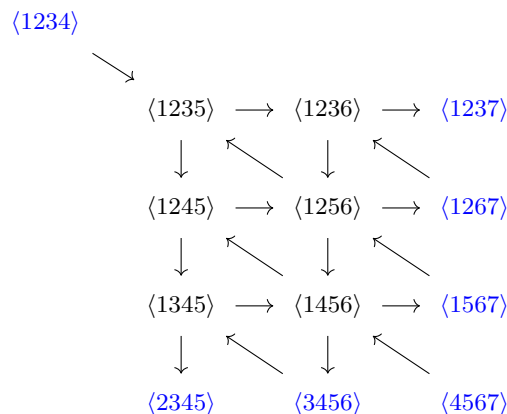


**Figure 10.3:** The Stasheff polytope with each face labelled with the corresponding $\mathcal{A}$-coordinate. The initial cluster corresponds to the top left vertex highlighted in red at the intersection of the faces $\langle 1235 \rangle$, $\langle 1245 \rangle$ and $\langle 1345 \rangle$.

### 10.2.2 $G(4,7)$

The initial cluster associated to $G(4,7)$ is depicted in Figure 10.4. By repeated mutation we generate 42 distinct active $\mathcal{A}$-coordinates distributed over 833 clusters. With each cluster containing six active nodes along with the seven frozen nodes.

$$\langle 1234 \rangle$$

$$\langle 1235 \rangle \longrightarrow \langle 1236 \rangle \longrightarrow \langle 1237 \rangle$$

$$\langle 1245 \rangle \longrightarrow \langle 1256 \rangle \longrightarrow \langle 1267 \rangle$$

$$\langle 1345 \rangle \longrightarrow \langle 1456 \rangle \longrightarrow \langle 1567 \rangle$$

$$\langle 2345 \rangle \qquad \langle 3456 \rangle \qquad \langle 4567 \rangle$$

**Figure 10.4:** The initial cluster of the $G(4,7)$ cluster algebra.

When the pair $(k,n)$ is coprime the frozen coordinates of $G(k,n)$ can be used to homogenise the active $\mathcal{A}$-coordinates [19], such is the case at seven points, where we may construct 42 homogenous letters in one-to-one correspondence with the 42 active $\mathcal{A}$-coordinates. These are given by the cyclic rotations of

$$a_{11} = \frac{\langle 1234 \rangle \langle 1567 \rangle \langle 2367 \rangle}{\langle 1237 \rangle \langle 1267 \rangle \langle 3456 \rangle}, \qquad a_{21} = \frac{\langle 1234 \rangle \langle 2567 \rangle}{\langle 1267 \rangle \langle 2345 \rangle},$$

$$a_{31} = \frac{\langle 1567 \rangle \langle 2347 \rangle}{\langle 1237 \rangle \langle 4567 \rangle}, \qquad a_{41} = \frac{\langle 2457 \rangle \langle 3456 \rangle}{\langle 2345 \rangle \langle 4567 \rangle},$$

$$a_{51} = \frac{\langle 1(23)(45)(67) \rangle}{\langle 1234 \rangle \langle 1567 \rangle}, \qquad a_{61} = \frac{\langle 1(34)(56)(72) \rangle}{\langle 1234 \rangle \langle 1567 \rangle}, \qquad (10.14)$$

which serve as the symbol alphabet for the construction of heptagon amplitudes. In the above we have introduced the notation

$$\langle 1(23)(45)(67) \rangle = \langle 1234 \rangle \langle 5671 \rangle - \langle 1235 \rangle \langle 4671 \rangle. \qquad (10.15)$$

We may view the cluster algebra as the six-dimensional $E_6$ polytope with 833 vertices and 42 codimension-one facets. Already at seven points it is not instructive to plot the entire cluster algebra. However, we can still learn about the subalgebra structure by mutating the initial cluster to the convenient form of the $E_6$ Dynkin diagram topology given in Figure 10.5. This makes clear the possible codimension-one subalgebras that are contained within the $E_6$ cluster algebra: upon freezing $a_{13}$ we obtain an $A_5$ subalgebra; freezing $a_{24}$ or $a_{33}$ generates

a $D_5$ subalgebra; freezing $a_{41}$ or $a_{51}$ generates an $A_1 \times A_4$ subalgebra; finally freezing $a_{62}$ would generate an $A_1 \times A_2 \times A_2$ subalgebra. We may go further into the boundary structure by considering adjacent pairs or codimension-two subalgebras. For instance the adjacent pair $\{a_{13}, a_{62}\}$ in the $E_6$ cluster corresponds to an $A_2 \times A_2$ subalgebra.

As was already emphasised each cluster corresponds to a vertex of the polytope whose six $\mathcal{X}$-coordinates constitute a local coordinate system such that the vertex is at the origin. The $\mathcal{X}$-coordinates may then be associated with one-dimensional edges of the polytope along which they range from 0 to $\infty$. The interior of the polytope is the region in which all $\mathcal{X}$-coordinates are positive.

$$a_{13}$$
$$\uparrow$$
$$a_{24} \longrightarrow a_{51} \longrightarrow a_{62} \longleftarrow a_{41} \longleftarrow a_{33}$$
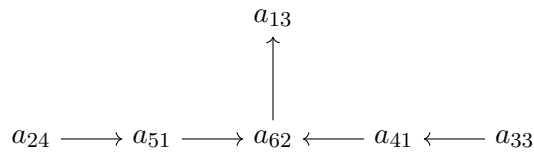
**Figure 10.5:** By mutation the initial cluster of $G(4,7)$ can be bought to the shape of an $E_6$ Dynkin diagram.

### 10.2.3   $G(4,8)$

At 8 points and beyond complications arise due to the underlying cluster algebra no longer being of finite type, and additional tools beyond that of the cluster algebra must be introduced in order to extract information for the symbol alphabet of the corresponding amplitude. There are two main reasons for this. First, the set of $\mathcal{A}$-coordinates becomes infinite which is not reflected by the finite set of letters needed to express say the two-loop NMHV octagon [134]. Therefore, some truncation procedure, such as topicalization [31–34], must be introduced to select a preferred subset of $\mathcal{A}$-coordinates. Second, the symbol alphabet starts to contain non-rational letters, with square roots appearing in the first instance for the two-loop NMHV octagon [134], the calculation of which revealed a set of 18 multiplicatively independent square root letters. More recently, the calculation of the 3-loop MHV octagon [135] revealed the same set of 18 algebraic letters along with an additional 24 rational letters.

Both issues were dealt with in [31] where the set of 180 rational letters of the two-loop NMHV octagon were recovered as rays of $\text{Trop}^+(I_{4,8})$, along with the 18 algebraic letters, associated to special *limit rays* arising from infinite affine sequences of mutations within the cluster algebra. Note, the additional 24 letters of the 3-loop MHV ampliutde were also covered by the predictions of [31]. Many other closely related approaches have been applied to the eight point case including plabic graphs, scattering diagrams to name a few [136–139].

In Chapter 11 we will use a new technique, which can be seen as a generalisation of the tropical approach, to extract the $\mathcal{A}$-coordinates of $G(4,6)$ and $G(4,7)$ along with their adjacency rules. Furthermore, in Chapter 12 we will review the methods used in [31] for

extracting square-root letters from infinite affine sequences in the more general setting of non dual conformal invariant 6-point kinematics.

## 10.3   Cluster Adjacency

The condition of cluster adjacency, initially proposed in [30], can be phrased as follows: *two $\mathcal{A}$-coordinates may appear adjacent in the symbol iff they appear together in some cluster.* This extends the role cluster algebras have to play in describing the analytic structure of scattering amplitudes beyond simply the union of their $\mathcal{A}$-coordinates and endows them with a geometric significance. In the language of the cluster polytope a pair of $\mathcal{A}$-coordinates are adjacent if their corresponding facets share a codimension-two boundary.

Note, the adjacency conditions are defined on the inhomogeneous $\mathcal{A}$-coordinates. Whereas the amplitudes are dual conformal invariant polylogarithmic functions on $\mathrm{Conf}_n(\mathbb{P}^3)$ whose symbol is written in terms of homogeneous multiplicative combinations of the $\mathcal{A}$-coordinates. However, these combinations can be expanded using (9.45) and (9.46) after which the adjacency conditions can be applied.

The conditions imposed by cluster adjacency are similar in spirit to that of the Steinmann relations. The Steinmann relations state that the double discontinuity of the (BDS-like normalised) amplitude must vanish when taken in overlapping channels, for the three-particle Mandelstams this can be summarised as

$$\mathrm{Disc}_{s_{jj+1j+2}}(\mathrm{Disc}_{s_{ii+1i+2}}\mathcal{E}_n) = 0, \quad \forall\, j = i \pm 1, i \pm 2. \tag{10.16}$$

Since, at the level of the symbol, the discontinuity around some letter $a = 0$ is obtained by isolating all terms beginning with $a$ and chopping it off, the Steinmann relations can be seen as placing constraints on the letters which can appear adjacently in the first two slots of the symbol. The importance of these relations in constraining the symbol of hexagon and heptagon amplitudes has been emphasised in [21, 22, 140].

In fact analogous constraints, the extended Steinmann relation [141], exist for adjacent slots all along the symbol. These extended relations are closely connected with the notion of cluster adjacency, with cluster adjacency implying the (extended) Steinmann relations, and (at six and seven points) the extended Steinmann relations together with the physical initial entry condition implying cluster adjacency.

At six points the adjacency conditions are best phrased by making use of the identification of $\mathrm{Conf}_6(\mathbb{P}^3)$ with $\mathrm{Conf}_6(\mathbb{P}^1)$. At the level of Plücker coordinates this is achieved by identifying the ordered four bracket $\langle ijkl \rangle$ with the ordered two bracket $\langle nm \rangle$, where $\{n, m\} = \{1, 2, 3, 4, 5, 6\} \backslash \{i, j, k, l\}$ and $n < m$, which in turn can be identified with a chord of the hexagon. In this way each cluster of the $A_3$ polytope can be seen as representing a

triangulation of the hexagon.
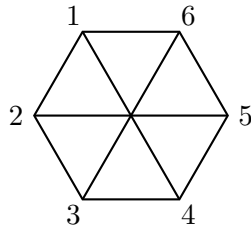


**Figure 10.6:** The three crossing chords corresponding to the square facets of the Stasheff polytope which each are never found in some cluster together.

In this language the statement of cluster adjacency becomes: two coordinates are forbidden (do not appear in a cluster together) iff their corresponding chords intersect. As an example consider the three square facets of the Stasheff polytope, corresponding to the crossing chords displayed in Figure 10.6, all of which are mutually forbidden pairs. Note, a similar statement of adjacency holds more generally for the Grassmannians $G(2, n)$ and chords of the $n$-gon.

In the case of $G(4, 7)$, and more generally $G(k, n)$ for $(k, n)$ coprime, we are able to use the frozen coordinates to homogenise the active $\mathcal{A}$-coordinate, and since the frozen coordinates appear in every cluster they cannot possibly spoil cluster adjacency. Therefore, cluster adjacency can be phrased directly on the 42 homogenous combinations defined in (10.14). The full set of adjacency conditions for $G(4, 7)$ were found in [30]. In particular out of the 903 pairs $\{a_{ij}, a_{kl}\}$ which can be constructed from the 42 letter alphabet 441 are adjacent and 462 are forbidden. We will see the 462 forbidden pairs arising in another context in the next chapter.

# Chapter 11

# Adjacency from the Gröbner fan

In this chapter we wish to reformulate the results of the last section in the new language of the Gröbner fan. This is inspired by the recent success of the application of Tropical geometry to scattering amplitudes [31–34], which the Gröbner fan can be thought as a generalisation of, and results from the mathematics literature [35, 36].

Our goal will be to extract the set of $\mathcal{A}$-coordinates and *forbidden* pairs from the Gröbner fan of the Plücker ideal $\mathrm{GF}(I_{k,n})$. As we will see the $\mathcal{A}$-coordinates will be encoded as non-prime factors of initial ideals associated to maximal cones of the positive tropical fan $\mathrm{Trop}^+(I_{k,n})$. Whereas, the forbidden pairs will be extracted from a single maximal Gröbner cone obtained after extending the Plücker ideal to the full set of $\mathcal{A}$-coordinates. We will demonstrate these techniques for $G(3, n)$ for $n = 6, 7, 8$ and discuss the possible outlook to the $n = 8$ case. This is of particular relevance for $G(3, 7)$ whose adjacency conditions dictate the structure of planar $\mathcal{N} = 4$ SYM amplitude symbols.

A benefit of this construction over the cluster approach is that it is very general, we can compute the Gröbner fan for any polynomial ideal we wish to write down. This poses the exciting question of whether similar techniques may be applied to scattering processes whose kinematics are not governed by the Grassmannian i.e. where dual-conformal symmetry is no longer present. We present an application of the Gröbner fan to non-dual conformal invariant 5-point massless scattering, where we will recover the entire non-planar alphabet $\mathbb{A}_{np}$ of [40], which we hope serves as a motivation to study the connection between Gröbner theory and scattering amplitudes.

## 11.1 Gröbner and Tropical fans

As was discussed at the beginning of Chapter **??** the Grassmannian can be thought as the projective variety inside $\mathbb{P}^{\binom{n}{k}-1}$ whose points vanish on the Plücker ideal $I_{k,n}$. As an example

the $G(2, n)$ Plücker Ideal is generated by the relations

$$I_{2,n} = \langle p_{ij}p_{kl} - p_{ik}p_{jl} + p_{il}p_{jk} : 1 \leq i < j < k < l \leq n \rangle. \tag{11.1}$$

Using this general viewpoint of the Grassmannian as an ideal generated by polynomial relations we can introduce a fan structure on $\mathbb{R}^{\binom{n}{k}}$ known as the Gröbner fan [142]. But, to begin to understand the structure of the Gröbner fan we must first introduce the notion of monomial orderings, initial ideals, and Gröbner bases our presentation of which follows that of [35].

Let $f$ be a polynomial in $n$ variables $(x_1, \ldots, x_n)$ with coefficients in an algebraically closed field $\mathbb{K}$ for which we use the notation

$$f = \sum_{\vec{\alpha}} c_{\vec{\alpha}} \mathbf{x}^{\vec{\alpha}}, \tag{11.2}$$

where we have introduced $\vec{\alpha} = (\alpha_1, \ldots, \alpha_n) \in \mathbb{Z}^n_{\geq 0}$, and $\mathbf{x}^{\vec{\alpha}}$ is understood as the monomial $x_1^{\alpha_1} \ldots x_n^{\alpha_n}$. Given some weight vector $w \in \mathbb{R}^n$ we can define the *initial form* of $f$ with respect to $\vec{w}$ as

$$\mathrm{in}_{\vec{w}}(f) = \sum_{\vec{\alpha}:\ \vec{\alpha}\cdot\vec{w}=m} c_{\vec{\alpha}} \mathbf{x}^{\vec{\alpha}}, \tag{11.3}$$

where $m = \min\{\vec{\alpha} \cdot \vec{w} :\ c_{\vec{\alpha}} \neq 0\}$. Furthermore, given an ideal $I \subset \mathbb{K}[x_1, \ldots, x_n]$, we can define its *initial ideal* with respect to $\vec{w}$ as the ideal generated by the initial forms of all functions $f \in I$ written as

$$\mathrm{in}_{\vec{w}}(I) = \langle \mathrm{in}_{\vec{w}}(f) : f \in I \rangle. \tag{11.4}$$

If for some finite set of generators $\mathcal{G} = \{g_1, \ldots, g_r\} \in I$, such that $I = \langle g_1, \ldots g_r \rangle$, we have $\mathrm{in}_{\vec{w}}(I) = \langle \mathrm{in}_{\vec{w}}(g) : g \in \mathcal{G} \rangle$ we call $\mathcal{G}$ a *Gröbner basis* of I with respect to $\vec{w}$.

The next definition we need is that of a *monomial order*. A monomial order $<$ on the set of monomials $\mathbf{x}^{\vec{\alpha}} \in \mathbb{K}[x_1, \ldots, x_n]$ is a total order which satisfies

$$i)\ 1 \leq \mathbf{x}^{\vec{\alpha}},$$

$$ii)\ \text{if } \mathbf{x}^{\vec{\alpha}} < \mathbf{x}^{\vec{\beta}} \implies \mathbf{x}^{\vec{\alpha}+\vec{\gamma}} < \mathbf{x}^{\vec{\beta}+\vec{\gamma}}.$$

This allows us to define the leading monomial of the polynomial $f$ as $\mathrm{in}_<(f) = c_{\vec{\beta}}\mathbf{x}^{\vec{\beta}}$, where $\mathbf{x}^{\vec{\beta}}$ is the leading monomial with respect to $<$ appearing in $f$ with non-zero coefficient i.e. $\mathbf{x}^{\vec{\beta}} = \max_<\{\mathbf{x}^{\vec{\alpha}} : c_{\vec{\alpha}} \neq 0\}$. Similarly, we can define the initial ideal of $I$ with respect to $<$ as

$$\mathrm{in}_<(I) = \langle \mathrm{in}_<(f) : f \in I \rangle. \tag{11.5}$$

Note, we may always choose some weight vector $\vec{w} \in \mathbb{R}^n$ such that $\mathrm{in}_{\vec{w}}(I) = \mathrm{in}_<(I)$. The converse is not generally true however.

By varying the weight vector $\vec{w}$ we may study all possible initial ideals of $I$. This leads us to the notion of the Gröbner fan $GF(I)$ on $\mathbb{R}^n$ as follows: two weight vectors $\vec{w}_1$ and $\vec{w}_2$ lie in the relative interior of the same cone $C$ if and only if $\text{in}_{\vec{w}_1}(I) = \text{in}_{\vec{w}_2}(I)$ i.e. they generate the same initial ideal. Note, each full-dimensional (maximal) Gröbner cone is associated to a monomial initial ideal specified by some monomial order $<$, consisting of all weight vectors $\vec{w} \in \mathbb{R}^n$ such that $\text{in}_{\vec{w}}(I) = \text{in}_<(I)$. A weight vector will lie on the boundary of a maximal cone when the associated initial ideal is no longer monomial. It is this collection of maximal Gröbner cones, together with their intersections, which we call the Gröbner fan $GF(I)$.

Note, we are always free to shift a weight vector by any element of the the lineality space of the Gröbner fan $GF(I)$ without altering the initial ideal, where the lineality space is defined as the linear subspace containing all elements $\vec{l}$ such that $\text{in}_{\vec{l}}(I) = I$.

We will also be interested in interesting subfans of the Gröbner fan, the first being the tropical fan $\text{Trop}(I)$ defined as the subfan

$$\text{Trop}(I) = \{\vec{w} \in \mathbb{R}^n : \text{in}_{\vec{w}}(I) \text{ contains no monomial}\}. \tag{11.6}$$

We may restrict further and define the totally positive tropical fan $\text{Trop}^+(I)$ given by

$$\text{Trop}^+(I) = \{\vec{w} \in \text{Trop}(I) : \text{in}_{\vec{w}}(I) \text{ is totally positive}\}, \tag{11.7}$$

where an ideal $I \subset \mathbb{R}[x_1, \ldots, x_n]$ is called *totally positive* if it does not contain any polynomial with all positive coefficients.

The above discussion is most easily demonstrated with an example, the simplest case being $G(2,4)$, whose Plücker ideal is generated by a single polynomial

$$I_{2,4} = \langle p_{12}p_{34} - p_{13}p_{24} + p_{14}p_{23} \rangle \subset \mathbb{R}[p_{12}, p_{13}, p_{14}, p_{23}, p_{24}, p_{34}]. \tag{11.8}$$

Let $\vec{w} = (w_{12}, w_{13}, w_{14}, w_{23}, w_{24}, w_{34}) \in \mathbb{R}^6$ and $f = p_{12}p_{34} - p_{13}p_{24} + p_{14}p_{23}$ which being the sole generator of $I_{2,4}$ constitutes a Gröbner basis for any choice of weight vector $\vec{w}$. A generic weight vector $\vec{w} \in \mathbb{R}^6$ can always be bought to the form $(x, y, 0, \ldots, 0)$ with some suitable choice of lineality shift. The resulting Gröbner fan $GF(I_{2,4})$ is depicted in the $(x, y)$ plane in Figure 11.1. The Gröbner fan $GF(I_{2,4})$ consists of three maximal cones labelled by the monomial initial ideals $\langle p_{12}p_{34}\rangle$, $\langle p_{13}p_{24}\rangle$ and $\langle p_{14}p_{23}\rangle$. The maximal cones intersect to give the three rays of the tropical fan $\text{Trop}(I_{2,4})$ given by $e_{12} = (1,0)$, $e_{13} = (0,1)$ and $e_{14} = (-1,-1)$, whose corresponding binomial initial ideals are $\langle p_{14}p_{23} - p_{13}p_{24}\rangle$, $\langle p_{12}p_{34} + p_{14}p_{23}\rangle$ and $\langle p_{12}p_{34} - p_{13}p_{24}\rangle$. The positive part of the tropical fan $\text{Trop}^+(I_{2,4})$ consists of the rays $e_{12} = (1,0)$ and $e_{14} = (-1,-1)$ highlighted in red whose generators contain terms of opposite sign, the ray $e_{13} = (0,1)$ is not contained in $\text{Trop}^+(I_{2,4})$ since it is generated by a polynomial with all positive coefficients.
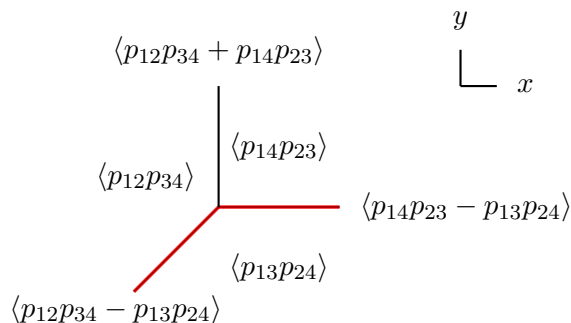
**Figure 11.1:** The Gröbner fan structure of $GF(I_{2,4})$ with each region labelled by its initial ideal. Each point in the $(x, y)$ plane corresponds to a 4-dimensional linear subspace of $\mathbb{R}^6$ consisting of all weight vectors lineality equivelent to $(x, y, 0, 0, 0, 0)$. The tropical fan corresponds to the three rays, whilst the positive tropical fan corresponds to the two red rays.

### 11.1.1   Forbidden pairs and $\mathcal{A}$-coordinates

Moving forward the final definition needed is that of a prime (or alternatively non-prime) ideal. An ideal $I$ is non-prime if there exists two polynomials $f \notin I$ and $g \notin I$ such that their product $f \cdot g \in I$. In this case we call $f$ and $g$ non-prime factors of $I$. Note, a non-prime ideal can always be decomposed into the intersection of finitely many prime components.

With all the necessary material reviewed let us remind ourselves of our goal: to extract (at least in the finite cases) the $\mathcal{A}$-coordinates and adjacency relations of the Grassmannian cluster algebras $G(k, n)$ from the Gröbner fan of the Plücker ideal $GF(I_{k,n})$, which in the case of $G(4, 6)$ and $G(4, 7)$ provide vital information for the amplitude bootstrap in the form of the symbol alphabet and adjacency rules. Such ideas were first presented in [35] for the case $G(2, n)$ and $G(3, 6)$ and more generally for any cluster algebra of geometric finite type in [36].

**$\mathcal{A}$-coordinates:** The Plücker ideal is defined on the $\binom{n}{k}$ Plücker coordinates $p_{i_1, \ldots, i_k}$. In the case of the Grassmannians $G(2, n)$ these make up the full set of $\mathcal{A}$-coordinates. However, for $G(3, 6)$, and more importantly $G(3, 7)$ relevant for heptagon amplitudes, $\mathcal{A}$-coordinates quadratic in the Plückers start to appear. As we shall explain these *missing $\mathcal{A}$-coordinates appear as non-prime factors of initial ideals inside the maximal cones of* $\mathrm{Trop}^+(I_{k,n})$.

**Forbidden pairs:** Generally, the rays of the positive tropical fan $\mathrm{Trop}^+(I_{k,n})$ will span multiple maximal Gröbner cones. That is to say taking a suitably general[1] weight vector $\vec{w}$ lying in the span of the rays of $\mathrm{Trop}^+(I_{k,n})$ we will generate multiple monomial initial ideals. However, upon extending the ideal by the missing $\mathcal{A}$-coordinates the rays of $\mathrm{Trop}^+(I_{k,n}^{\mathrm{ext}})$ resolve to span a single maximal Gröbner cone. The initial ideal of this maximal Gröbner cone provides us with a list of monomials which are exactly the forbidden pairs of $\mathcal{A}$-coordinates.

---

[1] A weight vector not lying in the intersection of maximal cones of the Gröbner fan.

Note, in the case of $G(2,n)$ all $\mathcal{A}$-coordinates are present already for $I_{k,n}$ and no extension procedure is needed.

In the remainder of this section we review these ideas for the case of $G(2,5)$. Later in Section 11.3 we return to the case of $G(3,6)$, already presented in [35], and further apply this discussion to $G(3,7)$ relevant for heptagon amplitudes. We also discuss the remaining finite case $G(3,8)$ and comment on the outlook beyond the finite type Grassmannians.

### 11.1.2  $GF(I_{2,5})$

We conclude this section with the example of $G(2,5)$. In the space of Plücker coordinates $(p_{12}, \ldots, p_{45})$ the five Plücker relations are given by

$$p_{ij}p_{kl} - p_{ik}p_{jl} + p_{il}p_{jk} = 0, \quad 1 \le i < j < k < l \le 5. \tag{11.9}$$

The Gröbner fan $GF(I_{2,5})$ is simplicial, containing 132 maximal cone and twenty rays, arranging the coordinates in lexicographic order

$$\{w_{12}, w_{13}, w_{14}, w_{15}, w_{23}, w_{24}, w_{25}, w_{34}, w_{35}, w_{45}\}, \tag{11.10}$$

they are defined as

$$e_{12} = (1, 0, 0, 0, 0, 0, 0, 0, 0, 0),$$
$$\vdots$$
$$e_{45} = (0, 0, 0, 0, 0, 0, 0, 0, 0, 1), \tag{11.11}$$

along with ten more given by $-e_{ij}$.

There are 60 cones with four $e_{ij}$ vertices and one $-e_{ij}$ vertex and 60 more with three $e_{ij}$ vertices and two $-e_{ij}$ vertices. The ten $e_{ij}$ vectors defined above make up the rays of the tropical fan, they are connected in a Petersen graph topology shown in Figure 11.2. The positive tropical fan contains the five rays the $e_{i,i+1}$ highlighted in red.

There is exactly one[1] Gröbner cone spanned by the five rays $\{e_{12}, e_{23}, e_{34}, e_{45}, e_{15}\}$ of $\text{Trop}^+(I_{k,n})$. This cone has a Gröbner basis whose initial monomials are the crossing chords (forbidden pairs) of the pentagon, i.e. $p_{13}p_{24}$ and cyclic. Therefore, from Gröbner theory, we have recovered the important (for amplitudes) content of the $G(2,5)$ cluster algebra i.e. the set of forbidden pairs of $\mathcal{A}$-coordinates!

The case of $G(2,n)$ was studied in detail in [35], where this construction was shown to hold for all $n$ i.e. the rays of the positive tropical fan span a single maximal Gröbner cone, whose

---

[1]There are eleven other maximal cones with all five vertices among the $\{e_{ij}\}$, corresponding to permutations of the above positive cone (i.e. different positive regions for other choices of ordering).
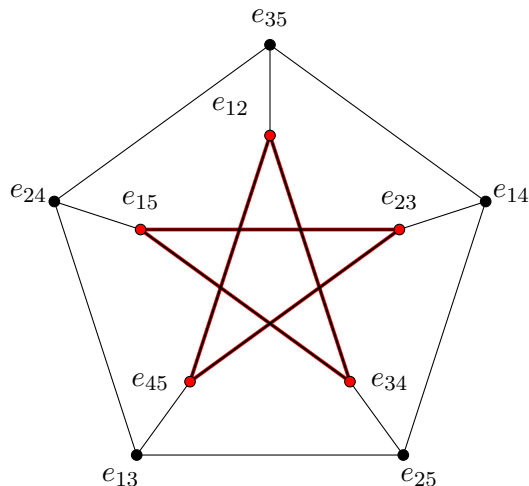
**Figure 11.2:** The tropical fan $\text{Trop}(I_{2,5})$ and its positive part highlighted red.

initial ideal is generated by the crossing chords of the $n$-gon, let us emphasise again these are exactly the set of forbidden pairs of $\mathcal{A}$-coordinates for the $G(2,n)$ cluster algebra. As was shown there for the case of $G(3,6)$, and we shall explain in Section 11.3, this is not the case generally. Instead to identify a single maximal Gröbner cone, whose rays are given by the positive tropical part, the ideal must first be extended by the missing $\mathcal{A}$-coordinates. In the next chapter we take a brief aside to describe how the positive tropical fan is calculated in practice before returning to this issue of missing $\mathcal{A}$-coordinates.

## 11.2   $\text{Trop}^+(I_{k,n})$ from the web matrix

In practice it is only possible to compute the entire Gröbner fan for the most simple of cases. Therefore, it is highly desirable to have an efficient route to calculating the positive tropical part $\text{Trop}^+(I_{k,n})$ directly without having it embedded in the entire Gröbner fan. In this section we review the methods of [143] on this direct construction. For a detailed discussion of this procedure and the structure of the resulting fans see [144, 145]. The cases of interest will be $\text{Gr}(3,n)$ for $n=6,7,8$ which along with $\text{Gr}(2,n)$ make up the finite type Grassmannian cluster algebras.

Generally, the $G(k,n)$ initial cluster has the form of a $(k-1) \times (n-k-1)$ array of active nodes, in addition to $k$ many frozen nodes, each labelled by an $\mathcal{A}$-coordinate. An example of the initial cluster for the case of $G(2,5)$ is given in Figure 11.3. Alternatively, we may instead assign to each active node a $\mathcal{X}$-coordinate, given by the product of incoming $\mathcal{A}$-coordinates over the product of the outgoing, which again organise themselves into a $(k-1) \times (n-k-1)$ array with elements $x_{rs}$.

Using $x_{rs}$ we can define the $k \times n$ web matrix $W^{(k,n)} = (\mathbf{I}_k|M)$. Where $M$ is given by the

$k \times (n-k)$ matrix elements

$$m_{ij} = (-1)^{i+k} \sum_{\vec{\lambda} \in Y_{ij}} \prod_{r=1}^{k-i} \prod_{s=1}^{\lambda_r} X_{rs}, \tag{11.12}$$

with the summation range $Y_{ij}$ given by $0 \leq \lambda_{k-i} \leq \dots \leq \lambda_1 \leq j-1$. The web matrix thus allows us to evaluate all $\mathcal{A}$-coordinates as subtraction free polynomials in the $\mathcal{X}$-coordinates by identifying the Plücker coordinates with the maximal minors of the web matrix i.e.

$$p_{i_i \dots i_k} = \det(W^{(k,n)}_{i_1,\dots,i_k})(x_{rs}) \tag{11.13}$$

where $W^{(k,n)}_{i_1,\dots,i_k}$ is understood as the matrix formed from $W^{(k,n)}$ by taking columns $i_i \dots i_k$.
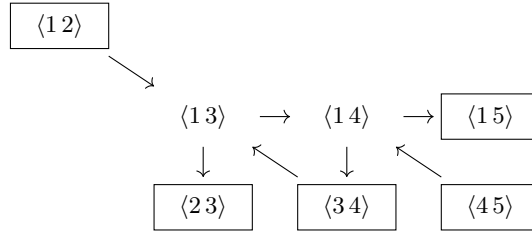


**Figure 11.3:** The initial cluster of $G(2,5)$.

Let us demonstrate this with the example of $G(2,5)$ whose initial cluster is depicted in Figure 11.3 from which we can read off the $\mathcal{X}$-coordinates, they are given by

$$x_{11} = \frac{\langle 12 \rangle \langle 34 \rangle}{\langle 14 \rangle \langle 23 \rangle}, \qquad\qquad x_{12} = \frac{\langle 13 \rangle \langle 45 \rangle}{\langle 34 \rangle \langle 15 \rangle}. \tag{11.14}$$

This in turn defines the web matrix to be

$$W^{(2,5)} = \begin{bmatrix} 1 & 0 & -1 & -1-x_{11} & -1-x_{11}-x_{11}x_{12} \\ 0 & 1 & 1 & 1 & 1 \end{bmatrix}. \tag{11.15}$$

By identifying the Plücker coordinates $p_{ij}$ with the maximal minor formed by columns $i$ and $j$ of the web matrix as

$$p_{ij} = \det(W^{(2,5)}_{ij})(x_{11}, x_{12}), \tag{11.16}$$

we immediately arrive at an expression for all $\mathcal{A}$-coordinates as subtraction free polynomials in the $\mathcal{X}$-coordinates. As an example we have

$$p_{25} = x_{11} + x_{12}x_{22},$$

We can now continue in tropicalizing the expressions for the $\mathcal{A}$-coordinates, which amounts to $+$ and $\times$ begin replaced by their tropical counterparts min and $+$. The tropical version

of the above Plücker is given by

$$\tilde{p}_{25} = \min(\tilde{x}_{11}, \tilde{x}_{11} + \tilde{x}_{12}) \,, \tag{11.17}$$

where $\tilde{p}$ and $\tilde{x}$ are used to emphasise that we are dealing with tropical expressions. This tropical expression defines a piece-wise linear map on $(x_{11}, x_{12})$, with regions of linearity separated by tropical hypersurfaces, and as such provide a fan structure on $(x_{11}, x_{12})$. For example the tropical hypersurface of $\tilde{p}_{25}$ is given by

$$\tilde{x}_{12} = 0 \,. \tag{11.18}$$

By tropicalizing different subsets of the $\mathcal{A}$-coordinates we can define different tropical fans given by the common refinement of all fans in the subset of tropical expressions. In practice we calculate the refinement of the tropical fan for a subset, $\mathcal{S}$, of $\mathcal{A}$-coordinates via the Minkowski sum of their Newton polytopes. The tropical expressions for the frozen coordinates do not contain any tropical hypersurface and hence do not contribute to the structure of the fan.

Our focus will be on two fans in particular: the Speyer-Williams fan [143], obtained by tropicalizing the set of all Plückers coordinates; and the cluster fan, where we choose to tropicalise the entire set of $\mathcal{A}$-coordinates. Note, for the case of $G(2,n)$ the Plücker coordinates themselves make up the entire set of $\mathcal{A}$-coordinates and hence the Speyer-Williams and cluster fans coincide. However, when considering $G(3,6)$, $\mathcal{A}$-coordinates quadratic in the Plückers begin to appear and hence the structure of the two fans begin to differ.

### 11.2.1   $\mathbf{Trop}^+(I_{2,5})$

Let us finish the example of $\text{Trop}^+(I_{2,5})$. The $G(2,5)$ web matrix, written in (11.15), allows us to write the 10 Plücker variables $p_{ij}$ in terms of the two $\mathcal{X}$-coordinates $(x_{11}, x_{12})$ as

$$
\begin{aligned}
p_{1i} &= p_{23} = 1, & p_{24} &= 1 + x_{11}, & p_{25} &= 1 + x_{11} + x_{11}x_{12}, \\
p_{34} &= x_{11}, & p_{35} &= x_{11} + x_{11}x_{12}, & p_{45} &= x_{11}x_{12}.
\end{aligned}
\tag{11.19}
$$

Taking these expressions as the input to the Minkowski sum operation of `gfan` [146] we obtain $\text{Trop}^+(I_{2,5})$. The resulting fan is depicted in Figure 11.4. It has five regions of linearity whose boundaries are given by the five rays

$$\{(1,0), (0,1), (-1,0), (0,-1), (1,-1)\}.$$

Note, the tropical fan as described above is parameterised in the space of the $(\tilde{x}_{11}, \tilde{x}_{12})$ variabels. However, as discussed in [144, 145], we can map the five rays above to those

presented in Section 11.1.2 by taking the scalar product of the unit vectors $e_{ij}$ with the vector of tropicalized Plücker coordinates i.e.

$$(\tilde{x}_{11}, \tilde{x}_{12}) \mapsto \sum_{1 \leq i < j \leq 5} \tilde{p}_{ij}(\tilde{x}_{11}, \tilde{x}_{12}) e_{ij}. \tag{11.20}$$

The five rays given above up to lineality map to $\{e_{12}, e_{45}, e_{23}, e_{15}, e_{34}\}$. In particular, the regions between the rays of Figure 11.4 map to the red edges between the corresponding rays in Figure 11.2.
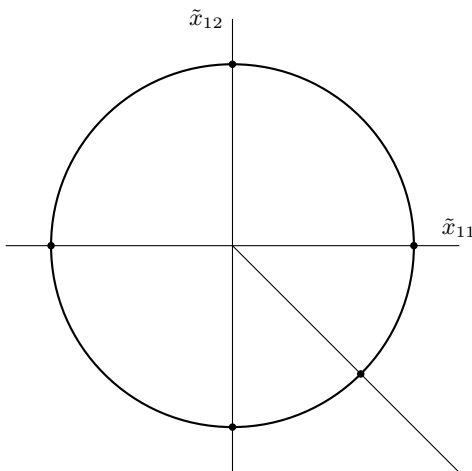


**Figure 11.4:** The tropical fan $\mathrm{Trop}^{+}(I_{2,5})$.

## 11.3 Adjacency from the Gröbner fan

As emphasised already in the case of $G(2, n)$ the Speyer-Williams and cluster fan coincide since the full set of $\mathcal{A}$-coordinates are given solely by the Plückers. But for the remaining finite type Grassmannians this is no longer the case. In this section we wish to begin with the Speyer-Williams fan, by tropicalizing only the Plücker coordinates, and see where the additional information of the missing $\mathcal{A}$-coordinates and adjacency conditions is hidden inside the structure of $\mathrm{Trop}^{+}(I_{k,n})$ and $GF(I_{k,n})$. Note, these questions were originally asked in [35] and later extended in [36]. Before we begin let us remind ourselves where we find this additional information:

$\mathcal{A}$**-coordinates**: The missing $\mathcal{A}$-coordinates appear as non-prime factors in the initial ideals of maximal cones of $\mathrm{Trop}^{+}(I_{k,n})$.

**Frobidden pairs**: Upon extending the ideal by the missing $\mathcal{A}$-coordinates the rays of $\mathrm{Trop}^{+}(I_{k,n})$ span a single maximal Gröbner cone. The initial ideal of this maximal Gröbner cone, of the extended ideal, provides us with a list of monomials which are exactly the forbidden pairs of $\mathcal{A}$-coordinates.

### 11.3.1   $G(3,6)$

The case of $G(3,6)$ was covered in detail in [35] we review here the relevant discussion and provide additional detail on the calculation. The Plücker Ideal $I_{3,6}$ is generated by three and four-terms relations of the form

$$p_{123}p_{145} + p_{125}p_{134} - p_{124}p_{135} = 0, \ldots \tag{11.21}$$

$$p_{123}p_{456} - p_{156}p_{234} + p_{146}p_{235} - p_{145}p_{236} = 0, \ldots \tag{11.22}$$

in the ring of polynomials in the 20 Plücker coordinates $p_{ijk}$. We obtain the Speyer-Williams [143] fan by tropoicalizing all Plücker coordinates as explained in the last section. The positive tropical fan is spanned by 16 rays given by

$$
\begin{array}{cccc}
(1,0,0,0), & (-1,0,0,0), & (1,-1,0,0), & (0,0,1,-1), \\
(0,1,0,0), & (0,-1,0,0), & (1,0,-1,0), & (-1,0,0,1), \\
(0,0,1,0), & (0,0,-1,0), & (1,0,0,-1), & (0,1,1,-1), \\
(0,0,0,1), & (0,0,0,-1), & (0,1,0,-1), & (1,-1,-1,0), \quad (11.23)
\end{array}
$$

in $\tilde{x}$ space with the ordering $(\tilde{x}_{11}, \tilde{x}_{21}, \tilde{x}_{12}, \tilde{x}_{22})$. The maximal cones of the fan are four-dimensional regions within which all minors are linear, which can be intersected with the unit sphere to produce 3-dimensional facets of a polyhedral complex. The fan has 48 maximal facets given by 46 terahedra and 2 bipyramids. They themselves have 2-dimensional boundaries corresponding to some minor being between two regions of linearity. There are 98 of these 2-dimensional boundaries, which themselves are bounded by 66 edges, which are further bounded by 16 points. The 16 points correspond to the intersection of the rays in (11.23) with the unit sphere. This information can be summarised by the $f$-vector given by $f_{3,6} = (16, 66, 98, 48)$. Sometimes we would also like to keep information on the number of vertices of each facet, for this we use the notation

$$f_{3,6} = (16_1, 66_2, 98_3, 46_4 + 2_5),$$

where we understand the right most element as 46 tetrahedrons (4-vertex objects) and two, non-simplicial, bipyramids (5-vertex objects).

In contrast with the $G(2,n)$ case, the Speyer-Williams fan does not single out an individual maximal Gröbner cone of $\text{GF}(I_{3,6})$. In fact, calculating initial ideals inside the span of the 16 positive rays of $\text{Trop}^+(I_{3,6})$ we find 9 maximal Gröbner cones. However, as shown in [35], we can resolve the positive tropical part into a single maximal Gröbner cone by extending the ideal. To decide how to extend the ideal we search the maximal non-prime cones of $\text{Trop}^+(I_{3,6})$ which will provide for us the missing $\mathcal{A}$-coordinates as non-prime factors.

Let us now describe this resolution in detail. Out of the 48 maximal cones only 2 are associated with non-prime initial ideals. They are given by two bipyramids each of which are spanned by 5 rays given by

$$
\begin{aligned}
b_1 &= \operatorname{span}\{(-1,0,0,1),(0,0,1,0),(-1,0,0,0),(0,1,0,0),(0,1,1,-1)\} \\
&:= \operatorname{span}\{b_{11},b_{12},b_{13}.b_{14},b_{15}\}, \\
b_2 &= \operatorname{span}\{(1,-1,-1,0),(1,0,-1,0),(1,-1,0,0),(0,0,0,-1),(1,0,0,-1)\} \\
&:= \operatorname{span}\{b_{21},b_{22},b_{23}.b_{24},b_{25}\}. \tag{11.24}
\end{aligned}
$$

The Gröbner fan structure $\operatorname{GF}(I_{3,6})$ splits each bipyramid into a collection of three tetrahedra, each with its own initial ideal, by introducing an additional edge between the poles of the bipyramids as indicated in Figure 11.5. This can be viewed as each bipyramid intersecting three of the nine maximal Gröbner cones spanned by the rays of $\operatorname{Trop}^+(I_{3,6})$. The three non-prime initial ideals generated inside $b_1$ can be written as the intersection of two prime ideals as

$$
\begin{aligned}
\operatorname{in}_{b_1\setminus\{b_{12}\}}(I_{3,6}) &= \langle\operatorname{in}_{b_1\setminus\{b_{12}\}}(I_{3,6})\cup M_1\rangle\cap\langle\operatorname{in}_{b_1\setminus\{b_{12}\}}(I_{3,6})\cup\{p_{256}p_{134}-p_{234}p_{156}\}\rangle, \\
\operatorname{in}_{b_1\setminus\{b_{13}\}}(I_{3,6}) &= \langle\operatorname{in}_{b_1\setminus\{b_{13}\}}(I_{3,6})\cup M_1\rangle\cap\langle\operatorname{in}_{b_1\setminus\{b_{13}\}}(I_{3,6})\cup\{p_{124}p_{356}-p_{123}p_{456}\}\rangle, \\
\operatorname{in}_{b_1\setminus\{b_{14}\}}(I_{3,6}) &= \langle\operatorname{in}_{b_1\setminus\{b_{14}\}}(I_{3,6})\cup M_1\rangle\cap\langle\operatorname{in}_{b_1\setminus\{b_{14}\}}(I_{3,6})\cup\{p_{126}p_{345}-p_{125}p_{346}\}\rangle.
\end{aligned}
$$
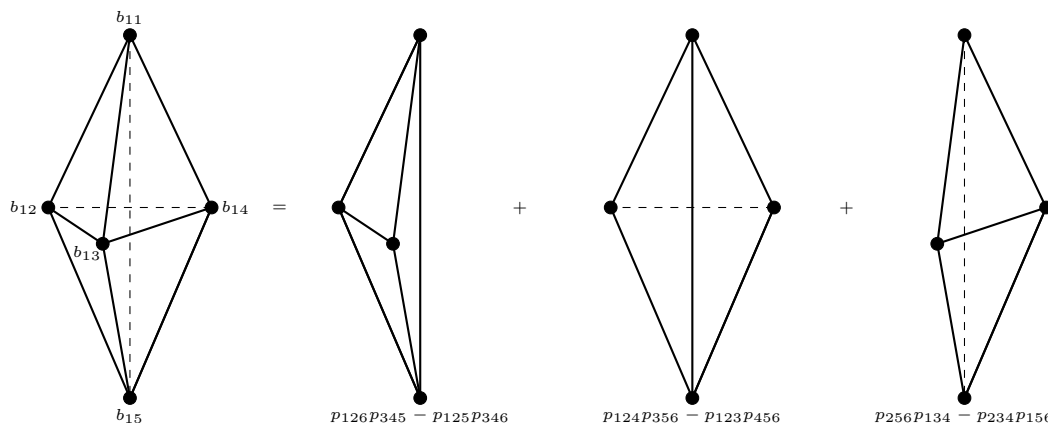


**Figure 11.5:** The bipyramid $b_1$ inside $\operatorname{Trop}^+(I_{3,6})$, on the left hand we have the full bipyramid with its 5 rays, on the right the bipyramid is split into three tetrahedra by the structure of the Gröbner fan. Each tetrahedron is labelled by the quadratic non-prime factor found in the initial ideal, note all three expressions are equivalent modulo the Plücker relations.

Similarly for $b_2$ we have the cyclic copy of the above given by

$$
\operatorname{in}_{b_2\setminus\{b_{22}\}}(I_{3,6}) = \langle\operatorname{in}_{b_2\setminus\{b_{22}\}}(I_{3,6})\cup M_2\rangle\cap\langle\operatorname{in}_{b_2\setminus\{b_{22}\}}(I_{3,6})\cup\{p_{145}p_{236}-p_{123}p_{456}\}\rangle,
$$

$$\mathrm{in}_{b_2\setminus\{b_{23}\}}(I_{3,6}) = \langle \mathrm{in}_{b_2\setminus\{b_{23}\}}(I_{3,6}) \cup M_2 \rangle \cap \langle \mathrm{in}_{b_2\setminus\{b_{23}\}}(I_{3,6}) \cup \{p_{136}p_{245} - p_{126}p_{345}\} \rangle,$$

$$\mathrm{in}_{b_2\setminus\{b_{24}\}}(I_{3,6}) = \langle \mathrm{in}_{b_2\setminus\{b_{24}\}}(I_{3,6}) \cup M_2 \rangle \cap \langle \mathrm{in}_{b_2\setminus\{b_{24}\}}(I_{3,6}) \cup \{p_{156}p_{234} - p_{146}p_{235}\} \rangle.$$

Where we understand for instance $\mathrm{in}_{b_1\setminus\{b_{11}\}}(I_{3,6})$ as the initial ideal of $I_{3,6}$ associated to the cone spanned by the rays $b_1 \setminus \{b_{11}\}$ and we have defined the sets of monomials

$$M_1 = \{p_{235}, p_{236}, p_{245}, p_{246}, p_{135}, p_{136}, p_{145}, p_{146}\},$$
$$M_2 = \{p_{124}, p_{125}, p_{134}, p_{135}, p_{246}, p_{256}, p_{346}, p_{356}\}.$$

Most importantly notice the three quadratic non-prime factors appearing in each cone modulo the Plücker ideal are equivalent to either

$$p_{12[34]56} \text{ or } p_{23[45]61}, \tag{11.25}$$

where we have defined $p_{ij[kl]mn} = p_{ijl}p_{kmn} - p_{ijk}p_{lmn}$. These are exactly the two missing $\mathcal{A}$-coordinates, which along with the 14 monomials contained in $M_1 \cup M_2$, make up the full set of active $\mathcal{A}$-coordinates!
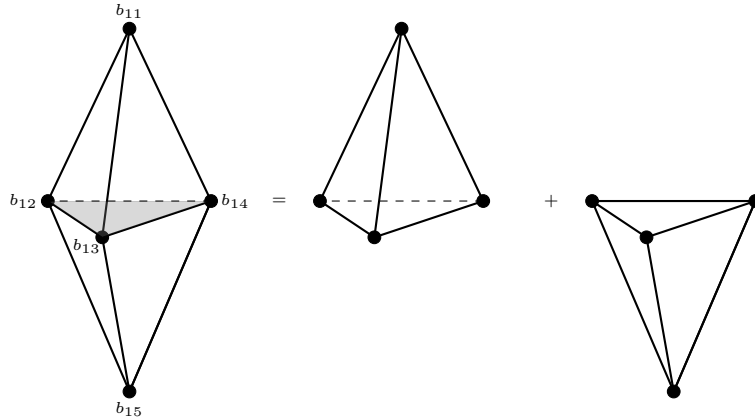


**Figure 11.6:** The bipyramid $b_1$ now depicted inside $\mathrm{Trop}^+(I'_{3,6})$, on the right hand side the bipyramid is split into two tetrahedra by the structure of the Gröbner fan both of which are associated to prime ideals.

Extending the Plücker ideal as

$$I'_{3,6} = I_{3,6} \cap \langle q_1 - p_{12[34]56} \rangle \subset \mathbb{R}[p_{123}, \dots, p_{456}, q_1], \tag{11.26}$$

defines a new ideal and hence a new Gröbner fan $GF(I'_{3,6})$. The positive tropical fan $\mathrm{Trop}^+(I'_{3,6})$ has the $f$-vector given by $f'_{3,6} = (16_1, 66_2, 99_3, 48_4 + 1_5)$ which now contains only a single non-prime bipyramid. The transition from $f_{3,6}$ to $f'_{3,6}$ can be seen as adding a triangle to the equator of the bipyramid $b_1$ as shown in Figure 11.6 which now splits into two terahedra with prime initial ideals. Note, also the rays of $\mathrm{Trop}^+(I'_{3,6})$ now span only 3

maximal Gröbner cones.

Extending the ideal further as

$$I_{3,6}^{\text{ext}} = I'_{3,6} \cap \langle q_2 - p_{23[45]61} \rangle \subset \mathbb{R}[p_{123}, \dots, p_{456}, q_1, q_2], \tag{11.27}$$

defines yet again a new Grobner fan $GF(I_{3,6}^{\text{ext}})$ whose positive tropical part $\text{Trop}^+(I_{3,6}^{\text{ext}})$ is simplicial, with $f_{3,6}^{\text{ext}} = (16_1, 66_2, 100_3, 50_4)$, and contains no non-prime maximal cones. Again this can be viewed as adding a triangle to bipyramid $b_2$.

Furthermore, the rays of $\text{Trop}^+(I_{3,6}^{\text{ext}})$ now span a single maximal Gröbner cone whose initial ideal is generated by

$$\{q_1 q_2, p_{124}q_2, p_{125}q_2, p_{134}q_2, p_{135}q_1, p_{135}q_2, p_{124}p_{135}, p_{136}q_1, p_{124}p_{136}, p_{125}p_{136}, p_{145}q_1, p_{146}q_1, p_{125}p_{146},$$

$$p_{135}p_{146}, p_{235}q_1, p_{124}p_{235}, p_{134}p_{235}, p_{146}p_{235}, p_{236}q_1, p_{124}p_{236}, p_{125}p_{236}, p_{134}p_{236}, p_{135}p_{236}, p_{145}p_{236},$$

$$p_{245}q_1, p_{134}p_{245}, p_{135}p_{245}, p_{136}p_{245}, p_{246}q_1, p_{246}q_2, p_{125}p_{246}, p_{134}p_{246}, p_{135}p_{246}, p_{136}p_{246}, p_{145}p_{246},$$

$$p_{235}p_{246}, p_{256}q_2, p_{134}p_{256}, p_{135}p_{256}, p_{136}p_{256}, p_{145}p_{256}, p_{146}p_{256}, p_{346}q_2, p_{125}p_{346}, p_{135}p_{346}, p_{145}p_{346},$$

$$p_{235}p_{346}, p_{245}p_{346}, p_{356}q_2, p_{124}p_{356}, p_{145}p_{356}, p_{146}p_{356}, p_{245}p_{356}, p_{246}p_{356}\},$$

which are exactly the 54 forbidden pairs of $\mathcal{A}$-coordinates!

### 11.3.2  $G(3,7)$

We now go beyond the results of [35] and consider $G(3,7)$. Again to obtain the Speyer-Williams fan for $G(3,7)$ we tropicalise the 35 Plücker coordinates. In the space of variables $(\tilde{x}_{11}, \tilde{x}_{12}, \tilde{x}_{13}, \tilde{x}_{21}, \tilde{x}_{22}, \tilde{x}_{23})$ the positive Tropical fan is spanned by 42 rays with 6-dimensional maximal cones. The structure of the fan is summarised by

$$f_{3,7} = (1, 42, 392, 1463, 2583, 2163, 595_6 + 63_7 + 28_8 + 7_9),$$

where we have included the information on the number of vertices for the maximal cones only.

We begin the search for the missing $\mathcal{A}$-coordinates by calculating the initial ideals associated to the $7_9$ maximal cones. Selecting one of the 7 nine-vertex maximal cones we find its initial ideal is non-prime and contains in particular the non-prime factors

$$\{p_{12[34]67}, p_{67[12]45}, p_{12[35]67}\},$$

with the remaining 6 maximal cones providing us with their cyclic copies [1]. In total we find

---

[1]Note, the first and second variables are already cyclic copies of one another.

all 14 missing quadratic $\mathcal{A}$-coordinates:

$$q_{51} = p_{12[34]56} \text{ and cyclic,}$$
$$q_{61} = p_{61[23]45} \text{ and cyclic,} \tag{11.28}$$

appearing as non-prime factors of the $7_9$ maximal cones. By extending the ideal by all 14 variables as

$$I_{3,7}^{\text{ext}} = I_{3,7} \cap \langle q_{51} - p_{12[34]56}, \ldots, q_{67} - p_{56[12]34} \rangle \subset \mathbb{R}[p_{123}, \ldots, p_{567}, q_{51}, \ldots, q_{67}], \tag{11.29}$$

the positive tropical fan $\text{Trop}^+(I_{3,7}^{\text{ext}})$ becomes simplicial with the $f$-vector

$$f_{3,7}^{\text{ext}} = (42_1, 399_2, 1547_3, 2856_4, 2499_5, 833_6).$$

Moreover, the rays of $\text{Trop}^+(I_{3,7}^{\text{ext}})$ span a single maximal Gröbner cone whose initial ideal gives us the list of 462 forbidden neighbours relevant for the symbol alphabet of heptagon amplitudes.

### 11.3.3   $G(3, 8)$

In the space of variables $(\tilde{x}_{11}, \tilde{x}_{12}, \tilde{x}_{13}, \tilde{x}_{14}, \tilde{x}_{21}, \tilde{x}_{22}, \tilde{x}_{23}, \tilde{x}_{24})$ the positive tropical Speyer-Williams fan is spanned by 120 rays with 8-dimensional maximal cones. The structure of the fan is summarised by

$$f_{3,8} = (1, 120, 2072, 14088, 48544, 93104, 100852, 57768, 13612),$$

with the maximal cones given by

$$9672_8 + 1696_9 + 1092_{10} + 480_{11} + 416_{12} + 104_{13} + 88_{14} + 32_{15} + 24_{16} + 8_{17}.$$

At this point the calculations become cumbersome, so let us emphasise the main differences to the previous two cases. First, there are 8 more $\mathcal{A}$-coordinates than there are rays of the Speyer-Williams fan, which must appear when we begin to extend the ideal. Second, the $\mathcal{A}$-coordinates not only contain expressions quadratic in the Plücker but also contain cubic expressions given by

$$\{p_{12[34]5[67]89}, p_{12[35]8[67]45}, p_{12[34]8[67]35}\} \text{ and cylic,} \tag{11.30}$$

where we have made the definition $p_{ij[kl]m[nr]st} = p_{ijl}p_{km[nr]st} - p_{ijk}p_{lm[nr]st}$.

Lets's start by addressing the missing rays. By searching as before a single $8_{17}$ cone we find

the following 6 non-prime factors

$$\{p_{81[23]45}, p_{81[23]46}, p_{56[78]14}, p_{56[78]23}, p_{23[45]71}, p_{23[46]71}\}. \tag{11.31}$$

With the remaining cones providing their cyclic copies. Note, this is only 48/56 of the missing quadratic $\mathcal{A}$-coordinates of $G(3,8)$, we are still missing the cyclic copies of $p_{23[45]71}$, this is in correspondence with the 8 missing rays mentioned earlier. However, extending the ideal by the 6 factors[1] of (11.31) and calculating the Trop$^+$ part generates one new ray! With the structure of the maximal cones now becoming

$$11454_8 + 1696_9 + 971_{10} + 412_{11} + 328_{12} + 89_{13} + 69_{14} + 28_{15} + 17_{16} + 7_{17}.$$

Which as we can see has borken up one of the 17-vertex maximal cones. An interesting question to ask is which of the maximal cones contain the new ray. They are given by

$$270_8 + 70_9 + 46_{10} + 18_{11} + 10_{12} + 4_{13} + 2_{14}.$$

By searching inside the $2_{14}$ cones we find the extra quadratic factors $p_{56[71]23}$ and $p_{81[24]56}$, whose cyclic copies are the 8 remaining $\mathcal{A}$-coordinates. We can repeat this procedure for each cyclic copy of (11.31) to find the 8 missing rays of the cluster fan and all quadratic $\mathcal{A}$-coordinates:

$$\{p_{81[23]45}, p_{81[23]46}, p_{56[78]14}, p_{56[78]23}, p_{23[45]71}, p_{23[46]71}, p_{56[71]23}\} + \text{cyclic}. \tag{11.32}$$

It would be interesting to understand whether such quadratics can be found without first extending the ideal.

We now move to a brief discussion of the missing cubic coordinates. First, we note that a preliminary search of the fan Trop$^+(I_{3,7})$ provided us with no cubic non-prime factors. However, by adding in all 56 quadratic we would expect the cubic $\mathcal{A}$-coordinates to appear as non-prime factors quadratic now in the full set of $\mathcal{A}$-coordinates. After extending the ideal with the missing cubics the results of [36], applying to any finite cluster algebra of geometric type, tell us that we would again see the rays of Trop$^+(I_{3,8}^{\text{ext}})$ spanning a single maximal Gröbner cone whose initial ideal is generated by the forbidden pairs of the cluster algebra. We did not perform this calculation here due to the computational complexity, and the fact that $G(3,8)$ is not relevant for $\mathcal{N} = 4$ SYM amplitudes. A more detailed exploration of this in the future would be interesting since it might provide an insight to the infinite case of $G(4,8)$.

The $\mathcal{N} = 4$ pSYM octagon alphabet is known to contain non-rational square root letters,

---

[1]We do not add all $6 \times 8$ cyclic copies at once as this slows down the computation. However, upon adding all 48 quadratics we would generate a fan with 128 rays, the same number as $\mathcal{A}$-coordinates.

accounted within the cluster algebra by considering coordinates associated to *limit rays*, arising from the limit of particular affine mutation sequences inside the $G(4,8)$ cluster algebra, as described in more detail in the next chapter. It would be interesting to study this phenomenon through the lens of the Gröbner fan.

## 11.4   Beyond the Grassmannian

So far our discussion has been focused on extracting $\mathcal{A}$-coordinates and adjacency rules from the Gröbner fan of the Plücker ideal for the finite type Grassmannians $G(3,n)$ for $n = 6, 7, 8$. In fact, in [36], this procedure was shown to work more generally for any geometric cluster algebra of finite type. However, what we are most interested in is how much physical information can be extracted from the Gröbner fan. For the cases of $G(4,6)$ and $G(4,7)$ the answer is the entire symbol alphabet and adjacency rules relevant for constructing the hexagon and heptagon amplitudes of $\mathcal{N} = 4$ SYM. This motivates the question of whether the Gröbner fan provides a useful tool for the study of other kinematic ideals beyond the dual-conformal invariant case?

In this section we hope to provide a positive answer to this question by considering the example of non dual conformal invariant 5-point massless scattering. Even in this more generalised case much of the discussion from Section 9.4 follows. Such amplitudes/integals may still be expressed in terms of polylogarithmic functions to which we can still associate a symbol and an alphabet. In fact, at two loops all functions relevant for two-loop planar five-particle scattering were computed in [37], leading to the 26 letter alphabet $\mathbb{A}_p$. This was later extended to 31 letters relevant for the non-planar case $\mathbb{A}_{np}$ in [40] where it was used to bootstrap individual two-loop Feynman integrals.

The goal of this section is to demonstrate how a *similar* exploration of the Gröbner fan associated to the five-point kinematic ideal $I_{5\text{pt}}$ can generate the *entire* non-planar alphabet relevant for constructing (at least at two loops) five-point massless amplitudes/integrals. Note, we do in fact miss one symbol letter $W_{31}$. However, the failure to recover $W_{31}$ is consistent with the various calculations made for five point processes, where it has been observed to be absent from (the suitably defined finite part of) the two-loop $\mathcal{N} = 4$ SYM [147, 148] and $\mathcal{N} = 8$ SUGRA [149, 150] amplitudes at two-loops. Similar two-loop observations have been made for the $q\bar{q} \to \gamma\gamma\gamma$ [151] and gluon amplitudes [152, 153] in QCD.

It is important to note that this computation is only an analogy to the Grassmannian cases for two reasons. First, in the case of the Grassmannian we imposed positivity conditions by considering only non-prime factors appearing in the positive part of the tropical fan $\text{Trop}^+(I_{k,n})$. However, for the five-point ideal, we do not impose any such positivity conditions and consider non-prime factors appearing in the full tropical fan $\text{Trop}(I_{5\text{pt}})$. Second, in

the case of the Grassmannian, having obtained the non-prime factors, we subsequently used them in order to extend the ideal, perhaps repeating this procedure multiple times as detailed for $G(3,8)$. This had the effect of eventually resolving the positive tropical fan, of the fully extended ideal, into a collection of simplices all with prime initial ideals. Furthermore, this singled out a single maximal Gröbner fan whose initial ideal contained the forbidden pairs of $\mathcal{A}$-coordinates, providing us with physical adjacency conditions on the symbol alphabet in the cases of $G(4,6)$ and $G(4,7)$. However, for the the five-point case we perform no such extension. Having obtained the non-prime factors appearing in the tropical fan we terminate the procedure, since the extension relies on a notion of positivity which we do not have for the five-point case, and the fact that we already find the full non-planar alphabet relevant for constructing amplitudes. Note, in particular this means we do not attempt to extract any adjacency rules. That being said it is encouraging the same idea of symbol letters appearing as non-prime factors inside maximal cones of the tropical fan of the kinematic ideal follows through to the five-point case.

### 11.4.1 The five-point two-loop symbol alphabet

The kinematics of five-point massless scattering is described on the 5 external momenta $p_i^\mu$ subject to the massless on-shell condition $p_i^2 = 0$ and momentum conservation $\sum_i p_i^\mu = 0$. Out of the momenta we can construct 10 scalar products $s_{ij} = 2p_i \cdot p_j$, five of which are independent, following the choice of [154] they are given by

$$v_i = s_{ii+1} = 2p_i \cdot p_{i+1}. \tag{11.33}$$

It will also prove useful to introduce the following Gram determinant

$$\Delta = \det(2p_i \cdot p_j) = (\mathrm{tr}_5)^2, \tag{11.34}$$

where we have introduced the notation $\mathrm{tr}_5 = \mathrm{tr}(\gamma_5 \not{p}_4 \not{p}_5 \not{p}_1 \not{p}_2)$. Note, when written in terms of '$\beta$-variables' [155] $\sqrt{\Delta} = \mathrm{tr}_5$ can be expressed as a purely rational function.

The planar (two-loop) five point alphabet $\mathbb{A}_p = \{W_1, \ldots, W_{20}\} \cup \{W_{26}, \ldots, W_{31}\}$ was originally obtained in [37] and consists of 26 letters given by

$$W_i = v_i, \qquad W_{5+i} = v_{i+2} + v_{i+3}, \qquad W_{10+i} = v_i - v_{i+3},$$

$$W_{15+i} = v_{i+3} - v_i - v_{i+1}, \qquad W_{25+i} = \frac{a_i - \sqrt{\Delta}}{a_i + \sqrt{\Delta}}, \qquad W_{31} = \sqrt{\Delta}, \tag{11.35}$$

where the $i$ indices run from 1 to 5 and we have introduced the notation

$$a_i = v_i v_{i+1} - v_{i+1} v_{i+2} + v_{i+2} v_{i+3} - v_i v_{i+4} - v_{i+3} v_{i+4}.$$

By closing the planar alphabet under permutations the authors of [40] generalised the alphabet to the non-planar case $\mathbb{A}_{np} = \mathbb{A}_p \cup \{W_{21}, \ldots W_{26}\}$, where we introduce the five additional non-planar letters given by

$$W_{20+i} = v_{i+2} + v_{i+3} - v_i - v_{i+1}. \tag{11.36}$$

As for the planar $\mathcal{N} = 4$ SYM case the non planar alphabet $\mathbb{A}_{np}$ provides the starting point for the construction of integrable polylogarithmic symbols relevant for the bootstrap of five-point massless non-planar amplitudes/integrals [40].

### 11.4.2   Non-planar alphabet from the Gröbner fan

Inspired by the appearance of symbol letters ($\mathcal{A}$-coordinates) as non-prime factors of the Plücker ideal we wish to apply *similar* ideas to the five-point ideal $I_{5pt}$ in order to generate the non-planar alphabet $\mathbb{A}_{np}$.

To define the kinematic space for general five-point massless scattering, instead of using momentum twistor variables, it is instructive to consider spinor-helicity variables. The spinor helicity variables are constrained by two sets of relations, the Schouten identity and momentum conservation, at five points these become[1]

$$\langle ij \rangle \langle kl \rangle - \langle ik \rangle \langle jl \rangle + \langle il \rangle \langle jk \rangle = 0; \quad [ij][kl] - [ik][jl] + [il][jk] = 0, \tag{11.37}$$

for $1 \leq i < j < k < l \leq 5$ and

$$\sum_{r=1}^{5} \langle nr \rangle [rm] = 0, \tag{11.38}$$

for $n, m \in \{1, 2, 3, 4, 5\}$. Collectively these equations generate the ideal, $I_{5pt}$, relevant for five-point massless kinematics whose Gröbner $\mathrm{GF}(I_{5pt})$ and Tropical fan $\mathrm{Trop}(I_{5pt})$ we now study.

The ideal $I_{5pt}$ is defined on the ten $a_{ij} := \langle ij \rangle$ and ten $\tilde{a}_{ij} := [ij]$ variables with $i < j$ organised as $(a_{12}, \ldots, a_{45}, \tilde{a}_{12}, \ldots, \tilde{a}_{45})$. We compute the tropical fan $\mathrm{Trop}(I_{5pt})$ with the help of `gfan` [146] and `macaulay2` [156] where we determine the fan is simplicial, containing 65 rays and an $f$-vector given by

$$f_{5pt} = (1, 65, 550, 1395, 1035).$$

The full set of 65 rays are given by: 20 unit vectors $\mathbf{e}_{ij}$ and $\tilde{\mathbf{e}}_{ij}$ where $\mathbf{e}_{ij}$ is the unit vector in the $a_{ij}$ direction and respectively $\tilde{\mathbf{e}}_{ij}$ is the unit vector in the $\tilde{a}_{ij}$ direction; 5 vectors of the form $\mathbf{z}_i = \sum_{j \neq i} \mathbf{e}_{ij}$ lineality equivalent to $\tilde{\mathbf{z}}_i = \sum_{j \neq i} \tilde{\mathbf{e}}_{ij}$; 10 permutations of $\mathbf{r}_{45} = \mathbf{v}_{123} + \tilde{\mathbf{e}}_{45}$,

---

[1]Note, the appearance of the two-brackets $\langle ij \rangle$ indicating the problem no longer has dual-conformal symmetry.

lineality equivalent to $\tilde{\mathbf{r}}_{45} = \tilde{\mathbf{v}}_{123} + \mathbf{e}_{45}$, where we have defined $\mathbf{v}_{ijk} = \mathbf{e}_{ij} + \mathbf{e}_{ik} + \mathbf{e}_{jk}$ and similarly for $\tilde{\mathbf{v}}_{ijk}$; finally the 30 permutations of $\mathbf{y}_{1,23,45} = \mathbf{v}_{123} + \tilde{\mathbf{v}}_{145} = \tilde{\mathbf{y}}_{1,23,45}$.
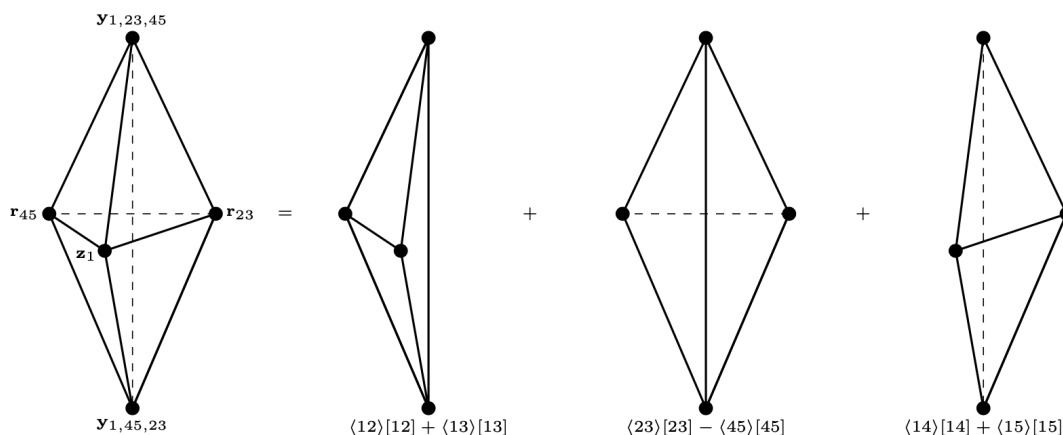


**Figure 11.7:** A bipyramid $b_1$ of $\text{Trop}(I_{5pt})$, on the left hand side we have the full bipyramid labelled by its 5 rays, on the right hand side the bipyramid is split into three tetrahedra. Each tetrahedron is labelled by the quadratic non-prime factor found in the initial ideal, where all three expressions are equivalent modulo $I_{5pt}$.

Amongst the 1035 maximal cones only 45 are non-prime: 30 given by the permutation copies of $\{\mathbf{y}_{1,23,45}, \mathbf{z}_1, \mathbf{r}_{45}, \mathbf{y}_{1,45,23}\}$; and an additional 15 given by the permutation copies of $\{\mathbf{y}_{1,23,45}, \mathbf{r}_{23}, \mathbf{r}_{45}, \mathbf{y}_{1,45,23}\}$. Note, these tertahedra fit together into 15 bipyramids. As an example consider Figure 11.7 where we have a single bipyramid: the left tetrahedron with the rays $\{\mathbf{y}_{1,23,45}, \mathbf{z}_1, \mathbf{r}_{45}, \mathbf{y}_{1,45,23}\}$, produces the non-prime factor $\langle 12 \rangle [12] + \langle 13 \rangle [13]$; transposing $2 \leftrightarrow 4$ and $3 \leftrightarrow 5$ we find the right tetrahedron with the rays $\{\mathbf{y}_{1,23,45}, \mathbf{z}_1, \mathbf{r}_{23}, \mathbf{y}_{1,45,23}\}$, and non-prime factor $\langle 14 \rangle [14] + \langle 15 \rangle [15]$; finally the middle tetrahedron has the rays given by $\{\mathbf{y}_{1,23,45}, \mathbf{r}_{23}, \mathbf{r}_{45}, \mathbf{y}_{1,45,23}\}$, which produces the non-prime factor $\langle 23 \rangle [23] - \langle 45 \rangle [45]$. As was the case for $G(3,6)$ the three non-prime factors appearing in the bipyramid are equivalent modulo the ideal $I_{5pt}$.

To generate the full set of non-prime factors modulo the ideal $I_{5pt}$ we need only take the permutation copies of $\langle 23 \rangle [23] - \langle 45 \rangle [45]$ which produces 15 quadratic expressions given by

$$
\begin{aligned}
&\langle 23 \rangle [23] - \langle 45 \rangle [45], &&\langle 24 \rangle [24] - \langle 35 \rangle [35], &&\langle 25 \rangle [25] - \langle 34 \rangle [34], \\
&\langle 13 \rangle [13] - \langle 45 \rangle [45], &&\langle 14 \rangle [14] - \langle 35 \rangle [35], &&\langle 15 \rangle [15] - \langle 34 \rangle [34], \\
&\langle 12 \rangle [12] - \langle 45 \rangle [45], &&\langle 14 \rangle [14] - \langle 25 \rangle [25], &&\langle 15 \rangle [15] - \langle 24 \rangle [24], \\
&\langle 12 \rangle [12] - \langle 35 \rangle [35], &&\langle 13 \rangle [13] - \langle 25 \rangle [25], &&\langle 15 \rangle [15] - \langle 23 \rangle [23], \\
&\langle 12 \rangle [12] - \langle 34 \rangle [34], &&\langle 13 \rangle [13] - \langle 24 \rangle [24], &&\langle 14 \rangle [14] - \langle 23 \rangle [23].
\end{aligned} \tag{11.39}
$$

Along with the $\{a_{ij}, \tilde{a}_{ij}\}$ this provides us with 35 expressions from which to form homogenous combinations.

To see that we are in fact recovering the same content as the symbol alphabet $\mathbb{A}_{np}$ we re-write the entire non-planar alphabet in terms of spinor helicity variables given by the cyclic copies of[1]

$$W_1 = \langle 12\rangle[12], \qquad\qquad\qquad W_6 = \langle 34\rangle[34] + \langle 45\rangle[45],$$

$$W_{11} = \langle 34\rangle[34] + \langle 35\rangle[35], \qquad\qquad W_{16} = \langle 13\rangle[13],$$

$$W_{21} = \langle 13\rangle[13] + \langle 34\rangle[34], \qquad\qquad W_{26} = \frac{\langle 45\rangle[51]\langle 12\rangle[24]}{[45]\langle 51\rangle[12]\langle 24\rangle},$$

$$W_{31} = [45]\langle 51\rangle[12]\langle 24\rangle - \langle 45\rangle[51]\langle 12\rangle[24]. \tag{11.40}$$

With this representation it is clear that letters $\{W_i\}_{i=1}^5 \cup \{W_i\}_{i=16}^{20} \cup \{W_i\}_{i=26}^{30}$ are given by multiplicative combinations of the $\{a_{ij}, \tilde{a}_{ij}\}$ variables. Furthermore, the remaining 15 letters $\{W_i\}_{i=6}^{10} \cup \{W_i\}_{i=11}^{15} \cup \{W_i\}_{i=21}^{25}$, themselves related by the $\mathcal{S}_5$ permutation symmetry, are exactly the 15 non-prime factors appearing in the Gröbner fan of the spinor-helicity ideal! To see this explicitly note we have

$$W_6 \; = \; \langle 34\rangle[34] + \langle 45\rangle[45] = \langle 12\rangle[12] - \langle 35\rangle[35],$$

$$W_{11} = \langle 34\rangle[34] + \langle 35\rangle[35] = \langle 12\rangle[12] - \langle 45\rangle[45],$$

$$W_{21} = \langle 13\rangle[13] + \langle 34\rangle[34] = \langle 14\rangle[14] - \langle 25\rangle[25], \tag{11.41}$$

all of which appear in (11.39). It follows then that taking homogenous combinations of letters $\{W_i\}_{i=1}^{30}$ is equivalent to taking homogenous combinations of $\{a_{ij}, \tilde{a}_{ij}\}$ and the permutations of the non-prime factors $\langle 23\rangle[23] - \langle 45\rangle[45]$. Note, as already emphasised, we do not recover the letter $W_{31}$. However, this is consistent with $W_{31}$ not appearing in the expressions for suitably defined amplitudes.

---

[1]Let us emphasise the fact that in spinor-helicity variables the rationality of letters $\{W_{26}, \ldots, W_{31}\}$ becomes manifest.

# Chapter 12

# Cluster algebras for massless kinematics

We have seen that the Grassmannian cluster algebras are very useful tools for extracting information on the branch cut structure of scattering amplitudes in planar $\mathcal{N} = 4$ SYM. In this chapter we wish to study a generalisation of the Grassmannian, the partial flag varieties $F(2, 4, n)$, naturally associated to $n$-point massless kinematics, to see how much information they contain relevant for the five and six -point massless alphabets[1]. As mentioned in the last section the planar five-point massless amplitude/integrals are constructed (at least at two-loops) from a 26-letter alphabet $\mathbb{A}_p$ [37]. At six points partial information of the symbol alphabet also exists [157–160] revealing a symbol alphabet consisting of both rational and square root letters. Note, the connection between these symbol alphabets for Feynman integrals and the Grassmannian cluster algebra $G(4, n)$ was studied in [161]. Where, using the alphabet for $G(4, 8)$ presented in [31], the authors were able to recover partial information. In particular by taking the line $(Z_7 Z_8)$ as the infinity twistor all but two of the letters of the planar five-point one mass integrals [157] were recovered, along with 22 letters of the five-point massless alphabet [37] which upon cyclic completion recovered the full $\mathbb{A}_p \setminus \{W_{31}\}$ alphabet. A similar analysis was also presented in [38], more recently the five-particle alphabet was obtained via *Schubert problems* in [39].

At five-points the cluster algebra associated to the partial flag $F(2, 4, 5)$ is of finite type containing 14 active $\mathcal{A}$-coordinates along with 6 frozen. Upon cyclic completion this generates a set of 25 expressions which can be used to form 20 of the symbol letters appearing in $\mathbb{A}_p$ leaving only 5 letters unaccounted for. Furthermore, as was carried out in [40], by completing this list of 20 symbol letters under permutations we generate the same set of 30 non-planar letters of the last section including the entire planar alphabet. At six points, like the case of the Grassmannian $G(4, 8)$, the cluster algebra associated to $F(2, 4, 6)$ is no longer of finite

---

[1]This chapter is based on incomplete work hopefully to appear in full on arXiv in the coming months.

type, and as such the symbol alphabet for 6 points contains algebraic square root letters. Following the methods of [31] we extract a single square root-letter $\Delta$ from so called *limit rays* of the $F(2,4,6)$ cluster algebra which appears in the symbol alphabet presented in [157] for five-point one-mass integrals.

As a final remark we emphasise that the cluster algebra $F(2,4,n)$ is contained as a sub-algebra inside the Grassmannian $G(4,n+2)$. So, in fact, we see that the dual-conformal invariant symbol alphabet at $n+2$ points contains information relevant for the $n$-point non dual-conformal invariant amplitude obtained by restricting to the appropriate sub algebra!

## 12.1   Partial flag varieties

To introduce the partial flag varieties we must first introduce the notion of a flag in a finite dimensional vector space $V$, this is given by an increasing sequence of linear subspaces each contained in the next i.e.

$$V_0 \subset V_1 \subset \ldots \subset V_k = V,$$

where defining $\dim(V_i) = d_i$ we have

$$0 = d_0 < d_1 < \ldots < d_k = n,$$

and $(d_1, \ldots, d_k)$ is referred to as the signature of the flag. The partial flag $F(d_1, \ldots, d_k)$ can then be described as the space of all flags of signature $(d_1, \ldots, d_k)$. The familiar case of the Grassmannian $G(k,n) = F(k,n)$ is just the case of flags of length 1 or the space of $k$-planes in $n$-dimensions.

First, let's see why such objects as partial flag varieties appear in the discussion of massless scattering. As described in the last section at five points the kinematic space relevant for massless scattering is given by the ideal generated by (11.37) in spinor helicity variables. Alternatively, a perhaps more appropriate choice of variables for the planar case is momentum twistors, in these variables the ideal is generated by[1]

$$\langle ij \rangle \langle kl \rangle - \langle ik \rangle \langle jl \rangle + \langle il \rangle \langle jk \rangle = 0, \tag{12.1}$$

for $1 \leq i < j < k < l \leq 5$ along with

$$\langle 15 \rangle \langle 1234 \rangle + \langle 14 \rangle \langle 1235 \rangle + \langle 13 \rangle \langle 1245 \rangle + \langle 12 \rangle \langle 1345 \rangle = 0 \tag{12.2}$$

and its cyclically related relations. This set of relations encodes the dependencies between ordered $2 \times 2$ and $4 \times 4$ minors of a $4 \times 5$ matrix i.e. the partial flag variety $F(2,4,5)$.

---

[1]Note, in contrast to the Grassmannian, the appearance of the two-brackets $\langle ij \rangle := \langle ijI_\infty \rangle$, where $I_\infty$ is the infinity twistor, indicates that the problem is no longer dual-conformal invariant.

More generally the ideal associated to $n$-point massless kinematics is given by the partial flag variety $F(2,4,n)$. Much like the Grassmannians [162] the partial flag varieties can be endowed with a cluster structure [163] which we outline in the next two sections for $F(2,4,5)$ and $F(2,4,6)$.

## 12.2   Five-particle alphabet from $F(2,4,5)$

The first example we consider is the case of $F(2,4,5)$ whose initial cluster is depicted in Figure 12.1 with active and frozen coordinates given by

$$\{a_1,\ldots,a_4\} = \{p_{14}p_{1235} - p_{15}p_{1234}, p_{1345}, p_{1235}, p_{1245}\},$$
$$\{f_1,\ldots,f_6\} = \{p_{2345}, p_{34}p_{1235} - p_{35}p_{1234}, p_{45}, p_{15}, p_{1234}, p_{12}\}. \tag{12.3}$$

Here, and in the remainder of this chapter, we switch to the notation $p_{ij} = \langle ij \rangle$ and $p_{ijkl} = \langle ijkl \rangle$. This cluster algebra is of finite type $D_4$, and by performing mutations we find the full set of 20 $\mathcal{A}$-coordinates distributed over 42 clusters, they are given by

$$\mathcal{A}_{F(2,4;5)} = \{p_{12}, p_{13}, p_{14}, p_{15}, p_{23}, p_{24}, p_{25}, p_{34}, p_{35}, p_{45}, p_{1234}, p_{1235}, p_{1345}, p_{1245}, p_{2345},$$
$$p_{14}p_{1235} - p_{15}p_{1234}, p_{34}p_{1235} - p_{35}p_{1234}, p_{35}p_{1245} - p_{45}p_{1235},$$
$$p_{34}p_{1245} - p_{45}p_{1234}, p_{24}p_{1235} - p_{25}p_{1234}\}. \tag{12.4}$$

Note, in particular there are two cyclic classes of quadratic coordinates, in the second and third lines, which do not come with their full cyclic completions. Therefore, we may cycle the entire cluster algebra to find all five cyclic copies of the quadratics given by

$$
\begin{array}{ll}
p_{14}p_{1235} - p_{15}p_{1234}, & p_{34}p_{1245} - p_{45}p_{1234}, \\
p_{12}p_{2345} - p_{25}p_{1234}, & p_{15}p_{2345} - p_{45}p_{1235}, \\
p_{13}p_{2345} - p_{23}p_{1345}, & p_{12}p_{1345} - p_{15}p_{1234}, \\
p_{34}p_{1245} - p_{24}p_{1345}, & p_{12}p_{2345} - p_{23}p_{1245}, \\
p_{35}p_{1245} - p_{45}p_{1235}, & p_{34}p_{1235} - p_{23}p_{1345}.
\end{array} \tag{12.5}
$$

This procedure generates 25 $\mathcal{A}$-coordinates[1] given by the $(p_{ij}, p_{ijkl})$ as well as the ten quadratics above. By taking homogenous combinations of these 25 expressions we are able to recover 20/26 of the known symbol letters of 5-point scattering which in momentum twistor variables now read

$$W_1 = \frac{p_{1235}}{p_{15}p_{23}}, \qquad\qquad W_6 = \frac{p_{34}p_{15}p_{2345} + p_{23}p_{45}p_{1345}}{p_{23}p_{34}p_{45}p_{15}},$$

---

[1]Note, these $\mathcal{A}$-coordinates do not necessarily belong to the same cluster algebra.

$$W_{11} = \frac{p_{34}p_{1235} - p_{23}p_{1345}}{p_{23}p_{34}p_{15}}, \qquad W_{15+i} = \frac{p_{13}(p_{12}p_{2345} - p_{25}p_{1234})}{p_{12}p_{15}p_{23}p_{34}},$$

$$W_{26} = \frac{p_{1245}(p_{23}p_{1345} - p_{13}p_{2345})}{p_{24}p_{1235}p_{1345}}, \quad W_{31} = \frac{p_{35}p_{1234}p_{1245} - p_{45}p_{1234}p_{1235} + p_{14}p_{1235}p_{2345}}{p_{12}p_{23}p_{34}p_{45}p_{51}}.$$

$$(12.6)$$

The 5 symbol letters of the planar alphabet $\mathbb{A}_p$ we fail to produce by this method, along with $W_{31}$ as explained in the last chapter, are $W_6$ and its cyclic copies. It is interesting to note that they are *trivially positive* i.e. after ensuring the $p_{ij}$ and $p_{ijkl}$ are positive the positivity of $W_6$ follows.

However, by completing $\{W_1, W_{11}, W_{15}, W_{26}\}$ under permutations of the external momenta not only do we produce the missing planar letters $W_6$ but also the non-planar letters $W_{20+i}$ given by

$$W_{21} = \frac{p_{12}p_{23}p_{45}p_{1345} - p_{12}p_{34}p_{45}p_{1235} + p_{12}p_{34}p_{15}p_{2345} - p_{23}p_{45}p_{15}p_{1234}}{p_{12}p_{23}p_{34}p_{45}p_{15}}, \qquad (12.7)$$

and it's cyclic copies. Hence, we recover the same 30/31 letters of $\mathbb{A}_{np}$ [40] as the last chapter by completing under permutations the $\mathcal{A}$-coordinates appearing in the $F(2,4,5)$ cluster algebra.
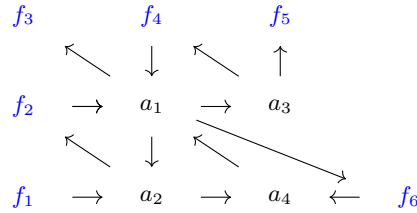


**Figure 12.1:** The initial cluster of the partial flag cluster algebra F(2, 4, 5).

### 12.2.1   $G(4, 7)$ **embedding**

As mentioned earlier the partial flag cluster algebra $F(2,4,5)$ appears as a codimension-two subalgebra of the $G(4,7)$ cluster algebra. This is demonstrated in Figure 12.2: the left hand side depicts a cluster appearing in $G(4,7)$ showing the 7 active coordinates, by freezing nodes $p_{1236}$ and $a_{53}$ and setting $p_{ij} := p_{ij67}$ we are left with the cluster subalgebra of the partial flag $F(2,4,5)$ on the right hand side. In this figure we have changed notation compared to Equation (10.14) where $a_{ij}$ is now understood as the non-homogenous $\mathcal{A}$-coordinates of

$G(4,7)$ i.e. those appearing in (12.8).

$$
\begin{array}{llllllll}
f_i: & \langle 1234\rangle & \langle 2345\rangle & \langle 3456\rangle & \langle 4567\rangle & \langle 1567\rangle & \langle 1267\rangle & \langle 1237\rangle \\
a_{1i}: & \langle 2367\rangle & \langle 1347\rangle & \langle 1245\rangle & \langle 2356\rangle & \langle 3467\rangle & \langle 1457\rangle & \langle 1256\rangle \\
a_{2i}: & \langle 2567\rangle & \langle 1367\rangle & \langle 1247\rangle & \langle 1235\rangle & \langle 2346\rangle & \langle 3457\rangle & \langle 1456\rangle \\
a_{3i}: & \langle 2347\rangle & \langle 1345\rangle & \langle 2456\rangle & \langle 3567\rangle & \langle 1467\rangle & \langle 1257\rangle & \langle 1236\rangle \\
a_{4i}: & \langle 2457\rangle & \langle 1356\rangle & \langle 2467\rangle & \langle 1357\rangle & \langle 1246\rangle & \langle 2357\rangle & \langle 1346\rangle \\
a_{5i}: & \langle 1(23)(45)(67)\rangle & \langle 2(34)(56)(71)\rangle & \langle 3(45)(67)(12)\rangle & \langle 4(56)(71)(23)\rangle & \langle 5(67)(12)(34)\rangle & \langle 6(71)(23)(45)\rangle & \langle 7(12)(34)(56)\rangle \\
a_{6i}: & \langle 1(34)(56)(72)\rangle & \langle 2(45)(67)(13)\rangle & \langle 3(56)(71)(24)\rangle & \langle 4(67)(12)(35)\rangle & \langle 5(71)(23)(46)\rangle & \langle 6(12)(34)(57)\rangle & \langle 7(23)(45)(61)\rangle
\end{array}
$$
$$(12.8)$$

Therefore, we see that information on the five-point alphabet can be recovered from the Grassmannian $G(4,7)$, where upon ignoring all $\mathcal{A}$-coordinates which do not treat the points 6 and 7 as a line, highlighted in red in (12.8), we recover the alphabet of $F(2,4,5)$.
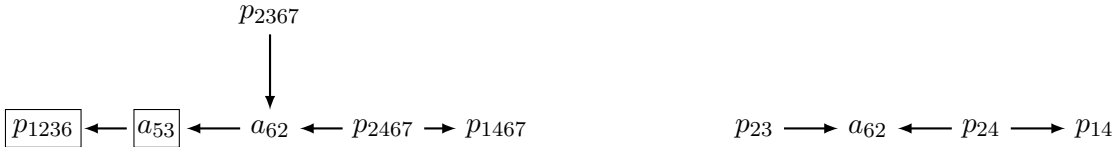


**Figure 12.2:** The embedding of flag $F(2,4,5)$ inside the Grassmannian $G(4,7)$.

Returning to the picture of lines in momentum twistor space this can be seen as taking the line $(Z_6 Z_7)$ as the infinity twistor $I_\infty$. With the two brackets defined as $p_{ij} = \langle ij67\rangle = \langle ijI_\infty\rangle$.
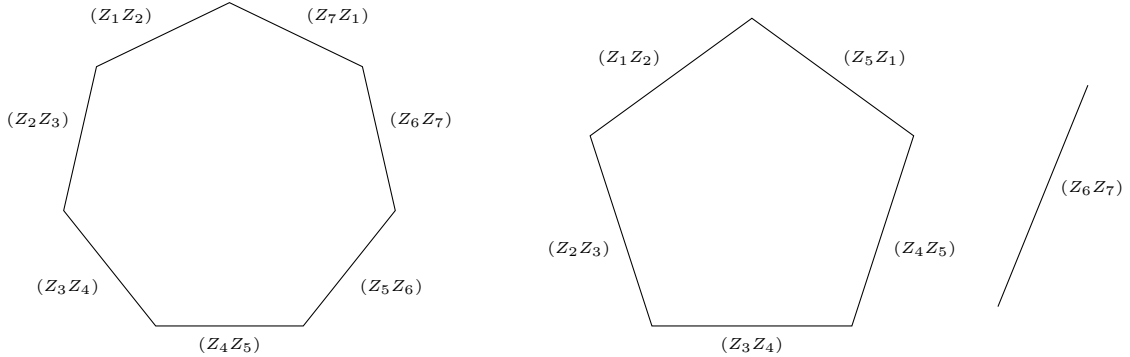


**Figure 12.3:** LHS: The configuration of lines in $\mathbb{CP}^3$ relevant for the case of seven point dual-conformal invariant kinematics. RHS: By taking the line $I_\infty^{AB} = (Z_6^A Z_7^B)$ as the infinity twistor we reduce to the case of general five-point massless kinematics.

## 12.3 An algebraic letter from $F(2,4,6)$

As discussed in Section 10.2.3 for the case of $G(4,8)$ complications arise when the underlying cluster algebra is no longer of finite type, and additional tools beyond that of the cluster algebra must be introduced in order to extract information for the symbol alphabet of the corresponding amplitude. The first complication being that the set of $\mathcal{A}$-coordinates becomes infinite which is not reflected by the finite set of letters needed to express say the two-loop

NMHV octagon [134]. Therefore, some truncation procedure, such as tropicalization [31–34], must be introduced to select a preferred subset of $\mathcal{A}$-coordinates. The second, related, issue is that the symbol alphabet starts to contain non-rational letters, with square roots appearing in the first instance for the two-loop NMHV octagon [134], the calculation of which revealed a set of 18 multiplicatively independent square root letters. Both issues were dealt with in [31] where the set of 180 rational letters of the two-loop NMHV octagon were recovered as rays of $\mathrm{Trop}^+(I_{4,8})$, along with the 18 algebraic letters, associated to special *limit rays* arising from infinite affine sequences of mutations within the cluster algebra.
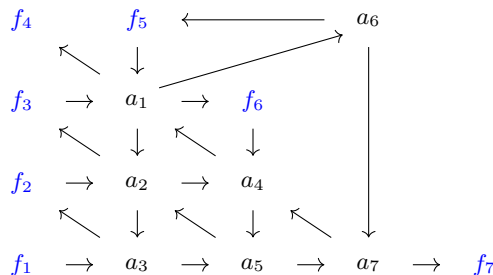


**Figure 12.4:** The initial cluster of the partial flag cluster algebra F$(2, 4, 6)$.

For the more general kinematics we consider in this chapter square root letters start to appear already at 6-points [157–160]. Therefore, we wish to follow the method presented in [31] to explore the set of square roots appearing in the $F(2, 4, 6)$ cluster algebra to see how they relate to square roots known to appear in 6-point integrals.

The cluster algebra associated to $F(2, 4, 6)$ is of affine $D_6$ type, its initial cluster is depicted in Figure 12.4, with active and frozen coordinates given by

$$\{a_1, \ldots, a_7\} = \{p_{15}p_{1236} - p_{16}p_{1235}, p_{1456}, p_{1345}, p_{1256}, p_{1245}, p_{1236}, p_{1235}\},$$
$$\{f_1, \ldots, f_7\} = \{p_{2345}, p_{3456}, p_{56}p_{1234} - p_{46}p_{1235} + p_{45}p_{1236}, p_{56}, p_{16}, p_{12}, p_{1234}\}. \qquad (12.9)$$

This is an example of an infinite type cluster algebra, however as a subalgebra of $G(4, 8)$, it is of finite mutation type. The infinity of $\mathcal{A}$-coordinates arise from rank two (affine $A_2^{(2)}$) cluster algebras connected by double arrows, as depicted in Figure 12.5, which generate an infinite mutation sequence by repeated mutation on nodes $w_0$ and $z_0$. This infinity may be organised by selecting from each $A_2^{(2)}$ sequence a single representative refered to as an *origin cluster*. Note, the origin cluster can always be bought into the form given at the left of Figure 12.6. In this picture we ignore all active coordinates not connected to the double arrow nodes (which do not play a role in the mutation rules) and combine all frozen nodes incoming to $z_0$ (outgoing from $w_0$) into $f_z$ ($f_w$). Similarly, we collect all active nodes connected to $w_0$ and $z_0$ as $b = b_1 b_2 b_3$.

Each origin cluster generates two infinite sequences of cluster $\mathcal{A}$-coordinates given by the
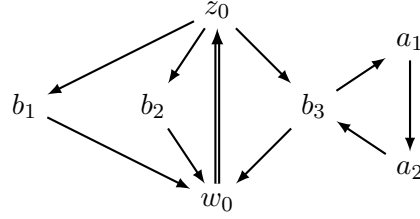
**Figure 12.5:** An example of an origin cluster with a doubled arrow between the two cluster $\mathcal{A}$-coordinates $(w_0, z_0)$ where frozen nodes are omitted. The $a_i$ nodes not connected to $(w_0, z_0)$ form an $A_2$ subalgebra of clusters containing the same $w_0$, $z_0$ and $b_i$ nodes and hence the same mutation sequence.

recursion relations

$$z_{n+2}z_n = \mathcal{C}_z\mathcal{F}^n + z_{n+1}^2; \quad w_{n+2}w_n = \mathcal{C}_w\mathcal{F}^n + w_{n+1}^2, \tag{12.10}$$

depending on whether the choice of initial mutation was $w_0$ or $z_0$ i.e. the top and bottom panels of Figure 12.6. Note, here we have defined the coefficients $\mathcal{C}_z = bf_z$ and $\mathcal{C}_w = bf_w$, similarly the factor $\mathcal{F}$ is defined as the product over frozen coordinates $\mathcal{F} = f_w f_z$.
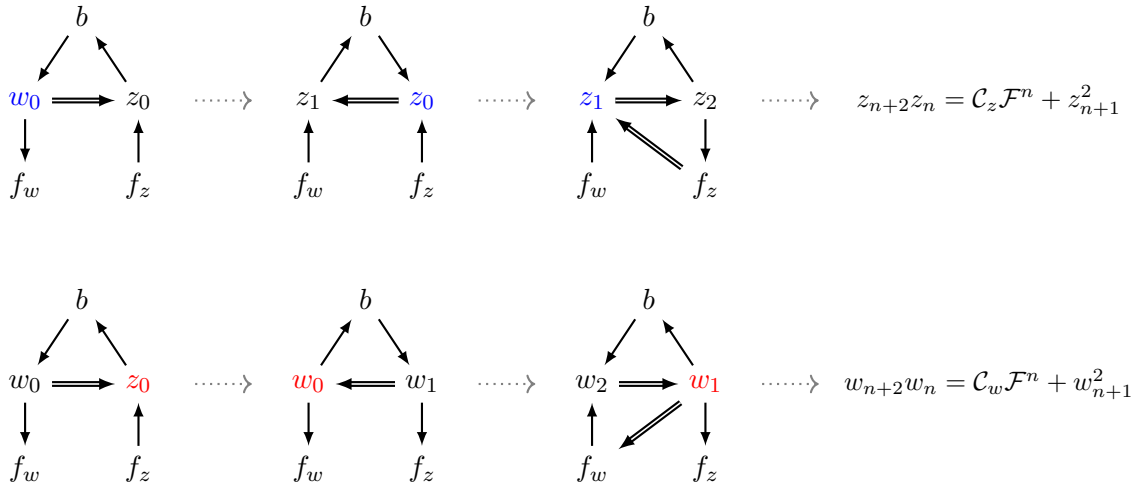


**Figure 12.6:** The double infinite mutation sequence $(z_n, w_n)$ generated by repeated mutations on the affine $A_2^{(2)}$ cluster subalgebra of the $F(2,4,6)$ cluster algebra. The two left hand clusters depict the origin clusters and the blue/red nodes indicate on which node we are performing the mutation.

The solution to this recursion relation was detailed in [31] and takes the form

$$z_n = \frac{1}{2^{n+1}}\left[(z_0 + B_z\sqrt{\Delta})(\mathcal{P}_z + \sqrt{\Delta})^n + (z_0 - B_z\sqrt{\Delta})(\mathcal{P}_z - \sqrt{\Delta})^n\right], \tag{12.11}$$

where we have defined

$$\mathcal{P}_z = \frac{f_z w_0 + z_1}{z_0}, \quad B_z = \frac{2z_1 - z_0 \mathcal{P}}{\Delta}, \quad \Delta = \mathcal{P}_z^2 - 4\mathcal{F}, \tag{12.12}$$

and similarly the solution for the $w$ sequence is obtained from the above formulae under swapping $z \leftrightarrow w$ under which $(\mathcal{P}_z, \mathcal{F}, \Delta)$ are invariant.

The sequence of **g**-vectors, associated to the $\mathcal{A}$-coordinates $(z_n{}^1, w_n)$, for such $A_2^{(2)}$ cluster algebras were studied already in [164] and have their own simple transformation rules. An example of the limit rays generated by the mutation sequences $z_n$ and $w_n$ are depicted in Figure 12.7. As can be seen from this figure by taking the limit of the sequence from both directions we approach the same *limit ray*, $\mathbf{g}_\infty$, depicted by the green line. Note, the square root $\sqrt{\Delta}$ appearing in a sequence $(z_n, w_n)$ will be the same for all sequences which asymptote to a given limit ray, and therefore to each limit ray $\mathbf{g}_\infty$ we may associate a single square root $\sqrt{\Delta}$.
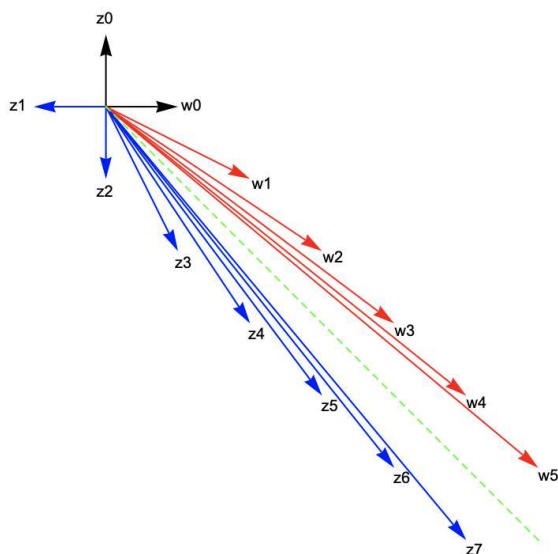


**Figure 12.7:** The **g**-vectors associated to the double infinite mutation sequence $(z_n, w_n)$. The two black arrows indicate the initial cluster with both sequences asymptoting to the same limit ray $\mathbf{g}_\infty$ indicated by the green line.

To search for origin clusters we perform all possible mutations of length $l$, starting from the initial cluster, selecting those which have the desired form. We find that the number of origin clusters saturates[2] to $16 \cdot 5$ already for mutation sequences of length $l = 11$, with the factor of 5 coming from performing mutations on the $A_2$ subalgebra of active nodes not connected to either $z_0$ or $w_0$. We find that all 16 origin clusters asymptote to the same limit

---

[1]Let us emphasise that the use of blue here does not correspond to frozen. But, is instead used to distinguish the took mutation directions.

[2]We have searched all sequences up to $l = 17$ which did not produce any additional origin clusters.

ray given by

$$\mathbf{g}_\infty = (1, -1, 0, 0, 1, -1, 0).$$

(12.13)

Note, this is in stark contrast with $G(4, 8)$ which contains infinitely many limit rays which themselves must be truncated using some other procedure such as tropicalziation [31, 165]. The square root associated to this limit ray is found to be given by

$$\Delta = p_{1256}^2 p_{34}^2 + p_{1234}^2 p_{56}^2 + p_{3456}^2 p_{12}^2$$
$$- 2(p_{1256}p_{1234}p_{34}p_{56} + p_{1256}p_{3456}p_{12}p_{34} + p_{1234}p_{3456}p_{12}p_{56}),$$

(12.14)

which is exactly the square root letter $\Delta_3$ appearing in the symbol alphabet at six-points e.g. see Equation (5.11) of [157]!

# Chapter 13

# Conclusion

In the second part of this thesis, following the work of [35, 36], we mapped the problem of extracting cluster algebra data relevant for the planar $\mathcal{N} = 4$ amplitude bootstrap to studying the structure of the Gröbner fan of the Plücker ideal. Most importantly we saw that

- The missing $\mathcal{A}$-coordinates appear as non-prime factors in the initial ideals of maximal cones of $\mathrm{Trop}^+(I_{k,n})$.

- Upon extending the ideal by the missing $\mathcal{A}$-coordinates the rays of $\mathrm{Trop}^+(I_{k,n})$ span a single maximal Gröbner cone. The initial ideal of this maximal Gröbner cone, of the extended ideal, provides us with a list of monomials which are exactly the forbidden pairs of $\mathcal{A}$-coordinates.

In particular this was applied to the case of $G(3, 7)$ whose set of $\mathcal{A}$-coordinates and adjacency rules are used as the starting point of the heptagon bootstrap.

Inspired by these results we wished to see whether the Gröbner fan could provide a useful tool in extending these ideas beyond dual conformal kinematics. The example of non-dual conformal kinematics we considered was five-point massless amplitudes whose (two-loop) planar $\mathbb{A}_p$ and non-planar alphabets $\mathbb{A}_{np}$ were discovered in [37, 40]. By inspecting the initial ideals of maximal cones of the Gröbner fan $\mathrm{GF}(I_{5\mathrm{pt}})$ we were able to recover the entire (relevant) non-planar alphabet as non-prime factors.

With these results there are a number of interesting questions to consider:

- Can we study $\mathrm{GF}(I_{4,8})$ to see square-root letters arising?

- At five-points does a similar extension procedure, as carried out for the Grassmannian, yield any useful information i.e. do the expressions which are produced after extending appear in the symbol alphabet at higher loops?

- How much of the symbol alphabets [157–160] of six-point non dual conformal invariant kinematics can be recovered from the analysis of the Gröbner fan $GF(I_{6pt})$?

We have also provided evidence that the family of partial flag varieties $F(2, 4; n)$ contain relevant information for the scattering of $n$-point non dual conformal invariant amplitudes analogous to the relation between Grassmannian cluster algebras and $\mathcal{N} = 4$ SYM amplitudes.

In the case of $F(2, 4, 5)$ we were able to obtain $20/25$ of the (relevant) symbol letters of the five-point planar alphabet $\mathbb{A}_p$ as cyclic completions of $\mathcal{A}$-coordinates. After completing under the full set of permutations this recovered the full non-planar alphabet $\mathbb{A}_{np}$. Furthermore, we saw that the cluster algebra $F(2, 4, 6)$ contains a single limit ray whose associated square root letter

$$
\begin{aligned}
\Delta = {}& p^2_{1256}p^2_{34} + p^2_{1234}p^2_{56} + p^2_{3456}p^2_{12} \\
& - 2(p_{1256}p_{1234}p_{34}p_{56} + p_{1256}p_{3456}p_{12}p_{34} + p_{1234}p_{3456}p_{12}p_{56}),
\end{aligned}
\tag{13.1}
$$

appears in the symbol alphabet at six-points i.e. Equation (5.11) of [157]!

Again there are a number of interesting questions to consider. First, why do we need to utilise the entire permutation symmetry to recover the planar letters $W_6$ and its cyclic copies, whereas the authors of [37] were able to recover these letters by considering limits of $G(4, 8)$? Second, how much of the rational alphabet at six-points can we recover from $F(2, 4, 6)$? Due to the connection to $G(4, 8)$ an interesting calculation would be to take the truncated $G(4, 8)$ alphabet presented in [31], remove all letters which do not treat points 7 and 8 as a line, complete under the cyclic (or full permutation) group, and see how much of the six-point alphabet [157–160] is recovered. Finally, can the connection to the $F(2, 4, n)$ partial flags be used to develop some organisation principle for the symbols of non dual conformal invariant amplitudes similar to cluster adjacency for the case of $\mathcal{N} = 4$ SYM?

# PART III

# APPENDIX

# Appendix A

# Window unmixing

## A.1  Unmixing subleading three-point functions

As an example let us consider the family of correlators $\langle 22pp\rangle$ first outlined in [1], which have the simplification of having a single $SU(4)$ channel $[0,0,0]$ whose degeneracy of operators is fully lifted at tree level. As we will see this allows us to obtain explicit expressions for the sub-leading supergravity and string corrected three-point functions. The one-loop $\log(u)$ OPE coefficient is given by

$$H^{(2,3)}_{22pp;\vec{\tau}} = \sum_{(qq)\in\mathcal{D}_{\vec{\tau}}} C^{(0,0)}_{22;\mathcal{K}_{qq}}(C^{(1,3)}_{pp;\mathcal{K}_{qq}}\eta^{(1,0)}_{\mathcal{K}_{qq}} + C^{(1,0)}_{pp;\mathcal{K}_{qq}}\eta^{(1,3)}_{\mathcal{K}_{qq}}) \tag{A.1}$$

where the labels are given by

$$\vec{\tau} = \{\tau, l = 0, [0,0,0]\},$$
$$\mathcal{D}_{\vec{\tau}} = \{(qq)|q \le \frac{\tau}{2}\}, \tag{A.2}$$

and $C^{(1,k)}_{pp,\mathcal{K}_{qq}}$ are the tree-level supergravity and string corrected three-point functions for $k = 0$ and $k = 3$ respectively. The three-point functions appearing in (A.1) can be extracted from the non-log$(u)$ contribution to tree-level correlators of the form $\langle ppqq\rangle$, whose window region is defined $p \le \frac{\tau}{2} < q$. The generalisation to $\langle ppqq\rangle$ is essential for the unmixing of degenerate operators.

As indicated in (A.1) there is not a one-to-one correspondence between three-point functions and conformal block coefficients. Therefore, to calculate the individual three-point functions we need to unmix the degenerate operators entering the block coefficients. The correlators $\langle 22pp\rangle$ do not provide enough information to solve this degeneracy problem, instead we must consider a more general set of correlators taking the form $\langle ppqq\rangle$. At each level in twist we have $(t-1)$ degenerate operators, where $t = \tau/2$, thus to solve we must consider

the set of $(t-1)$ families of correlators with $2 \leq p \leq t$. As mentioned before, the relevant information is encoded in the non-$\log(u)$ contribution to the tree-level correlators, whose OPE coefficients are given by

$$N_{ppqq,\vec{\tau}}^{(1,k=1,3)} = \sum_{i=1}^{t-1} (C_{pp,i}^{(0,0)} C_{qq,i}^{(1,k)}), \tag{A.3}$$

when looking at the window region $p \leq t < q$.

Having detailed where the required data can be found, the unmixing procedure is best illustrated with an example. With one operator at twist four, and therefore no mixing, the three-point functions can indeed be calculated just using data from the $\langle 22qq \rangle$ family. Thus, the first instructive case where operator mixing happens is at twist six.

At twist six we wish to compute the couplings $C_{qq,1}^{(1,k)}$ and $C_{qq,2}^{(1,k)}$ for $k = 0$ and $k = 3$ (supergravity and string corrected) respectively. Following the discussion above, to have enough information to perform the unmixing both the $\langle 22qq \rangle$ and $\langle 33qq \rangle$ family of correlators are needed. To ensure twist six lies within the window for both sets of correlators, we must have $q > 3$. As shown in (A.3), within the window region the conformal block coefficients are given by

$$\begin{aligned}
C_{22,1}^{(0,0)} C_{qq,1}^{(1,k=1,3)} + C_{22,2}^{(0,0)} C_{qq,2}^{(1,k=1,3)} &= N_{22qq,\tau=6}^{(1,k=1,3)}, \\
C_{33,1}^{(0,0)} C_{qq,1}^{(1,k=1,3)} + C_{33,2}^{(0,0)} C_{qq,2}^{(1,k=1,3)} &= N_{33qq,\tau=6}^{(1,k=1,3)},
\end{aligned} \tag{A.4}$$

for $\langle 22qq \rangle$ and $\langle 33qq \rangle$ respectively. This can be nicely repackaged in matrix form by

$$\begin{bmatrix} C_{22,1}^{(0,0)} & C_{22,2}^{(0,0)} \\ C_{33,1}^{(0,0)} & C_{33,2}^{(0,0)} \end{bmatrix} \begin{bmatrix} C_{qq,1}^{(1,k=1,3)} \\ C_{qq,2}^{(1,k=1,3)} \end{bmatrix} = \begin{bmatrix} N_{22qq,\tau=6}^{(1,k=1,3)} \\ N_{33qq,\tau=6}^{(1,k=1,3)} \end{bmatrix}, \tag{A.5}$$

from which the desired couplings can be readily obtained. This can be easily generalised to arbitrary twists

$$\mathbb{C}_t^{(0,0)} \vec{\mathbf{C}}_t^{(1,k=1,3)} = \vec{\mathbf{N}}_t^{(1,k=1,3)}, \tag{A.6}$$

$$(\mathbb{C}_t^{(0,0)})^{-1} \vec{\mathbf{N}}_t^{(1,k=1,3)} = \vec{\mathbf{C}}_t^{(1,k=1,3)}, \tag{A.7}$$

where the matrix is now $(t-1) \times (t-1)$ dimensional. During this process much new OPE data has been generated. We were able to find a closed formula for all order $\lambda^{-3/2}$ string corrected and supergravity three-point functions in the singlet with $\ell = 0$ and degeneracy labels $(i, r) = (1, 0)$.

The string corrected three-point functions are non-vanishing only for degeneracy label $i = 1$ (mirroring the behaviour of the string anomalous dimensions $\eta_i^{(1,3)}$) and are given, for $t < p$,

by the following formula

$$\frac{C^{(1,3)}_{pp,\mathcal{K}_{22}}(t)}{C^{(0,0)}_{22,\mathcal{K}_{22}}(t)} = \frac{\zeta_3}{1680}\frac{(-1)^t t^2 p(t-1)(1+t)^3(2+t)^2(3+t)\Gamma(p-t)\Gamma(p+2+t)}{\Gamma(p-1)\Gamma(p)}, \qquad (A.8)$$

where we have

$$C^{(0,0)}_{22,\mathcal{K}_{22}}(t) = \sqrt{105\cdot 2^{3-4t}\pi}\sqrt{\frac{\Gamma(t)\Gamma(t+2)}{(t+2)\Gamma(t+\frac{3}{2})\Gamma(t+\frac{5}{2})}}. \qquad (A.9)$$

The subleading supergravity three-point functions have also been calculated, again for $t < p$, and found to be

$$\frac{C^{(1,0)}_{pp,\mathcal{K}_{22}}(t)}{C^{(0,0)}_{22,\mathcal{K}_{22}}(t)} = \frac{(-1)^t pt(t+1)(t+2)}{720}(p(p+1)(p+2) - \frac{\Gamma(p-t)\Gamma(p+t+2)}{\Gamma(p-1)\Gamma(p)}). \qquad (A.10)$$

It is interesting to note that the ratio of the second term in (A.10) with A.9 is given by $\eta^{(1,0)}/\eta^{(1,3)}$.

# Appendix B

# Results

In this section we provide the full formulae for the Above Window, Window and Below Window functions appearing in the main text.

## B.1   Above Window

The function appearing in the Above Window is given by

$$
\begin{aligned}
w(\hat{s}, \check{s}, c_s; \Sigma) = \frac{1}{180}(\Sigma - 1)_3 \big( & 9c_s^4 - 54c_s^2\Sigma^2 - 18c_s^2\Sigma^2\check{s}^2 + 90c_s^2\Sigma\check{s}^2 - 108c_s^2\check{s}^2 + 54c_s^2\Sigma^2\check{s} - 126c_s^2\Sigma\check{s} \\
& - 36c_s^2\Sigma^2\check{s}\hat{s} + 144c_s^2\check{s}\hat{s} + 36c_s^2\check{s} - 18c_s^2\Sigma^2\hat{s}^2 - 90c_s^2\Sigma\hat{s}^2 - 108c_s^2\hat{s}^2 + 54c_s^2\Sigma^2\hat{s} + 126c_s^2\Sigma\hat{s} \\
& + 36c_s^2\hat{s} - 36c_s^2 + 45\Sigma^4 + 36\Sigma^2 + 2\Sigma^4\check{s}^4 - 28\Sigma^3\check{s}^4 + 142\Sigma^2\check{s}^4 - 308\Sigma\check{s}^4 + 240\check{s}^4 \\
& - 12\Sigma^4\check{s}^3 + 120\Sigma^3\check{s}^3 - 420\Sigma^2\check{s}^3 + 600\Sigma\check{s}^3 + 8\Sigma^4\check{s}^3\hat{s} - 56\Sigma^3\check{s}^3\hat{s} + 64\Sigma^2\check{s}^3\hat{s} + 224\Sigma\check{s}^3\hat{s} \\
& - 384\check{s}^3\hat{s} - 288\check{s}^3 + 40\Sigma^4\check{s}^2 - 254\Sigma^3\check{s}^2 + 518\Sigma^2\check{s}^2 - 364\Sigma\check{s}^2 + 12\Sigma^4\check{s}^2\hat{s}^2 - 156\Sigma^2\check{s}^2\hat{s}^2 \\
& + 432\check{s}^2\hat{s}^2 - 36\Sigma^4\check{s}^2\hat{s} + 120\Sigma^3\check{s}^2\hat{s} + 108\Sigma^2\check{s}^2\hat{s} - 480\Sigma\check{s}^2\hat{s} + 144\check{s}^2\hat{s} + 48\check{s}^2 - 66\Sigma^4\check{s} \\
& + 198\Sigma^3\check{s} - 168\Sigma^2\check{s} + 72\Sigma\check{s} + 8\Sigma^4\check{s}\hat{s}^3 + 56\Sigma^3\check{s}\hat{s}^3 + 64\Sigma^2\check{s}\hat{s}^3 - 224\Sigma\check{s}\hat{s}^3 - 384\check{s}\hat{s}^3 \\
& - 36\Sigma^4\check{s}\hat{s}^2 - 120\Sigma^3\check{s}\hat{s}^2 + 108\Sigma^2\check{s}\hat{s}^2 + 480\Sigma\check{s}\hat{s}^2 + 144\check{s}\hat{s}^2 + 80\Sigma^4\check{s}\hat{s} - 332\Sigma^2\check{s}\hat{s} + 48\check{s}\hat{s} \\
& + 2\Sigma^4\hat{s}^4 + 28\Sigma^3\hat{s}^4 + 142\Sigma^2\hat{s}^4 + 308\Sigma\hat{s}^4 + 240\hat{s}^4 - 12\Sigma^4\hat{s}^3 - 120\Sigma^3\hat{s}^3 - 420\Sigma^2\hat{s}^3 - 600\Sigma\hat{s}^3 \\
& - 288\hat{s}^3 + 40\Sigma^4\hat{s}^2 + 254\Sigma^3\hat{s}^2 + 518\Sigma^2\hat{s}^2 + 364\Sigma\hat{s}^2 + 48\hat{s}^2 - 66\Sigma^4\hat{s} - 198\Sigma^3\hat{s} - 168\Sigma^2\hat{s} \\
& - 72\Sigma\hat{s} \big). \tag{B.1}
\end{aligned}
$$

## B.2   Window and below window remainder functions

The residue function in the spherical harmonic basis is given by

$$
\mathtt{R}_{\bar{p}}^{-}(n, b) = \frac{1}{960}\big(64B^3 - 16B^2c_s^2 - 160B^2c_s - 32B^2c_{tu}^2 - 64B^2n\Sigma - 192B^2n + 16B^2\Sigma^2 + 224B^2\Sigma
$$

$$+ 448B^2 + 8Bc_s^2c_{tu}^2 + 32Bc_s^2n + 32Bc_s^2 + 64Bc_sc_{tu}^2 + 32Bc_sn - 64Bc_s\Sigma - 192Bc_s + 4Bc_{tu}^4$$

$$+ 32Bc_{tu}^2n\Sigma + 96Bc_{tu}^2n - 8Bc_{tu}^2\Sigma^2 - 96Bc_{tu}^2\Sigma - 208Bc_{tu}^2 - 32Bn\Sigma^2 - 224Bn\Sigma - 384Bn$$

$$+ 32B\Sigma^2 + 192B\Sigma + 256B - 16c_s^3n - c_s^2c_{tu}^4 - 8c_s^2c_{tu}^2n + 16c_s^2c_{tu}^2 + 16c_s^2n\Sigma + 32c_s^2n - 6c_sc_{tu}^4$$

$$- 24c_sc_{tu}^2n + 96c_sc_{tu}^2 + 16c_sn\Sigma^2 + 128c_sn\Sigma + 256c_sn - 4c_{tu}^4n\Sigma - 12c_{tu}^4n + c_{tu}^4\Sigma^2 + 10c_{tu}^4\Sigma + 16c_{tu}^4$$

$$+ 8c_{tu}^2n\Sigma^2 + 104c_{tu}^2n\Sigma + 224c_{tu}^2n - 16c_{tu}^2\Sigma^2 - 160c_{tu}^2\Sigma - 256c_{tu}^2 - 16n\Sigma^3 - 160n\Sigma^2 - 512n\Sigma - 512n).$$

$$(\text{B.2})$$

The 7 Window poles in the monomial basis are given by:

$$r_{\vec{p};6} = \frac{(\check{s} + \frac{\Sigma+c_s}{2} - 1)(\check{s} + \frac{\Sigma+c_s}{2})}{15},$$

$$r_{\vec{p};5} = \frac{(\check{s} + \frac{\Sigma+c_s}{2})(-30 + 11c_s + 2c_s^2 + 9\Sigma + 3c_s\Sigma + \Sigma^2 + c_{tu}^2 + 30\check{s} - 2\check{s}\Sigma - 12\check{s}^2)}{30},$$

$$r_{\vec{p};4} = \frac{1}{240}(240\check{s}^4 + 80\check{s}^3(\Sigma - 9) + 40\check{s}^2(30 - 2c_s^2 - 3c_s\Sigma - 11c_s - c_{tu}^2 - \Sigma^2 - 11\Sigma)$$

$$+ 4\check{s}(-3c_s^2\Sigma + 29c_s^2 - 6c_s\Sigma^2 + 30c_s\Sigma + 182c_s - 2c_{tu}^2\Sigma + 14c_{tu}^2 - 3\Sigma^3 + \Sigma^2 + 150\Sigma - 240)$$

$$+ (6c_s^4 + 18c_s^3\Sigma + 66c_s^3 + 8c_s^2c_{tu}^2 + 18c_s^2\Sigma^2 + 150c_s^2\Sigma + 116c_s^2 + 12c_sc_{tu}^2\Sigma + 40c_sc_{tu}^2 + 6c_s\Sigma^3$$

$$+ 102c_s\Sigma^2 + 104c_s\Sigma - 576c_s + c_{tu}^4 + 4c_{tu}^2\Sigma^2 + 32c_{tu}^2\Sigma - 20c_{tu}^2 + 18\Sigma^3 + 20\Sigma^2 - 480\Sigma + 64)),$$

$$r_{\vec{p};3} = \frac{1}{240}(2c_s^5 + 7c_s^4\Sigma - 4c_s^4\check{s} + 29c_s^4 + 6c_s^3c_{tu}^2 + 8c_s^3\Sigma^2 + 80c_s^3\Sigma - 40c_s^3\check{s}^2 - 16c_s^3\Sigma\check{s} - 32c_s^3\check{s} + 142c_s^3$$

$$+ 12c_s^2c_{tu}^2\Sigma - 12c_s^2c_{tu}^2\check{s} + 48c_s^2c_{tu}^2 + 2c_s^2\Sigma^3 + 66c_s^2\Sigma^2 + 210c_s^2\Sigma + 80c_s^2\check{s}^3 - 72c_s^2\Sigma\check{s}^2 - 384c_s^2\check{s}^2$$

$$- 24c_s^2\Sigma^2\check{s} - 96c_s^2\Sigma\check{s} + 96c_s^2\check{s} - 32c_s^2 + 2c_sc_{tu}^4 + 6c_sc_{tu}^2\Sigma^2 + 60c_sc_{tu}^2\Sigma - 40c_sc_{tu}^2\check{s}^2 - 24c_sc_{tu}^2\Sigma\check{s}$$

$$- 48c_sc_{tu}^2\check{s} + 58c_sc_{tu}^2 - 2c_s\Sigma^4 + 8c_s\Sigma^3 + 42c_s\Sigma^2 - 400c_s\Sigma + 160c_s\check{s}^4 + 160c_s\Sigma\check{s}^3 + 320c_s\check{s}^3$$

$$- 24c_s\Sigma^2\check{s}^2 - 480c_s\Sigma\check{s}^2 - 672c_s\check{s}^2 - 16c_s\Sigma^3\check{s} - 96c_s\Sigma^2\check{s} + 320c_s\Sigma\check{s} + 1056c_s\check{s} - 960c_s + c_{tu}^4\Sigma$$

$$- 4c_{tu}^4\check{s} + 5c_{tu}^4 + 12c_{tu}^2\Sigma^2 + 26c_{tu}^2\Sigma + 80c_{tu}^2\check{s}^3 - 8c_{tu}^2\Sigma\check{s}^2 - 144c_{tu}^2\check{s}^2 - 12c_{tu}^2\Sigma^2\check{s} - 48c_{tu}^2\Sigma\check{s} + 144c_{tu}^2\check{s}$$

$$- 104c_{tu}^2 - \Sigma^5 - 7\Sigma^4 - 26\Sigma^3 - 176\Sigma^2 - 384\Sigma - 320\check{s}^5 + 800\check{s}^4 + 80\Sigma^2\check{s}^3 + 320\Sigma\check{s}^3 - 1600\check{s}^3 + 8\Sigma^3\check{s}^2$$

$$- 96\Sigma^2\check{s}^2 - 320\Sigma\check{s}^2 + 2080\check{s}^2 - 4\Sigma^4\check{s} - 32\Sigma^3\check{s} + 96\Sigma^2\check{s} + 480\Sigma\check{s} - 1216\check{s} + 384),$$

$$r_{\vec{p};2} = -\frac{1}{480}(\check{s} - \frac{c_s + \Sigma}{2} - 1)(c_s^5 + 3c_s^4\Sigma - 2c_s^4\check{s} + 14c_s^4 + 8c_s^3c_{tu}^2 + 2c_s^3\Sigma^2 + 32c_s^3\Sigma - 40c_s^3\check{s}^2 - 8c_s^3\Sigma\check{s}$$

$$- 56c_s^3\check{s} + 112c_s^3 + 12c_s^2c_{tu}^2\Sigma - 16c_s^2c_{tu}^2\check{s} + 56c_s^2c_{tu}^2 - 2c_s^2\Sigma^3 + 12c_s^2\Sigma^2 + 80c_s^2\Sigma + 80c_s^2\check{s}^3 - 56c_s^2\Sigma\check{s}^2$$

$$- 272c_s^2\check{s}^2 - 12c_s^2\Sigma^2\check{s} - 104c_s^2\Sigma\check{s} - 264c_s^2\check{s} + 6c_sc_{tu}^4 + 40c_sc_{tu}^2\Sigma - 80c_sc_{tu}^2\check{s}^2 - 32c_sc_{tu}^2\Sigma\check{s} - 144c_sc_{tu}^2\check{s}$$

$$- 12c_sc_{tu}^2 - 3c_s\Sigma^4 - 16c_s\Sigma^3 - 80c_s\Sigma^2 - 480c_s\Sigma + 240c_s\check{s}^4 + 160c_s\Sigma\check{s}^3 + 800c_s\check{s}^3 + 8c_s\Sigma^2\check{s}^2 - 160c_s\Sigma\check{s}^2$$

$$- 16c_s\check{s}^2 - 8c_s\Sigma^3\check{s} - 40c_s\Sigma^2\check{s} + 240c_s\Sigma\check{s} + 1152c_s\check{s} - 960c_s - 12c_{tu}^4\check{s} + 6c_{tu}^4 - 4c_{tu}^2\Sigma^3 - 16c_{tu}^2\Sigma^2$$

$$- 12c_{tu}^2\Sigma + 160c_{tu}^2\check{s}^3 + 16c_{tu}^2\Sigma\check{s}^2 - 32c_{tu}^2\check{s}^2 - 16c_{tu}^2\Sigma^2\check{s} - 48c_{tu}^2\Sigma\check{s} + 240c_{tu}^2\check{s} - 144c_{tu}^2 - \Sigma^5 - 10\Sigma^4 - 48\Sigma^3$$

$$- 96\Sigma^2 + 192\Sigma - 480\check{s}^5 - 80\Sigma\check{s}^4 + 80\Sigma^2\check{s}^3 + 160\Sigma\check{s}^3 - 1440\check{s}^3 + 24\Sigma^3\check{s}^2 + 112\Sigma^2\check{s}^2 + 240\Sigma\check{s}^2 + 960\check{s}^2$$

$$- 2\Sigma^4\check{s} + 8\Sigma^3\check{s} + 120\Sigma^2\check{s} - 768\check{s} + 768),$$

$$r_{\vec{p};1} = -\frac{1}{240}(\check{s} - \frac{c_s + \Sigma}{2} - 1)_2(-c_s^3c_{tu}^2 + 4c_s^3\check{s}^2 + 8c_s^3\check{s} - 10c_s^3 - c_s^2c_{tu}^2\Sigma + 2c_s^2c_{tu}^2\check{s} - 6c_s^2c_{tu}^2 - 2c_s^2\Sigma - 8c_s^2\check{s}^3$$

$$+ 4c_s^2\Sigma\check{s}^2 + 16c_s^2\check{s}^2 + 8c_s^2\Sigma\check{s} + 72c_s^2\check{s} - 4c_s^2 - 2c_sc_{tu}^4 + c_sc_{tu}^2\Sigma^2 + 20c_sc_{tu}^2\check{s}^2 + 4c_sc_{tu}^2\Sigma\check{s} + 48c_sc_{tu}^2\check{s}$$

$$+ 10c_s\Sigma^2 + 56c_s\Sigma - 48c_s\check{s}^4 - 16c_s\Sigma\check{s}^3 - 224c_s\check{s}^3 - 4c_s\Sigma^2\check{s}^2 - 16c_s\Sigma\check{s}^2 - 192c_s\check{s}^2 - 8c_s\Sigma^2\check{s} - 80c_s\Sigma\check{s}$$

$$- 256c_s\check{s} + 112c_s + c_{tu}^4\Sigma + 4c_{tu}^4\check{s} + c_{tu}^4 + c_{tu}^2\Sigma^3 + 6c_{tu}^2\Sigma^2 - 6c_{tu}^2\Sigma - 40c_{tu}^2\check{s}^3 - 12c_{tu}^2\Sigma\check{s}^2 - 56c_{tu}^2\check{s}^2$$

$$+ 2c_{tu}^2\Sigma^2\check{s} - 16c_{tu}^2\Sigma\check{s} - 96c_{tu}^2\check{s} - 8c_{tu}^2 + 2\Sigma^3 - 4\Sigma^2 - 80\Sigma + 96\check{s}^5 + 32\Sigma\check{s}^4 + 240\check{s}^4 - 8\Sigma^2\check{s}^3 + 96\Sigma\check{s}^3$$

$$- 4\Sigma^3\check{s}^2 - 32\Sigma^2\check{s}^2 + 16\Sigma\check{s}^2 + 240\check{s}^2 - 8\Sigma^3\check{s} - 24\Sigma^2\check{s} + 96\Sigma\check{s} + 160\check{s} - 128 + 480\check{s}^3 + 26c_sc_{tu}^2),$$

$$r_{\vec{p};0} = \frac{1}{480}(\check{s} - \frac{c_s + \Sigma}{2} - 1)_3(16c_s^2\check{s} - c_sc_{tu}^4 + 8c_sc_{tu}^2\check{s}^2 + 24c_sc_{tu}^2\check{s} + 16c_sc_{tu}^2 - 16c_s\check{s}^4 - 96c_s\check{s}^3 - 128c_s\check{s}^2$$

$$- 96c_s\check{s} + c_{tu}^4\Sigma + 2c_{tu}^4\check{s} + 2c_{tu}^4 - 16c_{tu}^2\Sigma - 16c_{tu}^2\check{s}^3 - 8c_{tu}^2\Sigma\check{s}^2 - 48c_{tu}^2\check{s}^2 - 24c_{tu}^2\Sigma\check{s} - 72c_{tu}^2\check{s} - 32c_{tu}^2$$

$$+ 16\Sigma\check{s}^4 + 160\check{s}^4 + 96\Sigma\check{s}^3 + 352\check{s}^3 + 128\Sigma\check{s}^2 + 320\check{s}^2 + 16\Sigma^2\check{s} + 96\Sigma\check{s} + 128\check{s} + 32\check{s}^5 - 32c_s\Sigma\check{s}).$$

$$\text{(B.3)}$$

The 3 Below Window poles are given by:

$$b_{\vec{p};2} = \frac{4(\check{s} + \Sigma - 1)}{15},$$

$$b_{\vec{p};1} = \frac{(1 - 2\check{s} - \Sigma)(4\check{s}^2 - 4\check{s}(1 + 2\Sigma) + 16 - c_s^2 + 4\Sigma - 11\Sigma^2)}{15},$$

$$b_{\vec{p};0} = \frac{1}{60}(16\check{s}^5 - 64\check{s}^4\Sigma - 8\check{s}^3(c_s^2 - 15\Sigma^2 + 4) + 16\check{s}^2\Sigma(c_s^2 + 26\Sigma^2 - 29)$$

$$+ \check{s}(c_s^4 - 2c_s^2\Sigma^2 - 8c_s^2 + 289\Sigma^4 - 296\Sigma^2 + 16) + 12(\Sigma - 1)_3(5\Sigma^2 + 4 - c_s^2)). \quad \text{(B.4)}$$

## B.3   Combining $\mathcal{R}^W$ and $\mathcal{B}^{(BW)}$

Note first that we can rewrite the result for $\mathcal{B}^{(BW)}$ using the same split used for $\mathcal{R}^{(W)}$. In this way we can write

$$\mathcal{W}_{\vec{p}}^{(2)}(\hat{s}, \check{s}) = \sum_{z \geq 0} \frac{(\check{s} + p_{12} - z)_{z+1}\mathcal{P}_{\vec{p};z}^+(\hat{s}, \check{s}) + (\check{s} + p_{34} - z)_{z+1}\mathcal{P}_{\vec{p};z}^-(\hat{s}, \check{s})}{\mathbf{s} - z}, \quad \text{(B.5)}$$

where $\mathcal{W}_{\vec{p}}^{(2)}(\hat{s}, \check{s}) := \mathcal{R}_{\vec{p}}^{(W)} + \mathcal{B}_{\vec{p}}^{(W)}$ and

$$\mathcal{P}_{\vec{p}}^+ = \mathcal{P}_{\{-c_s, -c_t, c_u\}} \quad ; \quad \mathcal{P}_{\vec{p}}^- = \mathcal{P}_{\{+c_s, +c_t, c_u\}}, \quad \text{(B.6)}$$

Of course only the poles at $z = 0, 1, 2$ are modified by the addition of $\mathcal{B}^{(BW)}$ w.r.t. the contribution of $\mathcal{R}^{(W)}$.

Certain analyticity in $z$ can be made manifest for the $\mathcal{P}_{\vec{p}}^{(z)}$. Assuming we focus on $\mathcal{P}_z^-$ for concreteness, the idea is that the ratio $\mathcal{P}_z / \Gamma[1 + \frac{p_1 + p_2}{2} + \check{s}]\Gamma[-z + \frac{p_3 + p_4}{2} + \check{s}]$ can be further decomposed by writing $\mathcal{P}_z$ as a polynomial in Pochhammers. This is initially suggested by

the special form of $\mathcal{P}_6$ and $\mathcal{P}_5$ which have a partial factorised form of this sort, i.e.

$$\mathcal{P}_{\vec{p};6} = \frac{(\check{s}+\frac{\Sigma+c_s}{2}-1)(\check{s}+\frac{\Sigma+c_s}{2})}{15} \,,$$

$$\mathcal{P}_{\vec{p};5} = \frac{(\check{s}+\frac{\Sigma+c_s}{2})(-30+11c_s+2c_s^2+9\Sigma+3c_s\Sigma+\Sigma^2+c_{tu}^2+30\check{s}-2\check{s}\Sigma-12\check{s}^2)}{30} \,, \tag{B.7}$$

In this way we can absorb the $\check{s}$ dependence into the $z$-independent $\Gamma$, and get a structure of the form,

$$\frac{\mathcal{P}_z(\check{s}, c_s, c_t, c_u, \Sigma)}{\Gamma[1 + \frac{p_1+p_2}{2} + \check{s}]\Gamma[-z + \frac{p_3+p_4}{2} + \check{s}]} = \sum_{w \geq -1} \frac{\mathcal{P}_{z,w}(c_s, c_t, c_u, \Sigma)}{\Gamma[-z + \frac{p_3+p_4}{2} + \check{s}]\Gamma[-w + \frac{p_1+p_2}{2} + \check{s}]} \tag{B.8}$$

for each value of $z$. By doing so we find a lattice of points $(w, z)$ of the form



$$\tag{B.9}$$
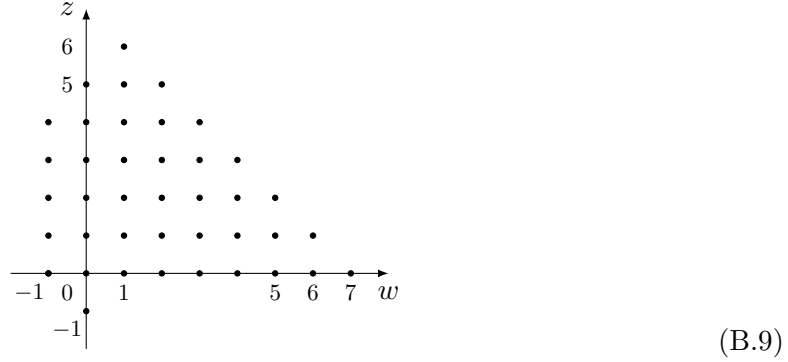
For example, the horizontal axis at $z = 0$ corresponds to a polynomial of degree eight in $\tilde{s}$, and therefore there are nine bullet points, the first of which counts for a degree zero contributions, going with $w = -1$, and the last one for a degree eight contribution, going with $w = 7$.

Rearranging the polynomials on the $-45°$ diagonals, we find simple analytic expressions. For illustration,

$$\begin{aligned}
\mathcal{P}_{z,w} &= \tfrac{1}{15} \, \texttt{Bin}\!\begin{bmatrix} 6 \\ z \end{bmatrix} && ; && z + w = 7 \\[4pt]
\mathcal{P}_{z,w} &= \tfrac{(6c_s+5\Sigma+3(2z-11))}{15} \, \texttt{Bin}\!\begin{bmatrix} 5 \\ z \end{bmatrix} && ; && z + w = 6 \\[4pt]
\mathcal{P}_{z,w} &= \tfrac{-(c_{tu})^2+(c_s)^2(31-6z)+\ldots}{30} \, \texttt{Bin}\!\begin{bmatrix} 5 \\ z \end{bmatrix} && ; && z + w = 5 \\
&\ \ \vdots
\end{aligned} \tag{B.10}$$

and so on so forth. The pattern of the binomial $\texttt{Bin}$ persists, and becomes $\texttt{Bin}\!\begin{bmatrix} -1+\#\bullet \\ z \end{bmatrix}$ where $\#$ counts the number of $\bullet$ on the various diagonals in (B.9). This binomial is always singled out by the fact that some of the top degree terms in $\mathcal{P}_{z,w}$, as function of $z$, contribute with a constant times such binomial. In the above formulae, these top degree terms are $(c_{tu})^0 \otimes \{c_s, \Sigma\}$ when $z + w = 6$, and $(c_{tu})^2$ when $z + w = 5$.

The analytic structure in (6.66) suggests from the very beginning a sort of analyticity of $\mathcal{P}_z$ in $z$, and the rearrangement into $\mathcal{P}_{z,w}$ in (B.10), is an example. On the other hand, had we started with a general parametrisation of $\mathcal{P}_z$ as a polynomial in $\check{s}, c_s, c_t, c_u, \Sigma$, and fitted data in- and below- Window, we would have found some free coefficients left. There is indeed a subtlety with a $\mathcal{P}_z$ so constructed, which is the following: Pieces of $\mathcal{P}_z$ cancel out in the sum

$$\frac{\left[ \frac{\Gamma[\check{s}+\frac{p_1+p_2}{2}+1]\mathcal{P}_z^+}{\Gamma[\check{s}+\frac{p_1+p_2}{2}-z]} + \frac{\Gamma[\check{s}+\frac{p_3+p_4}{2}+1]\mathcal{P}_z^-}{\Gamma[\check{s}+\frac{p_3+p_4}{2}-z]} \right]}{\Gamma[\check{s}+\frac{p_1+p_2}{2}+1]\Gamma[\check{s}+\frac{p_3+p_4}{2}+1]}. \tag{B.11}$$

Using that $\Gamma[X+1]/\Gamma[X-z] = (X-z)_{z+1}$ is polynomial in $X$, and expanding the whole numerator in (B.11), it is simple to see that contributions of the form $c_s^{2\mathbb{N}+1} f(\check{s}, c_s^2, c_t^2, c_u^2, \Sigma)$, for any function $f$, cancel out. We haven't encountered this subtlety in our discussion above because the functions in $\mathcal{R}^{(W)}$, nicely enough, do not have it.

# References

[1] J. M. Drummond, R. Glew and H. Paul, *One-loop string corrections for AdS Kaluza-Klein amplitudes*, *JHEP* **12** (2021) 072, [2008.01109].

[2] F. Aprile, J. M. Drummond, R. Glew and M. Santagata, *One-loop string amplitudes in $AdS_5 \times S^5$: Mellin space and sphere splitting*, 2207.13084.

[3] L. Bossinger, J. M. Drummond and R. Glew, *Adjacency for scattering amplitudes from the Gröbner fan*, 2212.08931.

[4] S. J. Parke and T. R. Taylor, *An Amplitude for n Gluon Scattering*, *Phys. Rev. Lett.* **56** (1986) 2459.

[5] R. Britto, F. Cachazo and B. Feng, *New recursion relations for tree amplitudes of gluons*, *Nucl. Phys. B* **715** , [hep-th/0412308].

[6] R. Britto, F. Cachazo, B. Feng and E. Witten, *Direct proof of tree-level recursion relation in Yang-Mills theory*, *Phys. Rev. Lett.* **94** (2005) 181602, [hep-th/0501052].

[7] J. M. Drummond and J. M. Henn, *All tree-level amplitudes in N=4 SYM*, *JHEP* **04** (2009) 018, [0808.2475].

[8] Z. Bern, L. J. Dixon, D. C. Dunbar and D. A. Kosower, *One loop n point gauge theory amplitudes, unitarity and collinear limits*, *Nucl. Phys. B* **425** (1994) 217–260, [hep-ph/9403226].

[9] N. Arkani-Hamed, J. L. Bourjaily, F. Cachazo, S. Caron-Huot and J. Trnka, *The All-Loop Integrand For Scattering Amplitudes in Planar N=4 SYM*, *JHEP* **01** (2011) 041, [1008.2958].

[10] N. Arkani-Hamed, F. Cachazo, C. Cheung and J. Kaplan, *A Duality For The S Matrix*, *JHEP* **03** (2010) 020, [0907.5418].

[11] L. J. Mason and D. Skinner, *Dual Superconformal Invariance, Momentum Twistors and Grassmannians*, *JHEP* **11** (2009) 045, [0909.0250].

[12] N. Arkani-Hamed, F. Cachazo and C. Cheung, *The Grassmannian Origin Of Dual Superconformal Invariance*, *JHEP* **03** (2010) 036, [0909.0483].

[13] J. M. Drummond, J. Henn, G. P. Korchemsky and E. Sokatchev, *Dual superconformal symmetry of scattering amplitudes in N=4 super-Yang-Mills theory*, *Nucl. Phys. B* **828** (2010) 317–374, [0807.1095].

[14] J. Drummond, J. Foster, O. Gürdoğan and G. Papathanasiou, *Cluster adjacency and the four-loop NMHV heptagon*, *JHEP* **03** (2019) 087, [1812.04640].

[15] L. J. Dixon, J. M. Drummond and J. M. Henn, *Bootstrapping the three-loop hexagon*, *JHEP* **11** (2011) 023, [1108.4461].

[16] L. J. Dixon, J. M. Drummond, M. von Hippel and J. Pennington, *Hexagon functions and the three-loop remainder function*, *JHEP* **12** (2013) 049, [1308.2276].

[17] L. J. Dixon, J. M. Drummond, C. Duhr and J. Pennington, *The four-loop remainder function and multi-Regge behavior at NNLLA in planar N = 4 super-Yang-Mills theory*, *JHEP* **06** (2014) 116, [1402.3300].

[18] L. J. Dixon and M. von Hippel, *Bootstrapping an NMHV amplitude through three loops*, *JHEP* **10** (2014) 065, [1408.1505].

[19] J. M. Drummond, G. Papathanasiou and M. Spradlin, *A Symbol of Uniqueness: The Cluster Bootstrap for the 3-Loop MHV Heptagon*, *JHEP* **03** (2015) 072, [1412.3763].

[20] L. J. Dixon, M. von Hippel and A. J. McLeod, *The four-loop six-gluon NMHV ratio function*, *JHEP* **01** (2016) 053, [1509.08127].

[21] S. Caron-Huot, L. J. Dixon, A. McLeod and M. von Hippel, *Bootstrapping a Five-Loop Amplitude Using Steinmann Relations*, *Phys. Rev. Lett.* **117** (2016) 241601, [1609.00669].

[22] L. J. Dixon, J. Drummond, T. Harrington, A. J. McLeod, G. Papathanasiou and M. Spradlin, *Heptagons from the Steinmann Cluster Bootstrap*, *JHEP* **02** (2017) 137, [1612.08976].

[23] S. Caron-Huot, L. J. Dixon, F. Dulat, M. von Hippel, A. J. McLeod and G. Papathanasiou, *Six-Gluon amplitudes in planar $\mathcal{N} = 4$ super-Yang-Mills theory at six and seven loops*, *JHEP* **08** (2019) 016, [1903.10890].

[24] L. J. Dixon, O. Gurdogan, A. J. McLeod and M. Wilhelm, *Bootstrapping a stress-tensor form factor through eight loops*, *JHEP* **07** (2022) 153, [2204.11901].

[25] S. Fomin and A. Zelevinsky, *Cluster algebras i: foundations*, *Journal of the American Mathematical Society* **15** (2002) 497–529.

[26] S. Fomin and A. Zelevinsky, *Cluster algebras ii: Finite type classification, arXiv preprint math/0208229* (2002) .

[27] S. Fomin and A. Zelevinsky, *Cluster algebras iv: coefficients*, *Compositio Mathematica* **143** (2007) 112–164.

[28] J. Golden, A. B. Goncharov, M. Spradlin, C. Vergu and A. Volovich, *Motivic Amplitudes and Cluster Coordinates*, *JHEP* **01** (2014) 091, [1305.1617].

[29] J. Golden, M. F. Paulos, M. Spradlin and A. Volovich, *Cluster Polylogarithms for Scattering Amplitudes*, *J. Phys. A* **47** (2014) 474005, [1401.6446].

[30] J. Drummond, J. Foster and O. Gürdoğan, *Cluster Adjacency Properties of Scattering Amplitudes in N = 4 Supersymmetric Yang-Mills Theory*, *Phys. Rev. Lett.* **120** (2018) 161601, [1710.10953].

[31] J. Drummond, J. Foster, O. Gürdogan and C. Kalousios, *Algebraic singularities of scattering amplitudes from tropical geometry*, *JHEP* **04** (2021) 002, [1912.08217].

[32] N. Arkani-Hamed, T. Lam and M. Spradlin, *Non-perturbative geometries for planar N = 4 SYM amplitudes*, *JHEP* **03** (2021) 065, [1912.08222].

[33] N. Henke and G. Papathanasiou, *How tropical are seven- and eight-particle amplitudes?*, *JHEP* **08** (2020) 005, [1912.08254].

[34] N. Henke and G. Papathanasiou, *Singularities of eight- and nine-particle amplitudes from cluster algebras and tropical geometry*, *JHEP* **10** (2021) 007, [2106.01392].

[35] L. Bossinger, F. Mohammadi, A. Nájera Chávez et al., *Families of gröbner degenerations, grassmannians and universal cluster algebras*, *SIGMA. Symmetry, Integrability and Geometry: Methods and Applications* **17** (2021) 059.

[36] N. Ilten, A. N. Chávez and H. Treffinger, *Deformation theory for finite cluster complexes*, *arXiv preprint arXiv:2111.02566* (2021) .

[37] T. Gehrmann, J. M. Henn and N. A. Lo Presti, *Analytic form of the two-loop planar five-gluon all-plus-helicity amplitude in QCD*, *Phys. Rev. Lett.* **116** (2016) 062001, [1511.05409].

[38] S. He, Z. Li and Q. Yang, *Kinematics, cluster algebras and Feynman integrals*, 2112.11842.

[39] S. He, J. Liu, Y. Tang and Q. Yang, *The symbology of Feynman integrals from twistor geometries*, 2207.13482.

[40] D. Chicherin, J. Henn and V. Mitev, *Bootstrapping pentagon functions*, *JHEP* **05** (2018) 164, [1712.09610].

[41] J. M. Maldacena, *The Large N limit of superconformal field theories and supergravity*, *Adv. Theor. Math. Phys.* **2** (1998) 231–252, [hep-th/9711200].

[42] S. Lee, S. Minwalla, M. Rangamani and N. Seiberg, *Three point functions of chiral operators in D = 4, N=4 SYM at large N*, *Adv. Theor. Math. Phys.* **2** (1998) 697–718, [`hep-th/9806074`].

[43] G. Arutyunov and S. Frolov, *Scalar quartic couplings in type IIB supergravity on AdS(5) x S**5*, *Nucl. Phys. B* **579** (2000) 117–176, [`hep-th/9912210`].

[44] G. Arutyunov and S. Frolov, *Some cubic couplings in type IIB supergravity on AdS(5) x S**5 and three point functions in SYM(4) at large N*, *Phys. Rev. D* **61** (2000) 064009, [`hep-th/9907085`].

[45] G. Arutyunov and S. Frolov, *Four point functions of lowest weight CPOs in N=4 SYM(4) in supergravity approximation*, *Phys. Rev. D* **62** (2000) 064016, [`hep-th/0002170`].

[46] G. Arutyunov, F. A. Dolan, H. Osborn and E. Sokatchev, *Correlation functions and massive Kaluza-Klein modes in the AdS / CFT correspondence*, *Nucl. Phys. B* **665** (2003) 273–324, [`hep-th/0212116`].

[47] G. Arutyunov and E. Sokatchev, *On a large N degeneracy in N=4 SYM and the AdS / CFT correspondence*, *Nucl. Phys. B* **663** (2003) 163–196, [`hep-th/0301058`].

[48] L. Berdichevsky and P. Naaijkens, *Four-point functions of different-weight operators in the AdS/CFT correspondence*, *JHEP* **01** (2008) 071, [`0709.1365`].

[49] L. I. Uruchurtu, *Four-point correlators with higher weight superconformal primaries in the AdS/CFT Correspondence*, *JHEP* **03** (2009) 133, [`0811.2320`].

[50] L. I. Uruchurtu, *Next-next-to-extremal Four Point Functions of N=4 1/2 BPS Operators in the AdS/CFT Correspondence*, *JHEP* **08** (2011) 133, [`1106.0630`].

[51] L. Rastelli and X. Zhou, *Mellin amplitudes for $AdS_5 \times S^5$*, *Phys. Rev. Lett.* **118** (2017) 091602, [`1608.06624`].

[52] L. Rastelli and X. Zhou, *How to Succeed at Holographic Correlators Without Really Trying*, *JHEP* **04** (2018) 014, [`1710.05923`].

[53] G. Mack, *D-independent representation of Conformal Field Theories in D dimensions via transformation to auxiliary Dual Resonance Models. Scalar amplitudes*, `0907.2407`.

[54] J. Penedones, *Writing CFT correlation functions as AdS scattering amplitudes*, *JHEP* **03** (2011) 025, [`1011.1485`].

[55] F. Aprile and P. Vieira, *Large p explorations. From SUGRA to big STRINGS in Mellin space*, *JHEP* **12** (2020) 206, [`2007.09176`].

[56] F. Aprile, J. Drummond, P. Heslop and H. Paul, *Double-trace spectrum of N = 4 supersymmetric Yang-Mills theory at strong coupling*, *Phys. Rev. D* **98** (2018) 126008, [1802.06889].

[57] S. Caron-Huot and A.-K. Trinh, *All tree-level correlators in $AdS_5 \times S_5$ supergravity: hidden ten-dimensional conformal symmetry*, *JHEP* **01** (2019) 196, [1809.09173].

[58] J. M. Drummond, D. Nandan, H. Paul and K. S. Rigatos, *String corrections to AdS amplitudes and the double-trace spectrum of $\mathcal{N}$ = 4 SYM*, *JHEP* **12** (2019) 173, [1907.00992].

[59] J. M. Drummond, H. Paul and M. Santagata, *Bootstrapping string theory on $AdS_5 \times S^5$*, 2004.07282.

[60] F. Aprile, J. M. Drummond, H. Paul and M. Santagata, *The Virasoro-Shapiro amplitude in $AdS_5 \times S^5$ and level splitting of 10d conformal symmetry*, *JHEP* **11** (2021) 109, [2012.12092].

[61] T. Abl, P. Heslop and A. E. Lipstein, *Towards the Virasoro-Shapiro amplitude in $AdS_5 \times S^5$*, *JHEP* **04** (2021) 237, [2012.12091].

[62] L. F. Alday, *On genus-one string amplitudes on $AdS_5 \times S^5$*, *JHEP* **04** (2021) 005, [1812.11783].

[63] L. F. Alday and X. Zhou, *Simplicity of AdS Supergravity at One Loop*, *JHEP* **09** (2020) 008, [1912.02663].

[64] F. Aprile, J. M. Drummond, P. Heslop and H. Paul, *Quantum Gravity from Conformal Field Theory*, *JHEP* **01** (2018) 035, [1706.02822].

[65] F. Aprile, J. M. Drummond, P. Heslop and H. Paul, *Loop corrections for Kaluza-Klein AdS amplitudes*, *JHEP* **05** (2018) 056, [1711.03903].

[66] F. Aprile, J. Drummond, P. Heslop and H. Paul, *One-loop amplitudes in $AdS_5 \times S^5$ supergravity from $\mathcal{N}$ = 4 SYM at strong coupling*, *JHEP* **03** (2020) 190, [1912.01047].

[67] J. M. Drummond and H. Paul, *One-loop string corrections to AdS amplitudes from CFT*, *JHEP* **03** (2021) 038, [1912.07632].

[68] Z. Huang and E. Y. Yuan, *Graviton Scattering in $AdS_5 \times S^5$ at Two Loops*, 2112.15174.

[69] J. M. Drummond and H. Paul, *Two-loop supergravity on $AdS_5 \times S^5$ from CFT*, 2204.01829.

[70] L. F. Alday and A. Bissi, *Loop Corrections to Supergravity on $AdS_5 \times S^5$*, *Phys. Rev. Lett.* **119** (2017) 171601, [1706.02388].

[71] L. F. Alday, A. Bissi and E. Perlmutter, *Genus-One String Amplitudes from Conformal Field Theory*, *JHEP* **06** (2019) 010, [`1809.10670`].

[72] S. Rychkov, *EPFL Lectures on Conformal Field Theory in D>= 3 Dimensions.* SpringerBriefs in Physics. 1, 2016, 10.1007/978-3-319-43626-5.

[73] D. Simmons-Duffin, *The Conformal Bootstrap*, `1602.07982`.

[74] F. A. Dolan and H. Osborn, *Conformal partial waves and the operator product expansion*, *Nucl. Phys. B* **678** (2004) 491–507, [`hep-th/0309180`].

[75] R. Rattazzi, V. S. Rychkov, E. Tonni and A. Vichi, *Bounding scalar operator dimensions in 4D CFT*, *JHEP* **12** (2008) 031, [`0807.0004`].

[76] S. El-Showk, M. F. Paulos, D. Poland, S. Rychkov, D. Simmons-Duffin and A. Vichi, *Solving the 3D Ising Model with the Conformal Bootstrap*, *Phys. Rev. D* **86** (2012) 025022, [`1203.6064`].

[77] E. D'Hoker and D. Z. Freedman, *Supersymmetric gauge theories and the AdS / CFT correspondence*, in *Theoretical Advanced Study Institute in Elementary Particle Physics (TASI 2001): Strings, Branes and EXTRA Dimensions*, pp. 3–158, 1, 2002. `hep-th/0201253`.

[78] L. Brink, J. H. Schwarz and J. Scherk, *Supersymmetric Yang-Mills Theories*, *Nucl. Phys. B* **121** (1977) 77–92.

[79] B. Eden, A. C. Petkou, C. Schubert and E. Sokatchev, *Partial nonrenormalization of the stress tensor four point function in N=4 SYM and AdS / CFT*, *Nucl. Phys. B* **607** (2001) 191–212, [`hep-th/0009106`].

[80] M. Nirschl and H. Osborn, *Superconformal Ward identities and their solution*, *Nucl. Phys. B* **711** (2005) 409–479, [`hep-th/0407060`].

[81] R. Doobary and P. Heslop, *Superconformal partial waves in Grassmannian field theories*, *JHEP* **12** (2015) 159, [`1508.03611`].

[82] F. A. Dolan and H. Osborn, *Conformal four point functions and the operator product expansion*, *Nucl. Phys. B* **599** (2001) 459–496, [`hep-th/0011040`].

[83] F. A. Dolan and H. Osborn, *Superconformal symmetry, correlation functions and the operator product expansion*, *Nucl. Phys. B* **629** (2002) 3–73, [`hep-th/0112251`].

[84] F. A. Dolan and H. Osborn, *Conformal partial wave expansions for N=4 chiral four point functions*, *Annals Phys.* **321** (2006) 581–626, [`hep-th/0412335`].

[85] O. Aharony, S. S. Gubser, J. M. Maldacena, H. Ooguri and Y. Oz, *Large N field*

*theories, string theory and gravity*, *Phys. Rept.* **323** (2000) 183–386,
[`hep-th/9905111`].

[86] H. Paul, *Aspects of four-point functions in N = 4 SYM at strong coupling*. PhD thesis,
Southampton U., 2020.

[87] E. Witten, *Anti-de Sitter space and holography*, *Adv. Theor. Math. Phys.* **2** (1998)
253–291, [`hep-th/9802150`].

[88] S. S. Gubser, I. R. Klebanov and A. M. Polyakov, *Gauge theory correlators from
noncritical string theory*, *Phys. Lett. B* **428** (1998) 105–114, [`hep-th/9802109`].

[89] E. D'Hoker, D. Z. Freedman, S. D. Mathur, A. Matusis and L. Rastelli, *Extremal
correlators in the AdS / CFT correspondence*, `hep-th/9908160`.

[90] G. Arutyunov and S. Frolov, *On the correspondence between gravity fields and CFT
operators*, *JHEP* **04** (2000) 017, [`hep-th/0003038`].

[91] G. Arutyunov, R. Klabbers and S. Savin, *Four-point functions of all-different-weight
chiral primary operators in the supergravity approximation*, *JHEP* **09** (2018) 023,
[`1806.09200`].

[92] F. Aprile, J. M. Drummond, P. Heslop, H. Paul, F. Sanfilippo, M. Santagata et al.,
*Single particle operators and their correlators in free $\mathcal{N} = 4$ SYM*, *JHEP* **11** (2020)
072, [`2007.09395`].

[93] T. W. Brown, *Half-BPS SU(N) correlators in N=4 SYM*, *JHEP* **07** (2008) 044,
[`hep-th/0703202`].

[94] D. J. Binder, S. M. Chester, S. S. Pufu and Y. Wang, *$\mathcal{N} = 4$ Super-Yang-Mills
correlators at strong coupling from string theory and localization*, *JHEP* **12** (2019) 119,
[`1902.06263`].

[95] L. F. Alday and S. Caron-Huot, *Gravitational S-matrix from CFT dispersion
relations*, *JHEP* **12** (2018) 017, [`1711.02031`].

[96] M. B. Green, H.-h. Kwon and P. Vanhove, *Two loops in eleven-dimensions*, *Phys. Rev.
D* **61** (2000) 104010, [`hep-th/9910055`].

[97] S. M. Chester, *Genus-2 holographic correlator on $AdS_5 \times S^5$ from localization*, *JHEP*
**04** (2020) 193, [`1908.05247`].

[98] S. M. Chester and S. S. Pufu, *Far beyond the planar limit in strongly-coupled $\mathcal{N} = 4$
SYM*, *JHEP* **01** (2021) 103, [`2003.08412`].

[99] M. B. Green and P. Vanhove, *The Low-energy expansion of the one loop type II
superstring amplitude*, *Phys. Rev. D* **61** (2000) 104011, [`hep-th/9910056`].

[100] F. A. Dolan, M. Nirschl and H. Osborn, *Conjectures for large N superconformal N=4 chiral primary four point functions*, *Nucl. Phys. B* **749** (2006) 109–152, [hep-th/0601148].

[101] F. Aprile, J. M. Drummond, P. Heslop and H. Paul, *Unmixing Supergravity*, *JHEP* **02** (2018) 133, [1706.08456].

[102] L. F. Alday, A. Bissi and T. Lukowski, *Lessons from crossing symmetry at large N*, *JHEP* **06** (2015) 074, [1410.4717].

[103] V. Gonçalves, *Four point function of $\mathcal{N}=4$ stress-tensor multiplet at strong coupling*, *JHEP* **04** (2015) 150, [1411.1675].

[104] A. L. Fitzpatrick and J. Kaplan, *Analyticity and the Holographic S-Matrix*, *JHEP* **10** (2012) 127, [1111.6972].

[105] M. B. Green, J. G. Russo and P. Vanhove, *Low energy expansion of the four-particle genus-one amplitude in type II superstring theory*, *JHEP* **02** (2008) 020, [0801.0322].

[106] L. F. Alday, T. Hansen and J. A. Silva, *AdS Virasoro-Shapiro from dispersive sum rules*, 2204.07542.

[107] S. Caron-Huot, F. Coronado, A.-K. Trinh and Z. Zahraee, *Bootstrapping $\mathcal{N}=4$ sYM correlators using integrability*, 2207.01615.

[108] S. Weinberg, *The quantum theory of fields*, vol. 2. Cambridge university press, 1995.

[109] N. Arkani-Hamed, T.-C. Huang and Y.-t. Huang, *Scattering amplitudes for all masses and spins*, *JHEP* **11** (2021) 070, [1709.04891].

[110] H. Elvang and Y.-t. Huang, *Scattering Amplitudes*, 1308.1697.

[111] P. Benincasa and F. Cachazo, *Consistency Conditions on the S-Matrix of Massless Particles*, 0705.4305.

[112] V. P. Nair, *A Current Algebra for Some Gauge Theory Amplitudes*, *Phys. Lett. B* **214** (1988) 215–218.

[113] M. T. Grisaru and H. N. Pendleton, *Some Properties of Scattering Amplitudes in Supersymmetric Theories*, *Nucl. Phys. B* **124** (1977) 81–92.

[114] M. T. Grisaru, H. N. Pendleton and P. van Nieuwenhuizen, *Supergravity and the S Matrix*, *Phys. Rev. D* **15** (1977) 996.

[115] A. Brandhuber, P. Heslop and G. Travaglini, *A Note on dual superconformal symmetry of the N=4 super Yang-Mills S-matrix*, *Phys. Rev. D* **78** (2008) 125005, [0807.4097].

[116] N. Arkani-Hamed, F. Cachazo and J. Kaplan, *What is the Simplest Quantum Field Theory?*, *JHEP* **09** (2010) 016, [0808.1446].

[117] H. Elvang, D. Z. Freedman and M. Kiermaier, *Recursion Relations, Generating Functions, and Unitarity Sums in N=4 SYM Theory*, *JHEP* **04** (2009) 009, [0808.1720].

[118] R. Penrose, *Twistor algebra*, *J. Math. Phys.* **8** (1967) 345.

[119] A. Ferber, *Supertwistors and Conformal Supersymmetry*, *Nucl. Phys. B* **132** (1978) 55–64.

[120] J. M. Drummond, J. M. Henn and J. Plefka, *Yangian symmetry of scattering amplitudes in N=4 super Yang-Mills theory*, *JHEP* **05** (2009) 046, [0902.2987].

[121] A. Hodges, *Eliminating spurious poles from gauge-theoretic amplitudes*, *JHEP* **05** (2013) 135, [0905.1473].

[122] J. M. Drummond, J. Henn, V. A. Smirnov and E. Sokatchev, *Magic identities for conformal four-point integrals*, *JHEP* **01** (2007) 064, [hep-th/0607160].

[123] C. Anastasiou, Z. Bern, L. J. Dixon and D. A. Kosower, *Planar amplitudes in maximally supersymmetric Yang-Mills theory*, *Phys. Rev. Lett.* **91** (2003) 251602, [hep-th/0309040].

[124] Z. Bern, L. J. Dixon and V. A. Smirnov, *Iteration of planar amplitudes in maximally supersymmetric Yang-Mills theory at three loops and beyond*, *Phys. Rev. D* **72** (2005) 085001, [hep-th/0505205].

[125] O. Steinmann, *Über den Zusammenhang zwischen den Wightmanfunktionen und den retardierten Kommutatoren.* PhD thesis, ETH Zurich, 1960.

[126] S. Caron-Huot, L. J. Dixon, J. M. Drummond, F. Dulat, J. Foster, O. Gürdoğan et al., *The Steinmann Cluster Bootstrap for N = 4 Super Yang-Mills Amplitudes*, *PoS* **CORFU2019** (2020) 003, [2005.06735].

[127] L. F. Alday, D. Gaiotto and J. Maldacena, *Thermodynamic Bubble Ansatz*, *JHEP* **09** (2011) 032, [0911.4708].

[128] E. Remiddi and J. A. M. Vermaseren, *Harmonic polylogarithms*, *Int. J. Mod. Phys. A* **15** (2000) 725–754, [hep-ph/9905237].

[129] A. B. Goncharov, *Multiple polylogarithms and mixed tate motives*, *arXiv preprint math/0103059* (2001) .

[130] A. B. Goncharov, M. Spradlin, C. Vergu and A. Volovich, *Classical Polylogarithms for Amplitudes and Wilson Loops*, *Phys. Rev. Lett.* **105** (2010) 151605, [1006.5703].

[131] V. Del Duca, C. Duhr and V. A. Smirnov, *An Analytic Result for the Two-Loop Hexagon Wilson Loop in N = 4 SYM*, *JHEP* **03** (2010) 099, [`0911.5332`].

[132] J. Drummond, J. Foster and O. Gürdoğan, *Cluster adjacency beyond MHV*, *JHEP* **03** (2019) 086, [`1810.08149`].

[133] S. Caron-Huot, *Superconformal symmetry and two-loop amplitudes in planar N=4 super Yang-Mills*, *JHEP* **12** (2011) 066, [`1105.5606`].

[134] S. He, Z. Li and C. Zhang, *Two-loop octagons, algebraic letters and $\bar{Q}$ equations*, *Phys. Rev. D* **101** (2020) 061701, [`1911.01290`].

[135] Z. Li and C. Zhang, *The three-loop MHV octagon from $\overline{Q}$ equations*, *JHEP* **12** (2021) 113, [`2110.00350`].

[136] J. Mago, A. Schreiber, M. Spradlin, A. Yelleshpur Srikant and A. Volovich, *Symbol alphabets from plabic graphs III: n = 9*, *JHEP* **09** (2021) 002, [`2106.01406`].

[137] Q. Yang, *Schubert Problems, Positivity and Symbol Letters*, `2203.16112`.

[138] L. Ren, M. Spradlin and A. Volovich, *Symbol alphabets from tensor diagrams*, *JHEP* **12** (2021) 079, [`2106.01405`].

[139] A. Herderschee, *Algebraic branch points at all loop orders from positive kinematics and wall crossing*, *JHEP* **07** (2021) 049, [`2102.03611`].

[140] J. Bartels, L. N. Lipatov and A. Sabio Vera, *BFKL Pomeron, Reggeized gluons and Bern-Dixon-Smirnov amplitudes*, *Phys. Rev. D* **80** (2009) 045002, [`0802.2065`].

[141] S. Caron-Huot, L. J. Dixon, F. Dulat, M. Von Hippel, A. J. McLeod and G. Papathanasiou, *The Cosmic Galois Group and Extended Steinmann Relations for Planar $\mathcal{N} = 4$ SYM Amplitudes*, *JHEP* **09** (2019) 061, [`1906.07116`].

[142] T. Mora and L. Robbiano, *The gröbner fan of an ideal*, *Journal of Symbolic Computation* **6** (1988) 183–208.

[143] D. Speyer and L. Williams, *The tropical totally positive grassmannian*, *Journal of Algebraic Combinatorics* **22** (2005) 189–210.

[144] J. Drummond, J. Foster, O. Gürdoğan and C. Kalousios, *Tropical fans, scattering equations and amplitudes*, *JHEP* **11** (2021) 071, [`2002.04624`].

[145] J. Drummond, J. Foster, O. Gürdogan and C. Kalousios, *Tropical Grassmannians, cluster algebras and scattering amplitudes*, *JHEP* **04** (2020) 146, [`1907.01053`].

[146] A. N. Jensen, "Gfan, a software system for Gröbner fans and tropical varieties." Available at `http://home.imf.au.dk/jensen/software/gfan/gfan.html`.

[147] D. Chicherin, T. Gehrmann, J. M. Henn, P. Wasser, Y. Zhang and S. Zoia, *Analytic result for a two-loop five-particle amplitude*, *Phys. Rev. Lett.* **122** (2019) 121602, [`1812.11057`].

[148] S. Abreu, L. J. Dixon, E. Herrmann, B. Page and M. Zeng, *The two-loop five-point amplitude in $\mathcal{N} = 4$ super-Yang-Mills theory*, *Phys. Rev. Lett.* **122** (2019) 121603, [`1812.08941`].

[149] S. Abreu, L. J. Dixon, E. Herrmann, B. Page and M. Zeng, *The two-loop five-point amplitude in $\mathcal{N} = 8$ supergravity*, *JHEP* **03** (2019) 123, [`1901.08563`].

[150] D. Chicherin, T. Gehrmann, J. M. Henn, P. Wasser, Y. Zhang and S. Zoia, *The two-loop five-particle amplitude in $\mathcal{N} = 8$ supergravity*, *JHEP* **03** (2019) 115, [`1901.05932`].

[151] S. Abreu, B. Page, E. Pascual and V. Sotnikov, *Leading-Color Two-Loop QCD Corrections for Three-Photon Production at Hadron Colliders*, *JHEP* **01** (2021) 078, [`2010.15834`].

[152] S. Badger, C. Bronnum-Hansen, H. B. Hartanto and T. Peraro, *Analytic helicity amplitudes for two-loop five-gluon scattering: the single-minus case*, *JHEP* **01** (2019) 186, [`1811.11699`].

[153] S. Abreu, J. Dormans, F. Febres Cordero, H. Ita, B. Page and V. Sotnikov, *Analytic Form of the Planar Two-Loop Five-Parton Scattering Amplitudes in QCD*, *JHEP* **05** (2019) 084, [`1904.00945`].

[154] T. Gehrmann, J. M. Henn and N. A. Lo Presti, *Pentagon functions for massless planar scattering amplitudes*, *JHEP* **10** (2018) 103, [`1807.09812`].

[155] Z. Bern, L. J. Dixon and D. A. Kosower, *One loop corrections to five gluon amplitudes*, *Phys. Rev. Lett.* **70** (1993) 2677–2680, [`hep-ph/9302280`].

[156] D. R. Grayson and M. E. Stillman, "Macaulay2, a software system for research in algebraic geometry." Available at `http://www.math.uiuc.edu/Macaulay2/`.

[157] S. Abreu, H. Ita, F. Moriello, B. Page, W. Tschernow and M. Zeng, *Two-Loop Integrals for Planar Five-Point One-Mass Processes*, *JHEP* **11** (2020) 117, [`2005.04195`].

[158] D. Chicherin, V. Sotnikov and S. Zoia, *Pentagon functions for one-mass planar scattering amplitudes*, *JHEP* **01** (2022) 096, [`2110.10111`].

[159] J. Henn, T. Peraro, Y. Xu and Y. Zhang, *A first look at the function space for planar two-loop six-particle Feynman integrals*, *JHEP* **03** (2022) 056, [`2112.10605`].

[160] S. Abreu, H. Ita, B. Page and W. Tschernow, *Two-loop hexa-box integrals for non-planar five-point one-mass processes*, *JHEP* **03** (2022) 182, [2107.14180].

[161] D. Chicherin, J. M. Henn and G. Papathanasiou, *Cluster algebras for Feynman integrals*, *Phys. Rev. Lett.* **126** (2021) 091603, [2012.12285].

[162] J. S. Scott, *Grassmannians and cluster algebras, arXiv preprint math/0311148* (2003) .

[163] C. Geiss, B. Leclerc and J. Schröer, *Partial flag varieties and preprojective algebras*, in *Annales de l'institut Fourier*, vol. 58, pp. 825–876, 2008.

[164] N. Reading, *A combinatorial approach to scattering diagrams, Algebraic Combinatorics* **3** (2020) 603–636.

[165] S. He, Z. Li and Q. Yang, *Truncated cluster algebras and Feynman integrals with algebraic letters*, *JHEP* **12** (2021) 110, [2106.09314].